



ANALYSIS AND SYNTHESIS OF SURFACE ACOUSTIC  
WAVE FILTERS USING AN ADMITTANCE MODEL

by

N.C.V. Krishnamacharyulu, B.E., M.E. (Hons.)

A Thesis

submitted for the Degree of  
DOCTOR OF PHILOSOPHY

in the

Department of Electrical Engineering  
University of Adelaide

February, 1975  
-----

CONTENTS

	<u>Page No.</u>
SUMMARY	(v)
PREFACE	(vii)
ACKNOWLEDGEMENTS	(viii)
CHAPTER 1 - INTRODUCTION	
1.1 Surface Acoustic Waves - an Historical Background	1
1.2 Role of Surface Acoustic Waves in Communications Engineering	3
1.3 Concept of Surface Acoustic Wave Filter	5
1.4 A Brief Survey of Literature on Surface Acoustic Wave Filters	6
1.5 An Outline of Thesis	15
CHAPTER 2 - ADMITTANCE MODEL FOR A PAIR OF INTERDIGITAL TRANSDUCERS	
2.0 Introduction	18
2.1 Basic Approach	19
2.2 Frequency Domain Transadmittance $y_{21}(\omega)$	21
2.2.1 $y_{21}(\omega)$ for a Pair of Uniform Transducers	24
2.3 Frequency Domain Input Admittance $y_{11}(\omega)$	29
2.4 Limitations in using $y_{21}(\omega)$ and $y_{11}(\omega)$	31
CHAPTER 3 - APPLICATION OF TRANSADMITTANCE TO THE SYNTHESIS OF A TV IF FILTER	
3.0 Introduction	34
3.1 TV IF Specification	34
3.2 Advantages of SAW TV IF Filters	37
3.3 Synthesis Procedure - Different Approaches	38
3.4 Synthesis of One Uniform and One Apodized Transducer, Filter 1	41
3.4.1 The Discrete Fourier Transform	44
3.4.2 The Fast Fourier Transform Algorithm	45
3.4.3 Computational Procedure	46
3.4.4 Transducer Configuration	51
3.4.5 Analysis of Modelled Transducer	52
3.4.6 Computer Program of Filter 1	54
CHAPTER 4 - EXPERIMENTAL AND COMPUTED RESULTS OF A TV IF FILTER	
4.0 Introduction	56
4.1 Choice of Suitable Substrate and Propagation Direction	57
4.2 Design and Fabrication of the Delay Line	58
4.2.1 Preparation of the Art-Work	59
4.2.2 Description of the Delay Line Fabrication	61
4.3 Frequency Response Measurement	62
4.3.1 Mounting Techniques	63
4.3.2 Tuning Circuit	64
4.3.3 Calibration of Instruments	66
4.3.4 Measurement Procedure	67
4.4 Discussion of the Results	71

## CHAPTER 5 - SYNTHESIS OF TV IF FILTERS USING OPTIMIZATION TECHNIQUES

5.0	Introduction	74
5.1	An Approach to Quadratic Cost Function Optimization	75
5.2	Mathematical Formulation of Quadratic Cost Function Optimization	76
5.3	Application to Nonlinear Phase Responses	81
5.4	Application to Linear Phase Responses, OPTIM METHOD	85
5.5	Computational Techniques	90
	5.5.1 Peak-Point Perturbation	90
	5.5.2 Coherent-Point Perturbation	92
	5.5.3 Independent-Point Perturbation	94
5.6	Optimization by Successive Iteration	95
	5.6.1 Zero-Order Iteration	95
	5.6.2 Nth-Order Iteration	98

## CHAPTER 6 - COMPUTER ILLUSTRATION OF OPTIMIZATION TECHNIQUES

6.0	Introduction	99
6.1	Synthesis of TV IF Filter using OPTIM METHOD, Filter 2	99
	6.1.1 Selection of Cost-Coefficients	100
	6.1.2 Design Considerations and Choice of Suitable Parameters	102
	6.1.3 Optimization Program, FILTER 2	103
	6.1.4 Discussion of the Results	104
6.2	Synthesis of TV IF Filter using Zero-Order Iteration Method, Filter 3	105
	6.2.1 Design Considerations and Choice of Suitable Parameters	105
	6.2.2 Optimization Program, FILTER 3	106
	6.2.3 Discussion of the Results	106
6.3	Synthesis of a TV IF Filter with Ideal Specifications using OPTIM METHOD, Filter 4	107
	6.3.1 Design Considerations and Choice of Suitable Parameters	108
	6.3.2 Optimization Program FILTER 4	110
	6.3.3 Discussion of the Results	110
6.4	Additional Illustration of OPTIM METHOD	111

## CHAPTER 7 - EXPERIMENTAL PERFORMANCE OF OPTIMIZED FILTERS

7.0	Introduction	113
7.1	Pattern Generation and Filter Fabrication	113
7.2	Experimental and Theoretical Results	114
	7.2.1 Transadmittance Program Y21FIL	114
7.3	Input-Output Admittances of the Filter	115
	7.3.1 Input Admittance of the Filter	116
	7.3.2 Output Admittance of the Filter	117
7.4	Insertion Loss due to Impedance Mismatch	118
	7.4.1 Other Sources of Insertion Loss	124
7.5	Discussion of the Results	125

CHAPTER 8 - SYNTHESIS OF A TV IF FILTER USING CHIRPED TRANSDUCERS		
8.0	Introduction	127
8.1	Basic Approach	128
	8.1.2 Application to SAW Filters	130
8.2	Synthesis Procedure with Two Identical Chirped Transducers	134
	8.2.1 Chirped Transducer Program	137
	8.2.2 Discussion of the Results	139
8.3	Synthesis Procedure with one Chirped and one Apodized Transducers	141
	8.3.1 Computational Procedure	142
	8.3.2 Improvement in Admittance Parameters	143
	8.3.3 Discussion of the Results	151
8.4	Conclusions on Chirped Transducer Design	152
CHAPTER 9 - SYNTHESIS OF A TV IF FILTER IN A HF LINEAR IC ENVIRONMENT		
9.0	Introduction	154
9.1	General Considerations	154
9.2	Choice of Suitable IC amplifiers	155
9.3	Definition of a Gain Function	158
9.4	Matching Networks	160
	9.4.1 Input Matching Networks	160
	9.4.2 Output Matching Networks	161
9.5	Analysis of Gain Function	163
9.6	Synthesis Procedure	165
CHAPTER 10 - SUMMARY AND CONCLUSIONS		168
APPENDIX A - COMPUTER PROGRAM LISTINGS		
A1	ARTWORK...Generation of Transducer Pattern	A1
	A1.1 Flow Chart of ARTWORK	A1
	A1.2 Listing of ARTWORK	A2
A2	FILTER 2...Optimization of Filter 1 using OPTIM METHOD	A8
	A2.1 Flow Chart of FILTER 2	A8
	A2.2 Listing of FILTER 2	A10
A3	FILTER 3...Optimization of Filter 1 using Zero Order Iteration Method	A24
	A3.1 Flow Chart of FILTER 3	A24
	A3.2 Listing of FILTER 3	A26
A4	FILTER 4...Synthesis of a Filter with given Ideal Specifications using OPTIM METHOD	A37
	A4.1 Flow Chart of FILTER 4	A37
	A4.2 Listing of FILTER 4	A39
A5	Y21FIL...Transadmittance of the Filter	A43
	A5.1 Flow Chart of Y21FIL	A43
	A5.2 Listing of Y21FIL	A44
A6	Y22APOD...Input Admittance of Apodized Transducer	A51
	A6.1 Flow Chart of Y22APOD	A51
	A6.2 Listing of Y22APOD	A52
A7	CHIRPTR...Filter Synthesis using Chirped Transducers	A58
	A7.1 Flow Chart of CHIRPTR	A58
	A7.2 Listing of CHIRPTR	A59

A8	PLT...General Purpose Plotting Program	A65
A8.2	Listing of PLT	A65

#### APPENDIX B - PHOTOFABRICATION TECHNIQUES

B1	Preparation of the Art-Work	B1
B2	First Stage Reduction Camera	B1
B3	Second Stage Reduction Camera	B2
B4	Substrate Preparation	B4
B5	Metal Coating	B4
B6	Photoetching	B5
B6.1	Photoresist Coating	B5
B6.2	Exposing to UV Source	B6
B6.3	Developing Exposed Photosensitive Resist Coating	B6
B6.4	Etching	B6

#### REFERENCES

R1

SUMMARY

This thesis describes the design, development, fabrication, experimental and theoretical performance of a surface acoustic wave filter with particular reference to a TV IF filter to meet the specifications for Australian standards. Conventional means of generating and detecting surface acoustic waves on piezoelectric media is followed and the frequency response of the filter is determined from the frequency selectivity of the input and output transducer structures.

First of all a brief survey of literature on surface acoustic filters is traced and then a brief review of the admittance formulaism and a detailed discussion of its merits in the synthesis of surface acoustic wave filters is presented.

Starting with a simple surface acoustic wave delay line configuration with one uniform broadband transducer with only a small number of fingers as the transmitting transducer, the receiving transducer is synthesized using the transadmittance formula for a typical TV IF specification as indicated by a major electronics industry in Australia. The design gives rise to a finger length weighted (apodized) comb structure with nonuniform finger spacings and the initial synthesis procedure is concerned only with the search for an optimum transducer length. The filter has been fabricated on a YX Quartz crystal substrate with aluminium metal electrodes and the experimental results agree quite well with the predicted performance.

The synthesis procedure outlined above although capable of providing an approximate representation of the desired response, deviates considerably from that of the actual specification as a result of truncating the time domain response of the apodized transducer, and hence suitable optimization techniques have been developed to bridge the gap as closely as possible. In the quadratic cost-function, optimization which is a main concern of the research project, the response

in the frequency domain is made closer to the specified one, while maintaining the same finger locations, but varying the overlaps in the apodized transducer. The same objective may be achieved with a successive truncation and weighting technique, referred to in the text as zero order successive iteration optimization method, but with less computing effort, which seems to be a fortuitous method. TV IF filters have been constructed and tested with both the approaches and the experimental results agree quite well with the theoretical predictions. Thus the transmittance formula used in conjunction with a computer optimization procedure, constitutes a novel technique for the synthesis of surface acoustic wave filters.

Another novel technique of designing TV IF filters using chirped-apodized transducer configuration, once again based on transmittance formulation, is also presented. Two identical transducers can also be used for realizing the TV IF responses, but the enormous number of fingers required, restricts their uses in practical situations.

The last part of the study involves in the synthesis of TV IF filters using HF linear IC amplifiers. In such a situation the overall response of the amplifier-delay line-amplifier chain together with the matching circuits is to be taken into consideration for the synthesis purpose. A complete synthesis procedure is presented for this configuration.

In conclusion, possible improvements in the filter design and the choice of a more appropriate substrate material for production of TV IF filters on a large scale basis are discussed.

PREFACE

This thesis contains no material which has been accepted for the award of any other degree or diploma in any University. To the best of the author's knowledge and belief, this thesis contains no material previously published or written by another person, except where due reference is made in the text.

(N.C.V. Krishnamacharyulu)



ACKNOWLEDGEMENTS

The author wishes to express deep indebtedness to his supervisor Dr. P.H. Cole for suggesting the topic of this thesis, for his constant encouragement, and continued advice during the preparation of this work which would have been rather impossible to complete without his able guidance and keen interest. The author is also grateful to Dr. D.W. Griffin and to Prof. R.E. Bogner who are also his supervisors for a certain period. Their suggestions in the research project are found to be quite helpful. The author is also indebted to his colleagues Dr. P.H.V. Sabine, Dr. A.S. Burgess for helpful discussions on different aspects of the work. Special thanks to Dr. A.S. Burgess for lending some of his computer programmes and photographs of the equipment in the clean room. Thanks are also to Mr. N.H. Le of this Department for his initial help in the filter design.

A number of people made important contributions to the success of this experiment work. The vacuum coating unit used in the filter fabrication was kindly made available by Prof. D.R. Miller of the Material Science Department. Thanks are also due to the workshop staff of the Electrical Engineering Department who assisted in the preparation of the necessary experimental facilities and to Mr. G.W. Pook for his expert and generous assistance in the laboratory.

Most respectful regards and thanks are also due to Mr. D.C. Pawsey, a senior staff member in the Department, for his kind cooperation and help in various aspects and, finally the author is grateful to the University of Adelaide, Adelaide, for providing the financial assistance to carry out this research project.

Acknowledgements are also due to Miss Carol Hedges and to Mrs. Marlene Molnar for carefully typing the manuscript.

## CHAPTER 1

## INTRODUCTION

1.1 Surface Acoustic Waves - an Historical Background

Elastic surface waves were first postulated by Lord Rayleigh (1)<sup>1</sup> in 1885. Rayleigh waves, or surface acoustic waves, the terminology most commonly used in electrical engineering, propagate along the stress free boundary surface of a semi-infinite elastically isotropic half-space. In the absence of mechanical dissipation, Rayleigh waves are non-dispersive, i.e. the velocity does not vary with frequency. The displacements are confined to the plane containing the direction of propagation on the surface and the normal to the surface. The penetration of displacements decreases exponentially below the surface and extends a distance of approximately one wavelength. The velocity is typically in the range 1 to 6 km/sec. i.e. about five orders magnitude lower than the velocity of electromagnetic waves.

Other kinds of surface acoustic waves which exist are interfacial waves near the boundary of two solids (1)<sup>3</sup> or near the boundary of a liquid with a solid (1)<sup>4,32</sup>. All elastic solids in general, can support surface waves whether the solid is isotropic (1)<sup>11,32</sup> or anisotropic-nonpiezoelectric (1)<sup>17,22,26,32,102</sup>, anisotropic-piezoelectric (1)<sup>32,100,101</sup>. Initially, Rayleigh waves have been of great concern to seismologists as these are the principle type of waves observed in earth tremors. Investigations of the progress of these waves through the earth's mantle led to analyses of propagation on curved surfaces and in layered media (1)<sup>4,5,6</sup>.

During the mid-50's, surface acoustic waves have been found considerable application in the ultrasonic range in the field of non-destructive material testing (1)<sup>8,9</sup>. The early transducers for

ultrasonic surface wave excitation usually consisted of a wedge arrangement (1)<sup>10</sup> which converted an homogeneous plane wave supported by the wedge into a surface wave along the interface region under the wedge. The surface wave so generated then propagated out onto the free surface. Thus the experimental work carried out with wedge and comb type transducers for transduction of surface waves in metals (1)<sup>11</sup> stimulated an increasing interest in a wide variety of materials mainly in the anisotropic media (1)<sup>14-18</sup>. Several authors (1)<sup>19-21</sup> have reported that low propagation loss could be obtained on using single crystal materials at frequencies up to and above 100MHz range. However, as the desired frequency is increased to the UHF and microwave region, the propagation loss increases considerably, and the existing transduction schemes become inefficient for launching the surface acoustic waves.

This barrier has been removed by depositing interdigital comb structures photoetched onto piezoelectric substrates (1)<sup>12</sup> and the technique is found to be quite efficient in generating and propagating surface acoustic waves even in the gigahertz frequency range (1)<sup>39,40</sup>. However, if the propagating medium is anisotropic for low transmission loss and piezoelectric for direct excitation, the surface wave phenomena becomes much more complex and numerical approximations have to be sought for solving the problems. The practical success of these interdigital transducers ushered in sudden upsurge of interest in the high frequency applications of surface acoustic waves. In addition, it encouraged the theoreticians to broaden existing analyses of anisotropic surface wave propagation (1)<sup>18</sup> to include the effect of piezoelectricity (1)<sup>23-25</sup> thus facilitating the search for substrate materials and orientations of high acoustoelectric coupling. Extended discussion of the surface wave phenomena in solids may be found in the recent books by Viktorov (1)<sup>11</sup>, Tiersten (1)<sup>27</sup>, Brekhovskikh (1)<sup>28</sup>,

Ewing et. al. (1)<sup>7</sup>, White (1)<sup>29</sup>, Holland and Eernisse (1)<sup>30</sup>, Musgrave (1)<sup>31</sup>, Mason (1)<sup>32,33</sup>, Redwood (1)<sup>34</sup>, Cove (1)<sup>35,36</sup>, Lim and Musgrave (1)<sup>37</sup>, Auld (1)<sup>38</sup>.

## 1.2 Role of Surface Acoustic Waves in Communication Engineering

With the efficient methods of transduction there has been a great interest during the past few years in the surface acoustic waves because of their potential application in signal processing devices. The reason for this stimulus is that the acoustic energy which is confined to the surface of the solid is accessible at any point along the path of propagation and this makes it possible to guide the surface waves, to amplify them, to switch them, and to manipulate them in other ways; and in fact it is possible to manipulate them in as many ways as one can do with the electromagnetic waves. Another important aspect motivating use of these devices is that they are simple in structure, compatible with microelectronic circuitry, convenient to fabricate by standard planar technology, easy to reproduce, stable with temperature, small in size so as to encapsulate them in an integrated circuit package and potentially they are inexpensive.

As a result, the last half-decade has seen a rather remarkable growth of surface wave technology in various parts of the world, as it applies to communications engineering. Today, a basic range of surface wave devices is being manufactured on a commercial scale and this component range is being extended steadily. It is appropriate at this juncture, to outline some prominent applications and the achievements of surface acoustic waves in communication technology.

The most basic application to which surface acoustic waves may be put is the provision of fixed or tapped time delay. Simple delay line structures providing delay times of up to 150 $\mu$ sec. and with folded delay lines of up to 250 $\mu$ sec. and with the use of surface acoustic amplifiers of up to 20msec. have been reported (1)<sup>41-47</sup>.

Delay lines with large bandwidth in conjunction with coded transducers are of particular importance in recirculating memories (1)<sup>48</sup>. An outstanding virtue of surface acoustic wave devices, apart from time delay, is that signals can be sampled along the path of the acoustic beam. Each sample can be acoustically weighted by phase or amplitude prior to its combination with other samples, thus forming a tapped delay line. Tapped delay lines have been operated with 50 taps at 50MHz bit rate on Y-X quartz and 127 taps on YZ lithium niobate (1)<sup>49</sup>. Tapped delay lines can be considered as a direct realization of a transversal filter and hence possess an excellent frequency filtering characteristic. Development of matched filters is quite rapid and the detailed design required to produce devices for pulse compressors and expanders, and pulse sequency generators and decoders, is available (1)<sup>50,54,55,56,57</sup>.

Considerable amount of research effort has also been devoted to the design and testing of microsonic devices which are acoustic analogues of familiar electromagnetic microwave components. Included in this category are surface acoustic wave guides (1)<sup>92,93,98</sup>, directional couplers (1)<sup>96</sup>, resonators (1)<sup>99</sup>, phase shifters (1)<sup>97</sup> and amplifiers and oscillators (1)<sup>93,94</sup>.

Surface wave devices are beginning to have an impact in both radar and communication systems (1)<sup>80</sup>. Radar applications include code generation, matched filters for pulse compression, analog variable delay lines, compressive receivers, correlation and convolution systems and simpler i.f. filters (1)<sup>51-54, 58-62</sup>.

Thus there has been a tremendous amount of work done in the surface acoustic wave studies for the last five years or so and it is not possible to describe them in detail in this brief summary, however, some of the recent review articles (1)<sup>63-91</sup> indicate the developments of SAW devices as applied to the communication engineering

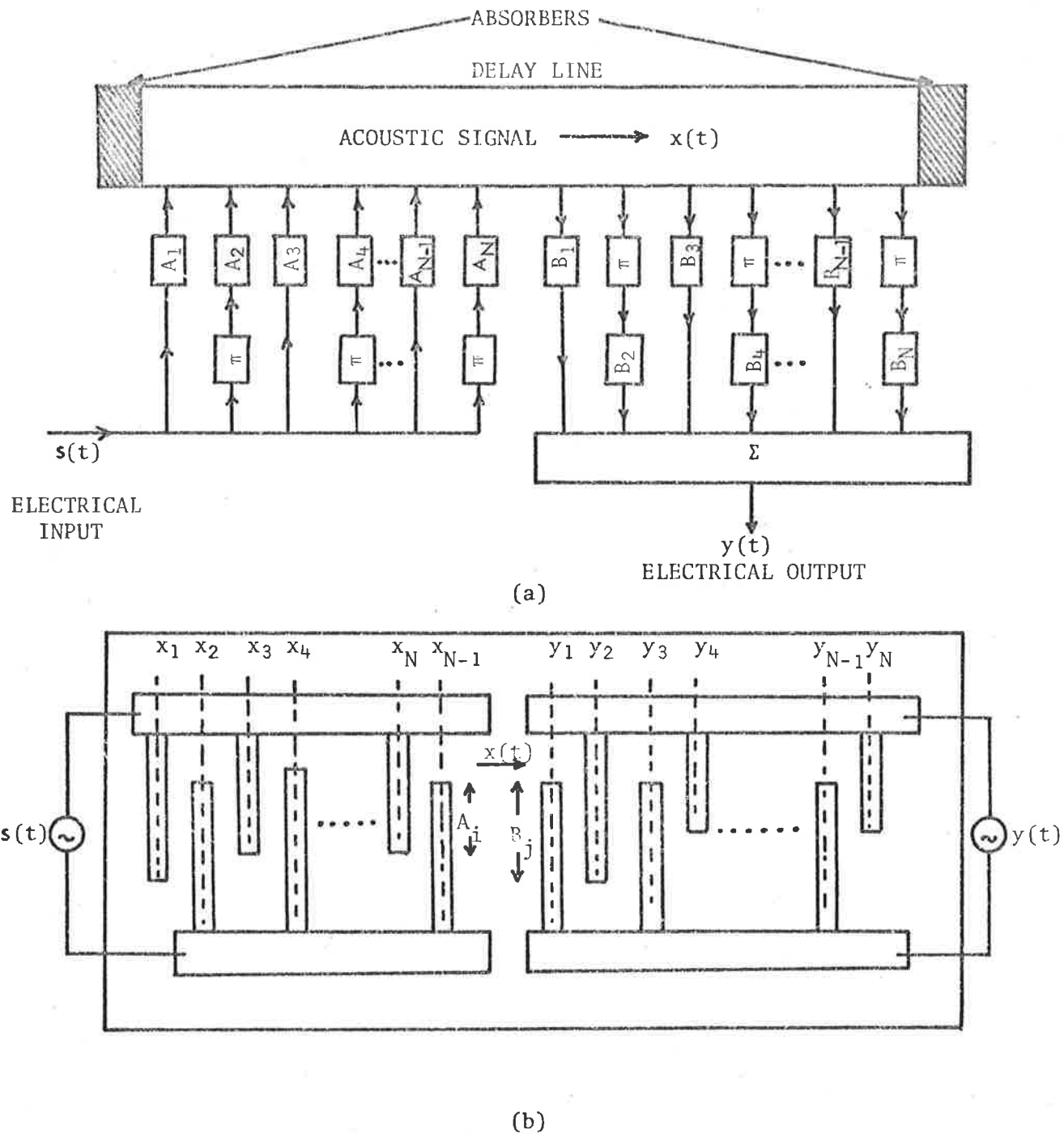


Figure 1.1 (a) Cascaded transversal filter equivalent with a launching transducer array and a receiving transducer array on a common acoustic path.

(b) SAW analogue with weightings  $A_i$  and  $B_j$ .

technology.

### 1.3 Concept of Surface Acoustic Wave Filter

Conceptually, acoustic surface wave filters are transversal filters (1)<sup>103</sup>, a generalised version of which is shown in Figure 1.1a. The signal propagating along the delay line is transversely tapped at appropriate places, suitably weighted and the weighted taps are summed up to form the output of the filter. The transfer function of the transversal filter has been derived under the conditions that the delay line is lossless and nondispersive with non-reflecting lightly coupled weighting taps (i.e. the taps do not perturb the propagating wave). A surface wave analogue with interdigital transducers on a piezoelectric substrate is shown in Figure 1.1b.

When the input array is excited by an electric field, periodic stresses are generated at the surface by the interaction of the resulting electric field with the piezoelectric medium, and a surface wave is launched. On the receiving side, the acoustic wave travelling under the transducer, by reciprocity, sets up periodic stresses which in turn induces an electric field in each electrode. The output voltage is obtained by adding together all voltages on the summing bus bars. The contribution from each electrode is proportional to the electrode overlap or in other words, the weighting is accomplished by the variation of the aperture of the electrodes in the array. If  $A_i$  is the weighting function for the input array and  $B_j$  is the weighting function for the output transducer, then the impulse response of the array pair is  $A_i^- * B_j$  which is the cross correlation of the input and output weighting functions, where  $A_i^-$  is the time reversed version of  $A_i$  and  $*$  denotes convolution. For matched filter applications, there is a specific relationship between the input signal and the impulse response of the filter. They are said to be matched if the impulse response is the delayed, time reversed, replica of the input

signal. The output of the matched filter  $y(t)$  is then given by the time shifted replica of the autocorrelation function of the input signal  $s(t)$ .

With accessibility of various weighting techniques and summing networks together with the simplicity of tap design, the matched filters have become more attractive in the surface acoustic wave devices. Other authors (1)<sup>50,103-110</sup> have described the transversal filter analogy in more detail.

#### 1.4 A Brief Review of Literature on Surface Acoustic Wave Filters

In this section a brief review of literature on surface acoustic wave filters with interdigital transducers is presented. SAW filters have become a prominent role in the surface wave device technology because of a variety of applications right from a few MHz to VHF, UHF and even microwave frequency range. SAW filters offer the same advantages as other surface acoustic wave devices, i.e. they are produced by planar technology, highly reproducible, reliable and inexpensive in large quantities etc. Typical applications include frequency (bandpass) filters, dispersive filters for generation and correlation of radar pulse compression waveforms, fixed and programmable analogue matched filters for phase-shifted-keyed waveforms and so on, but emphasis is given in this survey only to bandpass filters.

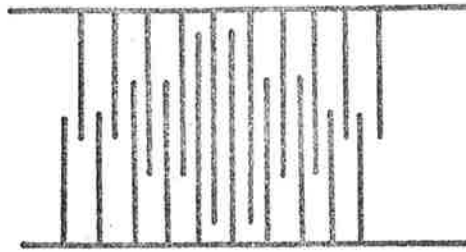
Fundamentally, frequency filtering can be obtained by constructive and destructive interference of the signal with itself. In a surface acoustic wave device the relative amplitudes of the signals at the taps (the weighting) are chosen so that the interference is constructive over the required passband and destructive elsewhere. Hence the frequency response is strongly dependent on the structure (weighting) of the input and output interdigital transducers. To date, several weighting schemes have been devised, including finger-length weighting, finger-period variation weighting, finger-orientation weighting



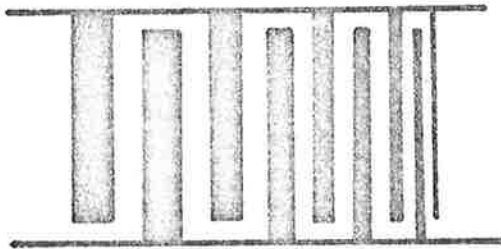
and finger-phase modulation weighting (Figure 1.2) or a combination of any of the above weightings. Each technique has its own advantages and disadvantages over the others and will be discussed at the appropriate sections (Chapter 3).

Before attempting to review the synthesis procedure it is appropriate to start with the analysis or the behaviour of the interdigital transducers. The substrate used being piezoelectric and anisotropic the analysis becomes very complex and laborious, and from an engineering point of view, it is unrewarding. It is more profitable to consider an approximate simplified theory and add sophistications when the occasion demands. R.M. White (1967) (1)<sup>74</sup> made use of the obvious analogy between the interdigital grid electrodes and an end fire antenna, and obtained reasonable agreement with the experimental findings. Probably the biggest single advance in this direction came with the publication by Smith et. al. (1969) (1)<sup>120,121</sup> who considered the transducer as an array of sources, each analogous to a piezoelectric plate transducer for launching bulk waves (Mason's equivalent circuit). Significant properties of the transducer can then be obtained by this simple model and the experimental results revealed good agreement with theoretical predictions even on strong coupling materials like lithium niobate. However, this model does not incorporate multiple reflections from the interdigital fingers and the theory becomes quite complex for multi-transducer structures. Later on this simple equivalent circuit model has been elaborated by several authors (1)<sup>111-116</sup> to include these factors as well.

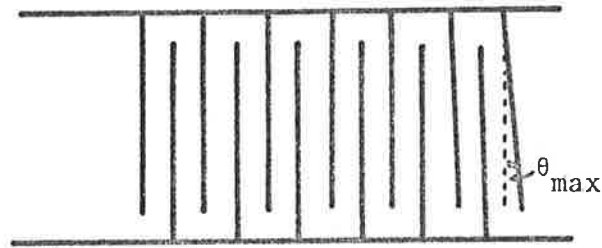
B.A. Auld (1969,1970) (1)<sup>117,118</sup> has successfully applied the microwave electromagnetic concepts to solve the electroacoustic field problems using two powerful approximation procedures viz., perturbation theory and variational techniques. Auld and Kino (1)<sup>119</sup> have used the so called normal mode theory for evaluating the interdigital



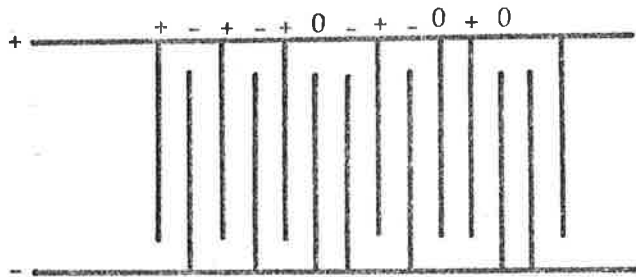
(a)



(b)



(c)



(d)

Figure 1.2 Different Weighting Configurations.

- (a) Finger length weighting configuration.
- (b) Finger period weighting configuration.
- (c) Finger orientation weighting configuration.
- (d) Finger phase weighting configuration  
(7-bit Barkercode, 1110010).

transducer input impedance and the expressions obtained are very much similar under certain conditions to those obtained by Smith et. al.

(1)<sup>120,121</sup>. A detailed analysis of the techniques used may be found in a recent book by Auld (1973) (1)<sup>38</sup>.

Another significant contribution, especially in the analysis and synthesis of SAW filters, has been published by Tancrell and Holland (1970 or 1971) (1)<sup>108</sup> who adopted a delta function model approach to describe the transfer function of the input and output transducer structures. In this approach each finger or finger edge is considered as a  $\delta$  function source of acoustic energy, which in a weak piezoelectric medium will become the driving source for the acoustic displacement. When the transmitter comb is excited by an external AC voltage, the analysis for the transmitter comb reduces to a summation of plane waves from the  $\delta$  function sources. For the receiver comb, the output is the sum of all these transmitted waves as they travel under each finger. No inter-electrode interactions (regeneration or reflections) are included, so this model is of particular importance to the low coupling materials only. Next, they extended the study to include interaction between the electric and acoustic portions of the piezoelectric medium through the Mason's equivalent circuit model and demonstrated both the approaches by considering a variety of structures, apodized (i.e. length weighted) as well as non-apodized and reported good agreement with the experimental results.

The main drawback in the above two approaches is that analysis becomes extremely time consuming even with the advent of large computers when considering dispersive transducers with large number of fingers, particularly if they are apodized. Another limitation of apodized comb structures is that diffraction due to short fingers becomes prominent particularly when strong coupling materials are used. Also the description assumes loss free propagation and negligible mass

loading of the metallic fingers, which can be significant at high frequencies otherwise, the theory is simple and straightforward if one transducer is unweighted and the other is weighted, in such a situation a direct Fourier transform relationship exists between the input and output transducers.

Hartman et. al. (1973) (1)<sup>122</sup> have developed an impulse model approach for the analysis and synthesis of SAW bandpass filters. They derived an expression for the impulse response of an array of interdigital transducers and deduced the frequency response and input admittance with much less effort than has been obtained by the simple equivalent circuit model approach. The design procedure consists of obtaining impulse responses of input and output transducers separately and once again the method becomes troublesome if both transducers require apodization. They also considered some of the secondary effects like electrical loading on the input and out terminals of the filter and the methods to reduce the loadings effect. They illustrated a few examples with this technique and seem to have obtained reasonable agreement with the experimental results.

Carlo Atzeni along with his colleagues (1971,72,73) (1)<sup>105,123,124</sup> derived the transducer configuration by sampling theory. This method is particularly useful for designing dispersive filters of linear FM (chirped) wave forms with constant amplitude impulse responses. The analysis can also be extended to realize nonlinear dispersive characteristics or to bandpass filters with an arbitrary frequency characteristic, provided that the time-bandwidth product is large. However, when the time-bandwidth product is large the design yields a large number of nonuniform samples and hence a large number of fingers in the transducer. To overcome this difficulty, Atzeni (1)<sup>125</sup> indicated that the samples may be taken at the intervals of  $K\pi$  ( $K$  is an odd integer) instead of  $\pi$  under certain conditions, thereby operating the

transducer at  $K$ th harmonic frequency instead of the fundamental; but the essential difficulty in this approach is that the output is also reduced by  $K$  times, a significant deficiency, especially on low coupling materials. A few examples have been given to illustrate this phase sampled impulse response method some with amplitude weighting also.

R.F. Mitchell and his associates at MRL, England (1970) (1)<sup>126</sup> have reported some experimental results of a SAW TV IF filter using length weighted transducers, but it seems that an explicit mathematical analysis or synthesis technique for the unsymmetrical input and output apodized transducer structure does not appear in this article or in the later publications by R.F. Mitchell (1)<sup>127,128,84</sup>.

The various methods described so far for filter analysis or synthesis are derived by considering individual transducer structures, whose immittance parameters are known (three-part model by Smith et. al. (1)<sup>120</sup>, normal mode theory by Auld and Kino (1)<sup>119</sup>, impulse model by Hartman et. al. (1)<sup>122</sup>, and so on). Normally, the input admittance which represents the effective power conversion from electric to acoustic or vice versa is different for an individual transducer and to that of a transducer pair in which the output transducer is shorted. Therefore, a practical performance of the filter can only be precisely predicted by considering the two transducers in tandem as a four terminal network, characterized by an admittance matrix. Gangully and Vassel (1)<sup>129</sup> derived expressions for the frequency response of a filter taking into consideration the effect of piezoelectric interactions and some of the secondary effects like multiple reflections, diffraction due to short fingers and illustrated the theory with some examples (1)<sup>130</sup>. Similar but much simpler expressions for the admittance model have been reported by Burgess and Cole (1)<sup>131</sup> on weak coupling materials. The derivation based on normal mode theory yields expressions for

transadmittance between a pair of transducers and the input admittance for a single transducer. The advantage of transadmittance parameter  $y_{21}(\omega)$  is that it is the most accurately measurable quantity in a SAW delay line and thus provides all the useful information for comparing theoretical and experimental performance of the device. Filter synthesis based on transadmittance formulation has been considered by the author and some of the results have been reported elsewhere (1)<sup>132</sup>.

The main features of the analysis and synthesis of SAW filters has been briefly reviewed so far, but various improvements with different weighting configurations depending on the specific requirements have been available in the literature but will be briefly scanned through, once again emphasizing only on those aspects which are of concern in the synthesis of bandpass filters. Tancrell and Engan (1973) (1)<sup>133</sup> reported the design and measurement of a bandpass filter consisting of two apodized transducers with a multistrip coupler (1)<sup>134,135</sup> which perform as the necessary integration across the beamwidth such that a unique impulse response can be assigned to each transducer. But the main disadvantage of a multistrip coupler is that it is practicable only on high  $K^2$  materials because the width of the coupler is inversely proportional to the couplings constant of the material. Later on Tancrell (1974) (1)<sup>109</sup> indicated an optimization technique to realize a bandpass filter with prescribed ripples in the passband as well as in the stopband and indicated their validity in practical situations. Vasile (1974) (1)<sup>136</sup> published a numerical Fourier transform technique for realizing bandpass filters, which does not require any iteration process and giving rise to an apodization function of finite length, thereby eliminating the truncation errors. He illustrated the method by considering a similar example used by Tancrell (1)<sup>109</sup> and reported good sidelobe rejection in the stopband and  $\pm 0.5$ dB ripple in the passband. The method seems to have no added advantage over window

function technique; further on observing the apodizing function in the finite duration the ratio of extreme sidelobes to the mainlobe is very small thereby diffraction losses become significant in the transducer. Very broad band filters (over 30 percent bandwidth) can be built with two dispersive transducers with finger width weighting and placing them in a nondispersive configuration. Swith et. al. (1972) (1)<sup>137</sup> have extended the circuit model theory to include the apodization and acoustic impedance discontinuity effects and reported results for a linear FM filter with two apodized identical transducers arranged in the above configuration. Dispersion can be introduced by arranging one transducer as the mirror image of the other. Gerard et. al. (1972) (1)<sup>138</sup> have developed a very broad band, low loss dispersive filter with a time-bandwidth product of 1000 using chirped transducers. In both articles it was pointed out that the Fresnel ripple, inherent with the unweighted nondispersive transducers, can be minimized or eliminated by weighting the transducers ; amplitude weighting in the case of the finger space-width (chirped) weighting and a window function weighting in the case of an amplitude weighting. Worely (1972) (1)<sup>139</sup> also discussed the realization of bandpass filters using the linear and nonlinear FM techniques but by a different approach, the so called stationary phase approximation method. Morgan (1972) (1)<sup>140</sup> introduced log-periodic transducers - analogous to log-periodic antennas in e. m theory to obtain wide bandwidths for SAW filters. Hartman (1971) (1)<sup>142</sup> , Budreau and Carr (1972) (1)<sup>141</sup> have considered narrow bandwidth SAW filters. When considering extremely narrow bandwidths problems arise because of a large number of fingers required to realize the responses and they have indicated two methods to reduce the number of fingers. Atzeni (1971) (1)<sup>125</sup> also indicated a reduced sampling procedure and demonstrated for the case of a linear FM signal: SAW filter responses can also be realized by phase weighting (1)<sup>143</sup> and explicit

mathematical derivations for coded delay line have been given by Speiser and Whitehouse (1971) (1)<sup>144</sup>, (which is out of the scope of the present work and will not be discussed further).

The methods described so far have been shown empirically to be capable of designing bandpass filters with smooth bandpass characteristics with no abrupt changes and further complications arise when designing SAW filters with such bandpass responses. Typical example is a TV IF response with complicated specifications. However, some authors have achieved the designing of TV IF filters with some success. R.F. Mitchell et. al. (1970) (1)<sup>126</sup> have produced some prototype filters to meet the U.K. colour TV IF specifications. A.J. de Vries et. al. (1971) (1)<sup>145,146</sup> at Zenith Radio Corporation (U.S.A.) have reported a measured colour TV IF response using three different surface wave integrable filters connected in series with discrete transistor amplifiers and tuning elements even then the required traps are not as deep as the desired ones. Chauvin et. al. (1971) (1)<sup>147</sup> have used an optimization procedure to obtain the finger locations and amplitudes of the apodized comb that will produce the required TV IF specification. The measured response seems to agree quite well with the theoretical one, but the original specification limits seem to be not quite rigid. Moreover, it would be more convenient to visualize trap levels, viz., the adjacent channel levels and the level at the sound carrier frequency had the graphs been plotted in dB scale. Lewis (1972) (1)<sup>148</sup> at the Hirst Research Centre has also reported the design and development of a prototype SAW TV IF filter. The results appear to be promising especially with deep traps less than 40dB down, but there is an ambiguity as to how the amplitude weightings  $A(x_1)$  were calculated. Highway and Deacon (1972) (1)<sup>149</sup> at Plessey Co. Ltd., England, have developed a design technique using linear dispersive transducers and demonstrated the technique for realizing a TV IF filter,



but the method seems to have failed to describe the behaviour of the filter at the band edges. Raalte Van (1974) (1)<sup>150</sup> also discussed the design of SAW TV IF filters. However, in the example considered, the desired response resembles like that of an ordinary bandpass response except with deep traps at the adjacent channel frequencies. Moreover, the experimental results of the designed filter are not available.

This brief survey of the literature is necessary to point out the potential applications of the surface wave devices in various fields and it is to be noted that still a great amount of work is to be done to assess the theoretical and experimental performance of the device, particularly to TV IF filters. The greatest of these is the choice of a suitable material with low insertion loss, easy to produce, stable with temperatures and above all inexpensive to implement in the industry. All the quantities cannot be met simultaneously and some trade-offs have to be made in practical situations. Even though SAW TV IF filters have been considered by some other research workers as pointed out before, production of the device on a commercial basis is still a real challenge.

The field of surface acoustic wave technology as a whole is growing rapidly, reflecting the high degree of research investment taking place. The theoretical and experimental techniques now available permit the design and manufacture of surface wave devices with considerable precision. Much of this knowledge has become available during the course of the present investigation and has made a significant contribution to the results achieved.

### 1.5 An Outline of the Thesis

The principle aim of the thesis is to synthesize surface acoustic wave filters with a given arbitrary frequency response (amplitude as well as phase). Several techniques are available in the literature for realizing regular (rectangular) bandpass filters, some utilizing optimization techniques, analogous to those used in designing nonrecursive digital filters. In these techniques the objective is to reduce the sidelobe level in the stopband and minimize the ripples in the passband. However, these techniques become more complex, highly nonlinear and time consuming in situations where the specified response is more complicated (like that of a TV IF filter) than the simple rectangular bandpass filters. In this thesis several synthesis techniques have been developed to meet such specific demands using an admittance model. Experimental verification has confirmed the validity of these techniques.

The preceding sections of the present chapter are concerned with a brief review of literature on SAW devices and their applications to communications engineering, in particular, emphasizing on those aspects which are of concern to bandpass filters.

Chapter 2 contains a brief review of the admittance formalism for a pair of interdigital transducer structures on a piezoelectric substrate and describes the advantages and limitations in using the formulae for filter synthesis.

In Chapter 3 the admittance formalism is illustrated for the synthesis of a TV IF filter. Initially a simple weighting configuration is considered. In this approach the transmitting transducer is assumed to have a small number of uniform fingers, which means a constant source function with  $\sin x/x$  frequency response and the source function of the receiving transducer is designed according to the above formalism. An approximate representation of the transducer geometry is then

developed which resulted in variable finger overlaps as well as in variable finger spacings. The frequency response of the filter with this transducer geometry is predicted once again using the admittance formula and good agreement was obtained between the two indicating that the approximate representation of the transducer geometry is a close representation of the designed source function.

In Chapter 4 the fabrication technique, the measurement procedure and the experimental results of the filter designed in Chapter 3 (referred as Filter 1) are presented. The slight discrepancy between the measured response and the theoretically predicted response is accounted mainly due to inaccuracy in photofabrication.

In Chapter 5 attention is focused on developing optimization techniques to improve the response of the filter with the same finite duration but by altering the finger overlaps. The quadratic cost function optimization which is a main concern of this investigation is a very simple technique, does not require any computer iteration and produces a closed form of synthesis procedure. Several schemes have been devised to simplify the numerical calculations involved with this technique and a simplified version referred as OPTIM METHOD in the text is presented for subsequent illustrations.

In Chapter 6 different filter responses with more tight specification limits are treated to illustrate the effectiveness of the various optimization techniques developed in Chapter 5 and the experimental performance of these various filters is investigated in Chapter 7. Apart from considering the frequency responses alone, attention is also given to calculate the insertion loss, input-output admittance of these various filters. Because of the high insertion loss obtained with the quartz substrate, some suitable techniques to improve the insertion loss are also discussed towards the end of this Chapter.

In Chapter 8 possibilities of using chirped transducers for TV IF filter design have been explored. Because of the complicated nature of the filter specification, a large number of fingers are needed if two identical chirped transducers have to be used and therefore, a novel technique in which only one transducer is chirped and the other is apodized, is presented. The advantages of this weighting configuration are clearly indicated, especially in the improvement of admittance parameters which in turn improves the insertion loss of the filter.

Although the TV IF filters have been synthesized reasonably well with interdigital transducers several basic problems still remained with these devices; one is, high insertion loss with low coupling materials and the other is high input-output impedances of the transducer which cause electrical mismatch at the input-output side of the transducer with the source and load impedances. To overcome these difficulties, a complete synthesis procedure using HF linear IC amplifiers is presented in Chapter 9. The advantage is clearly demonstrated through an example using FET transistors.

Finally, Chapter 10 contains the summary and conclusions of the results, suggested improvements in the admittance formulation and hence the suggested improvements in the filter design. An alternative substrate material for TV IF applications is also discussed.

Some of the computer programs developed to analyze, to synthesize and to plot the patterns for the surface acoustic wave filters are given in Appendix A and the photofabrication techniques followed to manufacture these devices are given in Appendix B.

## CHAPTER 2

ADMITTANCE MODEL FOR A PAIR OF INTERDIGITAL  
TRANSDUCERS2.0 Introduction

In this chapter basic information on the admittance formalism [2]<sup>1</sup> is presented to provide a background for the SAW filter analysis and synthesis. In filter applications, the transfer function of the device is of most concern and the admittance model expresses the transfer function in terms of admittance matrix elements, which are calculable from the material constants and the individual transducer geometrics. The diagonal elements of the admittance matrix represent the input admittances of the individual transducers, while the off-diagonal elements represent the acoustic coupling between a pair of transducers, all elements of the matrix being defined under short-circuited conditions. The transfer function in general depends on diagonal elements as well as off-diagonal elements, but under weak coupling approximation or to a first order approximation on moderate to strong coupling materials subject to certain conditions, it depends only on the off-diagonal element  $y_{21}(\omega)$ .

In the remainder of the chapter implicit expressions for the admittance coefficients and the basic assumptions under which they have been derived are presented. Finally, analytic formula for  $y_{21}(\omega)$  and  $y_{11}(\omega)$  for uniform transducers with equal mark-space ratio are derived with a suitable system of coordinates so as to visualize the group delay characteristic between the transducers more clearly and to facilitate the calculation of minimal Fourier transforms in the subsequent analysis and synthesis of SAW filters.

## 2.1 Basic Approach

The delay line having one input and one output transducers is considered as a general two-part structure as shown in Fig. 2.1a. The admittance matrix of the structure is defined by the equation

$$\begin{bmatrix} \dot{I}_1 \\ \dot{I}_2 \end{bmatrix} = \begin{bmatrix} y_{11}(\omega) & y_{12}(\omega) \\ y_{21}(\omega) & y_{22}(\omega) \end{bmatrix} \begin{bmatrix} \dot{V}_1 \\ \dot{V}_2 \end{bmatrix} \quad \dots (2.1)$$

where  $\dot{V}_1$  and  $\dot{I}_1$  are the complex phasors representing peak terminal voltages and currents at any instant, and  $y_{ij}(\omega)$  are the complex frequency functions. A knowledge of the admittance matrix at all frequencies provides a complete characterization of the delay line, a two-generator equivalent circuit of which is shown in Figure 2.1b. The voltage ratio transfer function terminated at both the ends is then given by,

$$\frac{\dot{V}_L(\omega)}{\dot{V}_S(\omega)} = \frac{-y_{21}(\omega)Z_L}{1 + y_{11}(\omega)Z_S + y_{22}(\omega)Z_L + \{y_{11}(\omega)y_{22}(\omega) - y_{12}(\omega)y_{21}(\omega)\}Z_L Z_S} \quad \dots (2.2)$$

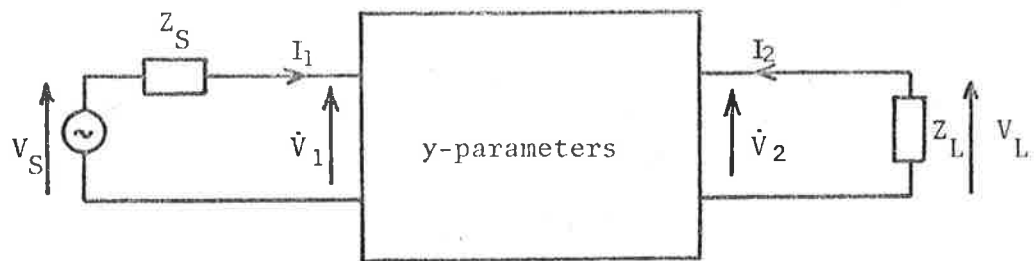
or the transfer function of the delay line alone is given by,

$$\frac{\dot{V}_L(\omega)}{\dot{V}_1(\omega)} = \frac{-y_{21}(\omega)Z_L}{1 + y_{22}(\omega)Z_L} \quad \dots (2.3)$$

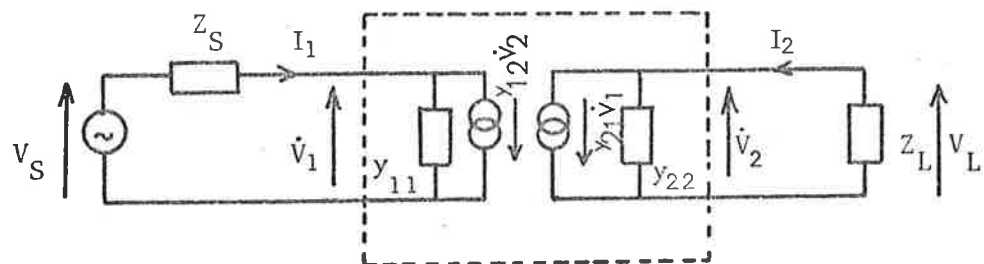
These expressions give the complete response of the two-part delay line, but in many situations these equations can be simplified by appropriate approximations. The admittance of a transducer at the synchronous frequency  $\omega_0$  in the simplest form is given by [2]<sup>2</sup>

$$Y(\omega_0) = \hat{G}_a(\omega_0) + j\omega_0 C_T$$

where  $\hat{G}_a(\omega_0)$  is the synchronism conductance given by  $\frac{4}{\pi} \omega_0 C_T K^2 N$  in which  $K^2$  is the familiar electromechanical coupling coefficient [2]<sup>3</sup> and  $N$  is the total number of fingers in the transducers and  $C_T$  is the total



(a)

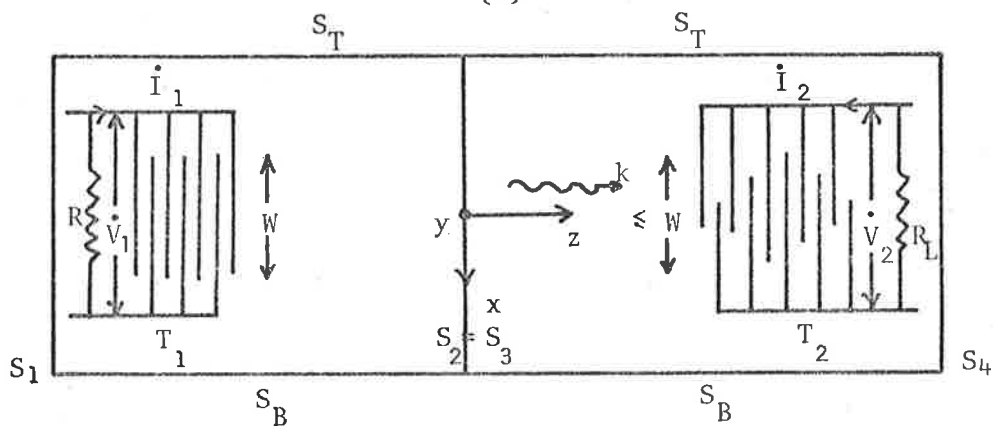


SOURCE

DELAY LINE

LOAD

(b)



(c)

Figure 2.1 Two-transducer structure configuration.

- (a) Representation of a general two-part structure.
- (b) Equivalent circuit of a two-part delay line in terms of  $y$ -parameters.
- (c) Transducer geometry and coordinate system used in the derivation of admittance parameters.

capacitance. When  $K^2N \ll 1$  the admittance is essentially given by the transducer capacitance alone and with the low impedance measurement system the quantities in equation (2.2) can be approximated to

$$\begin{aligned} |y_{11}(\omega)Z_S| &\ll 1 \\ |y_{22}(\omega)Z_L| &\ll 1 \\ |\{y_{11}(\omega)y_{22}(\omega) - y_{12}(\omega)y_{21}(\omega)\}Z_LZ_S| &\ll 1 \end{aligned} \quad \dots(2.4)$$

and hence the transfer functions become,

$$\frac{\dot{V}_L(\omega)}{\dot{V}_S(\omega)} \approx \frac{\dot{V}_L(\omega)}{\dot{V}_1(\omega)} \approx -y_{21}(\omega)Z_L \quad \dots(2.5)$$

This relation in fact shows that with high impedance transducers in a low impedance measurement system, the delay line frequency response is essentially given by the transadmittance between the transducers. This is the basic relationship used in the experimental measurements of the SAW filters. If the transducer static capacitances are tuned out with external tuning circuits, then the admittance at synchronous frequency is essentially given by the radiation conductance only and once again under weak-coupling approximation this term is fairly small and the tuning circuits may be included in the source and load impedances and, further, if the frequencies under consideration are not far from synchronous frequency the inequalities in equation (2.4) still hold good and the transfer function is again given by equation (2.4). Thus we assume that the static capacitances are always present in the admittance coefficients whether the tuning circuits are included or not. No attempt has been made with this approach to include second or higher order responses, even though they could be included in the analysis by manipulating the equation (2.2).



## 2.2 Frequency Domain Transadmittance $y_{21}(\omega)$

The system for which the transadmittance between a pair of transducers considered is shown in Figure 2.1c. First of all some of the basic assumptions under which it was derived will be briefly reviewed [2]<sup>1</sup>

For any surface acoustic wave device it is necessary to know how well the surface waves can be launched by applying a known electric potential to the electrode array. This information can be obtained by knowing the familiar piezoelectric coupling coefficient [2]<sup>3</sup> given by

$$K^2 \approx 2(v_f - v_M)/v_M = 2|\Delta v/v_M| \quad \dots(2.6)$$

where  $v_M$  is the surface wave velocity when a perfectly conducting massless metallic film is placed over the free surface of the solid and  $v_f$  is the velocity when this film is removed. Analysis of finding  $K^2$  for different materials and for different orientations have been carried out by several authors [2]<sup>4-10</sup> and the results for most commonly used materials can be found in the articles [2]<sup>11-18</sup>. When  $K^2$  is much smaller than unity then it is termed as weak-coupling approximation and under this situation the surface wave amplitudes (normal mode amplitudes) are obtained by neglecting the acoustic response of the substrate while calculating the relationship between the electrical potential on the surface and the applied voltage between the fingers of the interdigital transducer [2]<sup>19</sup>. It was further stated that the electromechanical-coupling constant calculated with the assumption of zero-stress permittivity  $\epsilon^T$  for this electrostatic problem agrees well with the experimentally observed values. The assumption of zero-stress permittivity permits the independent solution of the electric source field and the acoustic surface wave field, because the electric field of the surface wave can be neglected in the determination of the electric field of the electrodes. The weak-coupling approximation mentioned, thus, is the fundamental

assumption in the derivation of the admittance formalism.

The second important assumption in the derivation is that the acoustic scattering is zero while calculating the current in a short-circuited transducer; or in other words the reflections from a shorted transducer are zero. This is not a valid approximation on strong coupling materials or if the number of fingers is large even on weak-coupling materials.

Another significant factor is that the assumption of uniform plane waves for launching and detecting transducers; that means the effect of diffraction due to short fingers is neglected. The detecting transducer is assumed to be in the far-field region of the transmitting transducer (in an analogous way as in the antenna theory) so that the radiated field in the vicinity of the receiving transducer is essentially uniform plane wave.

With these assumptions the forward-transadmittance was derived to be equal to [2]<sup>1</sup>

$$y_{21}(\omega) = \frac{-|\omega| \Delta \epsilon_0^2}{W(\epsilon_0 + \epsilon_p)} \int_{S'} f'(x, z) e^{j\beta z} ds \int_{S''} f''(x, z) e^{-j\beta z} ds \quad \dots (2.7)$$

where  $\beta$  = the propagation vector at frequency  $\omega$  in the +z direction  
on the free surface of the substrate

$W$  = finger overlap width of the transducer  $T_1$

$\Delta = -\frac{K^2}{2}$ , normally specified as a negative number.

$\epsilon_0$  = electric permittivity of the free space.

$\epsilon_p$  = relative permittivity of the substrate

$T_1$  = Launching transducer on the x,z-plane occupying a  
surface  $S'$

$T_2$  = receiving transducer, uniform or apodized with maximum  
apodization  $\leq W$  on x,z-plane occupying a surface  $S''$

$f'(x,z)$  = source function of  $T_1$ , obtained from the potential distribution  $\phi_S$  and charge density  $\sigma_S$  on the underside of the finger

$f''(x,z)$  = source function of  $T_2$ , obtained in a similar way as that of  $T_1$ .

Further, the source function for either transducer  $T_1$  or  $T_2$  was shown to be equal to

$$f(x,z) = \frac{\pi}{1.854(z_{k+1}-z_k)} \sum_{n=0}^{\infty} (-1)^n \left( \frac{\epsilon_p}{\epsilon_0} + \frac{\beta}{\beta_n} \right) P_n(0) \cos \beta_n z'$$

for  $z_k \leq z \leq z_{k+1}$  ... (2.8)

where

$z_{k+1}-z_k$  = Distance between the electrical centres of the adjacent fingers (called the gapwidth)

$$\beta_n = \frac{(2n+1)\pi}{z_{k+1}-z_k}$$

$$z' = z - z_k$$

$P_n(0)$  = Legendre function of first kind of zero agreement.

In the numerical calculation of the behaviour of the transducers, only the first term, ( $n = 0$ ) is retained and also  $\beta/\beta_n$  is taken as unity. Hence equation (2.8) becomes,

$$f(x,z) = \frac{\pi}{1.854(z_{k+1}-z_k)} \left( \frac{\epsilon_p + \epsilon_0}{\epsilon_0} \right) \cos \pi \frac{z-z_k}{(z_{k+1}-z_k)} \quad \dots (2.9)$$

$$\text{for } z_k \leq z \leq z_{k+1}$$

As  $f(x,z)$  is independent of the variable  $x$ , we can write  $f(x,z) = f(z)$

and, therefore, (2.9) becomes

$$f(z) = \frac{\pi}{1.854(z_{k+1} - z_k)} \left( \frac{\epsilon_p + \epsilon_0}{\epsilon_0} \right) \cos \left\{ \pi \left( \frac{z - z_k}{z_{k+1} - z_k} \right) \right\} \quad \dots (2.10)$$

$$\text{for } z_k \leq z \leq z_{k+1}$$

Hence the transadmittance  $y_{21}(\omega)$  eqn (2.7) becomes

$$y_{21}(\omega) = \frac{-|\omega| \Delta \epsilon_0^2}{W(\epsilon_0 + \epsilon_p)} \int_{S'} f'(z) e^{j\beta z} ds \int_{S''} f''(z) e^{-j\beta z} ds \quad \dots (2.11)$$

It is to be noted that the surface integrals over  $S'$  and  $S''$  can be reduced to one dimensional integrals from the fact that  $f(x,z)$  is independent of  $x$ . Before attempting this step it is necessary to choose a more convenient coordinate system than has been defined in Figure 2.1(c) in order to evaluate these integrals more efficiently with numerical methods. One obvious choice is to select the origin to the far-left of transducer  $T_1$  and defining source functions only for positive values of  $z$ . i.e.

$$y_{21}(\omega) = \frac{-|\omega| \Delta \epsilon_0^2}{W(\epsilon_0 + \epsilon_p)} \int_{S'} f'(z) e^{j\beta z} ds \int_{S''} f''(z) e^{-j\beta z} ds \quad \dots (2.12)$$

where  $f'(z)$  and  $f''(z) \neq 0$  for  $z \geq 0$

and  $f'(z)$  and  $f''(z) = 0$  for  $z \leq 0$ .

This is the expression used in deriving the analytical expression for transadmittance between a pair of uniform transducers in the following section and numerical methods are presented in Chapter 3 for apodized transducers.

### 2.2.1 $y_{21}(\omega)$ for a Pair of Uniform Transducers

Recalling equation (2.12) and since the integrals are bounded we can write,

$$y_{21}(\omega) = \frac{-|\omega| \Delta \epsilon_0^2}{W(\epsilon_0 + \epsilon_p)} \int_{-\frac{W}{2}}^{\frac{W}{2}} \int_0^{\ell_1} f'(z) e^{j\beta z} dz dx \int_{-\frac{W}{2}}^{\frac{W}{2}} \int_0^{\ell_2} f''(z) e^{-j\beta z} dz dx \quad \dots(2.13)$$

where  $\ell_1$  and  $\ell_2$  are the lengths of the transducers  $T_1$  and  $T_2$  respectively and  $W$  is the width of each transducer as shown in the Figure 2.2. Further if we choose  $\ell_1 = \frac{N_1 \lambda_0}{2}$  and  $\ell_2 = \frac{N_2 \lambda_0}{2}$  and  $f'(z)$  starts at a distance  $L_1$  from the origin and  $f''(z)$  a distance  $L_2$  from the origin ( $L_2 > \ell_1 + L_1$ ), then equation (2.13) can be written as

$$y_{21}(\omega) = \frac{-|\omega| \Delta \epsilon_0^2 W}{(\epsilon_0 + \epsilon_p)} \int_{L_1}^{L_1 + \frac{N_1 \lambda_0}{2}} f'(z) e^{j\beta z} dz \int_{L_2}^{L_2 + \frac{N_2 \lambda_0}{2}} f''(z) e^{-j\beta z} dz \quad \dots(2.14)$$

Let

$$y_0 = \frac{-|\omega| \Delta \epsilon_0^2 W}{(\epsilon_0 + \epsilon_p)} \quad \dots(2.15)$$

$$\therefore y_{21}(\omega) = y_0 \int_{L_1}^{L_1 + \frac{N_1 \lambda_0}{2}} f'(z) e^{j\beta z} dz \int_{L_2}^{L_2 + \frac{N_2 \lambda_0}{2}} f''(z) e^{-j\beta z} dz \quad \dots(2.16)$$

The source functions from equation (2.10) can be written as

$$f'(z) = \frac{\beta_0}{\epsilon_0} \frac{(\epsilon_0 + \epsilon_p)}{1.854} \cos\{\beta_0(z - L_1)\} \quad \dots(2.17)$$

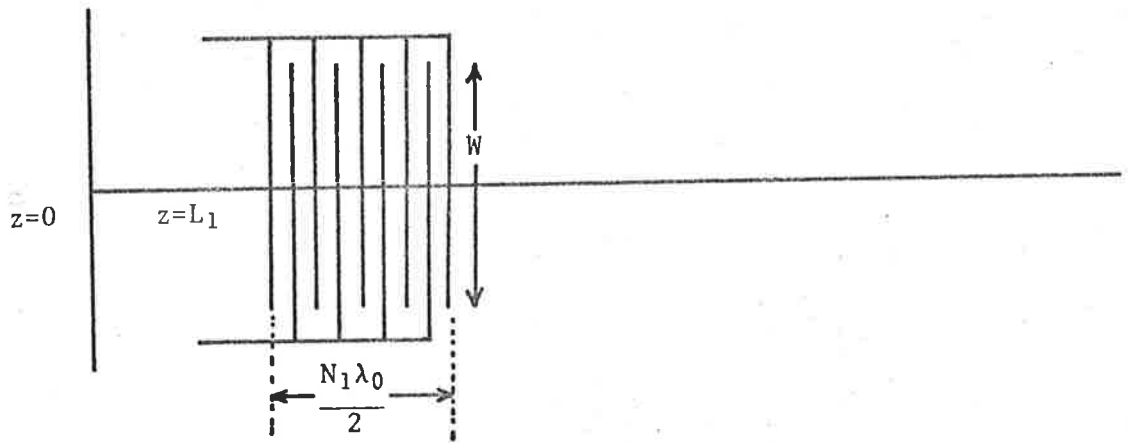
$$f''(z) = \frac{\beta_0}{\epsilon_0} \frac{(\epsilon_0 + \epsilon_p)}{1.854} \cos\{\beta_0(z - L_2)\} \quad \dots(2.18)$$

in which we have used the relation

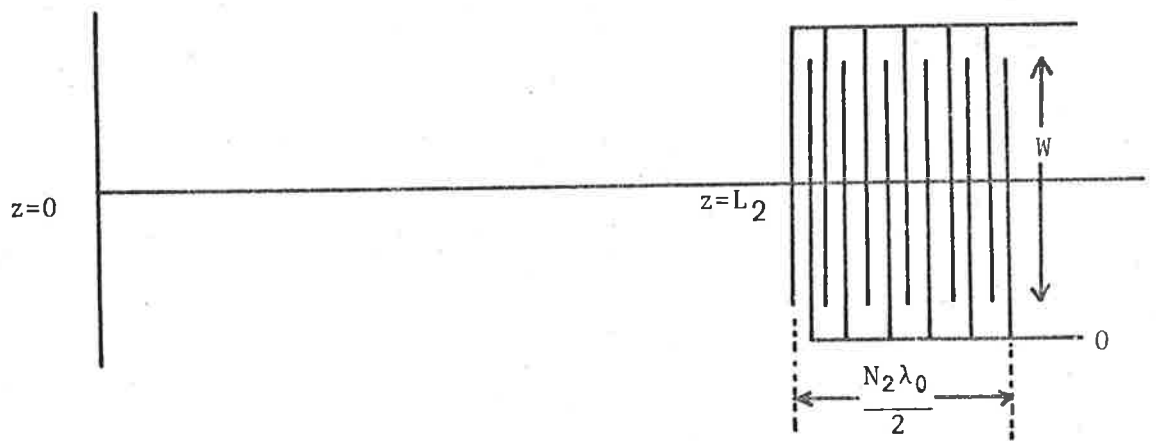
$$z_{k+1} - z_k = \frac{\lambda_0}{2} = \frac{\pi}{\beta_0}$$

Further, letting

$$K_x = \frac{\beta_0}{\epsilon_0} \left( \frac{\epsilon_0 + \epsilon_p}{1.854} \right) \quad \dots(2.19)$$



(a)



(b)

Figure 2.2 Coordinate System for Evaluating  $Y_{21}(\omega)$  for a Pair of Transducers.

(a) Transducer  $T_1$  of length  $l_1$ .

(b) Transducer  $T_2$  of length  $l_2$ .

the transadmittance equation (2.15) becomes

$$y_{21}(\omega) = y_0 K_x^2 \int_{L_1}^{L_1 + \frac{N_1 \lambda_0}{2}} \cos \beta_0 (z - L_1) e^{j\beta z} dz \int_{L_2}^{L_2 + \frac{N_2 \lambda_0}{2}} \cos \beta_0 (z - L_2) e^{-j\beta z} dz \quad \dots (2.20)$$

where  $N_1$  and  $N_2$  are the number of half-wavelengths in each transducer, can be either odd or even. Evaluating the integrals the equation (2.20) reduces to,

$$y_{21}(\omega) = y_0 K_x^2 \frac{N_1 \pi \beta}{\beta_0 (\beta + \beta_0)} \frac{\sin \left\{ \frac{N_1 \pi}{2} \frac{(\beta - \beta_0)}{\beta_0} \right\}}{\frac{N_1 \pi}{2} \frac{(\beta - \beta_0)}{\beta_0}} \times \frac{N_2 \pi \beta}{\beta_0 (\beta + \beta_0)} \frac{\sin \left\{ \frac{N_2 \pi}{2} \frac{(\beta - \beta_0)}{\beta_0} \right\}}{\frac{N_2 \pi}{2} \frac{(\beta - \beta_0)}{\beta_0}} \times \exp \left[ -j\beta \left\{ \left( L_2 + \frac{N_2 \lambda_0}{4} \right) - \left( L_1 + \frac{N_1 \lambda_0}{4} \right) \right\} + j \frac{N_2 - N_1}{2} \pi \right] \quad \dots (2.21)$$

on further substituting  $\beta = \frac{\omega}{v_f}$  and  $\beta_0 = \frac{\omega_0}{v_f}$ .

$$y_{21}(\omega) = y_0 K_x^2 \frac{N_1 \pi}{2 \beta_0} \left( \frac{2\omega}{\omega + \omega_0} \right) \frac{\sin \frac{N_1 \pi}{2} \left( \frac{\omega - \omega_0}{\omega_0} \right)}{\frac{N_1 \pi}{2} \left( \frac{\omega - \omega_0}{\omega_0} \right)} \times \frac{N_2 \pi}{2 \beta_0} \left( \frac{2\omega}{\omega + \omega_0} \right) \frac{\sin \frac{N_2 \pi}{2} \left( \frac{\omega - \omega_0}{\omega_0} \right)}{\frac{N_2 \pi}{2} \left( \frac{\omega - \omega_0}{\omega_0} \right)} \exp \left[ -j \frac{\omega}{v_f} \left\{ \left( L_2 + \frac{N_2 \lambda_0}{4} \right) - \left( L_1 + \frac{N_1 \lambda_0}{4} \right) \right\} + j \frac{N_2 - N_1}{2} \pi \right] \quad \dots (2.22)$$

Letting  $x_1 = \frac{N_1 \pi}{2} \left( \frac{\omega - \omega_0}{\omega_0} \right)$  ,  $x_2 = \frac{N_2 \pi}{2} \left( \frac{\omega - \omega_0}{\omega_0} \right)$

and

$$D = \left( L_2 + \frac{N_2 \lambda_0}{4} \right) - \left( L_1 + \frac{N_1 \lambda_0}{4} \right)$$

and substituting for  $y_0$  and  $K_x$ , the equation (2.22) can be written as

$$y_{21}(\omega) = \frac{-|\omega| \Delta W N_1 N_2 \pi^2 (\epsilon_p + \epsilon_0)}{4 \times 1.854^2} \left( \frac{2\omega}{\omega + \omega_0} \right)^2 \frac{\sin x_1}{x_1} \frac{\sin x_2}{x_2} \exp \left\{ -j \frac{\omega D}{v_f} + j \frac{N_2 - N_1}{2} \pi \right\} \quad \dots (2.23)$$

A number of conclusions can be drawn from the above equation.

- (1) The group delay which can be obtained by differentiating the phase with respect to ' $\omega$ ' and changing the sign is,

$$t_d = \frac{-d\phi}{d\omega} \quad \text{where } \phi = \frac{-\omega D}{v_f} - \left( \frac{N_2 - N_1}{2} \right)$$

$$\therefore t_d = \frac{D}{v_f} \quad \dots (2.24)$$

where  $D$  is the distance between the centres of the two transducers, as evident from Figure 2.2.

- (2) If the two transducers are of the same length i.e. having same number of fingers, then,  $N_1 = N_2 = N$

$$y_{21}(\omega) = \frac{-|\omega| \Delta W N^2 \pi^2 (\epsilon_0 + \epsilon_p)}{4 x 1.854^2} \left( \frac{2\omega}{\omega + \omega_0} \right) \left( \frac{\sin x}{x} \right)^2 \exp \left( -j \frac{\omega D}{v_f} \right) \quad \dots (2.25)$$

where

$$x = \frac{N\pi}{2} \left( \frac{\omega - \omega_0}{\omega_0} \right)$$

The output response of the transducer with a constant load resistance  $R_L$  for a unit impulse input is then given by, from equation (2.5),

$$\dot{V}_0(\omega) = -R_L y_{21}(\omega) \quad \dots (2.26)$$

or in time domain,

$$\dot{V}_0(t) = -R_L \mathcal{F}^{-1}\{y_{21}(\omega)\} = -R_L y_{21}(t) \quad \dots (2.27)$$

where  $\mathcal{F}^{-1}$  indicates the inverse Fourier transform and  $y_{21}(t)$  and  $y_{21}(\omega)$  from the Fourier transform pair i.e.  $y_{21}(t) \Leftrightarrow y_{21}(\omega)$ . The impulse response  $\dot{V}_0(t)$  can be easily evaluated through the numerical approach, especially with the use of fast Fourier transform algorithm.

- (3) For a positive input impulse, the sign of the central peak of the output response can also be predicted by the transadmittance



formula. From equations (2.23) and (2.24),

$$y_{21}(\omega) = \text{constant} \times |\omega| \times |F(\omega)|^2 \exp(-j\omega t_d) \quad \dots(2.28)$$

where

$$\text{constant} = \frac{-W\Delta N^2 \pi^2 (\epsilon_0 + \epsilon_p)}{4 \times 1.854^2} \quad \text{and} \quad |F(\omega)| = \left( \frac{2\omega}{\omega + \omega_0} \right)^2 \left( \frac{\sin x}{x} \right)^2$$

and from equation (2.27),

$$\dot{V}_0(t) = -R_L \times \text{constant} \times \int_{-\infty}^{\infty} |\omega| \times |F(\omega)|^2 e^{-j\omega t_d} e^{j\omega t} d\omega \quad \dots(2.29)$$

The sign of central or correlation peak is then obtained at

$$t = t_d \quad \text{i.e.} \quad \dot{V}_0(t)/t = t_d = -R_L \times \text{constant} \times \int_{-\infty}^{\infty} |\omega| \times |F(\omega)|^2 d\omega \quad \dots(2.30)$$

which is negative, since the integral in equation (2.30) is positive definite. Hence, in practical situations for a narrow positive input pulse we expect a negative central peak in time domain, provided that the connections of the input and output transducers to the source and load impedances are such that the connections followed for voltages and currents is maintained as shown in Figure 2.1(a).

(4) The voltage transfer function  $\left| \frac{\dot{V}_0(\omega)}{\dot{V}_1(\omega)} \right|$  from equation (2.25) can be seen to be proportional to  $|\frac{\omega}{\omega_0}| \times \left| \frac{2\omega}{\omega + \omega_0} \right|^2 \times \left( \frac{\sin x}{x} \right)^2$ , whereas several authors [2]<sup>2</sup> indicated that it is approximately of the form  $\left( \frac{\sin x}{x} \right)^2$ . This is quite true if the frequencies under consideration are not far from the central frequency  $\omega_0$ , in which case the two factors  $|\frac{\omega}{\omega_0}|$  and  $\left| \frac{2\omega}{\omega + \omega_0} \right|^2$  reduces approximately to unity. The dependence of transfer function on the two factors  $|\frac{\omega}{\omega_0}|$  and  $\left| \frac{2\omega}{\omega + \omega_0} \right|^2$  is that the response is tilted upwards, each factor contributing approximately a rise of 6dB per octave in the frequency domain. The second factor arises

because of uniform transducers while the first factor is inherent in the derivation of the transadmittance formula. The rise in frequency response in the passband is also observed by Smith et al. [2]<sup>21</sup> for unapodized linear FM transducers but their circuit model could not explain the reason for this upward tilt. They indicated that it is the characteristic of unweighted transducers. In order to remove the Fresnel ripple in the passband and obtain a flat band characteristic they pointed out that a slight apodization using a topped envelope of the transducers is necessary. Hartmal et al. [3]<sup>20</sup> also indicated in their impulse model design that transducers with log-tapered gaps must have overlap lengths multiplied by three-half power of frequency to achieve a flat frequency transfer function. Therefore, the  $|\omega|$  factor in the transadmittance model predicts this upward tilt in the passband as is clearly demonstrated for a logarithmically frequency-chirped transducer [2]<sup>1</sup>. In fact the  $|\omega|$  factor is applicable to all interdigital transducers including the uniform gap-width transducers.

### 2.3 Frequency Domain Input Admittance $y_{11}(\omega)$

The diagonal elements of admittance matrix of the two transducer structure as shown in Figure 2.1(c) represent the input and output admittances under short-circuit conditions. For identical transducers they are one and the same. The input admittance is derived under the same basic assumptions as those for the transadmittance. Hence, without going into details the input conductance of a single transducer is given by [2]<sup>22</sup>,

$$y_{11}(\omega) = \frac{j\omega \int_{-\infty}^{\infty} \phi(z)\sigma(z)dz}{\dot{V}_1^2} \quad \dots(2.31)$$

where,  $\phi(z)$  is the potential distribution on and between the fingers and  $\sigma(z)$  is the total charge on the fingers resulting from the peak value of a sinusoidal excitation voltage  $\dot{V}_1$ . The real part of  $y_{11}(\omega)$  is then

deduced as

$$G(\omega) = \frac{-|\omega|W\Delta}{(\epsilon_0 + \epsilon_p)V_1^2} |S(\beta)|^2 \quad \dots (2.32)$$

where  $S(\beta)$  is the Fourier transform of the source function  $f(x, z)$ . Hence  $G(\omega)$  can be calculated from the transadmittance  $y_{21}(\omega)$  itself by putting the transducer separation 'D' equal to zero. Therefore, for a uniform transducer the conductance  $G(\omega)$  is given by, from equation (2.25)

$$G(\omega) = \frac{-|\omega|\Delta WN^2\pi^2(\epsilon_0 + \epsilon_p)}{4 \times 1.854^2} \left(\frac{2\omega}{\omega + \omega_0}\right)^2 \left(\frac{\sin x}{x}\right)^2 \quad \dots (2.33)$$

in which as before  $x = \frac{N\pi}{2} \left(\frac{\omega - \omega_0}{\omega_0}\right)$  and 'N' is the number of half-wavelengths in each transducer. The radiation susceptance  $B(\omega)$  can be calculated from the first principles using the equation (2.31), however  $B(\omega)$  can be more readily calculated using the Hilbert-transform relationship, as pointed out by Nalamwer and Epstein [2]<sup>23</sup> i.e.

$$B(\omega) = \frac{1}{\pi} \int_{-\infty}^{\infty} \frac{G(x)}{x - \omega} dx \quad \dots (2.34)$$

This transform does not describe the admittance due to the static capacitance of the transducers, and in order to evaluate the total admittance of the transducer one has to include the contribution due to the static capacitance also. The expression derived for this quantity by Engan [2]<sup>24</sup> for equal finger-width to finger-ratio is

$$C_T = \frac{N}{2} \times W \times (\epsilon_0 + \epsilon_p) \quad \dots (2.35)$$

Therefore, the input admittance parameter is given by

$$y_{11}(\omega) = G(\omega) + j(B(\omega) + \omega C_T) \quad \dots (2.36)$$

A similar expression for output admittance parameter  $y_{22}(\omega)$  can be obtained. However, for apodized combs the simple approach followed for uniform transducers is not applicable for the reasons mentioned in the

next section of this chapter, but the method developed in Chapter 7 is somewhat similar to one described by Hartman et al. [2]<sup>20</sup>. Thus we have produced expressions for all the coefficients in the admittance matrix in terms of the transducer structures and the material parameters, so that the complete behaviour of the filter can be predicted.

It is to be noted from Figure 2.1(a) or (b), the input admittance of the two-port structure is given by

$$Y_{in}(\omega) = \frac{\dot{I}_1(\omega)}{\dot{V}_1(\omega)} = \frac{y_{11}(\omega) - \{y_{11}(\omega)y_{22}(\omega) - y_{12}(\omega)y_{21}(\omega)\}Z_L}{1 - y_{22}(\omega)Z_L}$$

Following the approximations as in equation (2.4)

$$Y_{in}(\omega) \approx y_{11}(\omega) \quad \dots (2.38)$$

Similarly we can prove that the output-admittance is

$$Y_0(\omega) \approx y_{22}(\omega) \quad \dots (2.39)$$

once again these relations - equations (2.38) and (2.39) show that with high impedance transducers in a low impedance measurement system the delay line input-output admittances are essentially given by the diagonal elements ( $y_{11}(\omega)$ ,  $y_{22}(\omega)$ ) of the transducer structure alone. In the next section some of the basic limitations imposed on in deriving all these admittance coefficients are discussed. Since the filter synthesis is developed in frequency domain and the source function is considered in time or position domain, restrictions involved in calculating the admittance coefficients in both the domains will be discussed.

#### 2.4 Limitations in Using $y_{21}(\omega)$ and $y_{11}(\omega)$

Basically the analysis is used for uniform identical transducers in which case straightforward analytical expressions can be obtained for calculating the source functions  $f'(z)$  and  $f''(z)$  and hence

$y_{21}(\omega)$  and  $y_{11}(\omega)$ . The analysis is equally simple for uniform but unequal number of fingers in each transducer. The analysis can be extended to uniform but varying finger-width to finger-gap ratio, transducers provided we assume an independent-gap approximation, that is the source function in any particular gap in the transducer is independent of the geometry of the adjacent gaps and is implicit in the analysis of other workers [2]<sup>21</sup>.

Analysis of transducers by this approach is simple, i.e. calculating frequency response for a given source function (finger positions and locations) but synthesis of transducers, i.e. calculating the source functions for a given arbitrary frequency response is not always feasible as explained more clearly in Chapter 8, dealing with shirped transducers.

The analysis and synthesis of transducers is quite simple if one of the transducers is uniform with uniform finger-width to finger-gap ratio and the other is apodized whose maximum apodization is less than or equal to the width of the uniform transducer. In this case a direct Fourier-transform relationship between the apodized comb and  $y_{21}(\omega)/\omega$  retained. However, calculating the input admittance of the apodized comb is more complicated but a procedure has been developed in Chapter 7.

The situation where both the transducers are apodized is more difficult to represent analytically because the propagating surface wave field onto which we must project the receiver source field is not independent of  $x$ , and the resulting expression for  $y_{21}(\omega)$  does not factorize into two separate integrals. The simplest practical solution in this case appears to be to divide the propagation path into a number of parallel strips selected so that each strip intersects the launching and receiving transducers in such a way that the restriction, that at least one of the transducers may be considered to be unapodized across that beam width, is satisfied [2]<sup>25</sup>. However, some methods are proposed later in the thesis to synthesize two apodized transducers without too much difficulty under certain conditions.

Thus this chapter provides the necessary information on admittance formalism and the next chapter deals with the basic design of a SAW filter.

## CHAPTER 3

APPLICATION OF TRANSMITTANCE TO THE SYNTHESIS  
OF A TV IF FILTER3.0 Introduction

The general philosophy of surface acoustic wave filter synthesis, using the transmittance formalism, will be demonstrated in this chapter. Filter synthesis can normally be developed in either frequency or time domain but here the former method is followed, since the transmittance formula has been developed in frequency domain. The example considered is that of a TV IF response and the synthesis yields a complicated wave form in the time-domain. Techniques have then been devised to represent these complicated time responses by approximate source functions, and from these source functions the finger-pattern or transducer geometry on the substrate is derived on an intuitive basis, so that equal mark-space ratio is maintained. The theoretical frequency response of the so-modelled transducer structure is then calculated once again using the transmittance formula and good agreement obtained with the frequency response of the designed complicated time wave form, thus ensuring that the transducer geometry which has been derived on an intuitive basis, is in fact, an appropriate representation. The step-by-step procedure of the synthesis technique is presented in this chapter while the experimental results are reported in Chapter 4.

3.1 TV IF Specification

The magnitude response of TV IF stage of a typical test receiver is shown in Figure 3.1 (by courtesy of Mr. Pascoe, Philips Electricals Pty. Ltd., Hendon, S.A., 1969). This is the response obtained with the conventional RLC modules, which gave a satisfactory result in a test

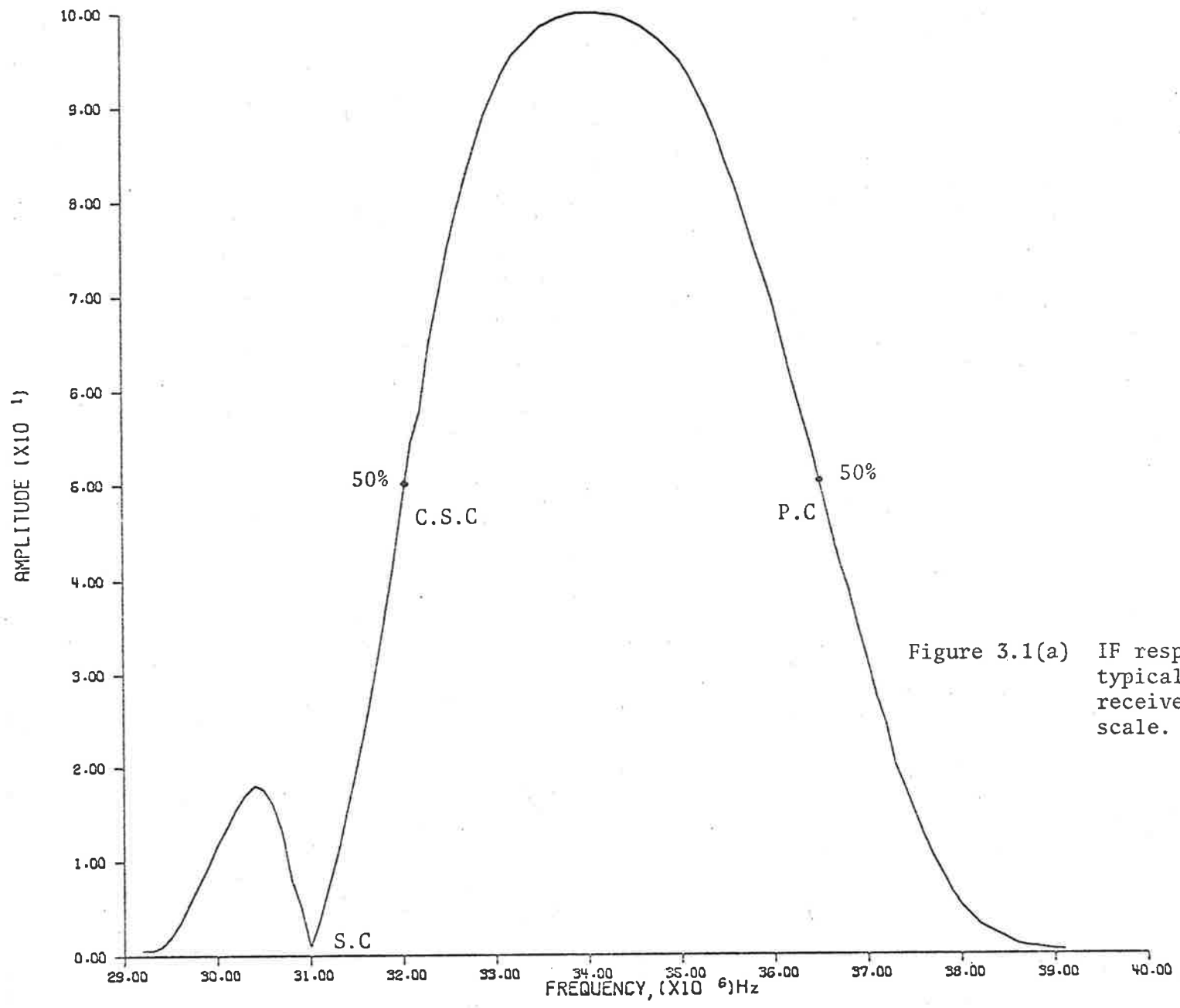


Figure 3.1(a) IF response of a typical test TV receiver in linear scale.



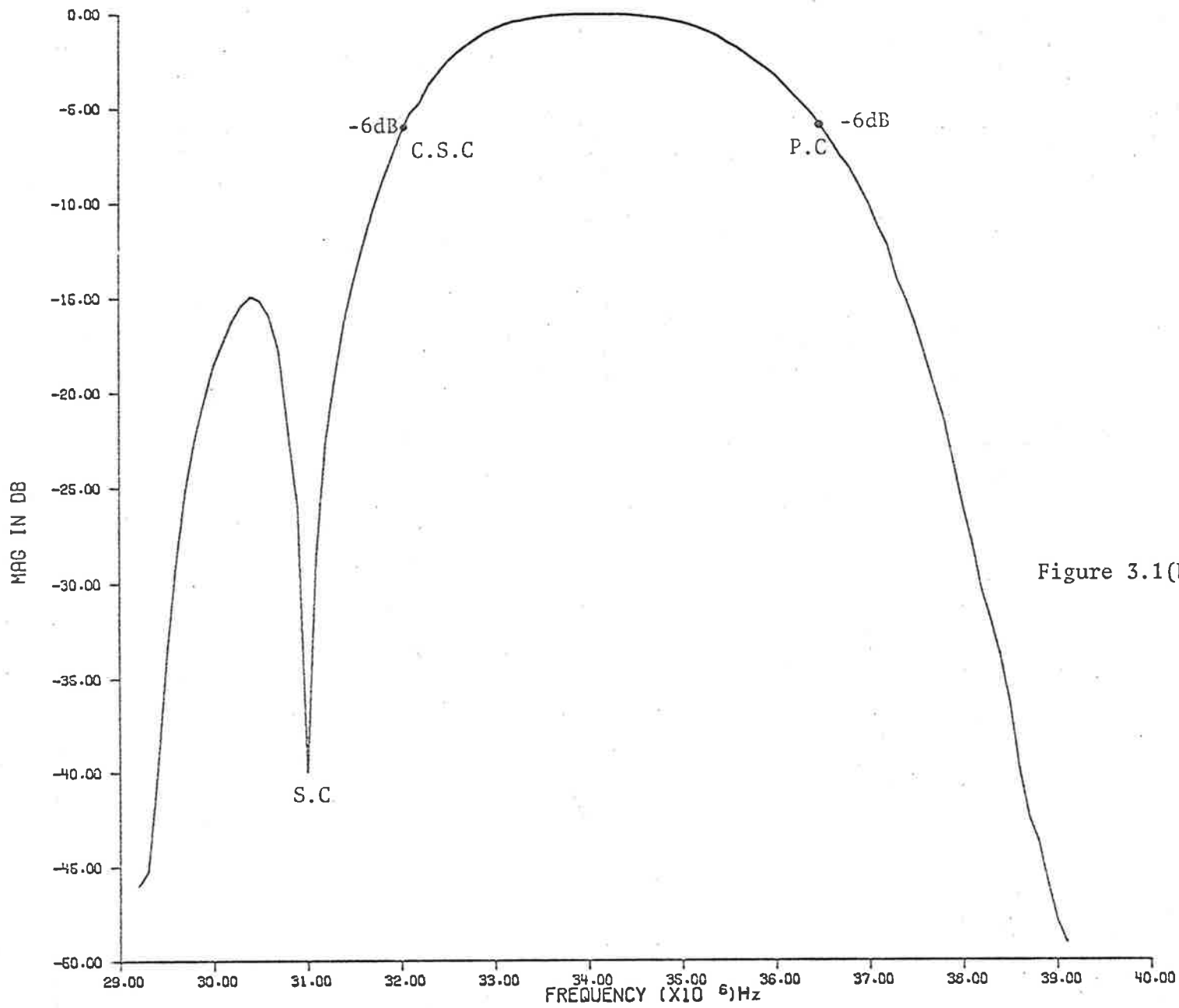


Figure 3.1(b) IF response of a typical test TV receiver in dB scale.

receiver. The initial aim of the project is to design a SAW filter whose response is close enough to that shown in Figure 3.1. Later on the synthesis is extended to achieve frequency response characteristic which lie within a given specified limit (Chapter 6). Before attempting to describe the synthesis procedure, it is appropriate to give a brief description about the peculiar shape of the TV IF response.

The IF section in a TV receiver is the most important part of the signal handling and processing functions. The faithfulness or otherwise of the video waveforms to the transmitted original, relies to quite a large extent on the characteristics and behaviour of this IF section. Unfortunately, the standards for the receiver IF passband characteristics are not laid down, apart from the intermediate frequencies which are, as recommended by the Australian Broadcasting Control Board [3]<sup>1</sup>, as follows:

Sound Carrier	...	...	...	30.5MHz	31.375MHz
					or
Vision Carrier	...	...	...	36MHz	36.875MHz

These frequencies should be adhered to within  $\pm 0.25\text{MHz}$  and the oscillator frequency should be above the channel frequency. It is up to the individual manufacturing companies to adopt their own specific characteristics to tie-in with the vestigial-side-band characteristics of the transmitted signal [3]<sup>2</sup> shown in Figure 3.2. The width of the television channel is 7MHz. Figure 3.2(a) indicates the various components in the spectrum allocation of a channel. Note that the side band components of the vision luminance information are asymmetrically transmitted. Upper side bands up to 5.0MHz are transmitted at full strength. Components beyond 5.0MHz are rapidly attenuated. Lower side bands down to 0.75MHz are transmitted at full strength. Below this point they are attenuated rapidly, and at 1.25MHz attenuated by some 60 dB.

Vision chrominance side bands are also transmitted asymmetrically.

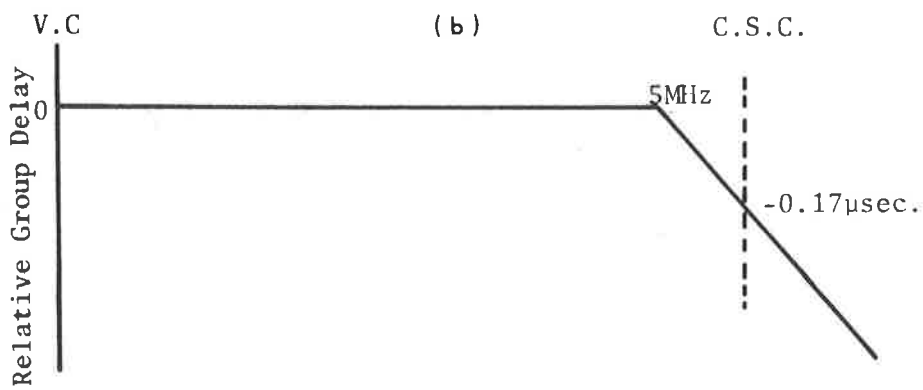
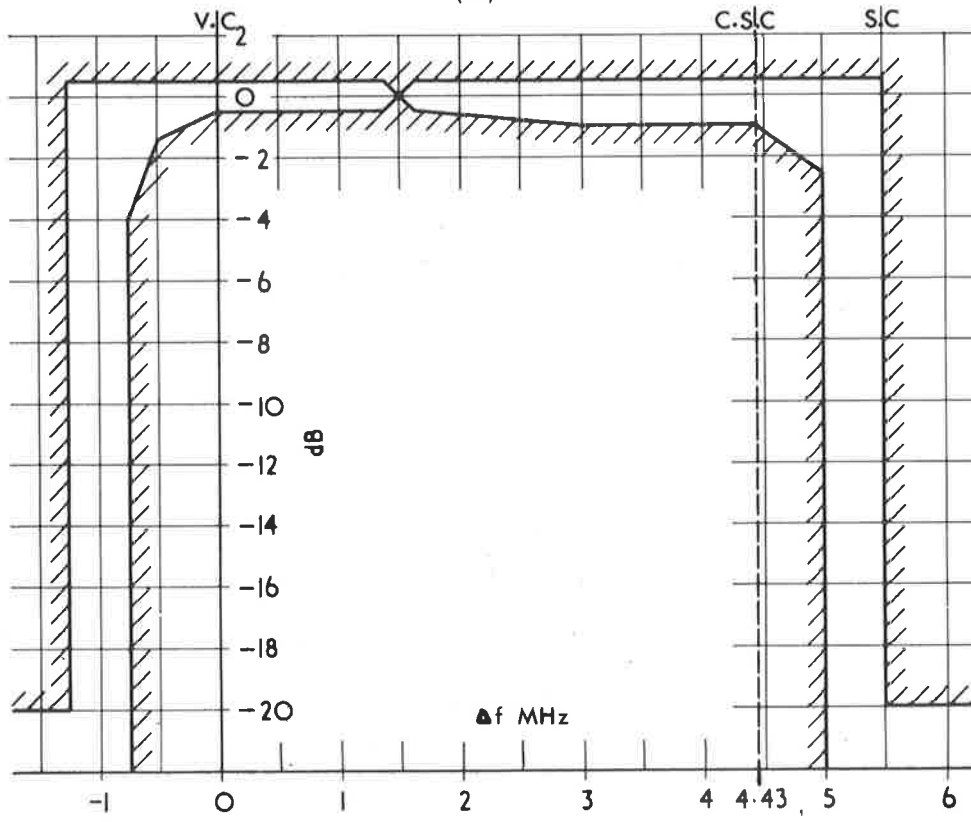
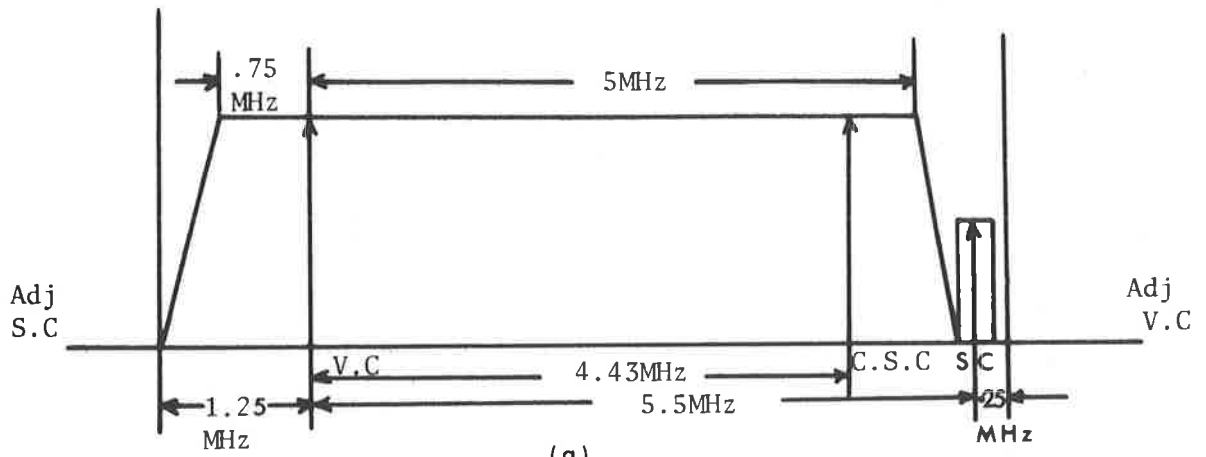


Figure 3.2 VSB Characteristic of the Transmitted Signal.  
 (a) VSB transmission characteristic  
 (b) Vision transmitter, amplitude/frequency response  
 (c) Transmitter group-delay specification

Lower chroma side-bands down to 1.3MHz below colour sub-carrier, and upper chroma side-bands up to 0.57MHz above colour sub-carrier are transmitted at full power. Thereafter, the chroma side-bands are attenuated considerably.

The sound carrier and its symmetrical side-bands to  $\pm 150$ MHz are transmitted at full power which has a maximum specified relationship for vision power  $[3]^2$ .

Figure 3.2(b) shows the amplitude v/s frequency response of the vision transmission with allowable tolerances. Note that the response at the television channel limits should have to be reduced at least 20dB relative to the response at 1.5MHz above the vision corner.

Figure 3.2(c) indicates the transmitted relative group delay specification to offset characteristics of an average receiver. The group delay of the transmitter and the standard vestigial side-band demodulator shall be flat to 5MHz. At the colour sub-carrier frequency the demodulator shall have a group delay of -0.17 microseconds relative to the delay at low frequencies. Normally tolerances of  $\pm 0.1$ usec in the specification are allowed.

Having known the VSB transmission characteristics the requirements for the IF passband can then readily be established. At the vision carrier the IF response should be down to 50% to correct the VSB transmission (6dB down) and it should rise more or less linearly as the frequency decreases until full response is reached about 34MHz. The linearity of the slope is essential to minimise the phase distortion in the receiver. Considerable attenuation is required at the sound carrier frequency of at least 25dB down than at the mid-band frequencies in order to avoid cross-modulation at the sound into the picture. For colour television signals much more higher attenuation is necessary of the order of 34dB down because of the presence of the large colour sub-carrier while it is absent in a monochromatic receiver. Further, very high attenuation at the adjacent

channel traps is needed to prevent interference from adjacent picture and sound carriers. Attenuation of the order of 50 to 60dB down is required for reception of signals at the extremely difficult areas. With all the aspects taken into consideration we get the unusual shape of the IF response as shown in Figure 3.1

### 3.2 Advantages of SAW TV IF Filters

The advantages of SAW filters, in general, have been discussed in Section 2 of Chapter 1, but the advantages of SAW filters for TV IF applications, in particular will be briefly described.

(1) The main advantage is that the SAW TV IF filter does not require any tuning circuits. Generally the IF passband response is obtained by means of a number of tuned circuits in the IF stages of the receiver. Normally, three IF stages hence, three tuned circuits are needed to provide the necessary passband characteristic and the gain for a monochrome receiver and possibly one more stage, hence one more tuned circuit for a colour receiver. Hence, tuning and servicing is difficult with the conventional RLC circuits. In a SAW device the whole IF response can be designed with simple interdigital transducer structures occupying only a few millimeters in area on a thin substrate. Hence, the filter is very small in size, light in weight and if the necessary gain is provided by means of integrated circuit amplifiers then the whole assembly can be encapsulated in a single package. Since the filter is permanently tuned, such a package has the additional advantage that it needs no further adjustments at the factory or afterwards.

(2) With SAW devices we can get a constant group-delay or linear phase over the entire passband which is not possible when using the conventional LC tuned circuits. Hence, video waveform distortion (phase distortion) can be minimized using SAW filter, thereby, improving the

quality of the picture.

(3) Since the IF response is determined by the geometry of the transducer structures, deep traps can be obtained by appropriately designing the structures which in turn reduces the cross-modulation of sound into picture and also interference due to adjacent channels.

### 3.3 Synthesis Procedure-Different Approaches

The different approaches of designing a SAW filter with a given arbitrary frequency response is mainly dependent on the assumptions under which the transmittance between a pair of transducer structures is derived. The fundamental assumption is that one of the transducers is uniform and the other transducer is either uniform or apodized whose maximum apodization is equal to or less than the width of the uniform transducer. The uniform or apodized transducer may have variable gap-widths e.g. chirped transducers [3]<sup>7</sup> and log periodic transducers [3]<sup>6</sup>. Analysis for two apodized transducers is very laborious while the synthesis is quite complicated if not impossible. Hence, only two choices are at our disposal for synthesis: either two uniform transducers or one uniform transducer and the other apodized transducer. It is not always possible to synthesize a given response with only two uniform transducers and hence some sort of weighting is necessary to achieve the arbitrary response. With the choice of transducers as mentioned above, possible weighting configurations are finger-width weighting for uniform transducer and finger-length weighting for the other transducer. The finger length weighed transducer may also have variable finger widths. The simplest case being, one unweighted transducer with only a small number of fingers whilst the other is weighted. In such a situation the unweighted transducer having a wide band characteristic does not influence very much the desired frequency response. TV IF filter synthesis is developed on this basis and is described in the following section. However, the advantages

and disadvantages of the various other approaches will be briefly described below.

(1) One unweighted and one apodized transducer configuration:

The advantages of this configuration are that only a single transducer needs to be designed and that the overlap weighting technique is easy to implement since a direct Fourier-transform relationship exists between  $y_{21}(\omega)/\omega$  and the apodizing function when the second transducer is of uniform beamwidths. The potential disadvantages are:

- (a) The total burden of producing a given response falls on one transducer;
- (b) the wide bandwidth of the second array can cause additional insertion loss;
- (c) the unweighted second array can cause undesired rounding of the filter response due to its  $\frac{\sin x}{x}$  frequency response; and
- (d) a symmetrical tuning and matching networks are necessary if they are to be used because of unequal input and output admittances of the transducers.

(2) Two apodized transducer configuration:

A seemingly obvious improvement is to use two overlap weighted transducers because all the difficulties associated with the unweighted transducer array are removed. Unfortunately, a synthesis procedure is not feasible except under certain circumstances since the transadmittance cannot be split up into two integrals describing the two array source functions and the two transducers cannot be designed independently. A technique whereby two overlap weighted transducers can be used and designed in terms of independent source functions is to couple the two transducers through a multi-strip coupler [3]<sup>3</sup>. In this case, the coupler performs the necessary integration across the beamwidth such that a unique source function can be assigned to each transducer. However, multi-strip

coupler design is practicable only on high coupling materials such as lithium niobate. The coupler width is given by [3]<sup>3</sup>  $L_T = \frac{\lambda}{2|\Delta|}$  and number of strips for equal mark-space ratio is given by  $N_T = \frac{1}{|\Delta|}$  where ' $\lambda$ ' is the wavelength of the surface wave velocity and  $|\Delta|$  is the electromechanical coupling constant. For YX quartz substrate  $|\Delta| \approx 0.1\%$  and the width of the coupler is approximately 500 wavelengths; at IF frequencies it is roughly equal to 5cm and the number of strips is roughly equal to 1000. This is quite impractical especially when micro-minaturization is the prime importance in the IF filters.

Identical apodized transducers can, however, be synthesized using transadmittance formula on reasons similar to those given by Gerard et al. [3]<sup>4</sup>, i.e. the product form of the source function integrals is still applicable provided that the time-bandwidth product is very large. A direct Fourier transform relationship between  $\sqrt{y_{21}(\omega)}/\omega$  and the source function exists, and the two transducers are then identical.

(3) Two uniform chirped transducer configurations:

Chirped transducers are extensively used for designing FM pulse compression filters. Fowel [3]<sup>5</sup> has developed a synthesis procedure for designing waveforms of this type which works well provided that the time-bandwidth product is large. These are particularly useful at high frequencies with regular bandpass characteristic. Another important aspect of this type of configuration is that the input-output admittances can be increased considerably, thereby reducing the insertion-loss of the filter. TV IF filter synthesis using chirped transducers is presented in Chapter 8.

(4) One uniform chirped and one apodized transducer configuration:

The requirement of large TB product for two uniform identically chirped transducers can be relaxed by using one uniform chirped transducer and apodizing the other transducer. Another advantage is that the ripple in the passband which is inherent with the uniform identical chirped



transducers can be minimized by using this type of configuration. Since the uniform chirped transducer will have a broadband characteristic, the transadmittance formula can well be used for synthesizing the apodized transducer. Further, if the uniform chirped transducer is so selected that its response is somewhat close to the desired response, then we can expect only a small amount of apodization in the other transducer, thus making it more advantageous than the first configuration (one uniform transducer with only a few number of fingers and the other apodized).

Once a particular type of finger weighting has been selected, there are several ways of representing the transducers [3]<sup>9,10,11</sup> depending upon the requirement. Loss due to bidirectionality can be minimized using unidirectional transducers [3]<sup>12,13</sup>. Various spurious signals which are of common problems in a surface wave device can also be suppressed by properly choosing the input and output transducers [3]<sup>8</sup>.

### 3.4 Synthesis of one Uniform and one Apodized Transducer-Filter 1

The actual synthesis technique developed for realizing the TV IF response shown in Figure 3.1 will now be discussed. Some of the further assumptions which are implied in the derivation of the transadmittance formula (Section 2.2) are as follows. The spurious effects such as bulk-wave generation, reflections between the fingers and the main loading of the surface by the interdigital transducer structure are neglected. These assumptions are shown to be fairly justified [3]<sup>14</sup> especially at IF frequencies and at moderate bandwidths.

From equations (2.5) and (2.11) we have

$$\frac{V_L(\omega)}{V_1(\omega)} \approx -y_{21}(\omega)Z_L = \frac{|\omega|\Delta\epsilon_0^2}{W(\epsilon_0+\epsilon_p)} Z_L \int_{s'} f'(z)e^{j\beta z} ds \int_{s''} f''(z)e^{-j\beta z} ds \dots$$

... (3.1)

Assuming a constant real load impedance ( $Z_L = R_L$ ) and noting that  $\beta = \omega/v_f$  the above equation can be written as

$$y_{21}(\omega) = - \frac{V_L(\omega)}{V_1(\omega)R_L} = - \frac{|\omega| \Delta \epsilon_0^2}{W(\epsilon_0 + \epsilon_p)} F_1(\omega) F_2(\omega) \quad \dots(3.2)$$

where  $F_1(\omega)$  is the frequency response arising due to source function  $f'(z)$  of the input transducer  $T_1$  and  $F_2(\omega)$  due to that of  $f''(z)$  of the output transducer  $T_2$ . Writing the expression in complex form we have,

$$|y_{21}(\omega)| e^{j\theta(\omega)} = - \frac{|\omega| \Delta \epsilon_0^2}{W(\epsilon_0 + \epsilon_p)} |F_1(\omega)| \times |F_2(\omega)| e^{j\theta(\omega)} \quad \dots(3.3)$$

where  $\theta(\omega)$  is the phase response of the filter. In general it is chosen so as to tie in with the group delay characteristic of the transmitted signal as shown in Figure 3.2(c). The amplitude functions  $|F_1(\omega)|$  and  $|F_2(\omega)|$  will have units of length, while the amplitude function  $|y_{21}(\omega)|$  will have units of siemens.

For a uniform input transducer of width  $W_1$  and length  $N_1$  half wavelengths the frequency response (Section 2.21) is given by,

$$|F_1(\omega)| = \frac{N_1 \pi W_1 (\epsilon_0 + \epsilon_p)}{2x \epsilon_0 \times 1.854} \left( \frac{2}{\omega + \omega_0} \right) \left| \frac{\sin \left\{ \frac{N_1 \pi}{2} \left( \frac{\omega - \omega_0}{\omega_0} \right) \right\}}{\frac{N_1 \pi}{2} \left( \frac{\omega - \omega_0}{\omega_0} \right)} \right| \quad \dots(3.4)$$

If the frequencies under consideration are not far from the central frequency  $\omega_0$  then the factor  $\left( \frac{2\omega}{\omega + \omega_0} \right)$  can be approximated to unity. Letting  $x = \frac{N_1 \pi}{2} \left( \frac{\omega - \omega_0}{\omega_0} \right)$ , equation (3.4) becomes

$$|F_1(\omega)| = \frac{N_1 \pi W_1 (\epsilon_0 + \epsilon_p)}{2x \epsilon_0 \times 1.854} \left| \frac{\sin x}{x} \right| \quad \dots(3.5)$$

Substituting equation (3.5) in (3.3) we have,

$$|y_{21}(\omega)| e^{j\theta(\omega)} = - \frac{|\omega| \Delta\epsilon_0 N_1 \pi W_1}{2xWx1.854} \left| \frac{\sin x}{x} \right| |F_2(\omega)| e^{j\theta(\omega)} \quad \dots(3.6)$$

Denoting the constant parameters on right-hand side of equation (3.6),

except  $W$  by  $\frac{1}{K_2} = - \frac{\Delta\epsilon_0 N_1 \pi}{2xWx1.854}$  then,

$$|F_2(\omega)| e^{j\theta(\omega)} = \frac{K_2}{|\omega|} \times \frac{|y_{21}(\omega)|}{W_1 \left| \frac{\sin x}{x} \right|} e^{j\theta(\omega)} \quad \dots(3.7)$$

Thus, knowing the magnitude and phase characteristic of the given TV IF response, we can calculate the frequency response of the output transducer and hence its source function through the Fourier transform relationship. In actual synthesis the phase response has been selected to be linear over the entire passband (hence, a constant group delay) instead of the required specification, for various reasons. The actual requirement is that from Figure 3.2 the phase is linear up to 5MHz with reference to vision carrier frequency, then can have non-linear variation in the rest of the bandwidth i.e. 0.75MHz. Most of the picture and colour information is transmitted in the 5MHz band with reference to VC frequency and the phase should be linear in this region and hence choosing a linear phase variation over the entire channel bandwidth (7MHz) does not effect the response significantly. The second reason is that, since  $|F_2(\omega)|$  is real and with a linear phase characteristic the source function is symmetrical over a point  $z = z_0$  and the optimization techniques developed in the subsequent parts of the thesis (Chapter 5) become simpler with symmetrical functions than with asymmetrical functions. Having thus established the phase relationship we can write now

$$\theta(\omega) = - \frac{z_0 \omega}{v_f} \quad \dots(3.8)$$

and equation (3.7) becomes to

$$|F_2(\omega)| e^{-j\frac{z_0}{v_f}\omega} = \frac{K_2}{|\omega|} \frac{|y_{21}(\omega)|}{W_1 \left| \frac{\sin x}{x} \right|} e^{-j\frac{z_0}{v_f}\omega} \quad \dots(3.9)$$

Now working in time-domain instead of position-domain we have,

$$|F_2(\omega)| e^{-jt_0\omega} = \frac{K_2}{|\omega|} \frac{|y_{21}(\omega)|}{W_1 \left| \frac{\sin x}{x} \right|} e^{-jt_0\omega} \quad \dots(3.10)$$

where  $t_0 = \frac{z_0}{v_f}$ , to be determined in accordance with the periodic interval of the source function in time domain. The time domain response  $F_2(t)$  of the transducer  $T_2$  is then obtained by taking the inverse Fourier transform of equation (3.10) i.e.

$$F_2(t) = \mathcal{F}^{-1}\{|F_2(\omega)| e^{-jt_0\omega}\} = \mathcal{F}^{-1}\left\{\frac{K_2}{|\omega|} \frac{|y_{21}(\omega)|}{W_1 \left| \frac{\sin x}{x} \right|} e^{-jt_0\omega}\right\} \quad \dots(3.11)$$

where  $\mathcal{F}^{-1}$  indicates inverse Fourier transform. Since the Fourier transform relationships from frequency to time and vice-versa are extensively used in this project it is appropriate at this juncture to indicate the algorithm used in evaluating the continuous Fourier transform integrals on digital computers.

#### 3.4.1 The Discrete Fourier Transform

To evaluate the Fourier transform of a function on a digital machine it is necessary to use the sampled version of the function and then use the discrete Fourier transform. The definition of DFT and its inverse used throughout this work is,

$$F_p\{(n-1)\Delta f\} = \Delta T \sum_{m=1}^N f_p\{(m-1)\Delta T\} e^{-\frac{j2\pi(m-1)(n-1)}{N}} \quad n = 1, 2, \dots, N \quad \dots(3.12)$$

and

$$f_p\{(m-1)\Delta T\} = \Delta f \sum_{n=1}^N F_p\{(n-1)\Delta f\} e^{\frac{j2\pi(m-1)(n-1)}{N}}$$

$$m = 1, 2, \dots, N \quad \dots (3.13)$$

where

- $N$  = total number of sampling points in either domain  
 $\Delta T$  = sampling interval in time domain  
 $\Delta f$  = sampling interval in frequency domain  
 $f_p$  = sampled version of continuous function,  $f_c$  in time domain  
 $F_p$  = sampled version of continuous function,  $F_c$  in frequency domain.  
 $\Delta f \cdot \Delta T = \frac{1}{N}$ .

This is a slightly modified version of the commonly adopted definition, in the sense that  $\Delta f$  and  $\Delta T$  do not appear before the summation terms and  $1/N$  is placed at either of the right-hand side equations (3.12) or (3.13). The present definition is convenient in one way that the amplitudes are scaled correctly while performing the transformation and no further scaling is necessary afterwards while in the commonly adopted definition a pre or post scaling of amplitudes is necessary.

### 3.4.2 The Fast Fourier Transform Algorithm

The fast Fourier transform is an efficient computational procedure for calculating the discrete Fourier transform of a function or its inverse. The FFT algorithm was published by Cooley and Tukey [3]<sup>15</sup> in 1965 and makes use of the cyclic properties of the exponential term in the integral definition to effect significant savings in computing time. The algorithm reduces the number of multiplications necessary to evaluate the DFT or its inverse for  $N$  samples from  $h_1 N^2$  to  $h_2 N \log_2 N$ , where  $h_1$  and  $h_2$  are constants of the order of unity and depend on the programming details.

A subroutine based on the version of the algorithm by Cooley Lewis and Welch [3]<sup>15</sup> and modified to the present definition equations (3.12) and (3.13) [3]<sup>16</sup> is used for evaluating the responses at various stages of the filter analysis and synthesis. The number of discrete samples is limited to  $2^{10}$  and for values greater than this number necessary changes have to be done in the subroutine. The use of FFT is fairly standard and needs no further explanation at this point. An extensive treatment of the algorithm may be found in the recent book by Oran Brigham (1974) [3]<sup>17</sup> and also on the IEEE special issue on FFT [3]<sup>18</sup>.

### 3.4.3 Computational Procedure

The steps involved in arriving at the time domain response of the output transducer will be described below. Recall equation (3.11)

$$F_2(t) = 7^{-1} \left\{ \frac{K_2}{|\omega|} \frac{|y_{21}(\omega)|}{W_1 \left| \frac{\sin x}{x} \right|} e^{-jt_0\omega} \right\}$$

(1) Choice of  $|y_{21}(\omega)|$ : The magnitude response  $|y_{21}(\omega)|$  is the specified response of the TV IF filter shown in Figure (3.1). The units of  $|y_{21}(\omega)|$  will be siemens and the magnitude response is selected arbitrarily. The peak amplitude is assigned a value of 100 siemens and the response is scaled accordingly. Since we need discrete representation of the functions for machine computation, the response is to be sampled at appropriate frequency intervals. Use of FFT algorithm requires uniform sampling. The sampling interval is selected such that all the details on the IF response are adequately taken into account. The most suitable frequency resolution was found to be equal to 0.2MHz. Hence  $|y_{21}(\omega)|$  is sampled at 0.2MHz for FFT operation.

(2) Choice of  $W_1 \left| \frac{\sin x}{x} \right|$ : Note that this factor arises due to uniform input transducer with only a few number of fingers. The choice of

$\left| \frac{\sin x}{x} \right|$  where  $x = \frac{N_1 \pi}{2} \left( \frac{\omega - \omega_0}{\omega_0} \right)$  depends on  $N_1$ , the number of half-wavelengths and  $\omega_0$  the centre frequency of the uniform transducer. The centre frequency can be selected to be approximately half-way between the edge frequencies of the IF characteristic Figure (3.1) and also on the flat portion of the response. Therefore, on examination of the IF response the centre frequency  $f_0 = \frac{2\pi}{\omega_0}$  will have a value around 34MHz. However, the exact value taken will be indicated while discussing the time resolution. The choice of  $N_1$  is such that the first nulls of  $\left| \frac{\sin x}{x} \right|$  response will be far-away from the edge frequencies of the IF characteristic. A 9-finger transducer was selected in the design and for uniform mark-space ratio  $N_1 = 8$ . Having selected  $N_1$  and  $\omega_0$ , the sampled response of  $W_1 \left| \frac{\sin x}{x} \right|$  is calculated. The units of  $W_1 \left| \frac{\sin x}{x} \right|$ , as indicated earlier, will be 'lengths'. The peak amplitude is assigned a value of 100 meters and the response  $W_1 \left| \frac{\sin x}{x} \right|$  is calculated accordingly.

(3) Choice of  $t_0$  in phase characteristic: The choice of periodic time interval  $T$  is governed by the frequency resolution. That is for frequency increments of 0.2MHz the time interval is given by  $T = \frac{1}{0.2\text{MHz}} = 5\mu\text{sec}$ . If we select  $t_0 = 0$  i.e. zero phase, the magnitude response in frequency domain, equation (3.11) is real and in view of the DFT as defined in equation (3.13),  $F_2(t)$  is real and symmetrical about the  $\left(\frac{N}{2} + 1\right)$ th sampling point corresponding to a time interval of  $\frac{T}{2}$ , and also maximum amplitude occurs at the first sampling point corresponding to zero time interval and the function, of course, repeats itself at  $(N+1)$ th sampling point corresponding to a time interval of  $T$ . This indicates that half of the main lobe starts at  $t = 0$  followed by sidelobes up to  $t = \frac{T}{2}$  and then the whole pattern folds over at  $t = \frac{T}{2}$ . This is not a convenient situation for the synthesis procedure or for making a finger pattern for the delay line. This difficulty can be removed by introducing the linear phase term and appropriately selecting  $t_0$ . The proper choice is that the

maximum amplitude occurs at  $t = t_0$  instead of at  $t = 0$ . This indicates that  $t_0 = \frac{T}{2}$  is a sensible choice. Therefore,  $t_0$  was selected to be equal to  $2.5\mu\text{sec}$ . With this choice, the mainlobe is symmetrical over  $\frac{T}{2}$  and the sidelobes follow on either side of the mainlobe in decreasing order.

(4) Choice of  $\frac{K_2}{|\omega|}$ : The constant  $K_2$  is determined from the substrate parameters and the finger-width on the substrate and in the synthesis procedure it is not necessary to include the actual values, however, because of the  $|\omega|$  factor in the denominator it can be used as a scale factor to reduce the index powers to reasonable level. In actual synthesis it was taken as  $10^8$ .

(5) Choice of sampling points and time resolution: The subroutine used for evaluating the FFT is capable for a maximum number of sampling points equal to 1024 and it was decided to make use of the whole number of points. Hence  $N = 1024$ . Therefore, time resolution is then given by  $\Delta T = \frac{T}{N} = \frac{5\mu\text{sec}}{1024} \approx 5\text{nsec}$ . We can also calculate the frequency period i.e.  $F = N \times \text{frequency resolution}$ . i.e.  $F = 0.2 \times 1024\text{MHz} = 204.8\text{MHz}$ . The centre frequency of the uniform transducer was selected to be equal to  $f_0 = \frac{1}{6\Delta T}$  so that there will be approximately six sampling points in each cycle of time response.

Having selected all the parameters in equation (3.11) we are now ready to perform the Fourier transform of the frequency response. Let us summarise the various parameters selected in order to perform the FFT operation.

Number of sampling points  $N = 1024$ .

Periodic time duration  $T = 5\mu\text{sec}$ .

Frequency resolution  $\Delta F = 0.2\text{MHz}$ .

Time resolution  $\Delta T \approx 5\text{nsec}$ .

Periodic frequency duration  $F = 204.8\text{MHz}$ .

Group delay  $t_0 = 2.5\mu\text{sec}$ .



Centre frequency of uniform transducer  $f_0 \approx 34.13\text{MHz}$ .

Lower frequency of IF characteristic  $f_1 = 29.4\text{MHz}$ .

Upper frequency of IF characteristic  $f_2 = 39.2\text{MHz}$ .

Frequency at sound trap  $f_s = 31\text{MHz}$ .

Maximum amplitude of IF characteristic = 100 siemens.

Maximum amplitude of  $W_1 \left| \frac{\sin x}{x} \right|$  response = 100 meters

(6) FFT operation for calculating  $F_2(t)$ : The method followed for evaluating the time response is similar to that indicated by Howard Helms [3]<sup>19</sup>. It is called "Four-T's" method i.e. Transform-Truncate-Transform-Test and is as follows:

(a) The frequency function in equation (3.11)

$$\left\{ \frac{K_2}{|\omega|} \frac{|y_{21}(\omega)|}{W_1 \left| \frac{\sin x}{x} \right|} e^{-j\frac{T}{2}\omega} \right\}$$

is calculated at the preformulated sequence of samples, in the range of interest i.e. in the passband and is set equal to zero outside this region. The spectrum due to negative frequencies is translated to the positive side of the frequency axis so that the overall response will have a complex conjugate symmetry over  $F/2$ .

(b) The inverse discrete Fourier transform of the above frequency response is computed using FFT routine. This produces a sampled response in time domain (can also be regarded as impulse response) with main lobe centred on  $\frac{T}{2}$  and the sidelobes extending on either side of the mainlobe. In an impulse response most of the energy is concentrated in the mainlobe and very little in the sidelobes: and also the amplitudes decrease very rapidly as they go further away from the mainlobe and tend to zero if the the periodic interval were taken to be infinitely large. Hence,

to make an inter-digital transducer corresponding to the complete impulse response is highly impracticable, since it requires a very large number of fingers and most of them will have a very small amount of overlap, compared to the maximum overlap. Therefore, it is necessary to truncate the sidelobes on either side of the mainlobe and the amount of truncation needed is a matter of trial and error method.

(c) Let  $NT$  be the number of sampling points of the central portion of the above time response we want to retain. The response at all other sampling points is set equal to zero. Note that  $NT$  will have to be selected in such a way that the symmetry of the response over  $T/2$  is maintained.

(d) The discrete Fourier transform of the above truncated time series is computed using FFT routine, producing a frequency response. Note that the frequency response occupies the whole frequency range 0 to  $F$  and the spectrum from  $F/2$  to  $F$  corresponds to the negative frequencies.

(e) The amplitude and phase response is calculated in the desired range of frequencies i.e. in the IF passband and is compared with that of the result in step (a). In particular observe the closeness of the result at the most critical regions namely at the edge frequencies and at the sound carrier frequency. The effect of truncation is an obvious advantage in the reduction of fingers but at the same time reduces the level of traps at the above critical frequencies, the most important one being at the sound carrier frequency.  $NT$  is varied and steps (c) to (e) are repeated until a best compromise is obtained. The best compromise will be to keep minimum number of sidelobes, following the mainlobe with reasonable level of trap at the sound carrier frequency. It was found that the sidelobes

are indeed necessary to provide the sound trap without which the sound trap is completely lost. Note that if  $NT$  is not taken to be symmetrical about  $(N/2 + 1)$ th point a phase error will result.

After a number of trails with different  $NT$ 's the truncated time response shown in Figure 3.3 is considered to be a best compromise between the number of fingers, number of sidelobes and the level of traps at the critical frequencies. Note that  $F_2(t)$  will have units of velocity. Total number of sampling points,  $NT$  for this response are 227 out of 1024 and the response is symmetrical about 513th point. The frequency response of the truncated time response is shown in Figure 3.4. This differs to some extent with the specified response especially the trap levels at the critical frequencies. Therefore, optimization techniques have been developed in Chapter 5 to improve the response by perturbing the amplitudes of the truncated time response.

Having obtained the time response of the output transducer the next task is to develop an approximate representation of the transducer finger configuration, i.e. we need to find the overlap length and gap-width for each pair of fingers. This is described in the ensuing section.

#### 3.4.4 Transducer Configuration

Transducer configuration we mean an approximate derivation of transducer geometry from the sampled version of the truncated time response. On examination of the computed results of Figure 3.5a shows that the time-response varies more or less uniformly having 3 to 4 sampling points in each half-cycle. It was decided that to represent one finger for each half-cycle so that one cycle corresponds to one finger pair. The distance between the centres of adjacent fingers, where the source function is assumed to have a maximum value, will be known as the gap-width of the finger-pair. These centres defined as electrical centres are the zero

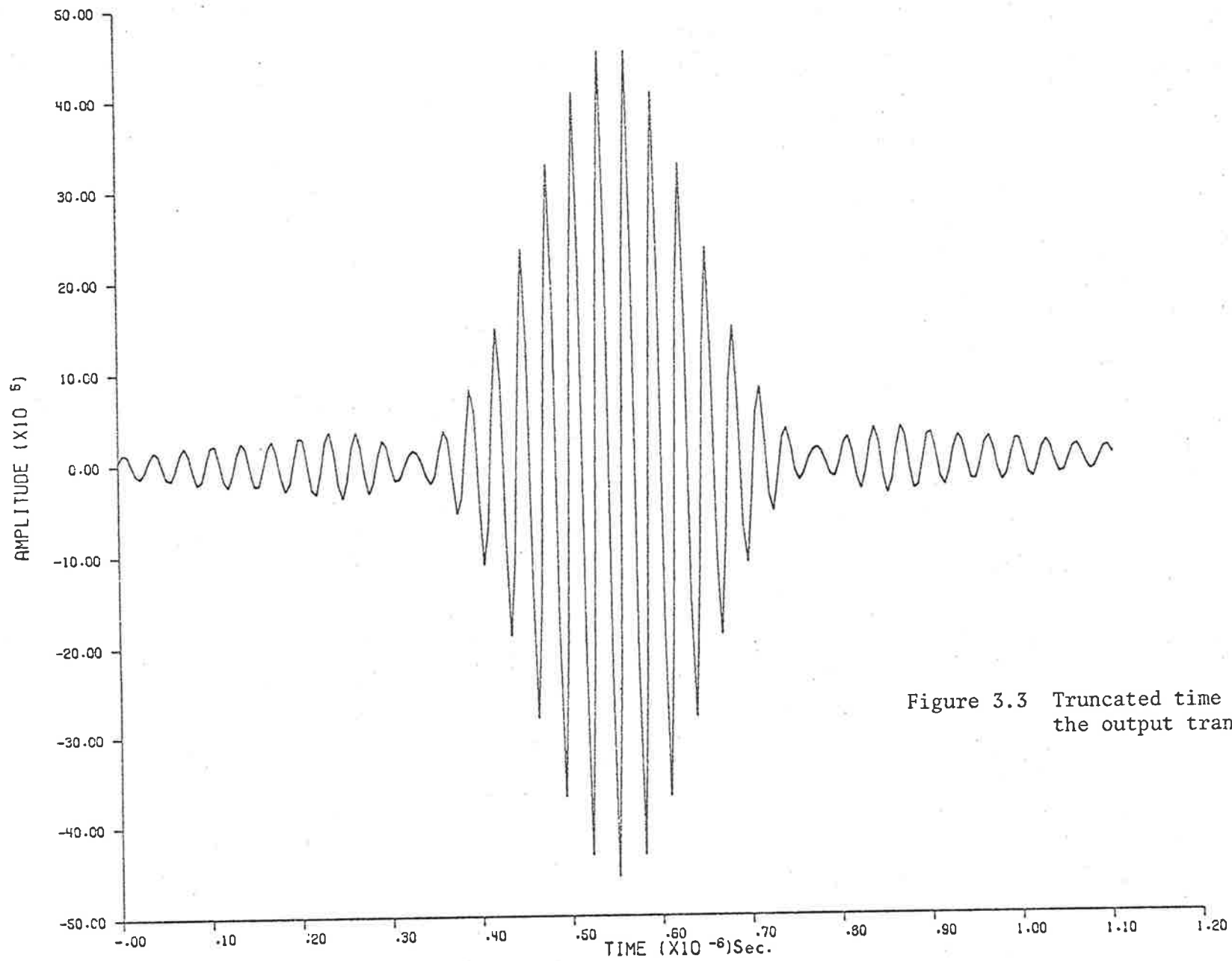
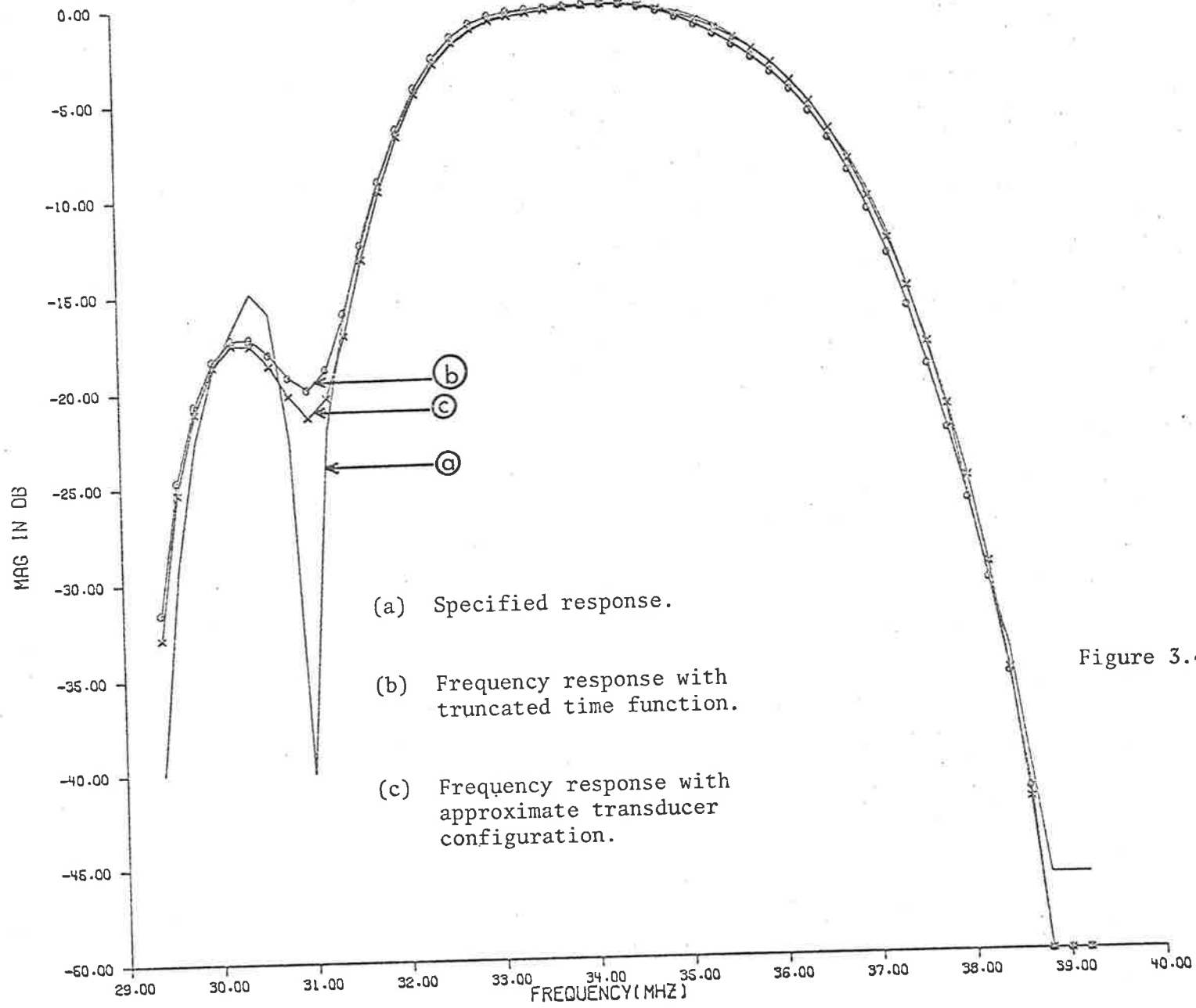


Figure 3.3 Truncated time response of the output transducer.



- (a) Specified response.
- (b) Frequency response with truncated time function.
- (c) Frequency response with approximate transducer configuration.

Figure 3.4 Theoretical performance of Filter 1, compared with the specified response.

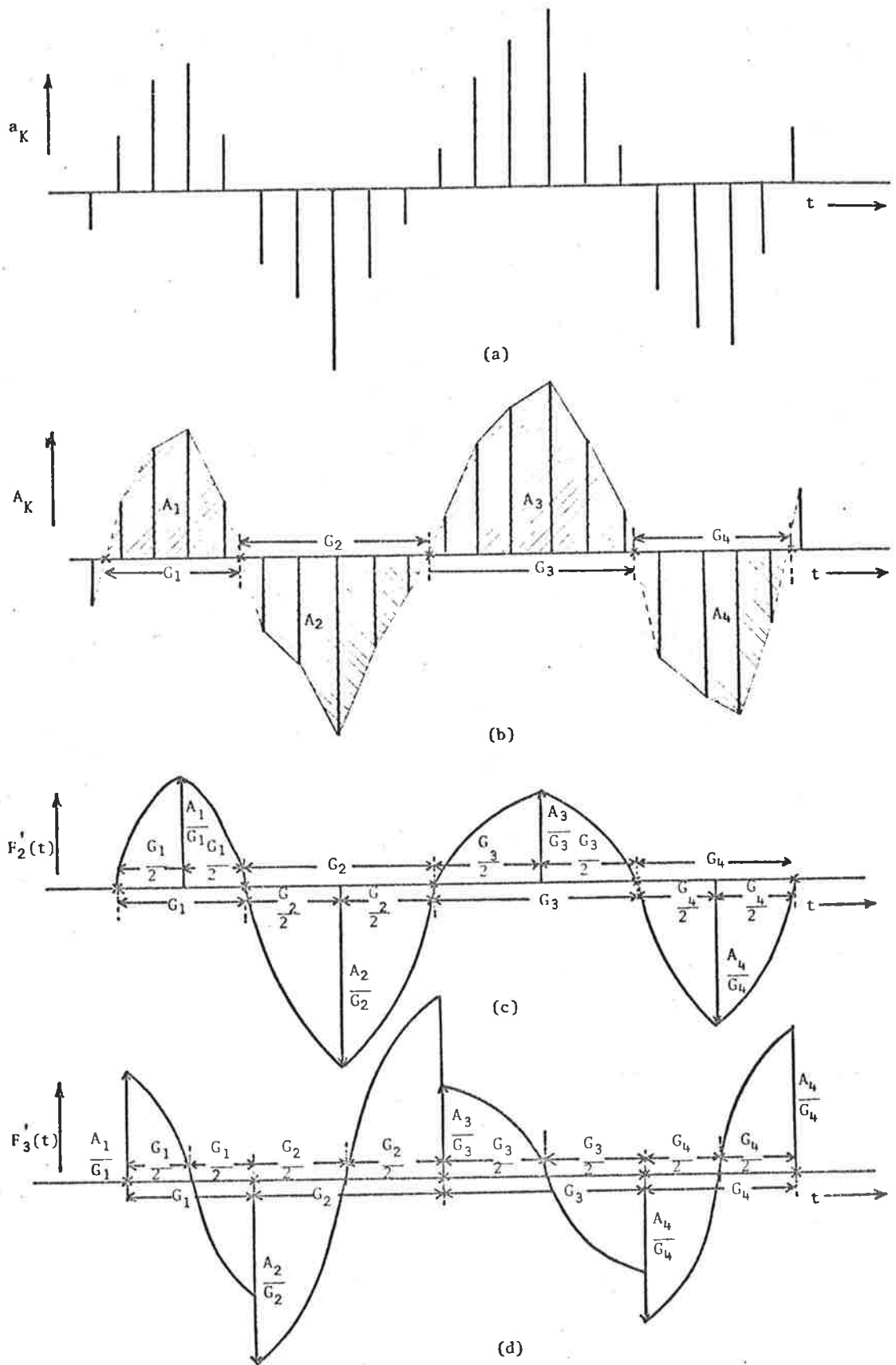


Figure 3.5 Source function representation from sampled response.

- (a) Sampled time response.
- (b) Overlaps and gap-widths of finger pairs.
- (c) Sinusoidal representation of source function.
- (d) Cosinusoidal representation of source function.

crossings of the time response i.e. where the response changes its sign. The zero crossings will be obtained by linear interpolation of the adjacent sampling points and hence the gap-widths, as shown in the Figure 3.5b.

The finger overlap can be obtained as follows. The source function equation (2.10) evaluated in  $z$  direction for an apodized transducer based on independent gap approximation can be written as,

$$f(z) = \frac{\pi(\epsilon_0 + \epsilon_p)}{1.854\epsilon_0} \sum_K \frac{W_K}{z_{K+1} - z_K} \cos \left( \pi \frac{z - z_K}{z_{K+1} - z_K} \right) \quad \dots (3.14)$$

but, as defined above  $z_{K+1} - z_K$  is the individual gap-width of the finger-pair. At the electrical centre  $z = z_K$  the finger overlap length  $\omega_K$  is proportional to peak amplitude of the source function multiplied by the gap-width. Hence, the finger overlaps can be selected by multiplying the peak amplitude in each half-cycle of the sampled time response with the corresponding gap-widths. However, we can also select the overlaps proportional to the total area under the envelope of samples in each half-cycle of the time response as shown in Figure 3.5b. Analysis, i.e. calculating the frequency response of the so selected transducer configuration with both the approaches, revealed that the later method of selecting overlaps gives a slightly better approximation to the specified response than the former method. Hence, selecting overlaps equal to the trapezoidal area of the samples between the zero-crossings for representing the finger-pattern is followed for the filter synthesized in this chapter and also for the optimized filters in Chapter 5.

#### 3.4.5 Analysis of Modelled Transducers

Having selected the appropriate overlaps and gap-widths of the apodized transducer it is necessary to evaluate the frequency response and compare it with that of the specified response to test the validity of so modelled transducer. The method adopted is briefly described as follows.

From the chosen overlaps calculate the peak amplitudes of the time response in each half-cycle by dividing by the respective gap-widths and place them in the middle of the zero crossings as shown in the Figure 3.5c. The time function is then constructed by assuming a sinusoidal representation between the zero-crossings and the peak amplitudes. The discrete representation of the continuous function is obtained by sampling the function at the appropriate sampling points and the frequency response is then calculated using FFT algorithm. The frequency response calculated thus for filter 1 is shown in Figure 3.4. The response compares well with the expected one (frequency response of the truncated time response), indicating the consistency of the assumed finger pattern configuration.

Another way of representing the time function from the given overlaps and gap-widths is shown in Figure 3.5d. The peak amplitudes are placed at the zero-crossings and the function is assumed to have zero value in between the zero-crossings. This allows us a cosine function representation in each gap-width. The source function representation in each gap of Figures 3.5(c) and 3.5(d) are identical except a 90 degree phase-shift in each gap-width. The Fourier transform of either functions Figure 3.5(c) or Figure 3.5(d) gives rise to approximately the same frequency response and we can adopt either representation for analysis of the transducer configurations. The first representation Figure 3.5c is used in the filter analysis before making the practical devices, while the second representation Figure 3.5d is used for predicting the behaviour of the practical filters. These different approaches have been followed for two reasons; firstly they give rise approximately same frequency response. This is because the source functions have been derived on an independent gap approximation and if the ratio of the adjacent gaps is approximately unity, which is the case in this filter synthesis, either representation will give rise to approximately the same result. Secondly, it was thought in the initial stage that the first representation is more appropriate and



programs have been developed and kept on permanent files. Later on it was found that the second representation is more exact and programs have been developed accordingly. Testing the various examples with both the approaches revealed approximately same results and hence it was decided to keep using both methods instead of modifying the program written for the first approach. Moreover, it does not influence the filter synthesis or the analysis of the device, it indicates only a rough estimate of the frequency response of the adopted time function.

#### 3.4.6 Computer program of Filter 1

A computer program has been developed to carry out the various stages described so far for Filter 1, and a flow-diagram is shown in Figure 3.6. The computer used is CDC6400 installed at the University of Adelaide, Adelaide. The program is written in FORTRAN IV language amenable with a RUN compiler. The main program and the various subroutines necessary, have been developed by the author except the FFT routine, which has been obtained elsewhere. The program generates an optimum truncated sampled time response for a specified frequency response and then calculates the overlap-lengths and the gap-widths for generating the finger pattern and finally analyses the so generated transducer configuration. A listing of the program is not included along with the other listings in the appendices, since this program is very much similar to the programs developed in Chapter 6 except for the optimization techniques. In other words the programs developed for optimized filters will always include the programs developed for Filter 1, and hence, it was felt that a separate listing for Filter 1 is unnecessary.

One important point to be noted while dealing with FFT is the proper choice of aliased function  $F_p(f)$  (equation 3.12). Aliased function we mean a periodic function formed by the superposition of the nonperiodic function  $F_c(f)$ , shifted by all multiples of a fundamental period, i.e.

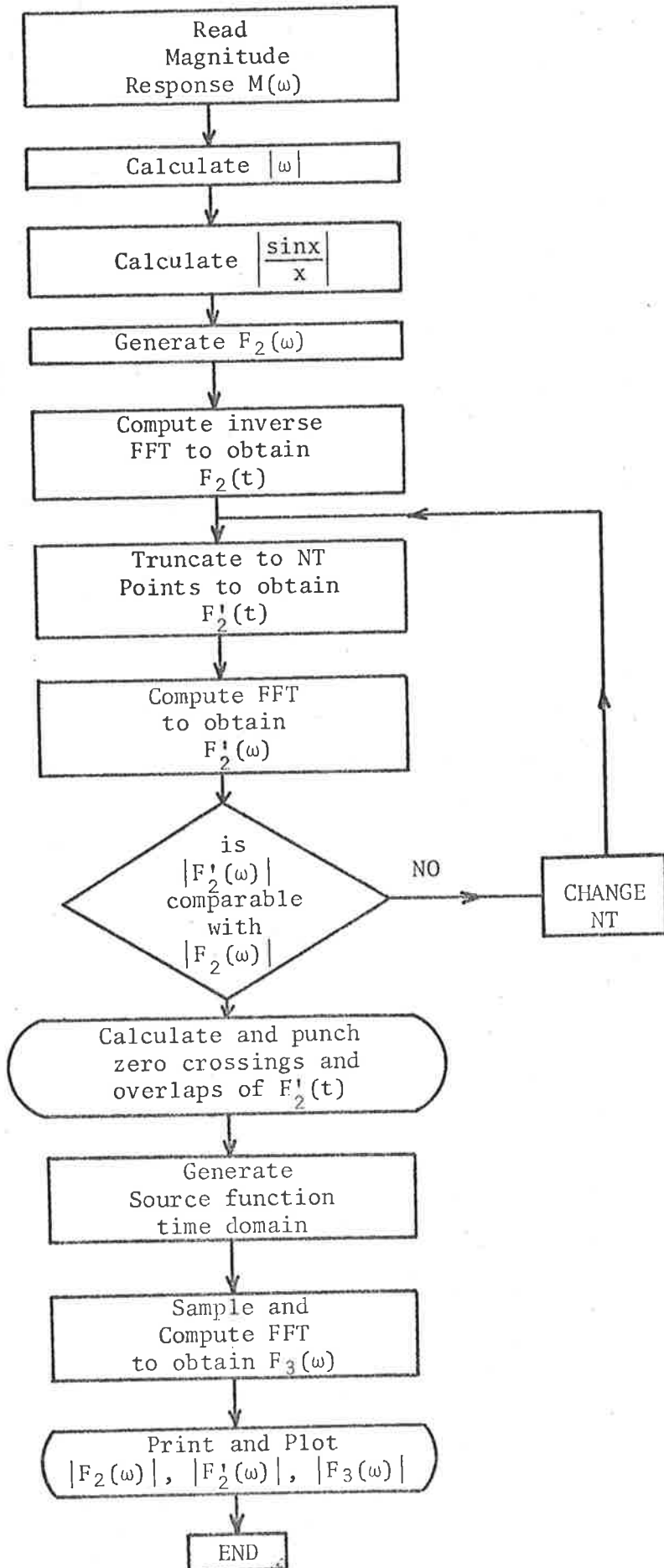


FIGURE 3.6

$$F_p(f) = \sum_{-\infty}^{\infty} F_c(f + KF) \quad \dots(3.15)$$

where  $F$  is twice the Nyquist frequency,  $1/2\Delta T$ . However, in FFT the periodic range is taken to be equal to zero to  $F$ , the negative  $f$ -half of  $F_c(f)$  is produced to the right of the positive  $f$  half of  $F_c(f)$ :

$$F_c(f) \approx F_p(f) \quad 0 \leq f \leq \frac{1}{2} F \quad \dots(3.16)$$

$$F_c(f-f) \approx F_p(f) \quad \frac{1}{2} F \leq f \leq F$$

From equations (3.12) and (3.13) it will be noted that periodic function  $F_p(f)$  is constructed by adding the set of functions  $F_c(f + KF)$  for  $K = 0, \pm 1, \pm 2, \dots$ . Hence, the error in approximating  $F_p(f)$  by  $F_c(f)$  in the range  $-\frac{1}{2} F < f < \frac{1}{2} F$ , is the sum of the  $F_c(f + KF)$ 's for  $K \neq 0$ . Thus, by choosing  $T$  small enough,  $F = \frac{1}{\Delta T}$  can be made sufficiently large so that this error is negligible in the frequency range of interest. This proper choice of  $F$  is the first choice to make in applying the algorithms. In order to minimize the error due to aliasing  $|f|$  must be greater than  $\frac{1}{2} F$ . For TV IF filters the frequency range is approximately from 30 to 40MHz and the fold-over frequency ( $\frac{1}{2} F$ ) must be at least greater than 40MHz. In the actual filter synthesis the fold-over frequency was selected to be equal to 104.2MHz which is much greater than 40MHz and hence, we can expect the errors due to aliasing will be negligibly small.

## CHAPTER 4

## EXPERIMENTAL AND COMPUTED RESULTS OF A TV IF FILTER

4.0 Introduction

The discussion so far has been directed principally towards the synthesis of a TV IF filter with a simple truncation in the time response of the apodized transducer. The design, however, does not yield a good agreement with the specified response as a result of the truncation operation. Before proceeding further to improve the response by optimizing the truncated version of the time response it was felt that it is better to test the validity of the admittance formalism for the filter concerned through a practical device and also to gain familiarity with the photofabrication technique which is necessary to build any surface acousticwave device. The fabrication process, basically, consists of optically polishing the single surface of the piezoelectric substrate, evaporating or otherwise depositing a metal film, and then patterning the metal to form the required transducer structures using standard photolithography techniques (4)<sup>4-6</sup> which have been highly developed for the semiconductor industry. The process is very inexpensive, highly repeatable, and most important, it can be used to produce line widths down to about 1.5  $\mu\text{m}$  corresponding to a transducer centre frequency of about 500 MHz for quartz or lithium niobate substrates.

However, the facilities available in this Department are very limited, developed for prototype manufacture of delay lines, but adequate enough for laboratory purpose for the frequencies up to 100 MHz. The actual facilities available in the laboratory, the author's contributions towards some of the developments in this area and the various steps followed in manufacturing the filters are given in Appendix B. Only the essential design considerations and the experimental performances of the filter are presented in this Chapter.

#### 4.1 Choice of Suitable Substrate and Propagation Direction

The most important consideration in a surface acoustic wave device is the choice of a suitable material and the propagation direction. There are several factors which need to be investigated in the choice of a suitable material for implementing in the industrial production, but we will not go into details in this aspect. However, we will mention the reasons for choosing a particular material and propagation direction for our laboratory experimental purpose.

Single crystal  $\alpha$ -quartz has been selected for use in the experiments on the basis of its relatively low cost and ready availability. Quartz is one of the most suitable materials for surface wave devices because of its low temperature co-efficient, chemical inertness and low signal attenuation. Despite the fact of its low electromechanical coupling co-efficient compared to some of the newer synthetic materials, its choice did permit advantage to be taken of its relatively greater durability, with regard to physical, thermal and chemical damage, in the fabrication processes and the experiments. Further, the choice of a low coupling material is necessary to test the validity of the admittance formulasim

Once the material has been selected the next question comes the choice of a suitable orientation for cutting the blanks and the direction of propagation of the wave vector on these blanks. A 'Y' cut zero rotated X propagation (YX) substrates have been selected for the filter experiments because of the accurate surface wave solutions are available for this configuration (4)<sup>1-4</sup> Moreover, it was decided to use fairly long delays (of the order of 10  $\mu$ sec) for convenience in the long pulse simulating CW measurements and also to ensure plane wave propagation which in turn require large size substrates. The YX quartz substrates of dimensions 1" x 1 $\frac{1}{2}$ " x 1/8",

optically polished on both sides, were obtained from SAWYER RESEARCH PRODUCT, INC., OHIO, U.S.A. Polishing on both sides is actually not necessary, but it was found beneficial in the repeated use of the substrates in the fabrication process.

#### 4.2 Design and Fabrication of the Delay Line

The fabrication of interdigital transducers requires the location of a grid of thin conducting electrodes, with suitable connections at the ends of the electrodes depending upon the grid phasing on the polished surface of a piezoelectric substrate. The whole process can be broken down into a series of steps as indicated below: -

- (1) Prepare the artwork.
- (2) Photograph the artwork on a suitable camera to make a photographically reduced working image of the desired pattern.
- (3) Evaporate a suitable metal film on the polished surface of the substrate.
- (4) Apply a thin coating of the photoresist solution on the metal surface.
- (5) Expose photoresist-coated surface to ultraviolet light, using the photographically reduced negative.
- (6) Develop the exposed photoresist in the proper developer.
- (7) Etch away the unexposed metal, leaving the pattern on the substrate.
- (8) Strip the photoresist from the pattern.

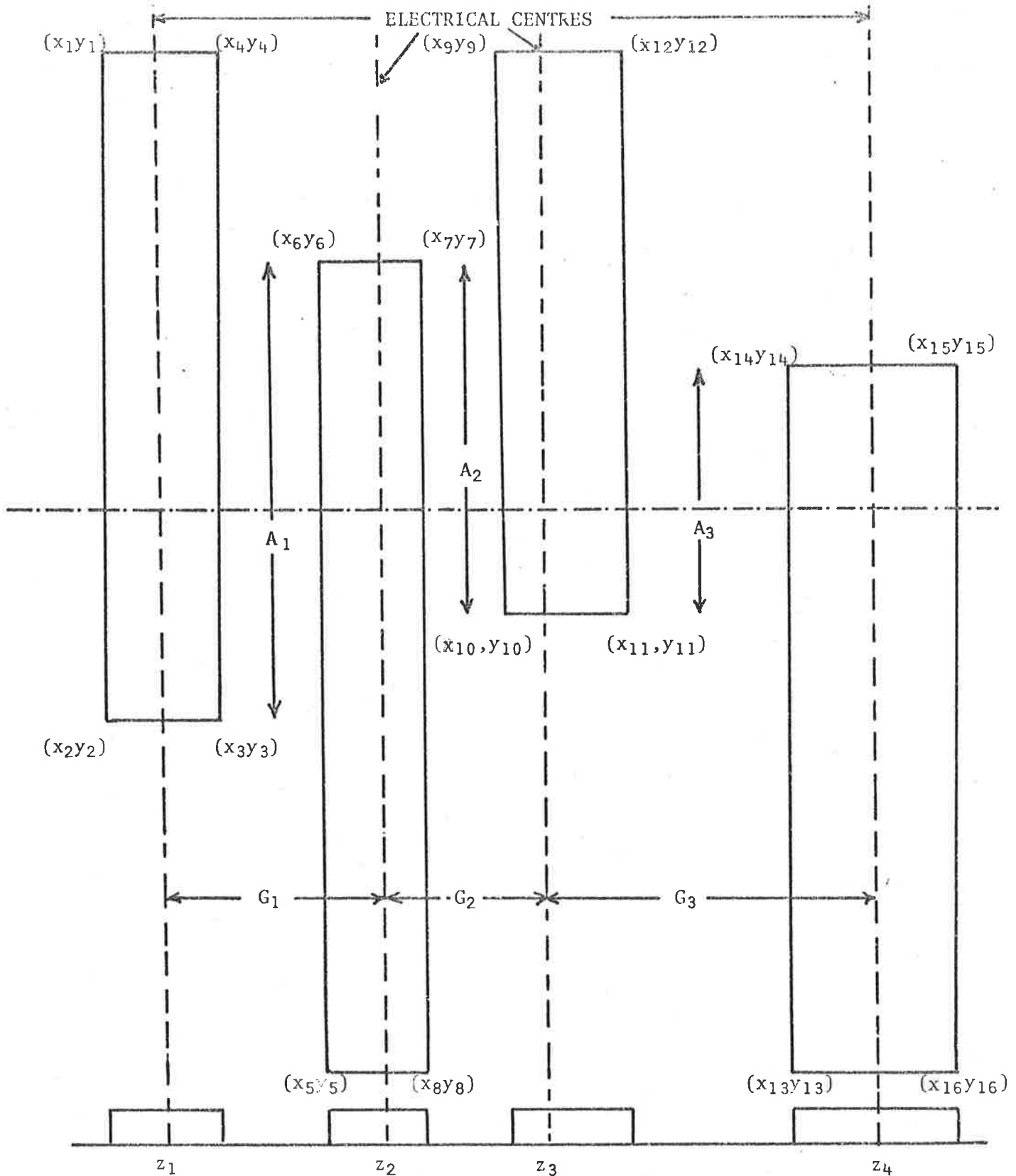
The techniques involved in each of these steps are clearly described in the Appendix B, except the preparation of the artwork which is described in the following section. The preparation of artwork for Filter 1 is different from that of the other filters described in Chapter 7. For Filter 1 the final transparency is produced in a two stage reduction process, while for other filters, it is produced in a single stage reduction thereby reducing considerable amount of time in photographic process.

#### 4.2.1 Preparation of the Artwork

First of all it is necessary to know the transducer finger geometry, i.e. the length and width of each finger in the transducer from the given gapwidths and overlaps (Program Filter 1, Chapter 3), for preparing the artwork. An illustration of calculating the boundaries of the fingers with the given gapwidths  $G_i$  and overlaps  $A_i$  is shown in Figure 4.1. Each finger is specified by a set of four pairs of co-ordinates and metalization has to be done within this set. It is to be noted from Figure 4.1 that a wider gap will produce a wider finger while a narrower gap will produce a thinner finger; thus maintaining nearly equal mark-space ratio in the entire pattern. The finger lengths are, of course, dictated by the given overlaps. For uniform transducers lengths, widths and spacings are all equal.

#### Design considerations in generating the mask

The original size of the finger pattern to be generated on the mask depends upon the available photographic equipment viz. the size of the copy board, the reduction ratios available on the cameras, and the size of the substrates onto which we wish to deposit the desired interdigital transducer finger configuration. The copy board size is 30" by 40" and the final transparencies used in the photofabrication are of size 2" by 2" Kodak high resolution plates. Various reductions are possible through two microphotographic cameras as mentioned in Appendix B. The quality of the final product greatly depends upon the quality of the original drawing and in the interest of minute details it is desirable to produce the artwork as large as possible and then reduce it to the final working size. However, using large reductions have other problems like producing barrel distortion and it is advisable to select an optimum reduction for a specific pattern. The author has contributed to calibrating the two cameras (as mentioned in Appendix B) and developed an optimum



$$\begin{array}{cccc}
 x_1 = x_2 = z_1 - \frac{G_1}{4} & x_5 = x_6 = z_2 - \frac{G_1}{4} & x_9 = x_{10} = z_3 - \frac{G_2}{4} & x_{13} = x_{14} = z_4 - \frac{G_3}{4} \\
 x_3 = x_4 = z_1 + \frac{G_1}{4} & x_7 = x_8 = z_2 + \frac{G_1}{4} & x_{11} = x_{12} = z_3 + \frac{G_2}{4} & x_{15} = x_{16} = z_4 + \frac{G_3}{4}
 \end{array}$$

The y coordinates are calculated with reference to a central axis.

Figure 4.1 Calculation of Coordinates for Plotting the Transducer Finger Pattern.



photographic process in each case.

For the filter concerned the maximum overlap for the apodized transducers is assumed to have a length of 50 wavelengths which corresponds to roughly 5mm and a minimum non overlap length of 1.25mm is selected for the connecting pads. The pattern is assumed to have 69 fingers occupying a length of roughly 3.5mm. Assuming a reduction ratio of 60 the pattern occupies an area of roughly 10" x 20" (without connecting pads) which is well within the dimensions of the copy board. Selection of a higher reduction ratio is possible but considering the optimum reduction ratios and for the other reasons mentioned earlier, the choice of 60 seems to be most appropriate.

It was decided to have a delay of approximately 7.5  $\mu$ sec between the transducers corresponding to a distance of about 50" after 60 reduction ratio and clearly we notice that both the input and output transducer patterns cannot be considered at the same time for photographic purpose. The calculation of co-ordinates for the uniform transducer is straight forward once we know the surface wave velocity and the centre frequency. The length of the uniform overlaps are, however, increased by about 25% of the maximum overlap length in the apodized transducer to take into diffraction effects due to the transmitting transducer.

#### Mask generation

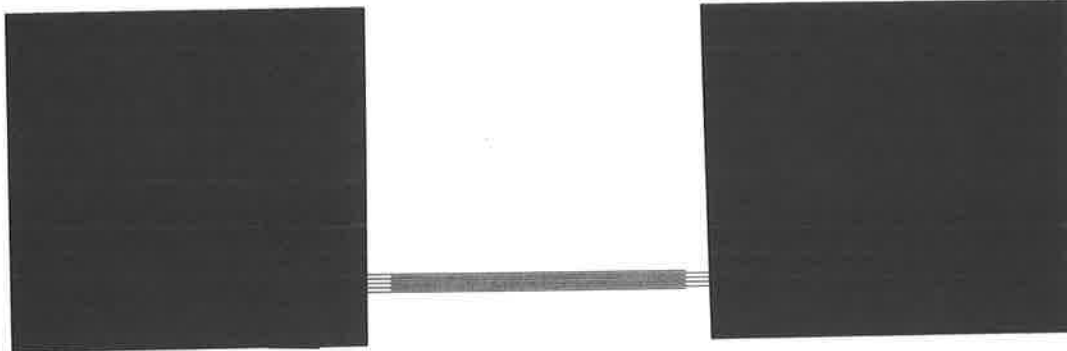
Having calculated the various co-ordinates for the uniform and apodized transducers, the next task is to prepare a master drawing or artwork for the photofabrication. There are several methods available ranging from simple hand drafting technique to automated or semi-automated drafting machines known as co-ordinatographs. In the early attempts of this project, patterns were cut directly onto Rubylith sheet by hand and it was found that it is quite tedious, especially when cutting fingers with varying widths and overlaps, and the results were not satisfactory in the final device.

Hence, a computer program developed by A.S. Burgess (4)<sup>4</sup>, suitably modified by the author to draw any number of fingers with any given reduction ratio, is used to generate the pattern on a 30" triacetate plastic sheet which can be mounted directly on the copyboard. A listing of the program, which calculates the required co-ordinates for the uniform transducer as well as for the apodized transducer with the given overlaps and gapwidths and then generates the required pattern suitable for a single stage reduction, is given in the Appendix A1 and is named as Program ARTWORK. The program plots only the pattern and the contact pads have to be provided by other means, the easiest way is to cut the Rubylith sheet to proper size and adhere it to the pattern. It is to be noted that for the filter concerned here the reduction ratio was selected to be 60 and as this cannot be achieved in a single stage, a two stage reduction (3x20) has to be adopted in the filter fabrication process. Accordingly, some of the parameters given in the program ARTWORK of Appendix A1 need to be changed. The required changes are the change in reduction ratio and the change in the pen tip size. These changes were implemented in the program and a master pattern was generated by the computer which is ready for other steps of photofabrication as described in Section 4.2. The filter configuration used for making the delay line is shown in Figure 4.2

#### 4.2.2 Description of Delay Line Fabrication

An outline of the delay line fabrication is presented, but exact description regarding the equipment used, details of the chemicals and processing times, etc. may be found in Appendix B.

The individual input and out transducer patterns generated by the computer were separately reduced by the first stage camera (3X) on to the 10"by 8"Kodalith Ortho Film, contact printed, suitably aligned, contact pads were added and then reduced to the final size by the second stage camera (30X) on to the 2 by 2 Kodak High resolution Plates (4)<sup>8</sup>.



P/09/110

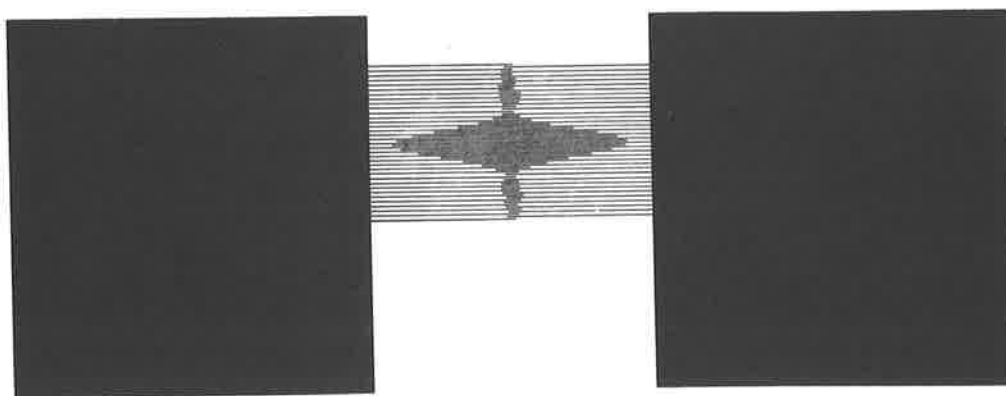


Figure 4.2 Transducer configuration of Filter 1.

A thin Aluminium metal film was then vacuum deposited on the polished surface of the substrate. The thickness of the film was designed to be of the order of  $0.1 \mu\text{m}$ . The Aluminium metal was selected for the thin film deposition because it was found that it gives a good adhesion to the surface of the substrate.

A resist film was then applied on the metal film, and the crystal was made to rotate on a spinning plate to ensure uniform thickness and then it was dried in a hotplate.

The next step was to expose the resist to ultraviolet lamp through the photo-mask made. This was carried on through the exposure jig and the lamphouse containing the UV source.

After development of the resist image according to the best prescriptions established in this laboratory, the last step was to etch away the metal to be removed. The part of the film constituting the transducer pattern was protected by the resist so that it was not easily removed by the etching fluid. A special etching solution was used for this purpose.

The final stage in the device fabrication was to remove the resist film without damaging the electrodes and this was done by immersing the crystal in a proprietary resist solvent solution and then drying it in a clean cabinet.

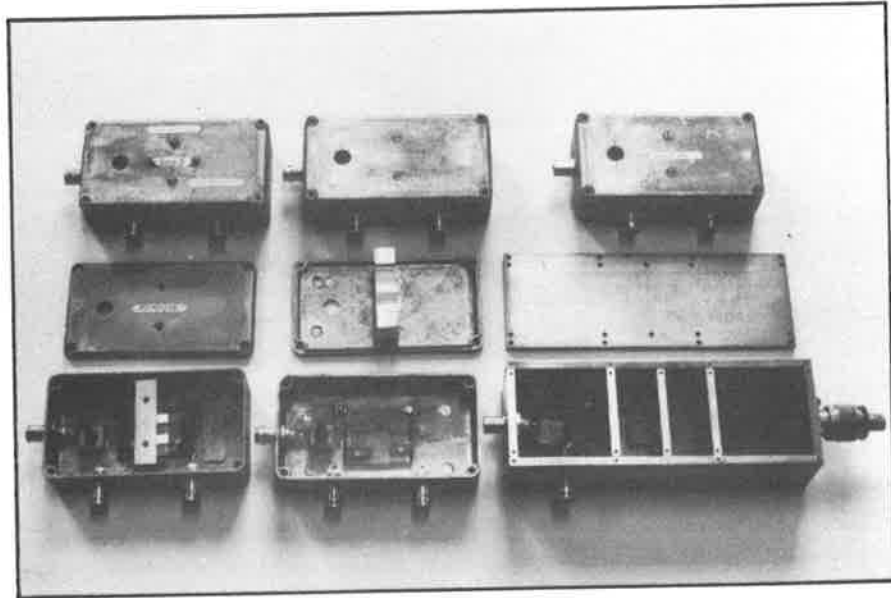
#### 4.3 Frequency Response Measurement

Having manufactured the SAW filter we are now interested in measuring the transmittance between the input and output transducer structures and compare it with the theoretical result as obtained in the last Chapter. The transmittance can be deduced by measuring the output voltages of the filter with a suitable load resistance or in other words by measuring the frequency response of the filter. However, some preliminaries are necessary before setting up the experimental work and these are indicated in the following sections.

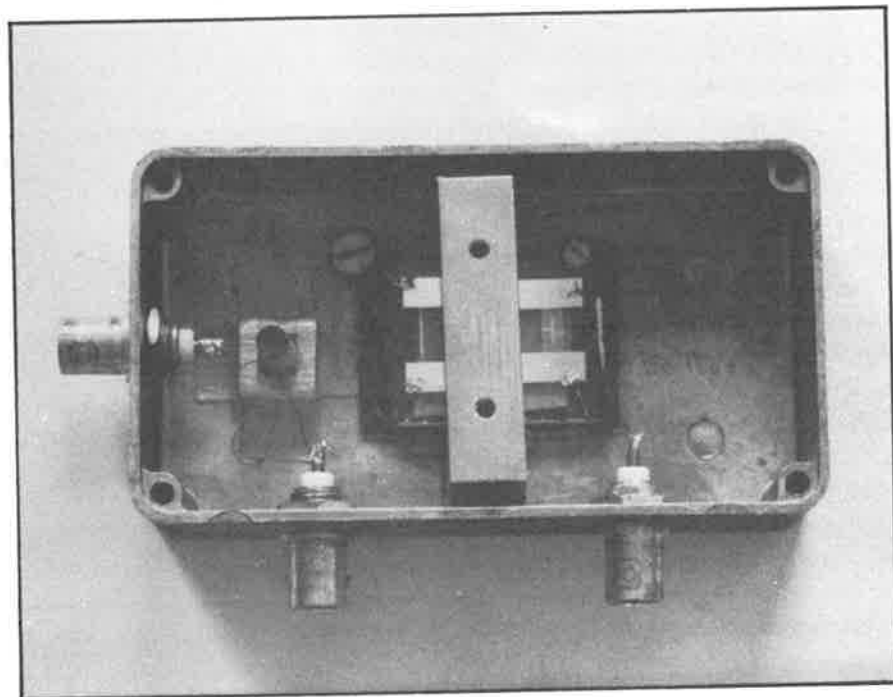
#### 4.3.1 Mounting Techniques

The first consideration is the design of a suitable jig for mounting the crystal (Filter) and appropriate connections according to the chosen set of experimental procedure. Care must be taken in designing the mounting jig, so that the crystal is adequately protected from possible accidental damage during the experimental investigation. In fact, it is worth sealing the crystal in a separate compartment and bring out the leads from the transducer pads, for connecting the filter to the external circuitry. Screening between the input and output transducer structures must also be taken into account while designing the mounting jig. Since there is a large separation between the structures an aluminium block of about half-inch thickness is used as the screening material between the two patterns. On one side of the aluminium block, a groove was machined approximately of the same height and width of the substrate and is bolted to one surface (top or bottom) of the jig. This arrangement provides that the nonmetalized surface between the input and output transducer structures is nearly in contact with the aluminium block providing good shielding between the input and output wiring thus minimizing the capacitive coupling between the two transducer structures. The arrangement may be seen in the Figure 4.3.

The crystal was held in position by a masking tape arranged in a double sided adhesive manner through a number of layers approximately of the same length as the substrate. The number of layers give some sort of spring type pressure which can be increased or decreased to hold the crystal in contact with the metal screening and at the same time avoids the possibility of breaking the crystal when trying to bolt the screening tightly to the mounting box.



(a)



(b)

Figure 4.3 (a) Some of the experimental mounting jigs used for measuring the frequency response of the filter.  
(b) Closer view of a typical jig showing the metal screening between the input-output transducer.

Gold wire of 0.127 mm diameter was used for connecting the transducer pads to the external connections and the method followed was to use pure indium solder (4)<sup>9</sup> (without any flux) with a low temperature soldering iron. Although the bond strength was quite low with this method, it was found that it is quite convenient to make or alter connections without any damage to the filter aluminium pads.

In many experiments involving long pulses or CW signals, it is desirable to avoid or minimise the backward travelling waves which cause undue interference with the incoming signal, and this can be done in a number of ways. It was found that edge reflections could be reduced by polishing a radius (large relative to the SAW wavelength) on the edge concerned or by applying an absorber such as adhesive masking tape or black wax (apiezon W). The last method is followed for this filter and other filters developed in Chapter 7. The black wax was applied on either side of the substrate by melting with a low temperature soldering iron. Some of the mounting jigs developed are shown in Figure 4.3. Provision was also made to include tuning networks in the mounting jigs and these will be discussed in the next section.

#### 4.3.2 Tuning Circuits

Tuning circuits in general are not desirable, especially in filter applications, since they cause unnecessary rounding of the filter response at the bond edges, but unavoidable when using high impedance ( $\text{low } K^2$ ) transducers into a low impedance measurement system. We wish to measure the transadmittance  $y_{21}(\omega)$  as accurately as possible so that the complete behaviour of the filter is known, particularly the deep trap levels at the sound carrier frequency and at the adjacent channel carrier frequencies. Untuned measurement with low source and load impedances, restricts the estimate of these deep traps, owing to high insertion loss of the filter (with  $\text{low } K^2$  material). On the other hand, if we use a tuning and matching circuit, with a high impedance termination on the output side, an accurate measurement

of  $y_{21}(\omega)$  is again difficult. The basic assumption of low impedance requirement in the derivation of the transadmittance formula is violated, moreover with high load impedences, the second and higher order responses will come into picture and make it difficult for an accurate measurement of  $y_{21}(\omega)$ . Therefore, a low impedance measurement system, with a  $50\Omega$  termination, without any tuning circuit on the output side is followed in this experimental procedure. A block diagram of which is shown in Figure 4.4 standard co-axial cables with  $52\Omega$  characteristic impedance,  $100\text{pf}/\text{m}$  are used for connecting the various instruments.

A single inductor tuning is employed on the input side; this will reduce the insertion loss of the filter to some extent and removes some of the difficulties mentioned in the measurement of  $y_{21}(\omega)$ . Since large voltages are available on the input side, we can use high impedance capacitive probe for measuring the voltages, and once we measure the voltages the high impedences does not enter in the  $y_{21}(\omega)$  measurement. A similar measurement system on the output side cannot be followed for the reasons mentioned in the first paragraph. In fact, the output transducer is directly connected to the preamplifier through a short cable with a  $50\Omega$  termination.

These are the reasons why we treated the input-output circuits separately. Note that the frequency response of the filter, defined as  $y_{21}(\omega) \cdot R_L$  does not depend upon the input tuning circuit.

A single variable inductor is employed for tuning the input circuit of the SAW filter. The variable inductance was obtained by winding 39 SWG copper wire on (722/1) bakelite formers using Neosid screw cores (4x5x12.7/F29). This assembly is well suited for tuning over the entire IF passband and the number of turns required is to be determined in accordance with the total capacitance on the input side. Hence, an accurate calculation of capacitance is necessary for the required adjustable inductance.



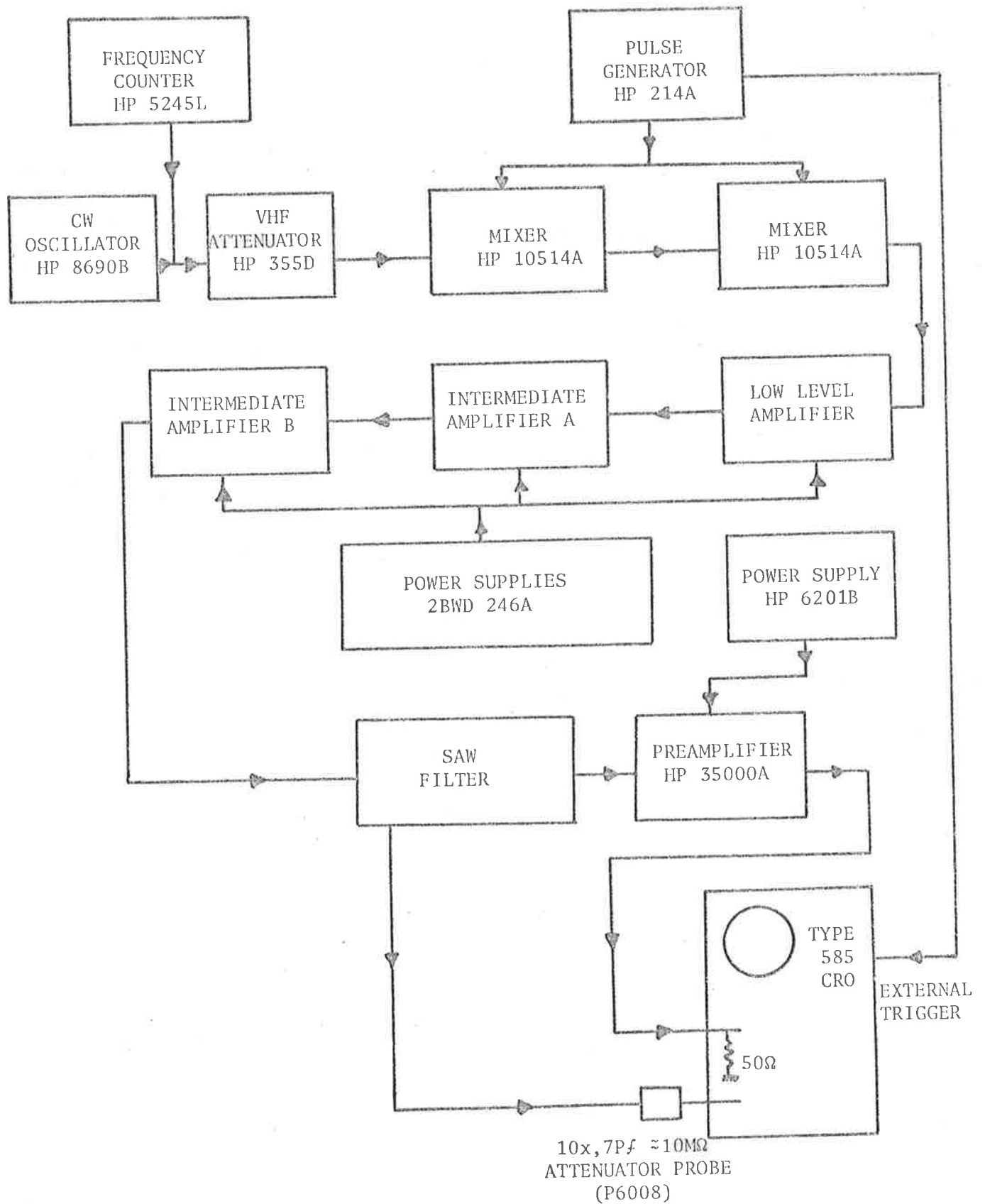


Figure 4.4 Block diagram of experimental setup for measuring the frequency response of the SAW filter.

The various capacitances incurred are (1) Input transducer static capacitance, (2), BNC connector capacitance on the filter assembly (jig), (3) The capacitance of the high impedance probe used for monitoring the input voltage on the transducer (see Fig.4.4), and (4) the various stray capacitances. The various capacitances were measured using a WAYNE KERR VHF Admittance Bridge and an estimate of total capacitance was made by adding all these capacitances and then the required inductance range was calculated for the range of frequencies concerned. Suitable number of turns were then wound on the 'former' to cover these frequencies for tuning purposes, once again measuring the inductances on the VHF Bridge. The tuning assembly may also be seen in the mounting jig shown in Figure 4.3.

#### 4.3.3 Calibration of Instruments

The accuracy of the transadmittance ( $|y_{21}(w)|$ ) measurement depends upon the accuracy of the equipment used (particularly on the output side of the transducer) in the experimental set-up and, therefore, it is necessary to calibrate the various instruments, at least the essential ones and thus ensuring minimum error in the measurement procedure.

For measurement of  $|y_{21}(w)|$  we need an accurate measurement of the input and output voltages across the transducer and the absolute value of the load admittance across the output transducer. Since the input - output voltages are measured on the Tektronix Oscilloscope, Type 585, the first calibration needed is the gain calibration of the channels A and B of the above oscilloscope (not the internal attenuators). The input voltage is measured using an high impedance attenuator probe (10x, 7 pf  $\approx$  10M $\Omega$ , P6008), hence, the next calibration required is the calibration of the high impedance probe.

The output voltage is measured across the output of the HP3500A amplifier terminated in a  $50\Omega$  load impedance. Therefore, apart from the gain calibration of the HP3500A amplifier, calibration of the input admittance of this amplifier with a  $50\Omega$  termination is necessary. Since the amplifier is directly connected to the output of the transducer, the input admittance of the amplifier (with  $50\Omega$  termination) forms the load admittance across the output transducer and, therefore, the measurement of the input admittance and the gain of the HP3500A amplifier plays a significant part in the accurate measurement of the  $|y_{21}(\omega)|$ .

The above instruments were calibrated carefully before the measuring the frequency response of the filter. The input admittance of HP3500A amplifier (with  $50\Omega$  termination) was calculated once again using WAYNE KEER VHF Admittance Bridge at the various frequencies.

Apart from the instrument calibrations, the circuit parameters on the output transducer side, which form the part of the load admittance, for example the capacitance and inductance of the external wiring up to the preamplifier (HP3500A), are also to be calculated before the measurement of the voltage transfer ratio. The static capacitance of the output transducer is also measured, which is necessary to include in the equivalent for the transducer configuration.

#### 4.3.4 Measurement Procedure

The standard apparatus used for evaluating the performance of the filter is shown in the block-diagram 4.4. The filter was excited with a pulse generator of  $50\Omega$  source impedance and the output voltage was observed after amplifying it through an amplifier. A schematic of the voltage measurement system of the filter is shown in Figure 4.5A. The filter was tuned to the centre frequency and initially, a very short pulse of RF signal was applied to the transmitting transducer to facilitate the identification of the undesired

propagating modes reaching the receiving transducer and also to verify the phase linearity of the output signal. The sidelobes were found to be very symmetrical, indicating the phase linearity of the filter and it was also found that the electromagnetically coupled signals (capacitive pulse) and the other spurious signals are negligibly small compared to the acoustic signals, ensuring that the techniques followed, mentioned in the earlier sections are well suited. The measurements were then performed using very long pulses simulating CW signals.

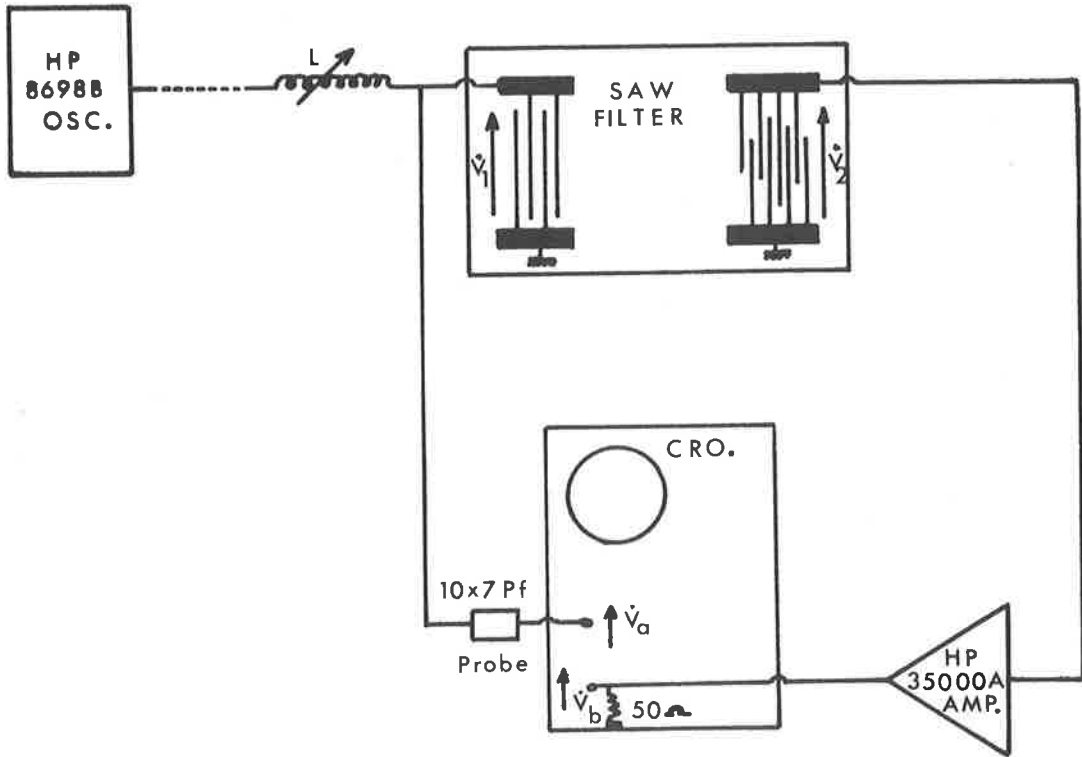
- (a) set HP8698B oscillator to desired frequency.
- (b) Tune L to obtain a large output response on the flat section of the output pulse. Ignore the initial and final transients.
- (c) Measure the input voltage  $\dot{v}_A$  and output voltage  $\dot{v}_B$
- (d) Interchange CRO inputs and re-measure voltages  $\dot{v}_A$  and  $\dot{v}_B$ .
- (e) Average the voltages  $\dot{v}_A$  and  $\dot{v}_B$  for the two different CRO connections and tabulate the results.
- (f) Go to step (a) and repeat to cover the various frequencies.

A typical oscilloscope picture for input, output signals at the centre frequency of the Filter 1 is shown in Figure 4.5b. The RF pulses of length 5.4  $\mu$ sec and amplitude 20V peak to peak were used in this experiment. The Tektronix oscilloscope Type 585 enabled us to measure readings down to 0.004V peak to peak which nearly occurred at the band edges of the IF response, beyond that it was found difficult to measure any readings.

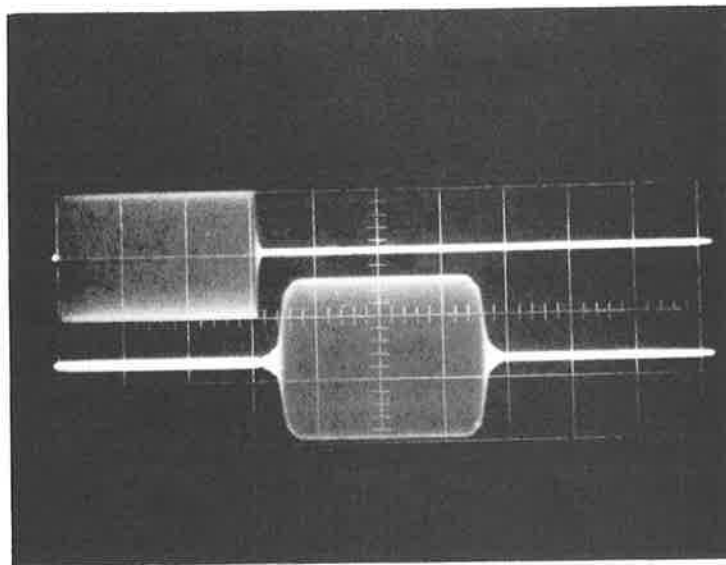
The other measurements carried out at this stage were the group delay between the input, out transducers, the approximate phase velocity of the surfacewave device, and the actual size of the pattern on the substrate compared to the designed value viz the achieved reduction ratio. The group delay can be measured by applying an extremely short pulse to the transmitting transducer, tuned to the centre frequency and measuring the time delay of the received pulse by 'Time Delay Multiplier facilities' on the oscilloscope. The group delay obtained in this manner was found to be approximately equal to 7.8  $\mu\text{sec}$ . The phase velocity can be obtained by measuring the distance between centres of the two transducers on the substrate with the help of a precision travelling wave microscope, and dividing the distance by above group time delay. The velocity obtained in this fashion was found to be equal to 3.145 km/sec. The reduction ratio can be obtained by measuring the distance between centres of the two transducer on the original art-work and dividing it by the corresponding distance on the substrate. The reduction ratio in this case was found to be equal to 63.3 against the designed value of 60.

No attempt was made to measure the input admittance parameters (radiation conductance and susceptance) of the uniform or apodized transducers, since they are negligibly small compared to the static capacitive reactances, hence they are neglected in evaluating the transmittance from the measured quantities. However, in the later part of the thesis (Chapter 7) computer programmes were developed to calculate theoretically these values for the uniform and apodized transducer structures.

The frequency response or the transfer function of the filter is simply obtained by the voltage ratio  $\hat{v}_2/\hat{v}_1$ , (Fig. 4.5a), which can be calculated from the measured values of  $\hat{v}_A$  and  $\hat{v}_B$ , knowing the gain of the amplifier and the attenuation of the high



(a)



(b)

Figure 4.5 Measurement of voltages.

- (a) Block diagram for measuring the input-output voltages of the filter.
- (b) Typical oscilloscope traces of long pulse CW simulating signals. Upper trace is the input signal (vertical scale 20V per cm). Lower trace is the acoustic output signal (vertical scale 0.2V per cm, with a 30dB amplifier gain). Horizontal scale for both traces is 2μsec. per cm.

impedance probe since the design was based upon the transadmittance between the two transducers we compare the measured value of the  $y_{21}(\omega)$  with the theoretical one which can be predictable from the geometry of the transducer structures alone, as discussed in the previous Chapter. The experimental value can be obtained from the measured values of  $\dot{v}_A$ ,  $\dot{v}_B$ , gain and input admittance of the HP3500A amplifier and the other circuit elements. An equivalent circuit for evaluating the  $y_{21}$ , is shown in Figure 4.6\* in which,

$C_1$  represents the static capacitance of the output transducer and other stray capacitances.

$L_1$  represents the stray inductance due to internal wiring,

$C_2$  represents the stray capacitances and the Capacitance due to BNC connectors.

$L_2$  represents stray inductance due to internal wiring and the inductance due to Bnc connectors,

$Y_{in}$  represents the input admittance of the HP3500A.

when terminated in a  $50\Omega$  load.

The series conductances<sup>of</sup>  $L_1$  and  $L_2$  have been neglected.

All these quantities were accurately measured as indicated in the Section 4.3.3.

If  $\dot{y}$  represents the admittance of the circuit, then we have,

$$\dot{y} = L_1 C_1 L_2 C_2 Y_{in} s^4 + L_1 C_1 C_2 s^3 + \{L_1 C_1 + L_2 (C_1 + C_2)\} Y_{in} s^2 + (C_1 + C_2) s + Y_{in} \dots \dots \dots (4.1)$$

where  $s = j\omega$

$$\therefore y_{21}(\omega) = \frac{\dot{v}_2}{\dot{v}_1} \dot{y} \dots \dots \dots (4.2)$$

\* The transducer radiation conductance and susceptance have been neglected as pointed out in section 2.1

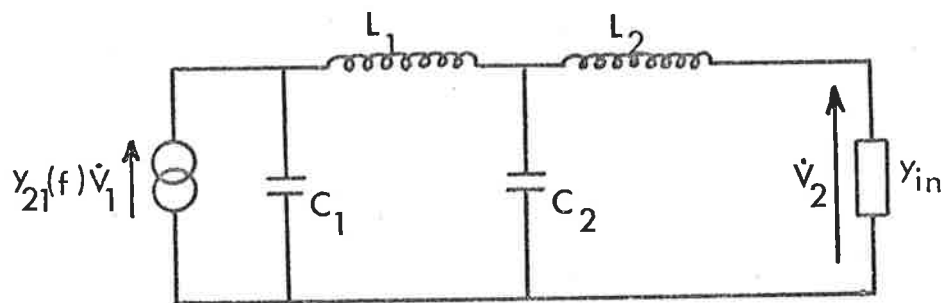


Figure 4.6 Equivalent circuit for evaluating  $y_{21}(\omega)$  of Filter 1.



A computer program was written to evaluate the transmittance  $y_{21}(\omega)$  for the frequencies concerned and the result is shown in Figure 4.7 compared with the theoretically calculated result. This program also included the theoretical calculation of  $y_{21}(\omega)$  of the designed filter transducer structures. The actual material parameters have not been used at this stage hence a comparison of the theoretical insertion-loss of the filter with the experimental one is not possible. The aim of the experiment was to test the validity of the transmittance formula for filter synthesis and this is clearly shown in Figure 4.7. However, a more elaborate program was developed in Chapter 7 to calculate this factor also.

#### 4.4 Discussion of the Results

The theoretically predicted performance of Filter 1 seems to agree fairly well with experimental observations, but some points of details deserve comment. It will be noted that from Figure 4.7, that the trap at the sound carrier has occurred at a frequency of 32.3 MHz against the designed frequency of 31.0 MHz - an increase of about 4.2%. Examination of the electrode pattern on a travelling microscope revealed a reduction ratio of 63.3 as against a designed value of 60 which shows an increased shift in frequency. It was also found that the measured surface wave velocity is  $3.145 \text{ km/sec}$ , while a different value of  $3.18 \text{ km/sec}$  was taken while drawing the master pattern. With these two corrections, the response of the filter was re-calculated and this is the response shown in Figure 4.7. The shift in frequency was correctly predicted, but the level at the sound carrier trap was slightly higher, of the order of 5dB more than the measured value, i.e. the measured response shows a better performance than the theoretically predicted response.

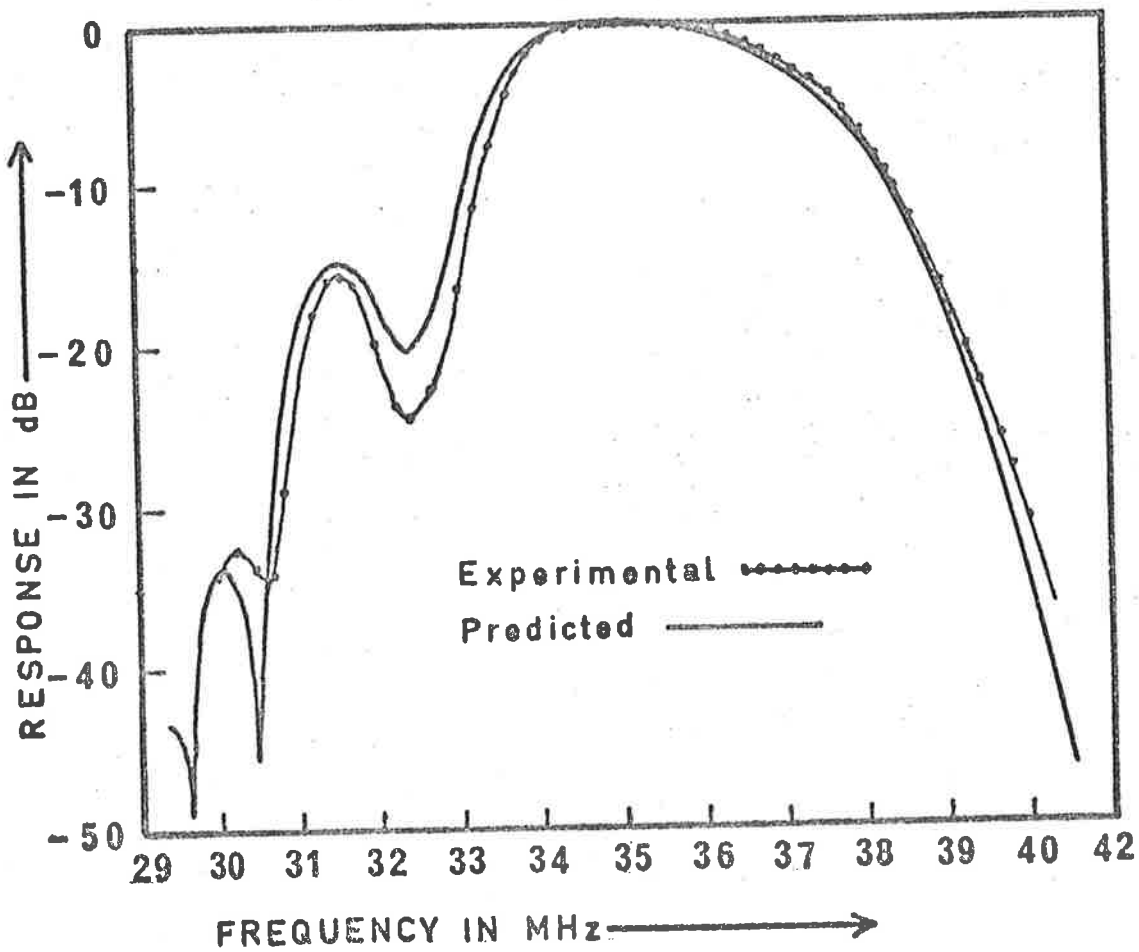


Figure 4.7 Experimental and theoretical performance of Filter 1.

The traps in the IF response or the IF response itself arised because of the interference between acoustic waves generated by each finger pair of the apodized interdigital transducer. The uniform transducer is assumed to transmit plane wave propagation. If there is a misalignment between the two transducer structures, because of the anisotropic nature of the substrate, the surface-wave velocity is different from that obtained by carefully aligned structures and the interference phenomenon is such that a deeper trap might have been caused at the sound carrier than expected. This misalignment of transducers is possible during the photofabrication right from the first stage reduction to final stage pattern on the substrate. The effect of misalignment can be easily investigated through a computer model, but it was felt that it is not necessary since the difference is very small.

Another point worth mentioning at this stage is that the load admittance to the output transducer (Figure 4.6) is mainly the input admittance of the preamplifier (HP 35000A) which is fairly constant and real (negligible imaginary component). A real load admittance is the basic assumption used in the synthesis of TV IF filter in Chapter 3 and the assumption is well justified in this situation. Hence, the graphs drawn in Figure 4.7 as magnitude of  $y_{21}(\omega)$  in dB scale, represent the magnitude response of the filter itself.

The measured insertion-loss of the filter,  $20 \log|\dot{v}_2/\dot{v}_1|$  with the  $50\Omega$  load termination at the centre frequency of 36 MHz was found to be of the order of 70dB down which is fairly high in practical situations and other design techniques using I C amplifiers to encompass the high insertion-loss of the substrate are presented in Chapter 9. The various loss mechanisms which deviate the ideal behaviour of the practical SAW filters will also be reviewed in Chapter 7.

The reciprocal nature of the SAW device was also tested by reversing the input-output connections i.e. by operating the apodized structure as the transmitting transducer and uniform structure as the receiving transducer and the same result was obtained as shown in Figure 4.7.

Thus, the good agreement obtained in the experiment with the theoretical result encouraged in developing some optimization techniques to improve the response and these are presented in Chapter 5.

## CHAPTER 5

SYNTHESIS OF TV IF FILTERS USING OPTIMIZATION  
TECHNIQUES5.0 Introduction

The basic synthesis procedure outlined in Chapter 3, although capable of providing an approximate representation of the desired response, suffers from significant inaccuracy as a result of truncating the time domain response of the output transducer  $T_2$ . Comparison of the theoretically calculated and experimentally measured performance of this filter (Chapter 4) shows that a significant gap exists between the specified response and the theoretically calculated response, although the latter forms a good match to the experimentally determined behaviour. Techniques for removing this error form a significant part of this chapter. Since SAW filters are analogous to non-recursive digital filters, many aspects of the design techniques developed in one area can also be applied to the other. During the past few years, considerable effort has been put forward in the latter area [5]<sup>1-14</sup> including some iterative optimization techniques for synthesizing the desired responses. However, these optimization schemes are well suited for realizing regular or smoothly varying bandpass characteristics while they become highly nonlinear with extreme complexity for irregular shapes like that of a TV IF response.

The optimization technique followed here for achieving the best agreement between the specified response and the adopted response is the least square error criterion. The method is fairly simple and well formulated in the network design [5]<sup>15</sup> but applying it to synthesize a SAW TV IF filter constitutes a novel technique. The procedure is easy to implement and requires no computer iteration process, much simpler than the

techniques developed for the above referenced non-recursive digital filters and yields a closed form of solution. The design technique becomes even simpler if the adopted response is even as pointed out in the 4th section of this chapter.

### 5.1 An Approach to Quadratic Cost Function Optimization

Before presenting the formalism of quadratic cost function optimization, it is worth discussing some of the existing techniques developed by other authors [5]<sup>9,10,11</sup> for non-recursive digital filters and the necessity to deviate from these techniques for the synthesis of TV IF filters.

The most straightforward approach is to use a window-function technique [5]<sup>16</sup>. This technique is quite useful to remove the undesirable ripples in the passband and in the stopband but cannot improve the skirt in the transition band. A preliminary computer investigation of window function technique for Filter 1 as synthesized in Chapter 3 revealed that the response is deteriorated instead of improving, viz. the trap at sound carrier is completely lost instead of increasing, indicating the failure of window-function technique for this kind of filter response. Other techniques e.g. [5]<sup>10,11</sup> make use of linear programming and iteration process which are time consuming and become extremely difficult for large number of constraints. Further, these techniques have been demonstrated for low-pass, band-pass or such other regular-shaped characteristic and it is not sure whether these techniques are capable of designing the complicated requirements of a TV IF filter. Even if they are, there is a further uncertainty whether they are applicable to SAW devices. The impulse response represents the finger pattern on the transducer and it may happen that the optimum designs are difficult to realize physically. This effect is quite clearly observed in the recent article by Tancrell [5]<sup>17</sup>.

Hence, it was decided to choose a simple optimization technique and develop the synthesis procedure from first principles to realize the given TV IF response. A very general shortcoming of all optimizing methods

is the lack of any assurance that the program will converge to the absolute (global) optimum, rather than to the nearest relative (local) optim. On studying the various simple optimization techniques, it was felt that the quadratic cost function optimization is well suited for the present case and it is hoped that the resulting optimum design will converge and is feasible to make practical filters.

## 5.2 Mathematical Formulation of Quadratic Cost Function Optimization

We will attempt to show here how the assumption of a quadratic cost function for departure from the ideal response in either the time domain or the frequency domain of an acoustic surface wave filter of finite duration can lead to the selection of an optimum response pattern in the time domain. The technique developed is most general and is applicable for designing a SAW filter for a given arbitrary frequency response (magnitude as well as phase). It will be shown later that certain simplifications are possible depending on the particular choice of the frequency response for example linear phase requirement rather than an arbitrary phase requirement, in which case the impulse response is even and the filter realization becomes simpler.

The following notation is used in deriving the error criterion:

$\underline{F}_2(\omega)$  = Frequency response in vector form of the output (apodized) transducer considered as the specified response in the optimization technique.

$\underline{F}_2(t)$  = Time domain response in vector form of the apodized transducer i.e. the Fourier transform of  $\underline{F}_2(\omega)$ .

$\underline{a}(t)$  = Finite duration time-domain response in vector form of  $\underline{F}_2(t)$  i.e. the truncated version of  $\underline{F}_2(t)$ .

$\underline{a}(\omega)$  = Frequency response in vector form of  $\underline{a}(t)$  i.e. the Fourier transform of  $\underline{a}(t)$ .

$\underline{p}(t)$  = Correcting vector necessary to add to  $\underline{a}(t)$ .

$\underline{r}(t)$  = Adopted response in vector form i.e.  $\underline{r}(t) = \underline{a}(t) + \underline{p}(t)$ .

$\underline{r}(\omega)$  = Achieved response in vector form i.e. the Fourier transform of  $\underline{r}(t)$ .

$\underline{F}_p$  = Transformation matrix with elements  $F_{pm,n} = \Delta T e^{-j2\pi \frac{(m-1)(n-1)}{N}}$  where m, and n may have N values.

$\underline{f}_p$  = Inverse transformation matrix with elements  $f_{pm,n} = \Delta f e^{j2\pi \frac{(m-1)(n-1)}{N}}$  where m and n may have N values.

$\underline{C}$  = Diagonal matrix with real, positive coefficients, called cost matrix or weighting matrix, with elements  $C_{mm}$ ,  $m = 1, 2, \dots, K$ .

It is to be remembered at this stage as mentioned earlier we are dealing with the discrete nature of the continuous functions, it is assumed that the above mentioned quantities are defined at the sampling intervals  $\Delta T$  in time domain and  $\Delta f$  in frequency domain with  $\Delta T \cdot \Delta f = \frac{1}{N}$ , where N is the total number of sampling points.

In the vectorial representation all the vectors are assumed to be column vectors, and the vectors  $\underline{a}(t)$ , and  $\underline{r}(t)$  will have components M values less than N and  $\underline{p}(t)$  will have components  $\leq M$  values while the vector  $\underline{F}_2(t)$  is assumed to have N components. The vectors  $\underline{a}(\omega)$ ,  $\underline{r}(\omega)$  and  $\underline{F}_2(\omega)$  will have components K values  $\geq M$  but  $\leq N$ . The row vectors are represented by transpose (T) of the column vectors.

With this notation we obtain the following relations:

$$\underline{F}_2(t) = \underline{f}_p \cdot \underline{F}_2(\omega) \quad (\text{for } N \text{ components of } t) \quad \dots (5.1)$$

$$\text{or} \quad \underline{a}(t) = \underline{F}_2(t) \quad (\text{for } M \text{ components of } t < N) \quad \dots (5.2)$$

$$\text{Therefore} \quad \underline{a}(\omega) = \underline{F}_p \cdot \underline{a}(t) \quad \dots (5.3)$$

We now wish to improve the response  $\underline{a}(\omega)$  in the frequency domain by modifying the truncated version of finite duration response, while retaining the same truncation limits. This can be achieved by adding a perturbation



vector  $\underline{p}(t)$  of dimension less than or equal to  $\underline{a}(t)$ , to obtain a new vector  $\underline{r}(t)$ , and a total response  $\underline{r}(\omega)$  in the frequency domain, i.e.

$$\underline{r}(t) = \underline{a}(t) + \underline{p}(t) \quad \dots(5.4)$$

Transforming  $\underline{r}(t)$  to frequency domain we get

$$\underline{r}(\omega) = \underline{Y} \underline{r}(t) \quad \dots(5.5)$$

where  $\underline{Y}$  is a transformation matrix of the same form as  $\underline{F}_p$  but is of different dimension.

$$\underline{r}(\omega) = \underline{Y}\{\underline{a}(t) + \underline{p}(t)\} \quad \dots(5.6)$$

Now we are interested in the extent to which the response matches the specified response,  $\underline{F}_2(\omega)$  and therefore, we form the difference  $\{\underline{r}(\omega) - \underline{F}_2(\omega)\}$  as a measure of this matching. In fact, if we adopt the assumption that the cost associated with lack of perfect match is a quadratic function of the difference, we obtain the following equation:

$$\tau = \{\underline{r}(\omega) - \underline{F}_2(\omega)\}^{\text{T}*} \underline{C} \{\underline{r}(\omega) - \underline{F}_2(\omega)\} \quad \dots(5.7)$$

where ' $\tau$ ' is the total cost and ' $\underline{C}$ ' is a diagonal matrix of real cost coefficients by which we assign different costs to departures from the ideal response in various portions of the frequency spectrum, and " $\text{T}^*$ " indicates transpose-conjugate operation. Substituting for  $\underline{r}(\omega)$  from equation (5.6) into equation (5.7), expanding the terms and noting that  $\underline{p}(t)$  and  $\underline{a}(t)$  are real we get

$$\tau = \underline{p}^{\text{T}}(t) \underline{A} \underline{p}(t) + \underline{b}^{\text{T}*}(t) \underline{p}(t) + \underline{p}^{\text{T}}(t) \underline{b}(t) + \tau_0 \quad \dots(5.8)$$

$$\text{where} \quad \underline{A} = \underline{Y}^{\text{T}*} \underline{C} \underline{Y} \quad \dots(5.8a)$$

$$\underline{b}^{\text{T}*}(t) = \{\underline{a}^{\text{T}}(t) \underline{Y}^{\text{T}*} - \underline{F}_2^{\text{T}*}(\omega)\} \underline{C} \underline{Y} \quad \dots(5.8b)$$

$$\underline{b}(t) = \underline{Y}^{T*} \underline{C} \{ \underline{Y} \underline{a}(t) - \underline{F}_2(\omega) \} \quad \dots(5.8c)$$

$$\tau_0 = \{ \underline{a}(\omega) - \underline{F}_2(\omega) \}^{T*} \underline{C} \{ \underline{a}(\omega) - \underline{F}_2(\omega) \} \quad \dots(5.8d)$$

For minimum cost we differentiate  $\tau$  with respect to the perturbation vector  $\underline{p}(t)$  and equate to zero i.e.

$$\frac{\partial \tau}{\partial \underline{p}(t)} = 2\underline{A} \underline{p}(t) + \{ \underline{b}(t) + \underline{b}^*(t) \} = 0 \quad \dots(5.9)$$

Since  $\underline{p}(t)$  is real, so also the constant term in the equation (5.9) it is sufficient to work out with the real coefficients of the matrix  $\underline{A}$ .

$$\therefore \text{Let } \underline{B} = \text{Real Part of } \underline{A} \quad \dots(5.10)$$

$$\text{and } 2\underline{d}(t) = \underline{b}(t) + \underline{b}^*(t)$$

Hence, equation (5.9) becomes

$$\frac{\partial \tau}{\partial \underline{p}(t)} = 2\underline{B} \underline{p}(t) + 2\underline{d}(t) = 0 \quad \dots(5.11)$$

In order to obtain an unique solution for  $\underline{p}(t)$  it is necessary that the matrix  $\underline{B}$  in equation (5.11) is non-singular. Referring to equation (5.8a) we see that the matrices  $\underline{Y}^{T*}$  and  $\underline{Y}$  are not square matrices in general while the matrix  $\underline{A}$  is an Hermitian matrix, since  $\underline{C}$  is a diagonal matrix by assumption. Therefore,  $\underline{B}$  is a real symmetric matrix, and assuming it to be non-singular the perturbations are given by,

$$\underline{p}(t) = -\underline{B}^{-1} \underline{d}(t) \quad \dots(5.12)$$

where  $\underline{B}^{-1}$  indicates the inverse of the matrix  $\underline{B}$ . Equation (5.12) indicates the solution of a large number of simultaneous linear equations and it is necessary to keep the number minimum as far as possible. Having found  $\underline{p}(t)$ , we can calculate the adopted response in time domain (equation 5.4) and hence the achieved response in frequency domain (equation 5.6). Before attempting the method to Filter 1, it is necessary to examine the

properties of the quantities defined in the equation (5.8).

(1) Matrix  $\underline{\underline{Y}}$ : The matrix  $\underline{\underline{Y}}$  is of the same form as  $\underline{\underline{F}}_p$  and in fact it represents a part of the whole matrix  $\underline{\underline{F}}_p$ . Therefore, the elements of  $\underline{\underline{Y}}$  are the same as the elements of  $\underline{\underline{F}}_p$ .

$$i.e. Y_{m,n} = \Delta T e^{-\frac{j2\pi(m-1)(n-1)}{N}}$$

in which 'm' will have K values ( $\geq M$ ) and 'n' will have M values, both K and M are less than N.

$$\therefore \underline{\underline{Y}} = \underline{\underline{F}}_p \quad \dots (5.13)$$

(2) Matrix  $\underline{\underline{Y}}^{T*}$ : The matrix  $\underline{\underline{Y}}^{T*}$  represents the complex conjugate of  $\underline{\underline{Y}}$ . Therefore, its elements are given by

$$Y_{n,m}^{T*} = \Delta T e^{+\frac{2\pi j(n-1)(n-1)}{N}}$$

as before, 'm' will have K values ( $\geq M$ ) and 'n' will have M values both being less than N. The elements  $Y_{n,m}^{T*}$  can also be written as,

$$Y_{n,m}^{T*} = \frac{\Delta T}{\Delta f} \left[ \Delta f e^{+\frac{j2\pi(m-1)(n-1)}{N}} \right],$$

but, from the definition of inverse transformation matrix,  $Y_{n,m}^{T*} = \frac{\Delta T}{\Delta f} f_{pm,n}$

$$\therefore \underline{\underline{Y}}^{T*} = \frac{\Delta T}{\Delta f} \underline{\underline{f}}_p \quad \dots (5.14)$$

(3) Matrix  $\underline{\underline{C}}$ : As mentioned earlier it is a diagonal matrix with K arbitrarily assigned coefficients.

(4) Matrix  $\underline{\underline{A}}$ : The matrix  $\underline{\underline{A}}$  is Hermitian of dimension M.

$$\text{i.e. } \underset{\sim}{A}_{(M \times M)} = \underset{\sim}{Y}^{T*}_{(M \times K)} \underset{\sim}{C}_{(K \times K)} \underset{\sim}{Y}_{(K \times M)}$$

(5) Matrix  $\underset{\sim}{B}$ : The matrix  $\underset{\sim}{B}$  is the real part of  $\underset{\sim}{A}$ , hence, it is a real, symmetric matrix with the same dimensions as that of  $\underset{\sim}{A}$ . For  $\underset{\sim}{B}$  to be non-singular 'K' must be  $\geq$  'M'.

(6) Vector  $\underset{\sim}{b}(t)$ : The vector  $\underset{\sim}{b}(t)$  can be interpreted from equation (5.9c) as the time domain response of the weighted error response in the frequency domain of positive spectrum only. It can be evaluated using the transformation matrices as defined earlier which in turn can be evaluated using the discrete FFT routine.

(7) Constant  $\tau_0$ : The constant  $\tau_0$  represents the initial cost before perturbations are applied, as is evident from equation (5.8). Its evaluation in the solution of linear equations is not necessary, however, the evaluation of total cost before and after optimization gives a good measure of the effectiveness of the technique.

(8) Perturbation vector  $\underset{\sim}{p}(t)$ : It is a real M-dimensional vector obtainable by solving a set of M dimensional equations (equations 5.11) using the standard matrix methods and we can expect a unique solution provided the number of variables in  $\underset{\sim}{p}(t)$  is the same as the number of conditions selected in the frequency domain.

Having thus established the mathematical development, we next apply it to the synthesis of SAW filters with arbitrary frequency response and then focus our attention to the case of filters with linear phase responses.

### 5.3 Application to Non-linear Phase Responses

If the specified response has a non-linear phase characteristic, then the time domain response  $\underset{\sim}{F}_2(t)$  is not even and because of the way the

discrete FFT algorithm written the sidelobes are centred around the half-periodic intervals and the principle-lobes towards the beginning and end of the periodic interval. However, by introducing an appropriate group-delay characteristic in the frequency domain, the time domain response  $\tilde{F}_2(t)$  can be made mainlobe centred around some time interval with the sidelobes falling on either side. This operation is necessary because of the convenience in truncating the sidelobes and the indices in the optimization program can be assigned to vary in an increasing order.

The basic equations are the same as derived in the last section, but here we show how to manipulate the matrices and vectors in a convenient way for computing purpose. Summarizing the formulae we get,

$$\begin{aligned}
 \tilde{p}(t) &= -\tilde{B}^{-1} \tilde{d}(t) \\
 \tilde{B} &= \text{Real part of } \tilde{A} \\
 \tilde{b}(t) &= \tilde{Y}^{T*} \tilde{C} \{ \tilde{Y} \tilde{a}(t) - \tilde{F}_2(\omega) \} \\
 \tilde{A} &= \tilde{T}^{T*} \tilde{C} \tilde{Y} \\
 \tilde{d}(t) &= \frac{1}{2} \{ \tilde{b}(t) + \tilde{b}^*(t) \} = \text{Real Part } \{ \tilde{b}(t) \} \\
 Y_{mn} &= \Delta T e^{-\frac{j2\pi(m-1)(n-1)}{N}} \\
 Y_{n,m}^{T*} &= \Delta T e^{\frac{j2\pi(n-1)(m-1)}{N}} \\
 \tilde{Y} &= F_{\tilde{z}_p} \\
 Y^{T*} &= \frac{\Delta T}{\Delta f} f_{\tilde{z}_p}
 \end{aligned} \tag{5.15}$$

We assign the cost coefficients at each frequency sampling point at which the response is specified, i.e. if the response is specified at  $K$  sampling points, then the cost coefficients are given by  $C_{ii}$ , where  $i = 1, K$ . Next, if the truncated time response  $\tilde{a}(t)$  is specified at  $M$  sampling point, and

if we perturb the response at all the  $M$  sampling points we obtain a perturbation vector  $\underline{p}(t)$  of  $M$  dimensions. Whatever the value of  $K$  (provided  $K \geq M$  for reasons mentioned earlier) we always end up with  $M$  simultaneous linear equations and the choice of  $K$  and  $M$  depends upon the number of constraints required in the frequency and time domains and is of course, limited by the computer storage and the time.

Now consider the matrix  $\underline{\underline{A}}$ : Since  $\underline{\underline{C}}$  is diagonal the elements of  $\underline{\underline{A}}$  are given by,

$$A_{I,J} = \Delta T^2 \sum_{k=1}^K e^{-\frac{j2\pi(J-I)(k-1)}{N}} \times C_{kk} \quad \dots (5.16)$$

where  $I, J$  will have  $M$  values, starting from the sampling point at which the perturbations are applied. The elements of  $\underline{\underline{B}}$  are given by the real part of the elements of  $\underline{\underline{A}}$ , and since  $\underline{\underline{B}}$  is symmetric it is sufficient to evaluate only the upper or lower triangular matrix of  $\underline{\underline{B}}$  and, therefore, we can restrict the index  $J$  to be greater than  $I$ .

Consider the vector  $\underline{b}(t)$ : The vector  $\underline{b}(t)$  can be evaluated directly as given in the equation (3.15), but it can be evaluated more efficiently by using FFT routine. Substituting equations (5.13) and (5.14) in equation (5.15)  $\underline{b}(t)$  vector can be written as,

$$\underline{b}(t) = \frac{\Delta T}{\Delta f} \underline{f}_{\underline{p}} \underline{\underline{C}}(\underline{F}_{\underline{p}} \underline{a}(t) - \underline{F}_2(\omega)) \quad \dots (5.17)$$

in which all the vectors are of dimension  $N$  with a number of zeros except in those regions of interest where the response is significant in either domain. The cost matrix  $\underline{\underline{C}}$  is also considered to be of dimension  $(N \times N)$  with diagonal elements present only in the region where the frequency response is specified and the rest of the elements being zero. In such a situation we can use the Fourier transform notation as defined in equation (3.12 and 3.13), and we obtain a vector  $\underline{b}_1(t)$  given by,

$$\underline{b}_1(t) = \frac{\Delta T}{\Delta f} f_p C_{kk} (F_p a(t) - F_2(\omega)) \quad \dots(5.18)$$

which can be evaluated using FFT routine and the vector  $\underline{b}(t)$  is obtained by selecting only that portion in time domain of  $\underline{b}_1(t)$  where the perturbations are to be evaluated. One point to be remembered while using FFT is that a conjugate frequency spectrum is necessary to give rise to a real time function, while equation (5.15) indicates that  $\underline{b}(t)$  is to be evaluated only for positive spectrum. If we use only positive spectrum in the FFT routine we obtain a complex time function whose real part is half the magnitude of the real time function obtained when both the positive and negative spectrums are considered. That means we actually obtain twice the required value of  $\underline{b}(t)$  in equation (5.18). Therefore, it is a simple matter to show that the  $\underline{d}(t)$  vector is given by,

$$\underline{d}(t) = \frac{1}{2} \underline{b}_1(t) \text{ (for } M \text{ components of } t) \quad \dots(5.19)$$

The perturbation vector is then calculated using the relation in equation (5.13) viz,

$$\underline{p}(t) = -\underline{B}^{-1} \underline{d}(t)$$

and the adopted response  $\underline{r}(t)$  from the equation (5.4) and hence the achieved response after optimization from the equation (5.5).

For a nonlinear phase response we have to solve  $M$  simultaneous equations whereas for a linear phase response this can be reduced to half the number, thus saving a considerable amount<sup>of</sup> computing time as well as storage. The same equations for  $\underline{B}$  and  $\underline{d}(t)$  can be used for this case also by varying the indices over half the range, and imposing symmetry in the other half range of the perturbation vector, however, we present in the next section an independent proof for this approach.

#### 5.4 Application to Linear Phase Responses - OPTIM Method

If the phase response is linear, the time domain response  $F_2(t)$  is even and can be made mainlobe centred at mid point of the periodicity interval as indicated in Chapter 3. If the response is truncated to  $M$  sampling points, we need to perturb the response  $\underline{a}(t)$  at  $M$  sampling points and hence solving of  $M$  simultaneous equations is necessary. The aim is to reduce the number of simultaneous equations, still preserving the linear phase characteristic in the frequency domain. This can be achieved by making use of the symmetry property of the truncated time response and we explain it more clearly on this approach, since this is the method followed for optimizing the Filter 1 and for other filters discussed in Chapter 6. We call this approach as OPTIM METHOD.

Consider an  $M$  dimensional perturbation vector  $\underline{p}(t_i)$  ( $i = 1, M$ ), symmetrical about its central point  $\left(\frac{M+1}{2}\right)$ ,  $M$  being an odd integer. We designate the left-half perturbations  $\underline{p}(t_i)$  by  $\underline{q}(t_i)$  and by symmetry the right-half perturbations are also equal to  $\underline{q}(t_i)$  in the reverse order, i.e.

$$\begin{aligned} \underline{q}(t_i) &= \underline{p}(t_i) \\ &= \underline{p}(t_{M+1-i}) \end{aligned} \quad \text{for } i = 1, \frac{M-1}{2} \quad \dots (5.20)$$

We assign only half the amplitude of  $\underline{p}(t)$  to the last value of  $\underline{q}(t)$ , i.e.

$$\underline{q}\left(t \frac{M+1}{2}\right) = \frac{1}{2} \underline{p}\left(t \frac{M+1}{2}\right) \quad \dots (5.21)$$

The relation between  $\underline{q}(t)$  and  $\underline{p}(t)$  can be expressed in a matrix form as follows:

$$\underline{p}(t) = \underline{S} \underline{q}(t) \quad \dots (5.22)$$

$$(M \times 1) \quad (M \times \frac{M+1}{2}) \quad (\frac{M+1}{2})$$

where  $\underline{S}$  is a matrix of the form





Having found  $q(t)$ , the total perturbations  $p(t)$  can be found from equation (5.20), and the adopted response  $r(t)$ , and hence the achieved response  $r(f)$  can be calculated as before.

The Relation between  $\underline{\underline{H}}$  and  $\underline{\underline{A}}$  Matrices:

To calculate  $\underline{\underline{H}}$  matrix it is not necessary to actually evaluate the  $\underline{\underline{S}}$  matrix but we make use of its properties in evaluating the  $\underline{\underline{H}}$  matrix elements in terms of  $\underline{\underline{A}}$  matrix elements. If we exclude the last perturbation of  $q(t)$  (central one in  $p(t)$ ) we can see that each element in  $\underline{\underline{H}}$  is composed of four elements in  $\underline{\underline{A}}$  in the following fashion:

$$\underline{\underline{H}}_{\gamma s} = \underline{\underline{A}}_{\gamma s} + \underline{\underline{A}}_{\dot{\gamma} s} + \underline{\underline{A}}_{\gamma \dot{s}} + \underline{\underline{A}}_{\dot{\gamma} \dot{s}} \quad \dots (5.29)$$

where the indices  $\gamma$  and  $s$  have values  $\frac{M-1}{2}$ . A dot on the index represents the conjugate point which we mean a point that is symmetrical about the central point in the truncated time response. For  $N$  samples in an FFT routine the conjugate point  $\dot{\gamma}$  is given by  $N + 2 - \gamma$ . With this notation the elements of  $\underline{\underline{A}}$  from equation (5.16) are given by

$$\left. \begin{aligned} \underline{\underline{A}}_{\gamma s} &= \Delta T^2 \sum_{k=1}^K e^{-\frac{j2\pi(s-\gamma)(k-1)}{N}} C_{kk} \\ \underline{\underline{A}}_{\dot{\gamma} s} &= \Delta T^2 \sum_{k=1}^K e^{+\frac{j2\pi(s-\gamma)(k-1)}{N}} C_{kk} \\ \underline{\underline{A}}_{\gamma \dot{s}} &= \Delta T^2 \sum_{k=1}^K e^{-\frac{2\pi j\{2-(s+\gamma)\}(k-1)}{N}} C_{kk} \\ \underline{\underline{A}}_{\dot{\gamma} \dot{s}} &= \Delta T^2 \sum_{k=1}^K e^{+\frac{j2\pi j\{2-(s+\gamma)\}(k-1)}{N}} C_{kk} \end{aligned} \right\} \dots (5.30)$$

Further, it is clear that,

$$A_{\gamma s} = (A_{\gamma s})^* \text{ and } A_{\gamma s} = (A_{\gamma s})^*$$

where '\*' indicates complex conjugate. Therefore the elements of  $\underline{H}$  are given by

$$H_{\gamma s} = 2 \text{ Real Part } (A_{\gamma s}) + 2 \text{ Real Part } (A_{\gamma s}) \quad \dots(5.31)$$

with an elementary algebra they can be shown to be equivalent to,

$$H_{\gamma s} = 4\Delta T^2 \sum_{k=1}^K \cos \frac{2\pi(s-1)(k-1)}{N} \cos \frac{2\pi(\gamma-1)(k-1)}{N} C_{kk} \quad \dots(5.32)$$

In the actual programming the elements are evaluated in a slightly different fashion, viz,

$$H_{\gamma s} = 4\Delta T^2 \sum_{k=1}^K \text{Real Part} \left[ e^{+ \frac{2\pi j(\gamma-1)(k-1)}{N}} \right] C_{kk} \text{Real Part} \left[ e^{- \frac{2\pi j(s-1)(k-1)}{N}} \right] \quad \dots(5.33)$$

which is identical to equation (5.32).

#### Relation between $\underline{g}(t)$ and $\underline{d}(t)$ Vectors

Once again excluding the last perturbation in  $\underline{q}(t)$  (the central one in  $\underline{p}(t)$ ), the  $\underline{e}^{T*}(t)$  vector can be obtained from equation (5.25) as,

$$\underline{e}^{T*}(t) = 2 \underline{b}^{T*}(t)$$

or

$$\underline{e}^*(t) = 2 \underline{b}^*(t) \text{ and } \underline{e}(t) = 2\underline{b}(t)$$

∴ from equation (5.27)

$$2\underline{g}(t) = 2(\underline{b}(t) + \underline{b}^*(t))$$

but,  $\underline{b}(t) + \underline{b}^*(t) = 2\underline{d}(t)$  from equation (5.10)

$$\underline{g}(t) = 2\underline{d}(t) \text{ (for } \frac{M-1}{2} \text{ components)} \quad \dots(5.34)$$

and whereas before  $\underline{d}(t)$  is given from equation (5.19)  $\underline{d}(t) = \frac{1}{2} \underline{b}_1(t)$  and

$\underline{b}_1(t)$  is obtained from equation (5.18). Note that the factor 2 can be cancelled in equations (5.33) and (5.34) and a computer program given in Appendix (A2) is written after implementing this cancelation.

Treatment of Last Perturbation in  $q(t)$  (Central one in  $p(t)$ )

Observing the matrix elements in equation (5.30) shows that the last perturbation point in  $q(t)$  or the central point in  $p(t)$  is also the conjugate point, hence, all the elements are the same and, therefore, equation (5.33) can still be used for evaluating the matrix elements corresponding to this point. However, for the  $\underline{g}(t)$  vector we can proceed as follows:

$$\text{from equation (5.25)} \quad \underline{e}^{T*} \left( \frac{t_{M+1}}{2} \right) = \underline{b}^{T*} \left( \frac{t_{M+1}}{2} \right)$$

$$\text{or} \quad \underline{e}^* \left( \frac{t_{M+1}}{2} \right) = \underline{b}^* \left( \frac{t_{M+1}}{2} \right)$$

$$\text{and} \quad \underline{e} \left( \frac{t_{M+1}}{2} \right) = \underline{b} \left( \frac{t_{M+1}}{2} \right) ,$$

but from equation (5.27),

$$\begin{aligned} 2\underline{g} \left( \frac{t_{M+1}}{2} \right) &= \underline{b} \left( \frac{t_{M+1}}{2} \right) + \underline{b}^* \left( \frac{t_{M+1}}{2} \right) \\ &= 2\underline{d} \left( \frac{t_{M+1}}{2} \right) \end{aligned}$$

$$\text{i.e.} \quad \underline{g} \left( \frac{t_{M+1}}{2} \right) = \underline{d} \left( \frac{t_{M+1}}{2} \right)$$

Thus we see that only half the magnitude of  $\underline{d}(t)$  (Ref. eqn. (5.34a) is required at this perturbation point and the equations for  $q(t)$  can be solved in the usual way, but the actual perturbation  $p(t)$  is to be multiplied by a factor of 2, thus obtaining all the perturbations in the required region.

## 5.5 Computational Techniques

In this section we present some of the computational techniques for the TV IF filter as synthesized in Chapter 3. Even for the symmetrical responses  $\underline{a}(t)$  we can apply the technique developed for nonlinear phase responses (Section 5.3); in this case the matrix  $\underline{B}$  is still real, symmetrical and nonsingular and the vector  $\underline{d}(t)$  is symmetrical and the perturbations  $\underline{p}(t)$  after solving the equations will come out to be automatically symmetrical because of the particular nature of the  $\underline{B}$  matrix and hence the total vector  $\underline{r}(t)$ , is symmetrical, thus retaining the linear phase response of the filter. The only drawback is that it takes considerable amount of time and storage compared to the OPTIM METHOD. In the early part of the project this technique was adopted and hence, we present the methods followed in this optimization scheme for achieving the desired response. The truncated response  $\underline{a}(t)$  in Filter 1 contains 227 sampling points starting from 400 to 626 (both inclusive) and if we perturb the response at all the sampling points, we need to solve 227 simultaneous linear equations and this is a formidable task, even with the modern high speed large digital computers. Considerable computational difficulties arise when handling with such large matrices and we have to devise ways and means to reduce the number to a feasible level and at the same time without losing the objective of the optimization technique. If we truncate the response to a lesser number of points, the error in the frequency domain is large and the present quadratic cost function optimization needs modification if departures in the error function is large. Several schemes have been developed by retaining the same number of sampling points but perturbing only at certain points and using the same optimization technique. These are illustrated as follows.

### 5.5.1 Peak-Point Perturbation

Observing the truncated version of the finite duration response  $\underline{a}(t)$  of Filter 1 we find that the response varies more or less uniformly,

having 3 to 6 sampling points in each half-cycle and there are about 71 half-cycles in the whole time duration of  $\underline{a}(t)$ . While making the filter-device we assigned one finger for each half-cycle and the overlap is proportional to area of each half-cycle. The significant contribution in the area is the peak amplitude of the response in the respective half-cycles, and hence it is appropriate to perturb only the peak amplitudes in each half-cycle, thus considering only 71 simultaneous equations instead of 227, reducing by a factor of about 3. Therefore  $M = 71$  in this case.

Recalling some of the equations from previous sections we have,

$$A_{I,J} = \Delta T^2 \sum_{k=1}^K e^{-\frac{j2\pi(J-I)(k-1)}{N}} C_{kk}$$

(I,J will have M values)

$$\underline{\underline{B}} = \text{Real part of } \underline{\underline{A}}$$

$$\underline{\underline{d}}(t) = \frac{1}{2} \underline{\underline{b}}_1(t) \quad \dots (5.34)$$

$$\underline{\underline{p}}(t) = -\underline{\underline{B}}^{-1} \underline{\underline{d}}(t)$$

$$\underline{\underline{r}}(t) = \underline{\underline{a}}(t) + \underline{\underline{p}}(t)$$

$$\underline{\underline{r}}(f) = F_p\{\underline{\underline{r}}(t)\}$$

It seems likely that a complete reduction of cost to zero is possible provided the number of variables in  $\underline{\underline{a}}(t)$  is the same as the number of conditions in the frequency domain i.e. by assigning the same number of cost coefficients to the error response. In this example the number of variables ( $M$ ) in the time domain is 71 and the cost coefficients ( $K$ ) will also have to be 71. The selection of cost coefficients is an arbitrary choice and the most proper choice is to assign higher values where the error is maximum and lower values where the error is minimum. In fact any other choice is permissible since the optimization technique does not depend upon the choice of the cost-coefficients. Having chosen the cost

coefficients the perturbation vector is evaluated through the various steps as indicated in the equation (5.35). A computer program was written to carry out all these stages and a flow-chart is shown Figure (5.1). Examination of the computed results revealed that the time response is severely distorted even though the response in the frequency domain is improved. By distortion we mean the smooth variation in the time wave form is completely lost. It was felt that perturbing at peak points alone will not be sufficient and an alternative approach is followed still keeping the same number of constraints in the frequency and time domains.

### 5.5.2 Coherent Point Perturbation

In this optimization strategy we retain the concept of perturbing 71 variables in the time domain in order to satisfy the 71 conditions in the frequency domain, but we hope to avoid the problem mentioned above by introducing an expansion matrix  $\underline{E}$  in order to perturb, in a coherent manner, all points of the time response in each half-cycle, in response to a single perturbation variable which pertains to that half-cycle. The result is that through the choice of 71 perturbation variables in the time domain perturbation of all the 227 points of the retained time window is possible. A number of policies whereby the expansion matrix may be calculated are available, but the one which has been investigated is as follows.

If the half-cycle contains 3 or 5 points, the central point is perturbed by one unit (for that half-cycle) and the surrounding points are perturbed by one half this amount, when however either 2 or 4 points of the time waveform fall on a given half-cycle the central points are perturbed by one unit (for that half-cycle) and the outer 2 points by half this amount. If the half-cycle contains only 2 sampling points the outer point is perturbed by one unit and the 1st one by half this amount; thus covering all the sampling points in the finite duration time response  $\underline{a}(t)$ .

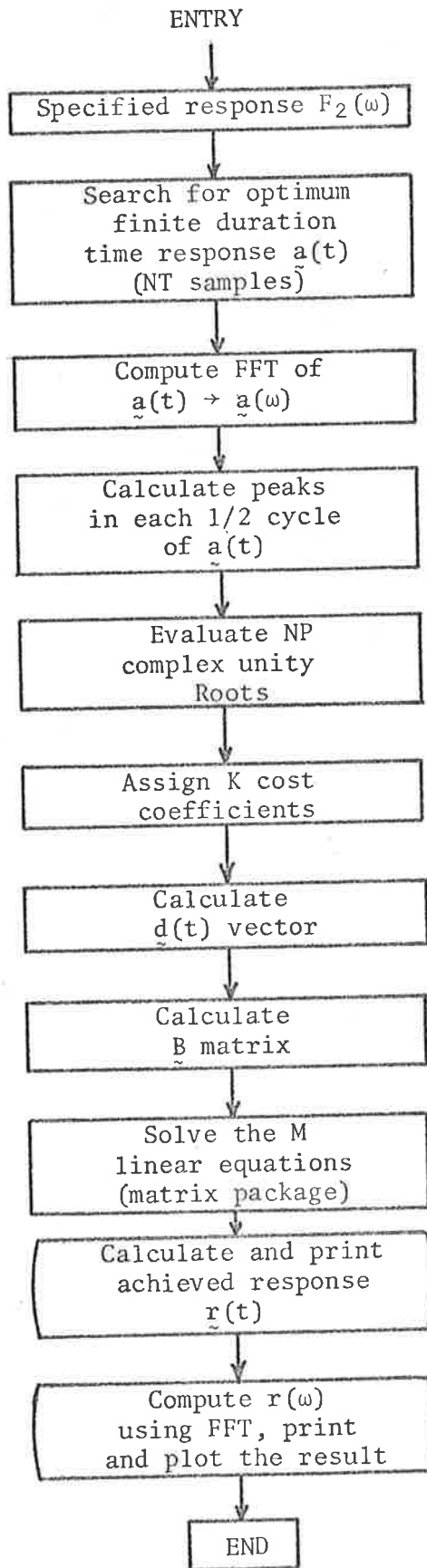


FIGURE 5.1 Flow-chart for peak point perturbation technique.





Note that it is not necessary to store the matrices  $\underline{\underline{A}}$ ,  $\underline{\underline{B}}$  or  $\underline{\underline{E}}$  but the steps (a), (b) and (c) can be performed within an operation and the resulting elements are stored in  $\underline{\underline{R}}$ .

$$(d) \quad \underline{\underline{d}}(t) = \frac{1}{2} \underline{\underline{b}}_1(t)$$

(227x1)

$$(e) \quad \underline{\underline{h}}(t) = \underline{\underline{E}}^T \underline{\underline{d}}(t)$$

(71x1)      (71x227)

$$(f) \quad \underline{\underline{s}}(t) = -\underline{\underline{R}}^{-1} \underline{\underline{h}}(t)$$

(71x1)      (71x71) (71x1)

$$(g) \quad \underline{\underline{p}}(t) = \underline{\underline{E}} \underline{\underline{s}}(t)$$

(227x1)      (227x71)(71x1)

Once again note that steps (e) and (g) are performed without using a stored matrix  $\underline{\underline{E}}$ . A computer program was written to carry out all these steps and a flow-chart is shown in Figure (5.2). Examination of the computed results revealed a similar effect with this approach also i.e. an undue distortion of the time response and appears likely to concentrate the effect of the perturbation in the higher harmonics. It was decided to increase the number of constraints in the frequency domain and this is followed for the rest of the filter synthesis (Chapter 6).

### 5.5.3 Independent Point Perturbation

In this method we attempt to independently perturb all the sampling points (227) in the time domain in order to minimize the sum of the squares of the differences between the specified response and the achieved response at 227 points in the frequency domain. Again we can expect that the method should produce complete reduction to zero of the frequency difference at the points of interest. However, the method is expected to

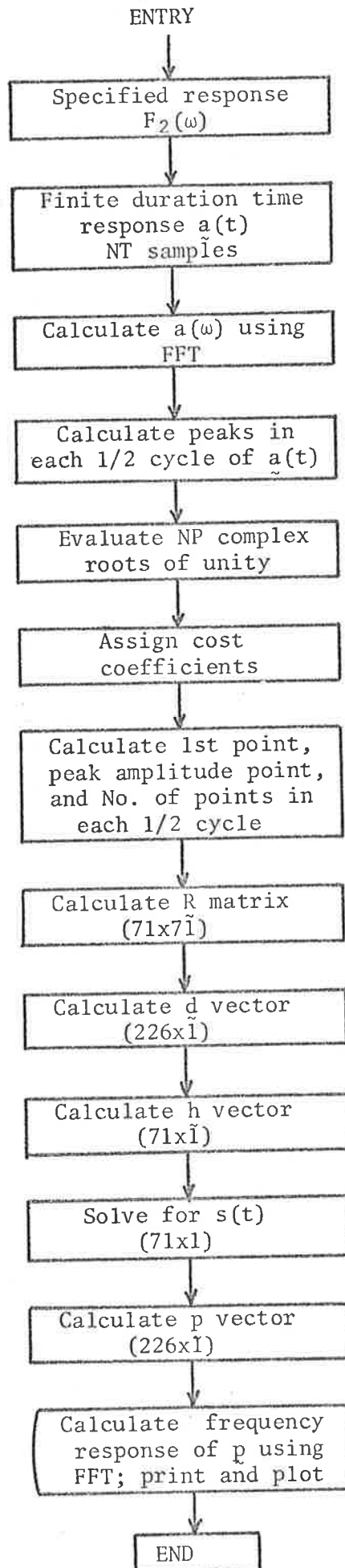


FIGURE 5.2. Flow-chart of coherent point perturbation technique.

be expensive of both computer storage and computer time. Hence, this method was not attempted.

## 5.6 Optimization by Successive Iterations

This is rather a fortuitous method and surprisingly produced fairly satisfactory results with much less effort than any of the above mentioned techniques. The term iteration does not mean the iteration process commonly used in the optimization techniques, rather it is used here to denote transformation from time to frequency domain or vice-versa. Because of the availability of the fast Fourier transform algorithms the method is considerably simpler even though several transformations are involved in the process. If the required perturbations are obtained in one set of transformations the method is termed as zero order iterations, and if the perturbations are obtained in two sets of transformations it is termed as first order iteration optimization technique, and finally for 'N' sets of transformations, it is termed as  $N^{\text{th}}$  order iteration.

### 5.6.1 Zero-Order Iteration

The procedure adopted here as follows: We start with a specified response in frequency domain of the output transducer  $T_2(F_2(\omega))$ . The response is set identically equal to zero at various sampling points other than at which it is specified, and the conjugate symmetry required by the FFT routine is imposed. The resulting response is then transformed to the time domain and subject to truncation to a length of seventy-one half-cycles (400 to 626 points, both inclusive). The time domain response is then expanded to a full 1024 points by zero filling. This response is then transformed to frequency domain using FFT routine and the difference between the resulting "achieved frequency response" and the specified response is calculated. This error response is retained only at frequency samples where the cost coefficients are specified and is set equal to zero

at other sampling points. The error response is then multiplied by the selected cost coefficients and the conjugate symmetry conditions required for FFT operation are imposed. The resulting response is then transformed to the time domain using FFT routine, where it is again truncated by retaining only those portions which fall within the region defined by the 71 half-cycles. The time response is then expanded to 1024 points by zero fill, transformed to frequency domain using FFT routines, truncated to the frequency range of interest, multiplied by the inverse cost coefficients, expanded to 1024 points by zero fill, subjected again to conjugate symmetry, transformed to time domain using FFT routine and finally changed in sign.

The required perturbations are those which fall within the truncated finite duration of the time response. The total time response which we attempt to synthesize is then the sum of the previously truncated time response  $\underline{a}(t)$  and the presently calculated perturbed response  $\underline{p}(t)$ .

More explicitly it will be explained in the following sequence

- (1) Let  $F_2(\omega)$  is the frequency response in the range  $f_1 \leq f < f_2$  of the apodized transducer to be synthesized. This is obtained following the procedure described in Section (3.4). (Note that  $\omega = 2\pi f$ ).
- (2) Calculate the adopted time response  $a(t)$  from  $F_2(t)$ , which is the inverse Fourier transform of  $F_2(\omega)$  and let the optimum duration of  $a(t)$  be  $t_1 \leq t \leq t_2$ .
- (3) Calculate the achieved response in frequency domain  $F_2'(\omega)$  of  $a(t)$ . This is obtained by taking the Fourier transform of  $F_2(t)$  retaining only that portion between  $t_1 \leq t < t_2$  and zero elsewhere.
- (4) Calculate the error response in the range of interest i.e. form the difference between  $F_2'(\omega)$  and  $F_2(\omega)$  for  $f_1 \leq f \leq f_2$  and assume zero error elsewhere. Note that the requirement of conjugate symmetry in the frequency domain is always imposed while transforming it the time domain.

- (5) Multiply the error response by the chosen cost-coefficients,  $C_{xx}$  and form the resulting response  $F_3(\omega) = C_{xx}\{F_2'(\omega) - F_2(\omega)\}$
- (6) Transform the error weighted response  $F_3(\omega)$  to time domain and truncate it to  $t_1 \leq t \leq t_2$ , i.e. the response is assumed to be zero outside these limits. Let us denote the retained window by  $a_1(t)$ .
- (7) The retained window  $a_1(t)$  is transformed to frequency domain and the resultant response is retained within the interval  $f_1 \leq f \leq f_2$  and assumed zero elsewhere. Let us denote the resultant frequency response by  $F_4(\omega)$ .
- (8) The resultant response  $F_4(\omega)$  is multiplied by the inverse cost-coefficients i.e. by  $\frac{1}{C_{xx}}$  and then transformed to time domain, once again truncating to  $t_1 \leq t \leq t_2$ . Let this new time function be denoted by  $a_2(t)$ .
- (9) Now the corrections (perturbations) that are to be added to  $a(t)$  for improving the achieved response in frequency domain are given by  $-a_2(t)$  and therefore, the resulting adopted time response  $r(t)$  is given by  $\{a(t) - a_2(t)\}$ .

Symbolically the perturbations are given by

$$p(t) = -\mathcal{F}^{-1} \left\{ \frac{1}{C_{xx}} F_4(\omega) \right\} \quad \dots (5.36)$$

where  $\mathcal{F}^{-1}$  indicates the inverse Fourier transform operation and  $F_4(\omega)$  is obtained as indicated in step (7). The whole sequence of operations from (1) to (9) is termed as one set of transformations and if the required perturbations are obtained in one set of transformations, it is defined as zero order iteration process as indicated earlier.

### 5.6.2 N<sup>th</sup> Order Iteration

This procedure is the N<sup>th</sup> order iteration of the zero order process just described. In this iteration the adopted response is considered to be the sum of the previously adopted response and just calculated perturbation. A new value on the achieved response is calculated as the Fourier domain transform of this now adopted response. The next round of optimization procedure then follows the sequence. Calculation of the difference in the frequency domain, truncation and weighting in the frequency domain, transformation to the time domain, truncation in the time domain, transformation to the frequency domain, truncation and inverse weighting in the frequency domain, and finally change of sign, transformation to and truncation in the time domain to produce a new value of the perturbation.

The need for this technique did not arise because the achieved response obtained with zero-order iteration is nearly optimum and the whole sequence of steps took less than 10sec of CP time on CDC6400 computer, indicating the effectiveness of this fortuitous method.

Thus we conclude this chapter with the various optimization techniques developed for the synthesis of SAW filters and some of the results obtained for optimized TV IF filters are presented in the next chapter.

## CHAPTER 6

## COMPUTER ILLUSTRATION OF OPTIMIZATION TECHNIQUES

6.0 Introduction

In this chapter we present the theoretical results of the synthesized TV IF filters using the techniques developed in Chapter 5. Since we assumed a linear phase characteristics in the specified IF response we follow the OPTIM METHOD for illustrating the synthesis technique. Filters other than IF responses like bandpass responses are also considered to illustrate the feasibility of the technique. Results obtained by zero order successive iteration are of particular interest because of the way the method is developed. The choice of suitable parameters and other design considerations for each of the examples chosen are discussed in detail and the variation of the parameters and their influence on the behaviour of filter are also presented. All the computer programs have been developed in terms of a number of subroutines, assigning a specific operation for each of the subroutine. A brief description of the program is given for each of the examples considered.

6.1 Synthesis of TV IF Filter using OPTIM METHOD, Filter 2

We apply the OPTIM METHOD introduced in Chapter 5 for optimizing the Filter 1, developed in Chapter 3, we recall that the finite duration sampled response  $\underline{a}(t)$  of the output transducer  $T_2$  is symmetrical over its half-periodic interval  $\frac{T}{2}$  corresponding to 513<sup>th</sup> sampling point and the response extends from 400<sup>th</sup> sampling point to 626<sup>th</sup> sampling point, both inclusive assuming a total of 1024 sampling points. In the OPTIM METHOD we need to consider half the response in  $\underline{a}(t)$  and hence, it is sufficient to perturb only at half the number of sampling points i.e. from 400<sup>th</sup> to 513<sup>th</sup> sampling points, both inclusive. Thus we have to



solve 114 simultaneous linear equations.

#### 6.1.1 Selection of Cost-coefficients

Selection of cost coefficients seems to be a significant design parameter in the whole optimization process. In the early attempts it was felt that it is proper to select the same number of cost-coefficients in the frequency domain as there are the number of perturbation variables in the time domain. If we wish to perturb the response at all the 114 points we have to assign 114 cost coefficients and then a question arises to which portion of the frequency domain we have to assign the cost coefficients. An obvious answer is to assign the cost coefficients to that region where the specified response is centred around the 114 samples in the frequency domain. A preliminary computer investigation with this choice indicated that the response is not improved to the satisfactory level and at the same time it was found that the resulting time response is distorted very much, i.e. the smooth variation of 3 or 4 sampling points per cycle is destroyed and abrupt changes with huge amplitudes at the adjacent sampling points are found. This results in an unrealizable SAW device. In the frequency domain it was observed that response in the low-frequency range is not small compared to the original specification, and it was thought that the huge amplitudes in the time domain response may be due to this large low frequency component. Hence it was found that selecting cost coefficients as the same number of variables is not a suitable criterion.

In another attempt the cost coefficients are assigned to that region not only covering the IF passband but also right up to zero frequency component. In this case the number of cost coefficients selected were 210 while the number of perturbations are still 114 which ensures a non-singular matrix for H equation (5.28). The selection of the amplitudes of the cost coefficients is quite arbitrary, however, an appropriate choice will be to allocate higher cost coefficients where the error

response is lower. With this criterion an appropriate choice of cost-coefficients was made and once again a computer investigation by perturbing all the 114 sampling points revealed that the optimized response is very close to the specified response in frequency domain but with a distorted resultant waveform in the time domain. By distorted waveform we mean the smooth variation in the original finite duration time response  $\tilde{a}(t)$  with 3 to 4 samples per half-cycle is destroyed and abrupt changes with large variations in amplitudes are found so that a SAW filter cannot be built with this waveform representation. However, when we compare the reduction in cost it is quite promising. For the criterion followed in the optimization technique we expect a reduction of cost and in fact calculation of the above approach indicated a reduction in cost of about 94% after optimization indicating the effectiveness of the method. The level at sound trap increased from 19dB to 32dB while the levels at band edges are also increased by about 10dB, showing a good agreement with the specified response.

With these preliminary investigations it was found that it is necessary to assign cost coefficients throughout the frequency spectrum, not simply to a portion of it, whatever the number of perturbation variables in the time domain are. That means we have to assign 513 cost coefficients in the frequency domain and this requires a considerable amount of computing time if we wish to perturb at all the 114 sampling points in the time domain, because of the large number of computations required in evaluating the  $\tilde{H}$  matrix. Hence, it is better if we can further reduce the number of equations i.e. by considering less number of points than 114. In Chapter 3 it was mentioned that the sidelobes in time domain are responsible for forming the sound trap in the frequency domain, hence, a suitable choice will be to consider all the sampling points in the sidelobes and few sampling points in the mainlobe, thus reducing the number of equations considerably. In the program given in Appendix A2 for Filter 2 only 86 points are perturbed starting from the sidelobe end.

Returning back to the cost coefficients, we indicate here a choice of amplitudes for the 513 selected cost coefficients. The 50 cost coefficients at the specified frequency sampling points are taken to be approximately inversely proportional to the absolute values of the specified response at these sampling points and the remaining values at the other sampling points are selected arbitrarily. If the remaining coefficients are selected to be large (larger than the peak amplitude in the above 50 sample intervals) then we are trying to optimize the response in the sidelobe region of the frequency domain i.e. we are trying to achieve zero sidelobe response and this is difficult to achieve in practice. Moreover, our motive is to optimize the response in the specified range, not in the sidelobe range and anyhow they are negligibly small compared to the main response. On the other hand if they were selected to be small (much smaller than the minimum amplitude in the above 50 sample intervals) we are trying to optimize the response only in the desired range of interest and we might encounter the same difficulty faced at the beginning i.e. optimizing the response in the desired range of interest alone will produce a distorted time waveform which is unrealizable through a SAW device. Therefore, the remaining cost coefficients are to be selected in a compromising way. The best compromise was found to be to select the amplitudes of the order of 0.1% of the peak amplitude of the coefficient selected in the specified range of frequencies. In the program of FILTER 2 they were selected to be equal to 0.01.

#### 6.1.2 Design Considerations and Choice of Suitable Parameters

Design of the filter up to finite duration time response of the apodized transducer is the same as indicated in Chapter 3. Some of the design parameters are:

Number of sampling points  $N = 1024$

Periodic time duration  $T = 5\mu\text{sec}$

Frequency resolution  $\Delta f = 0.2\text{MHz}$ .

Initial sampling point of the specified response in  
frequency domain IFI = 148

Final sampling point of the specified response in frequency  
domain IFF = 197

Results obtained from program of FILTER 1 (Figure 3.6) are:

Initial sampling point of finite duration time response

ITI = 400

Final sampling point of finite duration time response

ITF = 626

Total number of samples in the finite duration including

ITI and ITF, NT = 227

Choice of parameters for optimization are:

Number of cost coefficients NC = 513

Number of perturbations starting from ITI, KP = 86

Following the arguments of Section (6.1.1)

$$C_i = \frac{1}{|F_2(\omega_i)|} \quad \text{for } i = \text{IFI, IFF}$$

$$= 0.01 \quad \text{for } i < \text{IFI and } > \text{IFF}$$

where  $F_2(\omega)$  is the specified response.

Having selected the various parameters a computer program was written to carry out the OPTIM METHOD.

### 6.1.3 Optimization Program FILTER 2

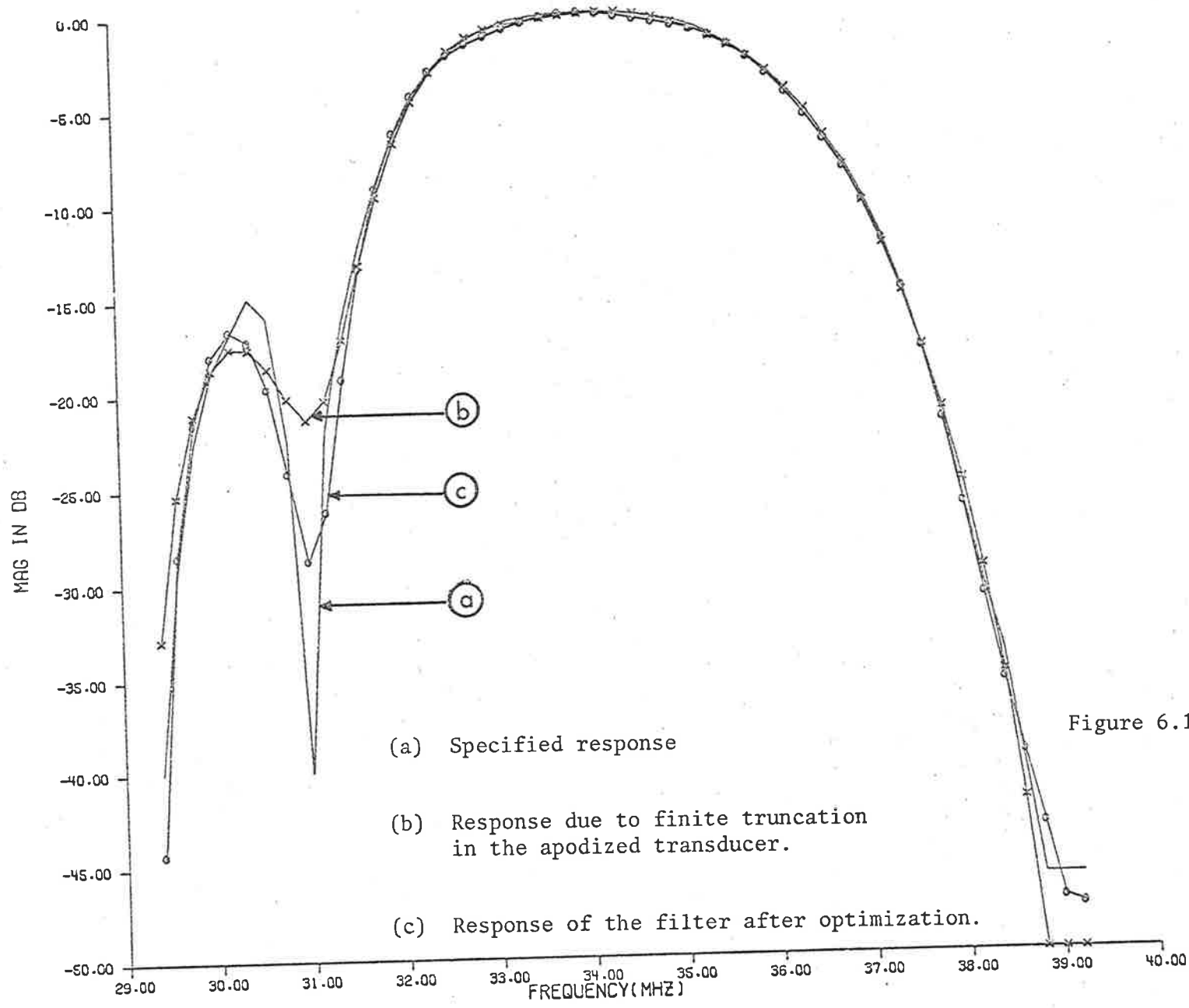
The program used for computing perturbation solution by OPTIM METHOD is called FILTER 2 and a listing is presented in Appendix A2 preceeding with a flow chart. A matrix subroutine called LSSS is used for solving the linear simultaneous equations, which makes use of the symmetry property of the matrix. The program calculates the optimum solution, adopted response and the achieved response <sup>in</sup> ~~is~~ frequency domain.

The results are shown in Figure 6.1. Further, the program generates, the gap-width and the overlaps necessary for plotting the pattern and then calculates the expected response of this pattern by assuming a sinusoidal representation of the source function in each gap.

#### 6.1.4 Discussion of the Results

If the achieved response after optimization Figure (6.1c) is not satisfactory, we may have to change some of the design parameters and repeat the whole optimization process once again. Possible changes in parameters are (i) increase the value of KP at the expense of computing time, (ii) a different set of  $C_i$ . Both approaches have been tried and it was found that the parameters presented in the program are the optimum for the achievable response. Increase in KP did not improve the response anything better than that presented in Figure (6.1c), except increase in computing time. This is expected because large perturbations are observed to occur at sidelobes rather than at the mainlobe in the time response, and increasing the perturbation points near the mainlobe does not influence the optimized response very much. A slightly different set of cost coefficients have also been tried, bearing in mind the precautions mentioned in Section 6.1.1 and it was found that the change in response is negligibly small.

An estimate of the total cost before and after optimization indicated a reduction of about 65% which is much less than for the case when we considered for 114 costs only. This is also expected because we are trying to reduce the sidelobes to zero by assigning cost coefficients throughout the spectrum and this will be difficult to achieve in general. Had the response been specified with small amount of sidelobes instead of zero values, we can expect a higher reduction in cost than 65%. But including sidelobes may arise aliasing problems when using the FFT routine. However, a reduction in cost of 65% is quite substantial and the requirements are nearly achieved in the frequency domain indicating the



- (a) Specified response
- (b) Response due to finite truncation in the apodized transducer.
- (c) Response of the filter after optimization.

Figure 6.1 Theoretical performance of Filter 2.

effectiveness of this method.

## 6.2 Synthesis of TV IF Filter using Zero-order Iteration

### Method, Filter 3

This method is considered to be fortuitous as indicated earlier, and is capable of yielding satisfactory results with much less effort. An outline of the method is presented in Section 5.6.1, but the theoretical results will be presented here applying the technique to the same finite duration time response of Filter 1.

#### 6.2.1 Design Considerations and Choice of Suitable Parameters

Design of the filter up to the finite duration time response of the apodized transducer is the same as indicated in Chapter 3. The various parameters up to the selection of cost coefficients and the number of perturbations are the same as indicated in Section 6.1.2. Summing up the results briefly we have,

$$N = 1024$$

$$T = 5\mu\text{sec}$$

$$\Delta f = 0.2\text{MHz}$$

$$\text{IFI} = 148$$

$$\text{IFF} = 197$$

$$\text{ITI} = 400$$

$$\text{ITF} = 624$$

$$\text{NT} = 227$$

We consider perturbing the response at all the sampling points of the retained window i.e. 227 perturbations, but assigning only 50 weighting coefficients in the frequency domain. The weighting coefficients selected are

$$C_{kk} = \frac{1}{|F_2(\omega_k)|} \quad \text{where } k = 1, 50$$

Having selected the various parameters, the perturbations are given by (equation 5.36),

$$p(t) = -7^{-1} \left\{ \frac{1}{C_{kk}} F_4(\omega) \right\}$$

where  $F_4(\omega)$  is calculated as described in Section 5.6.1.

### 6.2.2 Optimization Program FILTER 3

The computer program used for computing the perturbation solution by zero order successive iteration method is called FILTER 3 and a listing along with a flow chart is given in Appendix A3. The program calculates the 227 perturbations by successive truncation, weighting and transformation operations, as outlined in Chapter 5, evaluates the adopted response and the achieved response in the frequency domain. Further, the program generates the gap-widths and the overlaps necessary for plotting the pattern and then calculates the expected response of this pattern using a sinusoidal representation of the source function in each gap. The results obtained by this method are shown in Figure 6.2.

### 6.2.3 Discussion of the Results

If the achieved response after optimization is not satisfactory, we may have to change some of the design parameters and repeat the whole successive operation once again. The only variable available in this method is the choice of a different set of weighting coefficients. A slightly different set, has not produced any appreciable change in the optimized response, however large variations in the weighting coefficients either too small or too large compared to the present set of values have deteriorated the response after optimization. The same effect has also



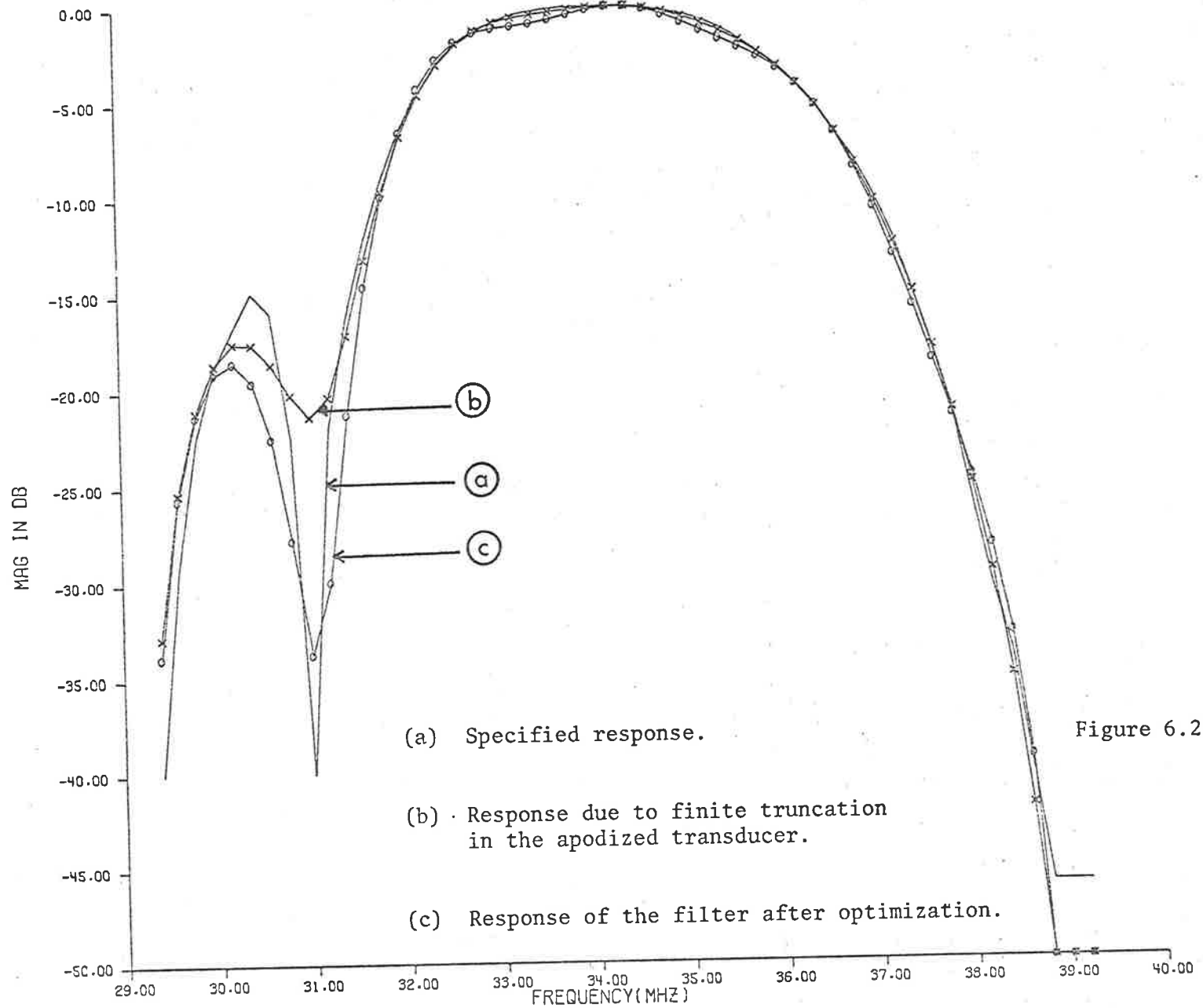


Figure 6.2 Theoretical performance of Filter 3.

been found by increasing the number of weighting coefficients than the present set of values and hence, it was found that it is difficult to draw any conclusion regarding the choice of weighting coefficients, however, with the present choice the method proved to be successful with much less effort. The solution does not require any matrix inversion and took less than 20sec of CP time compared to about 350sec of CP time of the previous method.

### 6.3 Synthesis of a TV IF Filter with Ideal Specifications using OPTIM METHOD, Filter 4

In the procedure described so far we have been trying to design a filter to achieve a given response as closely as possible, but in actual practice certain tolerances are permitted and it is sufficient if the response falls within these limits. We now consider a TV IF response with a given specified limit and try to synthesize a filter whose response lie within these limits. The ideal magnitude response of a typical TV IF system as indicated by one of the major electronics companies in Australia, with the prescribed limits is shown in Figure 6.3. The basic synthesis procedure is to assume an average characteristic which lie between the prescribed limits and then follow the method described in Chapter 3 and apply the optimization techniques developed in Chapter 5. Once again if we assume a linear phase characteristic the ideal technique is to apply OPTIM METHOD. As we see from Figure 6.3 that the lower limit is infinitely large at the band edges\* (adjacent channel carriers) and that flat band responses in some portions of the entire characteristic connected with steep slopes are present, an ideal characteristic is difficult, in fact impossible to achieve in practice. It is also to be noted that deeper the traps at the band edges and at the sound carrier the better will be the

---

\* However, a 60dB is assumed for plotting purposes.

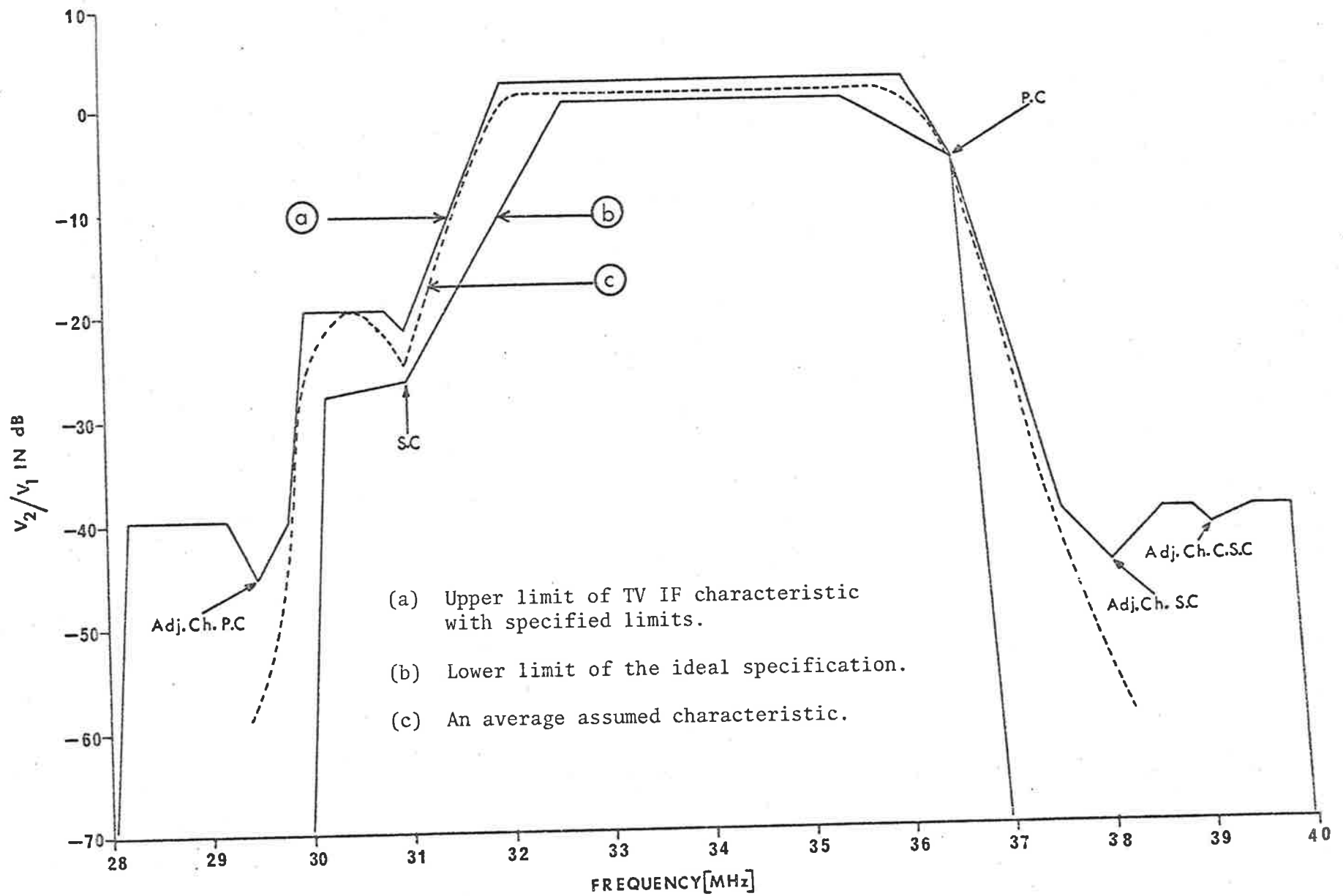


Figure 6.3 Magnitude response of TV IF characteristic with specified limits.

design for various reasons discussed in Chapter 3. From Figure 6.3 we note that a minimum limit of 45dB at the band edges and about 22dB at the sound carrier is necessary while designing the filter. We also know that flat band characteristics will produce undue ripples in the IF response because of the finite truncation in the time response (Gibb's phenomena). Ripples in the passband, however, is not a serious problem so long as they are within the prescribed limits. Further, the optimization will reduce the ripples to some extent (the amplitudes but not the number). Another aspect of reducing the ripples is to choose the response in a smooth variation rather than sharp changes. All these factors have to be taken into consideration while selecting the average characteristic of the IF response. The deep trap at the band edges may be obtained to some extent by adjusting the number of fingers in the uniform transducer and this will be discussed in the following section.

### 6.3.1 Design Considerations and Choice of Suitable Parameters

In the procedures described so far the proportions of input transducer  $T_1$  have been arbitrarily set to 9 fingers with a centre frequency of roughly 34.0MHz, so that the contribution due to  $F_1(\omega)$  is assumed to be fairly constant over the desired IF range. However, by increasing the number of fingers, the mainlobe is made narrower and if the first nulls are made to fall at the band edges, we can expect deep traps at these edges. With the average characteristic shown in Figure 6.3c, the central portion of the response (4.2MHz out of 7MHz band) is fairly flat. Choosing a narrow band response for  $|F_1(\omega)|$  produces large amount of ripple in the passband region and we have to seek an optimum number of fingers which produce minimum amount of ripple and at the same time increases the levels at the band edges. A preliminary computer investigation revealed that a choice of 11 number of fingers is a most suitable parameter in calculating the  $|F_1(\omega)|$  with a centre frequency of 34.0MHz. Hence  $N_1 = 10$  and  $f_0 = 34\text{MHz}$  in the expression  $\left| \frac{\sin x}{x} \right|$  where

$x = \frac{N_1 \pi}{2} \left( \frac{\omega - \omega_0}{\omega_0} \right)$ . The response is assumed to have specified from 29.4MHz to 38.2MHz with a sampling frequency of 0.2MHz giving rise to a total number of 45 samples in the specified region of interest. The other parameters for computing the FFT routine are the same as indicated in the previous programs, i.e.  $N = 1024$  and  $T = 5\mu\text{sec}$ . Design of the filter up to truncated time response of the apodized transducer is the same as indicated in Chapter 3. Summarizing the results we have,

$$N = 1024$$

$$T = 5\mu\text{sec}$$

$$\Delta f = 0.2\text{MHz}$$

$$\text{IFI} = 148$$

$$\text{IFF} = 192$$

The optimum finite duration time response in this case was found to be equal to 79 half-cycles corresponding to 251 sampling intervals in the time domain.

$$\text{i.e.} \quad \text{ITI} = 388$$

$$\text{ITF} = 638$$

Since the optimization technique followed is the same as for Filter 2 we apply the same conditions as indicated in Section 6.1.2 i.e.

$$\text{Number of coefficients } \text{NC} = 513$$

$$\text{Number of perturbations starting from ITI, KP} = 86.$$

Following the arguments of Section 6.1.1, cost coefficients are

$$C_i = \frac{1}{|F_2(\omega_i)|} \quad \text{for } i = \text{IFI}, \text{IFF}$$

$$= 0.01 \quad \text{for } i < \text{IFI} \text{ and } > \text{IFF}$$

where  $|F_2(\omega)|$  is the specified response.

Having selected all the parameters a computer program was written to obtain the optimum solution for Filter 4.

### 6.3.2 Optimization Program Filter 4

The computer program developed for evaluating the optimum solution using OPTIM METHOD for achieving the ideal specified response is called FILTER 4 and a listing along with the flow chart is given in the Appendix A4. The program evaluates the symmetrical time response, calculates the optimum solution by considering KP samples and then the adopted response and the achieved response of the filter. The results are shown in Figure 6.4. Further the program generates the zero crossings and the overlaps necessary for plotting the pattern and then calculates the expected response of this pattern by approximating a sinusoidal source function representation in each gapwidth.

### 6.3.3 Discussion of the Results

The effect of change in cost coefficients or the number of perturbations is the same as discussed for Filter 2 in Section 6.1.4. Since the specified response of the filter has a flat characteristic for most of the IF passband, the response of the apodized transducer has a downward slope in this region so also the ripples in the frequency domain of the adopted time response. It was observed that, more the number of fingers in the transmitting transducer, more will be the slope and hence a large amount unequal ripples in the IF region. In order to minimize this effect it is necessary to reduce the number of fingers in the transmitting transducer which in turn reduces the level at the band edges. A compromise of 11 fingers was found to be most satisfactory. Further, it was found that it is necessary to increase the truncation limits in the finite duration time response than in the previous example to keep the sound trap to a reasonable level.

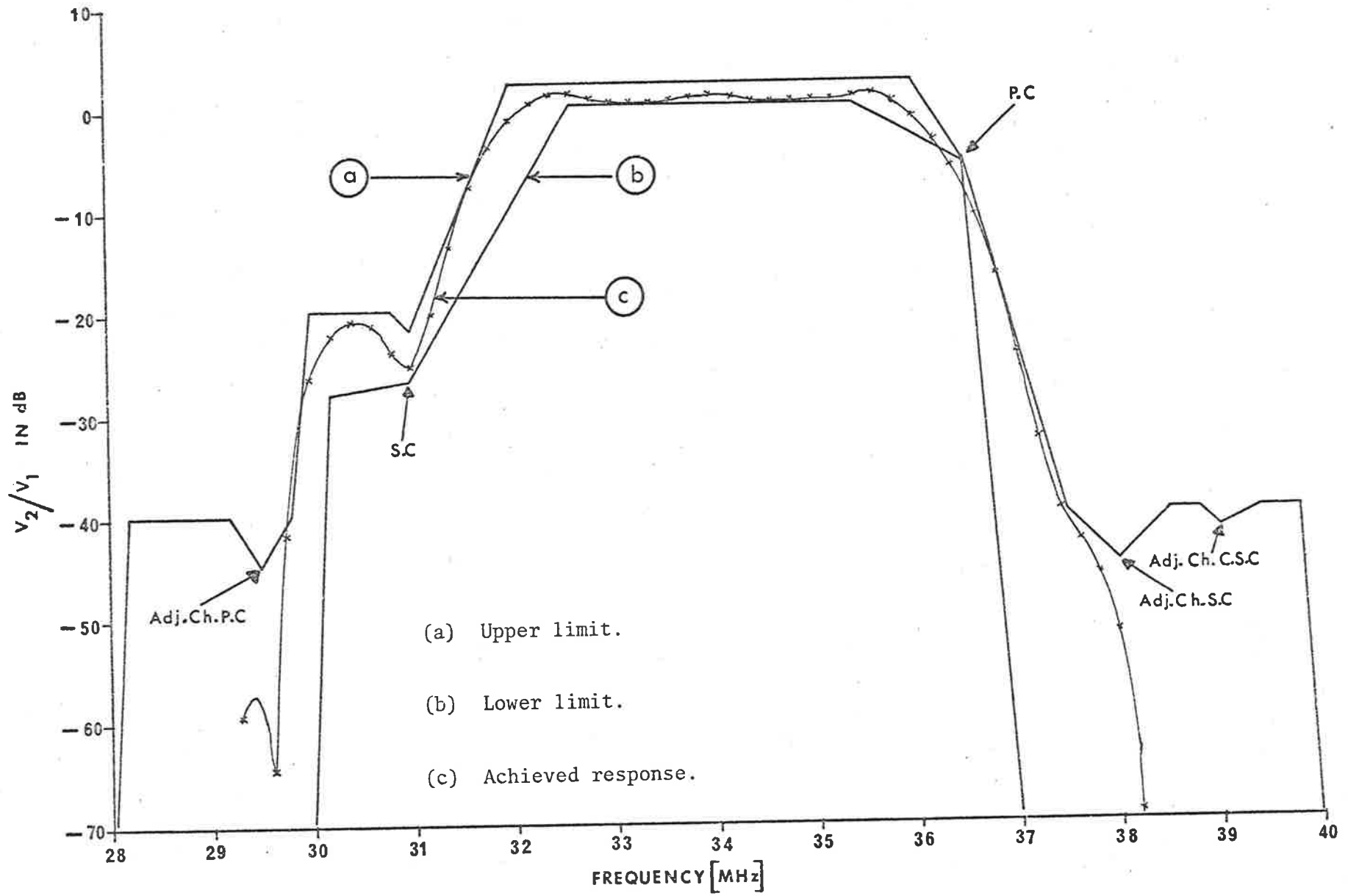


Figure 6.4 Ideal specifications and the achieved response with the OPTIM METHOD.

In general it was found that any attempt to improve the level at the band edges will deteriorate the level at the sound carrier or vice versa, even though some allowance was given to the ripple in the passband. The optimum design will depend upon the number of fingers in the transmitting transducer, truncation limits in the apodized transducer and the number of perturbations in the optimization technique. Of the various trials, the present parameters indicated in Section 6.3.1 seems to be the best compromise for achieving this ideal response. For all the filters synthesized with OPTIM METHOD it was found that major perturbations were occurred in the sidelobe region than near the mainlobe region.

#### 6.4 Additional Illustrations of OPTIM METHOD

We present here some of the additional examples considered using OPTIM METHOD. The simple example considered is a rectangular bandpass filter. The basic parameters are the same as used for Filter 1 but instead of using the IF response a bandpass response is introduced in its place. Hence, the variables used are:

$$N = 1024$$

$$T = 5\mu\text{sec}$$

$$\Delta f = 0.2\text{MHz}$$

$$\text{IFI} = 148$$

$$\text{IFF} = 197$$

The magnitude of the bandpass filter is constant throughout the entire region, except at the band edges where it is assumed to be 40dB down. The filter is then synthesized with similar approach as used for the synthesis of Filter 1, except that the response is truncated arbitrarily in the time domain. The sampled response is retained only at 109 sampling points out of 1024, starting from 459<sup>th</sup> point.

$$\text{i.e.} \quad \text{ITI} = 459$$



ITF = 567

The frequency response of this retained window is then calculated using FFT routine, and obviously the response is quite different from the specified one. The levels at the band edges are only of the order of 15dB, while a large amount of ripple is present in the passband with wide skirts at the band edges. The OPTIM METHOD is then applied to the retained window assigning same number of cost coefficients as there are the number of variables and perturbing all the samples in the finite response. The optimized response is very close to the specified response, with a reduction of about 95% in the total cost. The levels at the band edges increased to about 40dB while the skirt slopes are also increased considerably. The ripples, though increased in number, reduced in size to a great extent. However, the resultant time response distorted considerably and SAW filter cannot be devised with this waveform representation. When the cost coefficients are assigned in the whole frequency spectrum, a realizable pattern was obtained with a satisfactory improvement in the frequency domain.

The example of bandpass filter is presented here to show the effectiveness of the OPTIM METHOD, and it is not the purpose to make a practical SAW device. Moreover, well established techniques are available in the literature for synthesizing the bandpass filters, but the purpose is to show that the method is most general and is applicable to synthesize any sort of filter.

Thus we conclude this chapter illustrating the optimization techniques developed in the previous chapter. The experimental performances of the synthesized filters will be presented in the next chapter.

## CHAPTER 7

## EXPERIMENTAL PERFORMANCE OF OPTIMIZED FILTERS

7.0 Introduction

In this Chapter we present the experimental performance of some of the optimized filters, synthesized in Chapter 6 and compare their theoretical responses by evaluating the transmittance formula developed in Chapter 2. Theoretical and experimental investigation of the filter insertion loss is also presented. Precise details of the filter fabrication and measurement procedures have been documented as described in Chapter 4, except the generation of the original artwork, the essential difference being that the artwork was drawn to be amenable to a single stage reduction for the final transparency, instead of two stage reduction as followed for Filter 1. Tuning and mounting techniques are exactly the same as described in an earlier Chapter (Chapter 4), except for a few refinements in the techniques. Commercially available Eddy-stone boxes were used as the mounting jigs and the internal screening is prepared in the Departmental workshop.

Computer programs have been developed to evaluate the input-output admittance parameters in the admittance model of the filter and the results are illustrated for a typical optimized filter.

7.1 Pattern Generation and Filter Fabrication

The filter patterns were generated by the computer using the program ARTWORK as described in the Appendix A1. The patterns were designed for a single stage reduction and the electrodes were drawn using black ink with a pen tip of 0.3 mm size. The filters which we describe in the chapter are similar in construction, hence they will be dealt with together. After a choice of suitable substrate, the working area of the interdigital digital transducer structures was selected and with an appropriate reduction ratio, the filter patterns were drawn as described above. A summary of the filters description is given in Table 7.1. Filter 1 was already discussed in Chapter 4, but it is presented here simply for comparison purpose

Filter Identification	Response Specification	Method of Optimization	Transmitting transducer		Receiving transducer		Group delay between the transducers	Reduction ratio	Choice of substrate and propagation direction	Assumed surface wave velocity
			No. of fingers	Maximum overlap length	No. of fingers	Maximum overlap length				
Filter 1	IF response of a typical test receiver	Four-T's method	9	6.25mm	69	5.0mm	7.8 $\mu$ sec (2.47cm)	60	YX Quartz (1 $\frac{1}{2}$ "x1"x $\frac{1}{8}$ ")	3.16km/sec
Filter 2	Same as Filter 1	OPTIM METHOD	9	6.25mm	72	6.0mm	6.8 $\mu$ sec (2.14cm)	25.2	"	3.145km/sec
Filter 3	Same as Filter 1	Zero order iteration	9	6.25mm	72	5.0mm	6.8 $\mu$ sec (2.14cm)	25.2	"	3.145km/sec
Filter 4	Response with ideal specification	OPTIM METHOD	11	6.25mm	78	5.0mm	6.8 $\mu$ sec (2.15cm)	25.2	"	3.145km/sec

TABLE 7.1 Description of the filters drawn by the computers using Program ARTWORK

with other filters. The program, ARTWORK given in Appendix A1, is for Filter 2 and appropriate data has to be changed for drawing the other filters, the necessary requirements being mentioned in the program itself. The electrode patterns of the three filters, Filter 2, Filter 3 and Filter 4 are shown in Figures 7.1, 7.2 and 7.3 respectively.

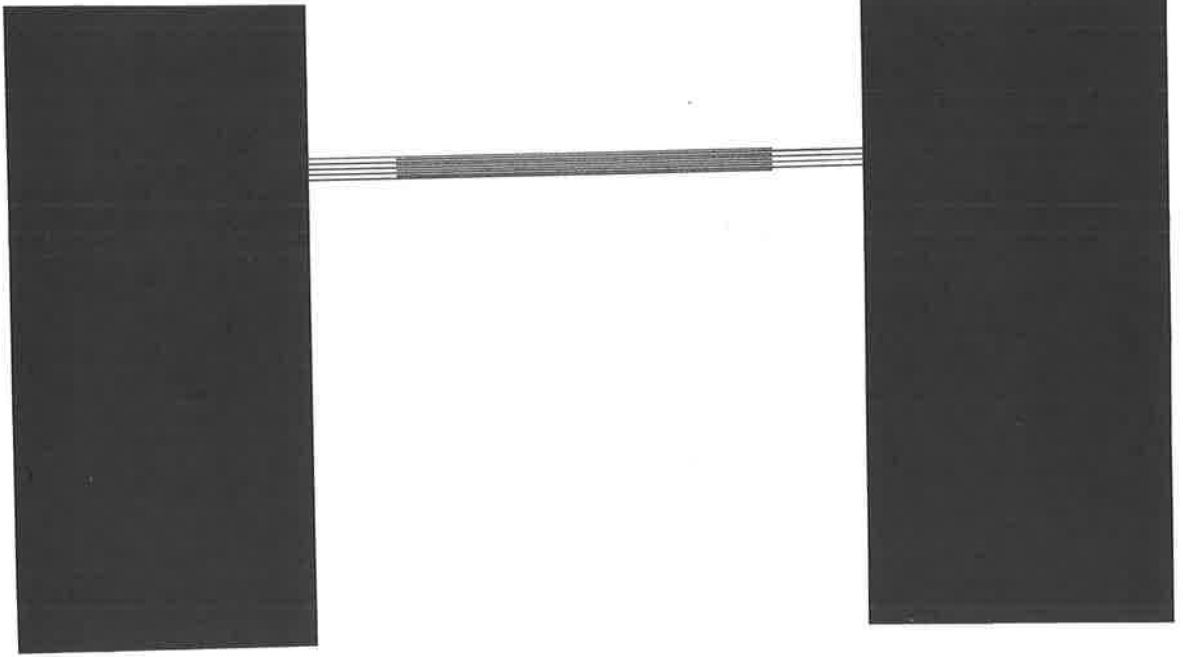
The filters were then fabricated using the photolithographic techniques mentioned in Appendix B mounted in metal boxes following the same principles as described in Section 4.3.1 and a 50ohm termination was adopted for measuring the frequency response characteristics as shown in Figure 4.4.

## 7.2 Experimental and Theoretical Results

The frequency response of the filter was measured in the same manner as described in Section 4.3.4 and the results are shown in Figures 7.4, 7.5 and 7.6 for the three respective filters, compared with the theoretically predicted response using the trans-admittance model, a computer program of which is described below.

### 7.2.1 Transadmittance Programs, Y21FIL

The program used for computing the theoretical performance of the filter is identified as Y21FIL and the listing of a typical example (Filter) is presented in Appendix A5, preceding a flow chart. The program evaluates the frequency response of the uniform and apodized transducer structures by approximating an independent cosinusoidal source function representation in between the gaps and then calculates the transadmittance in siemens with the given material contents. The program can also calculate the insertion loss of the filter, if the load admittance across the output transducer is provided or calculated in a subroutine with given circuit parameters. Provision is also made to include small changes in reduction ratio or surfacewave velocity or both, if required, in order to compare the theoretical results with the



P10911P2

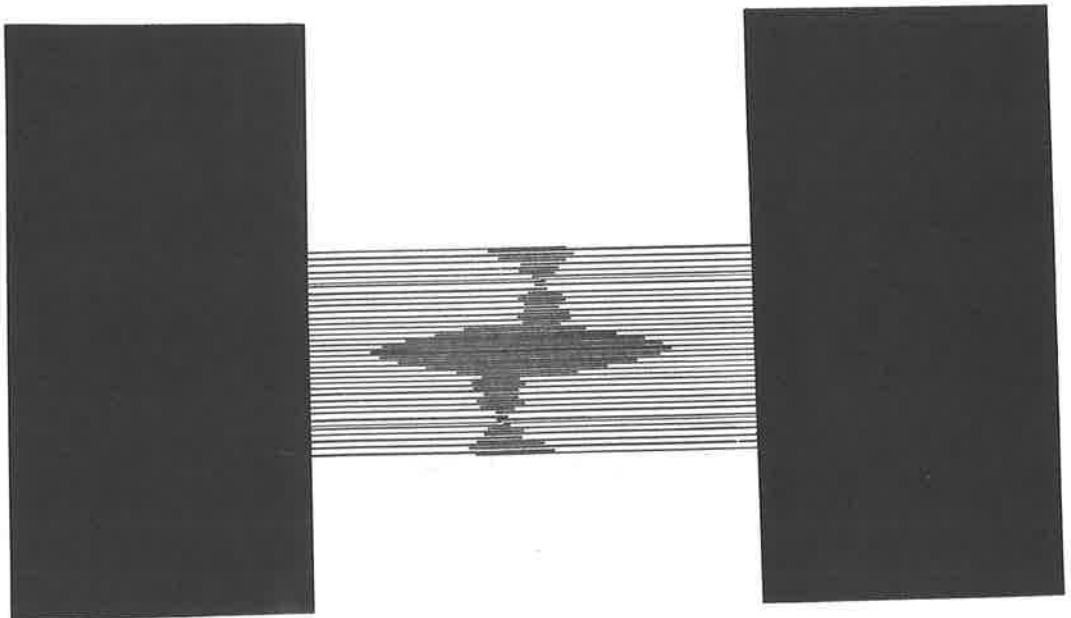
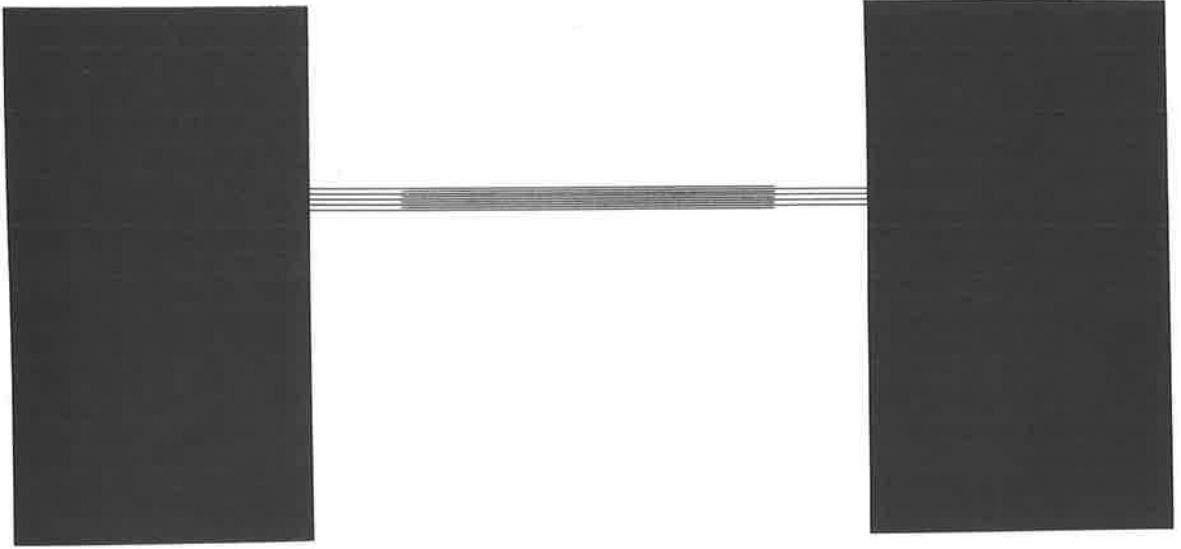


Figure 7.1 Electrode pattern of Filter 2.



P/09/1112

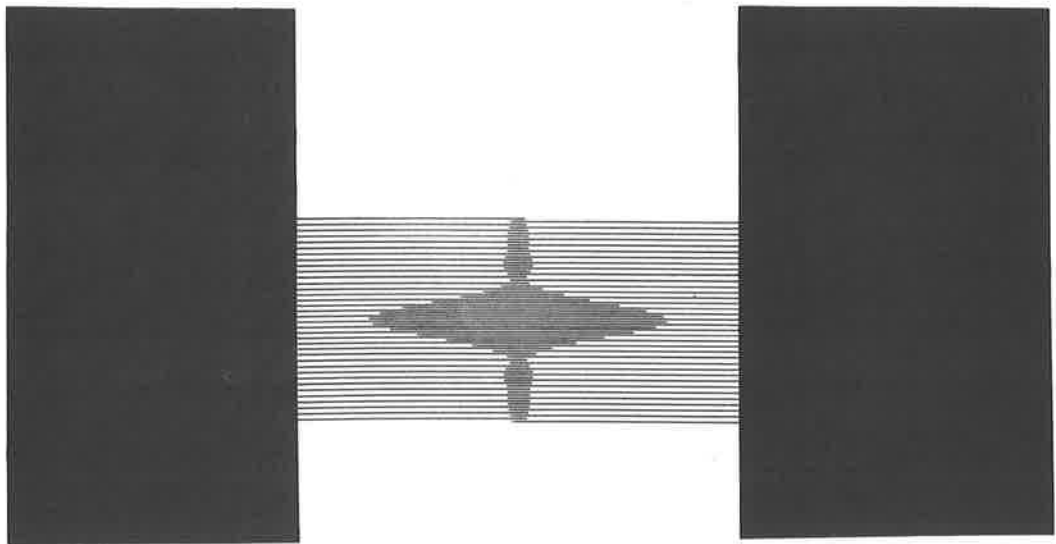
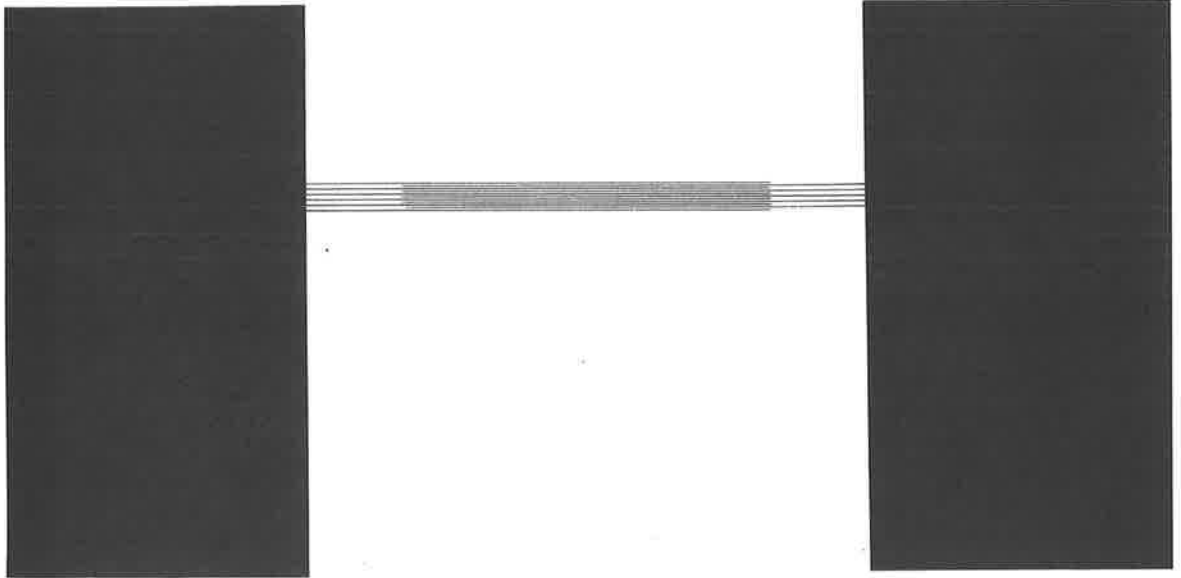


Figure 7.2 Electrode pattern of Filter 3.



A17111P2

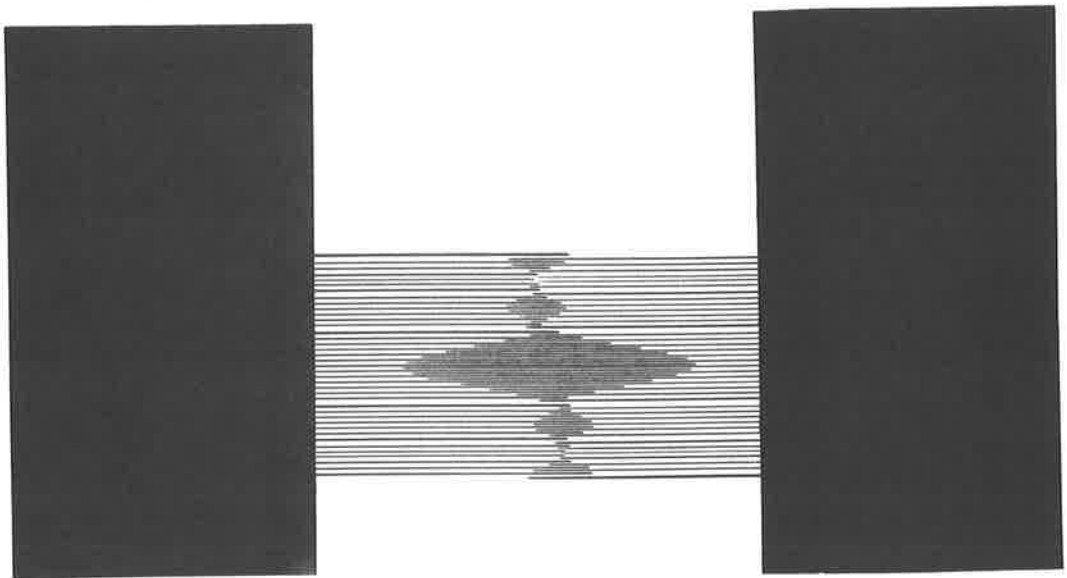


Figure 7.3 Electrode pattern of Filter 4.

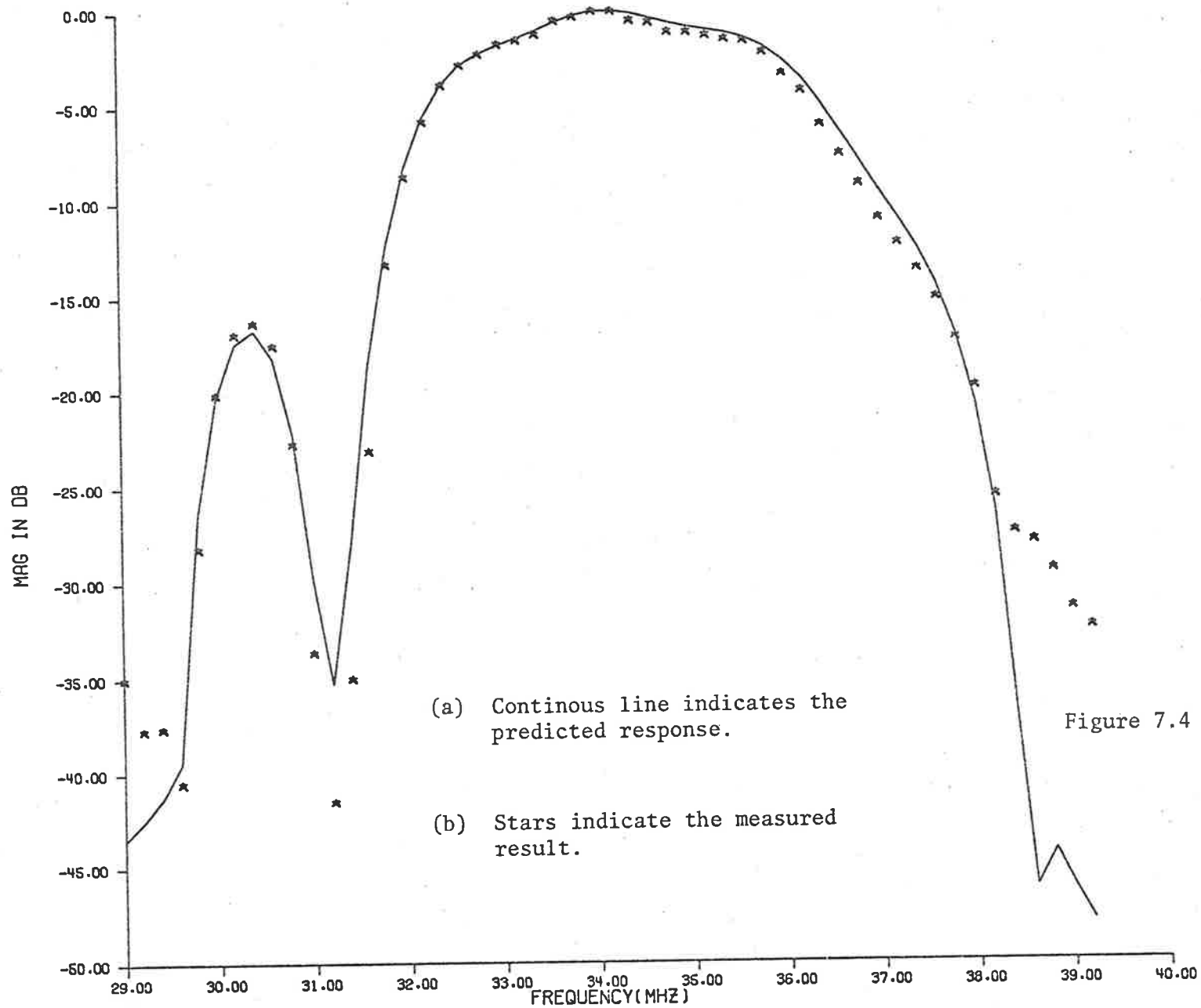
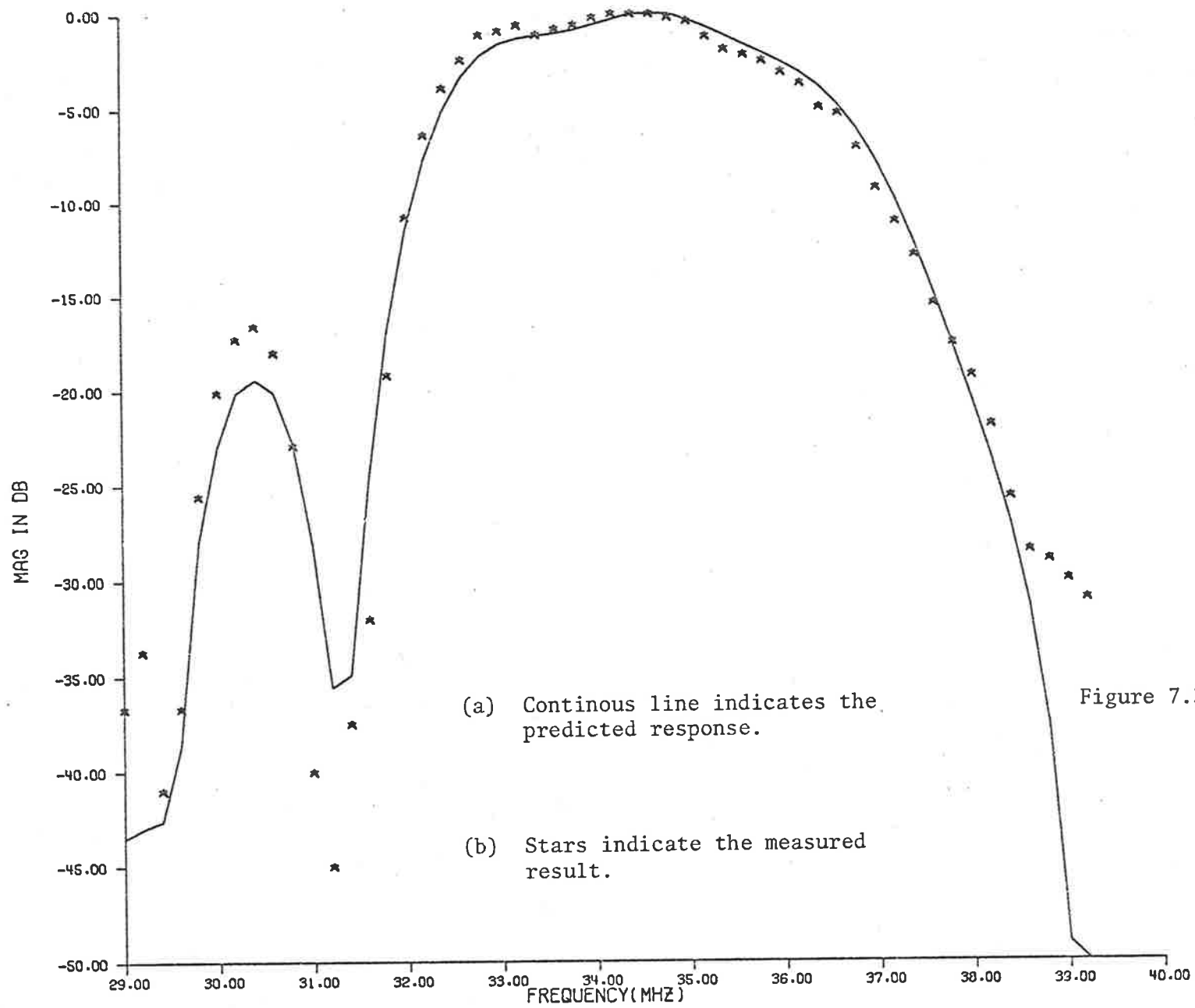


Figure 7.4 Theoretical and experimental frequency response of Filter 2.





(a) Continuous line indicates the predicted response.

(b) Stars indicate the measured result.

Figure 7.5 Theoretical and experimental response of Filter 3.

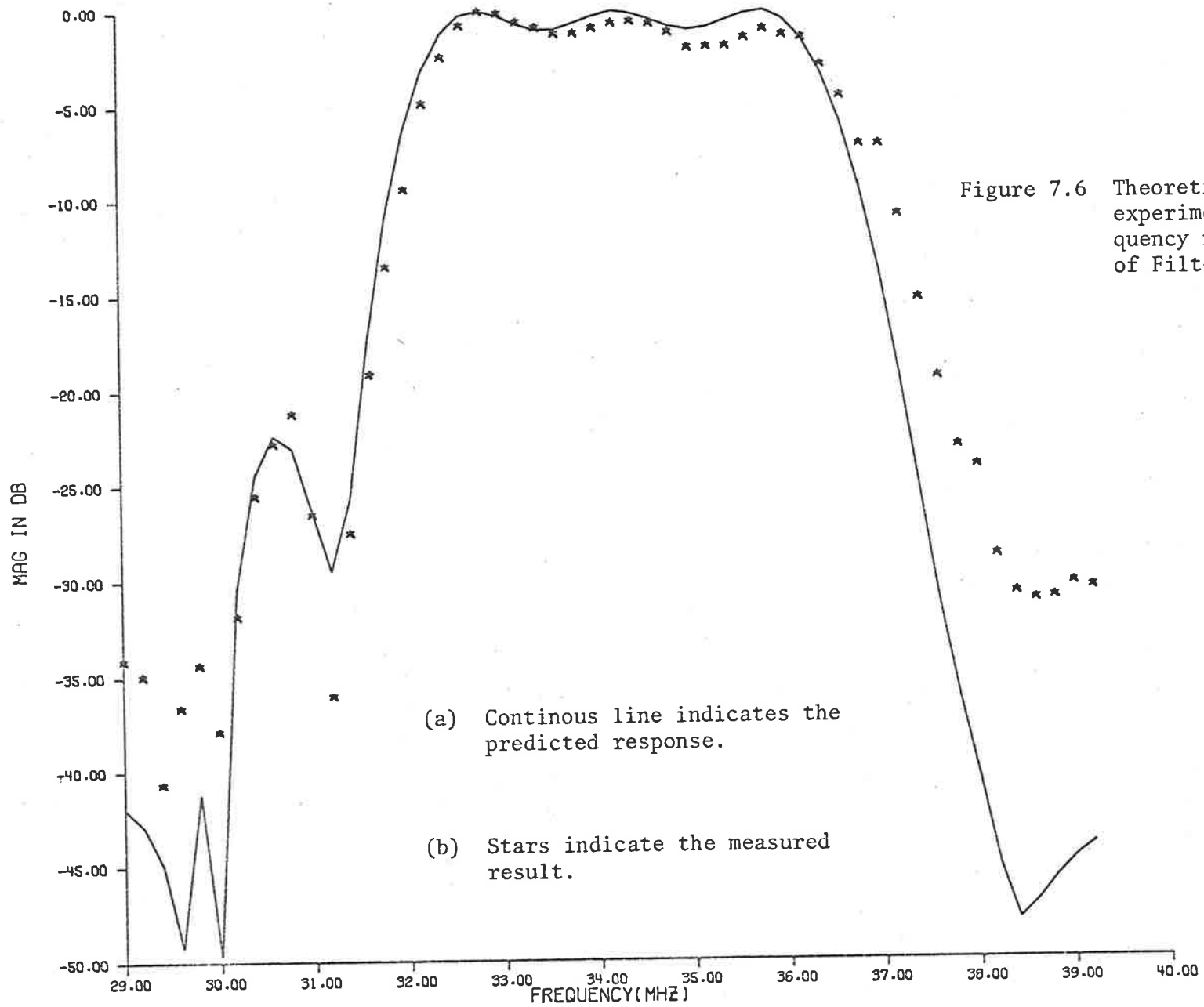


Figure 7.6 Theoretical and experimental frequency response of Filter 4.

experimental ones. The graphs shown in Figures 7.4, 7.5 and 7.6 are the voltage transfer ratio of the filter and the product of transadmittance and load impedance of the filter (equation 2.5), plotted in dB scale, maximized with respect to peak amplitude. The radiation conductance and susceptance of the input-output transducers have been neglected in both the measurement procedure and in the theoretical evaluation of the filter frequency response. As pointed out in the beginning of Chapter 2, their magnitudes are negligibly small compared with the static capacitive reactances.

### 7.3 Input-output Admittances of the Filter

By input-output admittances of the filter we mean the input-output admittance parameters of the uniform and apodized transducer structures under short-circuit conditions as defined in the admittance model (Chapter 2). For the experimental devices presented in this Chapter or for the filter presented in Chapter 4, measurement of these quantities is extremely difficult, except for the static capacitances, because of low coupling material and only a small number of fingers are used in each transducer, (particularly for the uniform transducer). As an illustration, consider the input admittance of a uniform transducer. Recall equations (2.33), (2.34), (2.35) and (2.36) and at the synchronous frequency,

$$Y_{11}(\omega_0) = G(\omega_0) + j\omega_0 C_T \quad \dots (7.1)$$

$$= \frac{-|\omega_0| \Delta W N^2 \pi^2 (\epsilon_0 + \epsilon_p)}{4 \times 1.854^2} + j\omega_0 C_T \quad \dots (7.2)$$

$$= \frac{-|\omega_0| C_T N}{4 \times 1.854^2} + j\omega_0 C_T \quad \dots (7.3)$$

For YX quartz substrate  $\Delta_x \approx 0.1\%$  and even for 201 fingers ( $N = 100$ ),

the magnitude of first term is approximately 0.1 times the magnitude of the capacitance reactance term, for a 9 finger transducer this is much smaller than 0.1 and there is considerable difficulty in measuring such a small quantity, however, we can calculate the input admittance for the uniform transducer, using the expressions derived in Section 2.3 or using the transadmittance  $Y_{21FIL}$ , by considering two identical transducers and putting the separation between them equal to zero.

### 7.3.1 Input-admittance of the Filter

The input admittance parameters of the filters concerned, comprise the admittance parameters of the uniform transducer alone when the reflections from the shorted apodized transducer are neglected. This is, of course, one of the basic assumptions in the admittance formulism. Computer programs have been written to evaluate the input admittance parameters of the uniform transducers and the magnitude responses  $G(\omega)$ ,  $B(\omega)$  and  $\omega C_T$ , obtained are similar to those published by other workers [7]<sup>1,2</sup>, except for the fact that the responses  $G(\omega)$  and  $B(\omega)$  are not symmetrical over the synchronous frequency,  $\omega_0$ , and so also the side-lobes because of the  $|\omega|$  factor in the input admittance formula of the admittance model. The results are fairly obvious, hence, the graphical representations of the responses  $G(\omega)$  and  $B(\omega)$  are not presented here. However, as a specified example, for a 9 finger transducer of 6.25mm width on YX quartz substrate, at the synchronous frequency of 34.4MHz the following quantities were obtained.

$$G(\omega_0) = 2.765 \mu \text{ siemens}$$

$$B(\omega_0) = -0.18 \mu \text{ siemens}$$

$$\omega_0 C_T = 260 \mu \text{ siemens}, C_T = 1.2 \text{ pF (theoretical)}$$

$$\omega_0 C_T = 540 \mu \text{ siemens}, C_T = 2.5 \text{ pF (measured)}$$

In all the transducer capacitance measurements, it was found

that the measured values are higher than the predicted values by an amount of 1 to 2 pF, the exact amount being dependent upon the layout of the pattern and of the circuit wiring.

### 7.3.2 Output-admittance of the Filter

The output admittance parameters of the filter concerned, comprise the admittance parameters of the apodized transducer alone, with the same reasoning given in the preceding section. However, calculation of the admittance parameters is not as simple as that for uniform transducers for the reasons mentioned in Section 2.4 of Chapter 2. The method followed here is similar to that described by Hartmen et al. [7]<sup>3</sup> in their impulse model design of acoustic surface wave filters. A computer program was developed by the author to evaluate the admittance parameters of the symmetrical apodized transducers, a listing of which is given in Appendix A6. The program is called Y22APOD and evaluates the radiation conductance by dividing the apodized transducer into a number of uniform but unequal width strips and adding the contributions from each strip. The radiation susceptance is again given by Hilbert transform of the radiation conductance, and the capacitance reactance is calculated from the relation,

$$\omega C_T = \frac{1}{2} \omega (\epsilon_0 + \epsilon_p) \sum_{i=1}^N (A_i) \quad \dots (7.4)$$

where  $A_i$  are the overlap lengths on the apodized transducer of  $N$  half-wavelengths long and  $\epsilon_0$  and  $\epsilon_p$  are the material constants. The program can also be used for uniform transducers in which case it divides the transducer into a single strip and the rest of the calculations follow thereafter. The computed results for a typical optimized filter (Filter 2) are shown in Figure 7.7. It is interesting to see that the radiation conductance characteristic is similar to the magnitude response of the filter itself, the probable reason being that the total burden of producing the filter response is bestowed upon the apodized transducer alone

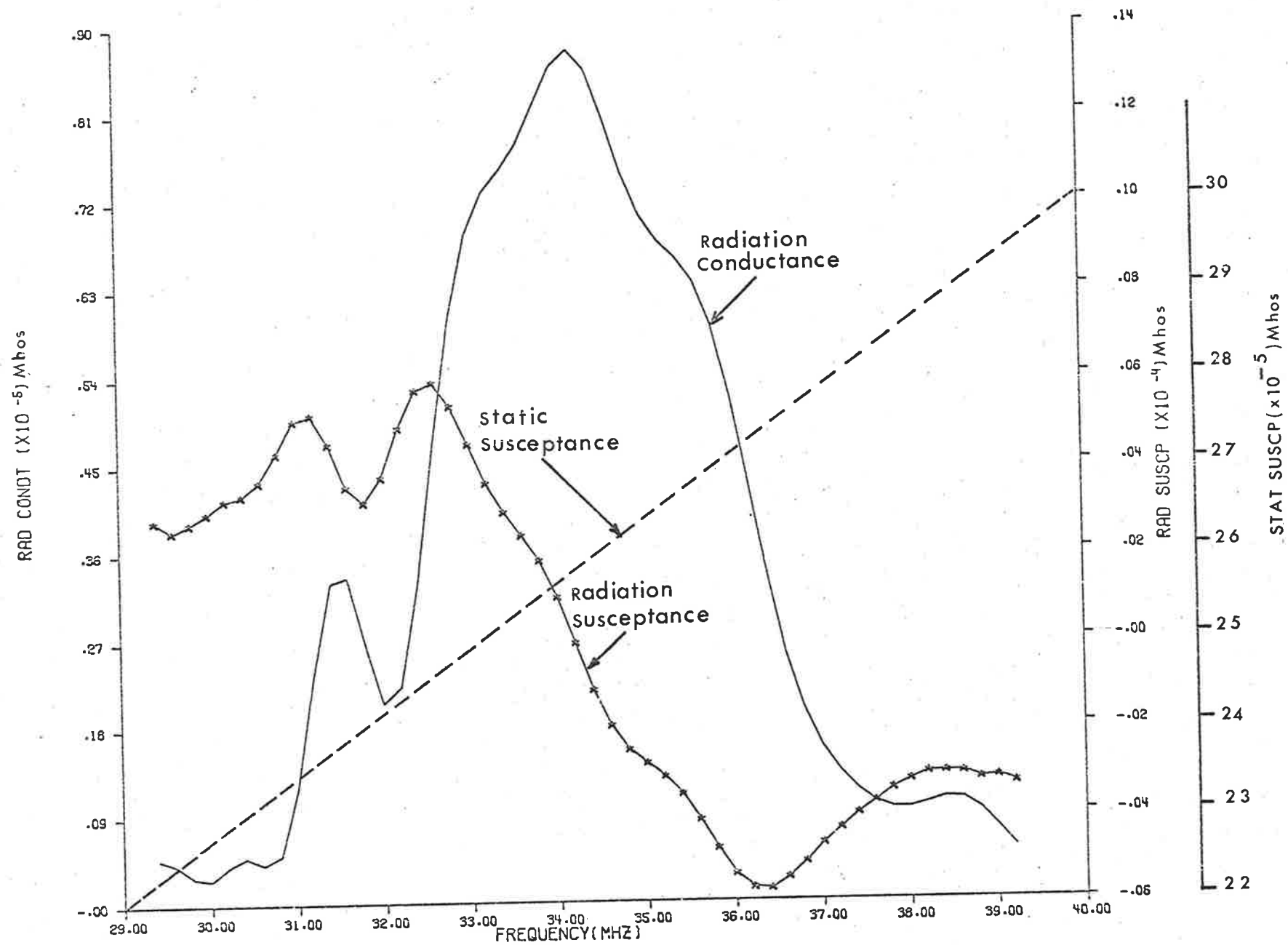


Figure 7.7 Radiation conductance and susceptance of apodized transducer in Filter 2.

and the contribution from the uniform transducer is assumed to be constant. Had the overlaps been the same we expect a  $\left(\frac{\sin x}{x}\right)^2$  characteristic but because of the particular apodization to realize the desired frequency response the radiation characteristic is also similar to the desired frequency response. At the centre frequency of 34.4MHz the following quantities were obtained.

$$G(\omega_0) = 8.75 \mu \text{ siemens}$$

$$B(\omega_0) = -7.9 \times 10^{-2} \mu \text{ siemens}$$

$$\omega_0 C_T = 460 \mu \text{ siemens } (C_T = 2.12 \text{ pF theoretical})$$

$$\omega_0 C_T = 855 \mu \text{ siemens } (C_T = 4 \text{ pF measured})$$

No attempt was made to measure the quantities  $G(\omega)$  and  $B(\omega)$  because with these transducers it is completely dominated by the static susceptances. In this situation, the static susceptance and parasitic strays are of more concern to the filter design, than  $G(\omega)$  and  $B(\omega)$  and, therefore,  $G(\omega)$  and  $B(\omega)$  may be neglected.

#### 7.4 Insertion-loss due to Impedance Mismatch

The theoretical and experimental insertion-loss of the filter with a  $50\Omega$  load termination, agree quite well apart from an average of 3dB difference in the IF passband and this can be attributed due to various losses in the practical SAW devices. The theoretical insertion-loss is calculated from the relation  $20 \log\{|y_{21}(\omega)|R_L\}$  and the measured insertion-loss is calculated from the relation  $20 \log\left(\frac{V_2}{V_1}\right)$ . The calculation of these values is incorporated in the program called Y21FIL given in Appendix A5. The observed value of the insertion-loss at the centre frequency, is rather high of the order of 72dB down (further increasing on either side) and is due to impedance mismatch of the transducer with the source and load impedances. The high impedance of the low transducer is due to the use of the low  $K^2$  material, while a low impedance measurement

system is necessary for the various reasons mentioned earlier. Thus, we see a great amount of mismatch in the impedances and this fact will be elaborated more clearly as follows.

First of all, a comment on the definition of the insertion-loss will be made. The term insertion-loss, referred in this investigation means the voltage transfer ratio expressed in decibels, i.e.  $20 \log \left( \frac{\dot{v}_2}{\dot{v}_1} \right)$  (also approximately equal to  $20 \log |y_{21}(\omega) R_L|$ , where  $\dot{v}_2$  is the output voltage across the filter and  $\dot{v}_1$  is the input voltage to the filter. This facilitates comparison between the theory and the experiment for both passband shape and the insertion-loss at the band centre. However, it is more appropriate to define the insertion-loss of the filter as the power transfer ratio expressed in decibels, i.e.  $10 \log \left( \frac{P_L}{P_I} \right)^*$ , where  $P_L$  is the power delivered to the load and  $P_I$  is the power delivered by the source. These two results viz.  $20 \log \left( \left| \frac{\dot{v}_2}{\dot{v}_1} \right| \right)$  and  $10 \log \left( \frac{P_L}{P_I} \right)$  are not the same in general, except under certain circumstances.

For the purpose of illustrating the insertion-loss, we assume the filter has the source and load conductances  $G_S$  and  $G_L$  respectively, as shown in Figure 7.8(b), and the radiation conductances and susceptances are neglected. This will be a reasonable assumption on weak-coupling materials, least for anything other than very narrow band-widths.

The power delivered by the source to the transducer at band centre is given by

$$P_I = \frac{I_1^2}{4G_S} \quad \dots(7.5)$$

the power delivered to the load is given by

$$P_L = \frac{|y_{21}(\omega)|^2 I_1^2}{G_L G_S^2} \quad \dots(7.6)$$

where  $|y_{21}(\omega)|$  is the magnitude of the transadmittance between the transducers and  $I_1$  is the input current source and  $G_L$  is the load conductance  $\left( \frac{1}{R_L} \right)$ . Therefore, the insertion-loss of the filter according to the power transfer ratio definition is given by,

---

\* In normal terminology it represents the power gain but it is termed here as the insertion-loss.



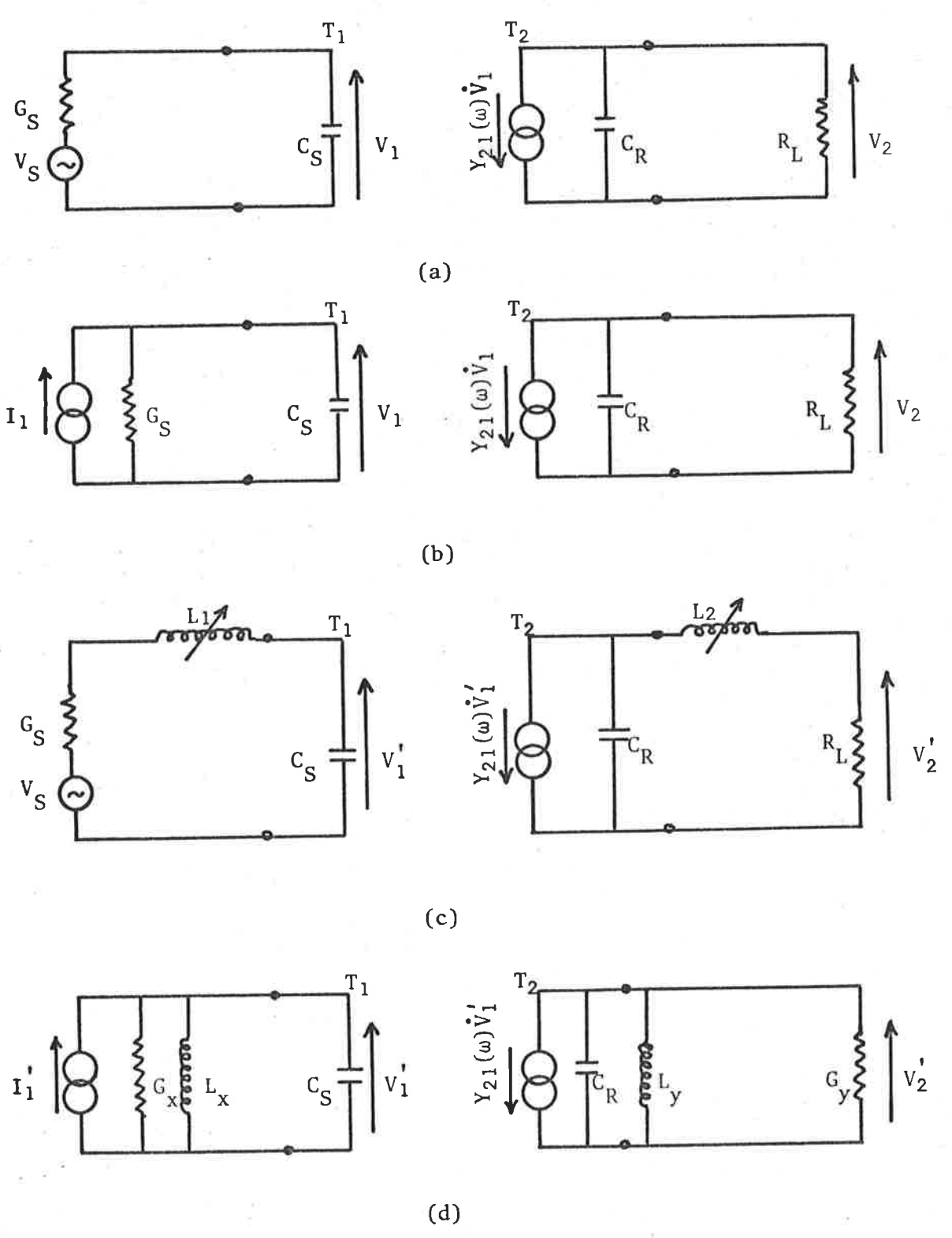


Figure 7.8 Equivalent Circuit Representation for Illustrating the Insertion-loss of the Filter.

- (a) Without tuning inductors (series representation).
- (b) Same as (a) but with shunt representation.
- (c) With series tuning inductors (series representation).
- (d) Same as (c) but with shunt representation.

$$P_{in}(\omega) = \frac{P_L}{P_I} = \frac{4|y_{21}(\omega)|^2}{G_L G_S} \quad \dots(7.7)$$

When  $G_L = G_S$  the expression for  $P_{in}(\omega)$  in dB scale is similar to that of voltage transfer ratio expressed in dB scale i.e.  $20 \log \left| \frac{\dot{V}_2}{\dot{V}_1} \right|$  or  $20 \log \{ |y_{21}(\omega)| R_L \}$  except that  $P_{in}(\omega)$  will be 6 dB lower. Therefore, we assume  $G_L = G_S$  (the untuned load and source conductances) and explore the ideas for improvements in the insertion-loss of the filter.

Figure 7.8(c) shows two series inductor tunings in the input-output circuits and an equivalent shunt representation is shown in Figure 7.8(d). The equivalent shunt conductance in the input circuit is given by

$$G_x = \frac{G_S}{(1+Q_1^2)} \quad \dots(7.8)$$

where

$$Q_1 = \omega_0 L_1 G_S = \frac{G_S}{\omega_0 C_S}$$

Similarly the equivalent shunt conductance in the output circuit is given by,

$$G_y = \frac{G_L}{(1+Q_2^2)} \quad \dots(7.9)$$

where

$$Q_2 = \omega_0 L_2 G_L = \frac{G_L}{\omega_0 C_R}$$

The equivalent shunt inductances can be calculated in a similar way if required, but is not necessary in this situation. With these tuning inductors, the insertion-loss of the filter is given by,

$$P_{in}(\omega_0) = \frac{P_L}{P_I} = \frac{4|y_{21}(\omega_0)|^2}{G_x G_y} \quad \dots(7.10)$$

For improvement in the insertion-loss the expression in equation (7.10) is maximized by making  $G_x$  and  $G_y$  as small as practicable. The conductances, however, must be kept large enough to maintain a reasonable bandwidth in the input-output circuits. The Q-factors of the parallel circuit, Figure 7.8(d), are given by

$$Q_S = \frac{\omega_0 C_S}{G_x} * \quad \dots(7.11)$$

and

$$Q_L = \frac{\omega_0 C_R}{G_y}$$

where  $C_S$  and  $C_R$  are the transducer static capacitances. If we use the relation (7.11) to eliminate  $G_x$  and  $G_y$  from equation (7.10), we obtain,

$$P_{in}(\omega_0) = \frac{4|y_{21}(\omega_0)|^2 Q_S Q_L}{\omega_0^2 C_S C_R} \quad \dots(7.12)$$

Thus we see to calculate the insertion-loss we must know the forward transmittance, the input-output capacitances and must be prepared to decide what are the highest values of  $Q_S$  and  $Q_L$  which will give acceptable responses. As an example consider the case of Filter 2. The calculated value of transmittance (Program Y21FIL, Appendix A5) was,

$$|y_{21}(\omega_0)| = 3.925\mu \text{ siemens} \quad \dots(7.13)$$

with a low impedance termination ( $\approx 50\Omega$ ) and assuming the same source and load conductances, the untuned insertion loss of the filter from equation (7.7), is,

$$P_{in}(\omega_0) = -66\text{dB} \text{ (-72dB according to voltage transfer ratio definition)} \quad \dots(7.14)$$

in which we have assumed  $G_L = G_S = 15.6\text{m siemens}$ . Thus we see by using low source and load impedances we have obtained a very high value of insertion-loss.

Now we consider the case when the transducer capacitances are tuned out with the respective inductances. Taking the measured values of  $C_R$  and  $C_S$  from Sections (7.3.1 and 7.3.2) and calculating the respective inductances required at resonance and substituting in equations (7.8) and (7.9) we have,

---

\* From equations (7.8) and (7.9) it is easy to prove that  $Q_S \approx Q_1$  for  $Q_1 \gg 1$   
and  $Q_L \approx Q_2$  for  $Q_2 \gg 1$

$$Q_1 = 28.8 \quad \dots(7.15)$$

$$Q_2 = 18.2$$

Therefore, the equivalent shunt conductances are, from equations (7.8) and (7.9)

$$G_x = 18.8\mu \text{ siemens} \quad \dots(7.16)$$

$$G_y = 46.7\mu \text{ siemens}$$

∴ The insertion-loss of the filter is, from equation (7.10)

$$P_{in}(\omega_0) \approx -11.55\text{dB} \quad \dots(7.17)$$

The associated Q-factors are, from equation (7.11)

$$Q_S \approx 28.8 \quad \dots(7.18)$$

$$Q_L \approx 18.2$$

Thus we see we are able to improve the insertion-loss of the filter considerably, with the tuned circuits but at the expense of high Q-factors, equations (7.15) or (7.18), which severely restricts the filter performance, because of the narrow bandwidth and hence operating the filter with such high Q-factors is not desirable. There are several ways to reduce the Q-factors equations (7.8, 9 and 11) for obtaining reasonable amount of insertion-loss and at the same time maintaining the adequate bandwidth of the filter. In view of the equations (7.8), (7.9) and (7.11) the possible approaches are 1) increase static capacitances,  $C_S$  and  $C_R$ , 2) reduce tuning inductances  $L_1$  and  $L_2$ , 3) use low admittance sources  $G_L$  and  $G_S$ .

The first factor is not desirable, since the static capacitances depend upon the substrate material and the number of fingers. The number of fingers depend upon the filter design and hence cannot be increased. The static capacitance can be increased by using a high  $K^2$  material but using high  $K^2$  materials have their own problems as discussed in Chapter 10 and is not preferred.

The second factor is interrelated with the first factor and cannot be

reduced any further. Therefore, the third factor, viz use of low conductance values for  $G_L$  and  $G_S$  is quite possible by using high impedance IC operational amplifiers. For example if we wish to use Q-factors of 5 ( $Q_S = Q_L = 5$ ) for the input-output circuits, then the source and load conductance will be from equations (7.8) and (7.11),

$$G'_S = (1 + Q_1^2) \frac{\omega_0 C_S}{Q_1} = 1.34 \text{m siemens} \quad \dots(7.19)$$

$$G'_L = (1 + Q_2^2) \frac{\omega_0 C_R}{Q_2} = 2.37 \text{m siemens}$$

and these values can be easily achieved with the help of suitable IC amplifiers, with capacitances nearly matching with that of the transducer capacitances. The insertion-loss with these new source and load conductances will be from equation (7.11).

$$P_{in}(\omega_0) = -19 \text{dB} \quad \dots(7.20)$$

Thus we will be able to improve the untuned insertion-loss (with  $\approx 50\Omega$  source and load conductances) from -66dB to -19dB with tuned circuits and with source conductance of 1.3m siemens and load conductance of 2.37m siemens.

In fact it is possible to improve the insertion-loss without any tuned circuits, and incorporating the HF linear IC amplifiers to match the transducer impedances. Referring to equation (7.7), if we select suitable IC amplifiers (eq. FET transistors) say with  $G_L = 1 \text{ms}$  and  $G_S = 0.5 \text{ms}$ , then the insertion-loss would be from equation (7.7)

$$P_{in}(\omega_0) = \approx -39 \text{dB} \quad \dots(7.21)$$

Thus we see the potential advantage in using IC amplifiers in improving the insertion-loss of the filter. The filter design has to be modified to incorporate the responses of these amplifiers and of matching circuits if any, and the design procedure is presented to some extent in Chapter 9.

As a final remark we have to remind ourselves that the insertion-

loss of -66dB mentioned in this section is referred to the untuned source and load conductances, each approximately having values of 15.6mA/v. However in the experimental procedure, we have used a series of inductance tuning in the input circuit and the input voltage is monitored with a high impedance capacitive probe, while the output is directly connected with an amplifier terminated with a 50Ω resistance. In this situation the insertion-loss at the band centre is given by referring to Figure 7.6(d),

$$P_{in}(\omega_0) = \frac{(1 + Q_i^2) |y_{21}(\omega_0)|^2}{G_L G_S} \quad \dots(7.22)$$

where  $Q_i = \omega_0 L G_S$ , and 'L' is the inductance required to tune the total capacitance in the input circuit, viz, the transducer static capacitance, stray capacitances, the capacitance of the BNC connectors, and the capacitance of the high impedance probe. As an example, considering once again for Filter 2, from the measured results we obtained the following results

$$Q_i = 6.05$$

and

$$P_{in}(\omega_0) = -50.5\text{dB}$$

...(7.23)

#### 7.4.1 Other Sources of Insertion-Loss

The insertion-loss discussed so far arises due to electrical mismatch at the filter input-output terminals to the source and load impedances. However, there are several other sources of losses which can occur in a SAW device [7]<sup>3</sup>. Some of them are, 1) bidirectionality loss, 2) electrical dissipative losses in the transducer pattern, 3) losses in the matching networks, 4) propagation losses in the substrate, 5) losses due to beam spreading, 6) apodization losses and 7) losses due to transducer misalignment of the list mentioned above, loss due to bidirectionality in the prominent one and the others are usually small if proper care is exercised in design and fabrication of the filter.

The filter configurations considered in this thesis have an inherent bidirectionality loss of 6dB [7]<sup>1</sup>, half of which occurs because the input transducer radiates only half of the power toward the output transducer, because by reciprocity it can only reconvert half of the acoustic power incident on it into electrical output. There are several schemes proposed [7]<sup>4</sup> to minimize or eliminate [7]<sup>5,6</sup> bidirectionality loss but at the expense of added complexity of transducer fabrication.

The loss due to bidirectionality has been included in the derivation of the transadmittance formula and adding the contributions due to other factors mentioned above probably explains the average 3dB difference between the measured and the calculated insertion loss of the filter.

#### 7.5 Discussion of the Results

On the whole, the experimental results of the optimized filters agree quite well with the theoretical results. It was found that minor changes in the reduction ratio and the surfacewave velocity were observed than the estimated values because of the limited facilities in the photofabrication procedure. However, considerable improvement was observed in measured results of the filters which have been fabricated with a single stage reduction process than with a two stage reduction process. Had accurate techniques been available, the specified response, the predicted response of the model and the experimental response of the filter can be compared together and precise frequency specifications can be obtained.

The good agreement obtained achieved in the experiments can also be taken to provide empirical justification in the derivation of the approximate source functions in the transadmittance formulism. Although only quartz substrate materials have been used in these experiments, we can use any other weak coupling substrate materials for characterisation of the surfacewave filter using the transadmittance formulation. There are several other new materials appearing in the field and a choice of

suitable material regarding the cost and ease of fabrication in the SAW IF filter will be discussed towards the end of the thesis (Chapter 10). Even though the observed acoustic signal was not distorted much in the experiments, some of the factors contributing to the distortion effects will also be discussed in the same chapter.



## CHAPTER 8

## SYNTHESIS OF A TV IF FILTER USING CHIRPED TRANSDUCERS

8.0 Introduction

A novel technique of designing TV IF filters using chirped transducers is presented in this Chapter. A chirped transducer is one in which the spacings of the interdigital electrodes are graded from one end of the array to the other while maintaining the same electrode lengths throughout the array, SAW filters can be designed using two such arrays as input-output transducers and suitably modifying the spacings between the electrodes. There are two types of such filters (8)<sup>1</sup>. If the two transducers in the filter are similar, viz., identical in finger spacings and in orientation, the filter is dispersionless and the linear phase response is retained. On the other hand, if one transducer is the mirror image of the other, the filter exhibits dispersive characteristics and the group delay becomes frequency dependent. Broadbandwidths can be achieved with both types of filters, but however dispersive filters have received considerable attention in recent years (8)<sup>2,3,4,5,6</sup>, in particular linear FM dispersive filters, because of their many important applications in radar and communication systems. A linear FM dispersive filter is designed to have a constant envelope and linear group delay (quadratic phase) versus frequency. In a linear FM dispersive filter, the transducers are designed to have uniform finger overlaps and a constantly decreasing finger spacings. The two transducers are of course arranged as the mirror images of one another.

The advantages of using uniform finger overlaps is discussed in Chapter 3, the main advantage being increase in input-output admittances which in turn reduces the insertion-loss of the filter. The design of linear FM dispersive filters is straightforward and has been studied by

several authors (8)<sup>14</sup>. Bandpass filters with regular passband characteristics have been studied by Worley (8)<sup>15</sup> using nonlinear FM techniques. The synthesis procedure followed here for TV IF filters makes use of the techniques developed by Fowle (8)<sup>16</sup> for designing FM pulse compression signals. The first technique discussed consists of designing two identical input-output chirped (FM) transducers, the FM function which describes the transducer structure is determined according to the required IF characteristic. Later on a method is presented in which only one of the transducers is chirped and the other is apodized.

### 8.1 Basic Approach

The basic principles involved in designing an FM signal for obtaining a desired magnitude frequency response will be briefly reviewed. Suppose we have a narrowband signal  $s(t)$  centred at a carrier frequency  $f_0$  with an envelope  $u_e(t)$  and a phase modulation  $\phi(t)$ , then we have,

$$s(t) = u_e(t) \cos\{2\pi f_0 t + \phi(t)\} \quad \dots \quad (8.1)$$

$$= \operatorname{Re}\left[u_e(t) e^{j\{2\pi f_0 t + \phi(t)\}}\right] \quad \dots \quad (8.2)$$

$$= \operatorname{Re}\{v_i(t)\} \quad \dots \quad (8.3)$$

where

$$v_i(t) = u_e(t) e^{j\{2\pi f_0 t + \phi(t)\}} \quad \dots \quad (8.4)$$

is the complex FM signal. For simplicity in algebra we work out with complex quantities and, therefore,  $v_i(t)$  will be taken as the input signal. In practical situations only the real part will be

considered. Suppose  $v(f)$  is the Fourier transform of  $v_i(t)$ , with magnitude spectrum  $v_m(f)$  and phase spectrum  $\theta(f)$  i.e.

$$v(f) = v_m(f) e^{j\theta(f)} = \mathcal{F}\{v_i(t)\} \dots \quad (8.5)$$

The signal autocorrelation function,  $R_{11}(\tau)$  is then given by,

$$R_{11}(\tau) = \int_{-\infty}^{\infty} v_i(t) v_i^*(t-\tau) dt = \int_{-\infty}^{\infty} v_i^*(t) v_i(t+\tau) dt \dots \quad (8.6)$$

where \* represents complex conjugate and by autocorrelation theorem (8)<sup>17</sup>  $R_{11}(\tau)$  can be written as,

$$R_{11}(\tau) = \int_{-\infty}^{\infty} v_m^2(f) e^{j2\pi f\tau} df \dots \quad (8.7)$$

Thus when  $R_{11}(\tau)$  is chosen, the magnitude spectrum  $v_m(f)$  can be determined by the inverse Fourier transform of  $R_{11}(\tau)$ . Therefore

$$v_m(f) = \left[ \int_{-\infty}^{\infty} R_{11}(\tau) e^{-j2\pi f\tau} d\tau \right]^{\frac{1}{2}} \dots \quad (8.8)$$

Thus we see designing an FM signal of arbitrary envelope shape to have a specified autocorrelation function is equivalent to that of designing a signal of arbitrary time envelope or modulus so that its Fourier transform will have an arbitrary modulus. With the two modulus functions  $u_e(t)$  and  $v_m(f)$ , specified, Fowle (8)<sup>16</sup> derived approximate phase functions  $\phi_1(t)$  and  $\theta_1(f)$  for the phase functions  $\phi(t)$  and  $\theta(f)$  in terms of the quantities derived from  $v_m(f)$  and  $u_e(t)$  alone so as to form the approximate Fourier transform pair, i.e.

$$v_m(f) e^{j\theta_1(f)} \Leftrightarrow u_e(t) e^{j\{2\pi f_0 t + \phi_1(t)\}} \quad \dots \quad (8.9)$$

or more specifically to say, given  $v_m(f)$  and  $u_e(t)$ , we can calculate  $\phi_1(t)$  and  $\theta_1(f)$  so that

$$|\mathcal{F}\{u_e(t) e^{j\{2\pi f_0 t + \phi_1(t)\}}\}| \approx v_m(f)$$

or

$$|\mathcal{F}^{-1}\{v_m(f) e^{j\theta_1(f)}\}| \approx u_e(t)$$

It is to be noted that, once we calculate the phase function in one domain, we also obtain the associated phase function in the inverse domain, and we have no control over the phase functions obtainable in either domains.

### 8.1.2 Application to SAW Filter

In order to implement the FM technique mentioned in the previous section to SAW filters, it is necessary to choose a scheme for employing two transducers which together produce the desired frequency response. Specifically, it is necessary to find two source functions from which the two individual transducers are to be designed. It will be shown here how this can be achieved through the use of transadmittance mode.

We know that the transadmittance between the transducers  $T_1$  and  $T_2$ , each having a real source function  $f(t)$  in the time domain is given by, according to equation (2.7)

$$Y_{21}(f) = K F_1(f) F_1^*(f) e^{-j2\pi f t_0} \quad \dots \quad (8.10)$$

where  $F_1(f)$  is the frequency response of  $T_1$  and  $F_1^*(f) e^{-j2\pi f t_0}$  is

the frequency response of  $T_2$  and  $t_0$  is the constant group delay representing the separation between the two transducers. The contribution due to  $|\omega|$  factor has been neglected for the time being. We also know that  $y_{21}(f)$  represents the filter transfer function when the load impedance is constant, hence it can also be considered as the specified response. Let  $f(t)$  be of the form  $r(t) \cos\{2\pi f_0 t + \alpha(t)\}$  which is the desired FM function, and for convenience it is choosed to be the real part of a complex function  $R(t)$ , where

$$R(t) = r(t) e^{j\{2\pi f_0 t + \alpha(t)\}} \quad \dots \quad (8.11)$$

Let the frequency response of  $R(t)$  be  $U(f)$  with magnitude spectrum  $U_m(f)$  and phase spectrum  $\psi(f)$ , i.e.

$$\begin{aligned} U(f) &= U_m(f) e^{j\psi(f)} \\ &= \mathcal{F}\{R(t)\} = \mathcal{F}\left[r(t) e^{j\{2\pi f_0 t + \alpha(t)\}}\right] \end{aligned} \quad \dots \quad (8.11a)$$

The source function  $f(t)$  can be written as,

$$f(t) = \frac{1}{2} r(t) \left[ e^{j\{2\pi f_0 t + \alpha(t)\}} + e^{-j\{2\pi f_0 t + \alpha(t)\}} \right] \quad \dots \quad (8.11b)$$

Assuming  $f(t)$  to be a narrowband signal (function) which is normally true in practice (the value of ' $f_0$ ' whether at radio frequencies (RF) or at intermediate frequencies (IF), will always be several times greater than the bandwidth of the filter), the Fourier transform of the first term on the right hand side of the equation (8.11b) gives rise to a spectrum which is

centred around the positive frequency ' $f_0$ ' to a great extent and is negligible in the rest of the frequency domain. But the spectrum of this first term around ' $f_0$ ' is equal to the Fourier transform of  $f(t)$ , within the same range, i.e.,

$$\mathcal{F}\left[\frac{1}{2} r(t) e^{j\{2\pi f_0 t + \alpha(t)\}}\right] \approx \mathcal{F}\{f(t)\} \quad \dots \quad (8.11c)$$

and by definition,

$$\mathcal{F}\{f(t)\} = F_1(f)$$

$$\mathcal{F}\left[r(t) e^{j\{2\pi f_0 t + \alpha(t)\}}\right] = U(f)$$

$\therefore$  from equation (8.11c),

$$U(f) = 2F_1(f) \quad \dots \quad (8.11d)$$

provided  $f$  is near  $f_0$ .

Substituting right hand side of equation (8.11d) in equation (8.10), the transadmittance in frequency domain can be written, for  $f$  near  $f_0$ , as

$$y_{21}(f) \approx K^1 U(f) U^*(f) e^{-j2\pi f t_0} \quad \dots \quad (8.11e)$$

where  $K^1$  is a constant ( $=\frac{1}{4}K$ ).

Now considering the magnitudes only in equation (8.11e), we have,

$$|y_{21}(f)| \approx K^1 U_m(f) \quad \text{for } f \text{ near } f_0 \quad \dots \quad (8.11f)$$

The transadmittance in time domain is given by the inverse Fourier transform of  $y_{21}(f)$  in equation (8.11e)

$$y'_{21}(t) = \mathcal{F}^{-1}\{y_{21}(f)\} \approx \mathcal{F}^{-1}\{K^1 U_m^2(f) e^{-j2\pi f t_0}\} \\ \text{for } f \text{ near } f_0 \quad \dots \quad (8.11g)$$

or this can be written as

$$y'_{21}(t+t_0) = \mathcal{F}^{-1}\{|y_{21}(f)|\} \approx K \mathcal{F}^{-1}\{U_m^2(f)\} \dots \quad (8.11h)$$

for  $f$  near  $f_0$

Thus we see the time delayed version of the transmittance equation (8.11h) is similar to the equation for an autocorrelation function described in equation (8.7), hence we can use the same techniques developed by Fowle (8)<sup>16</sup> for synthesizing the SAW filters.

Thus knowing  $U_m^2(f)$  (in this case the specified response of the filter) and assuming an arbitrary time envelope  $r(t)$  in equation (8.11) we shall be able to find the approximate phase functions for  $\alpha(t)$  and  $\psi(f)$  and then be able to obtain the approximate frequency response of the filter. On obtaining the phase function in time domain fingers in the transducer are located at the points where the instantaneous phase is a multiple of  $\pi$ . The source functions  $f(t)$  can be obtained by taking the real part of  $R(t)$  in equation (8.11). Note that  $U_m(f)$  is the square root of the magnitude of the specified response and corresponds to the frequency response of one transducer. Thus we shall be able to design one of the two identical transducers in the filter and the other transducer is simply obtained by duplicating the first transducer. One drawback in the FM techniques is that, with the given modulus functions we obtain uncontrollable phase functions in other domains. The fingers are located according to the FM phase functions in time domain and the associated phase function in the frequency domain may have any kind of characteristic. Thus we obtain an uncontrolled phase response in the frequency domain for each transducer. However, as we have assumed two identical transducers, identical in finger locations and in orientation, the associated phase response of each transducer, will not effect the overall linear phase response of the filter, with this configuration.

This is the basic approach followed in designing chirped transducers using transmittance model contemplating with the FM techniques developed by Fowle (8)<sup>16</sup>. Even though the basic principles are the same, the method followed here is somewhat different from that, indicated by Fowle,

the exact treatment and the results obtained will be presented in the following sections.

## 8.2 Synthesis Procedure with Two Identical Chirped Transducers

We will now demonstrate the synthesis of uniform amplitude waveforms with appropriate phase modulation for obtaining the desired frequency response. This can be done through the use of the stationary phase principle. A detailed theoretical derivation of the principle is given by Fowle (8)<sup>16</sup>, as indicated in the previous section, and hence, only the pertinent equations are shown here. Rewriting equation (8.11a) we have

$$U_m(f) e^{j\psi(f)} = \mathcal{F}\{r(t) e^{j\{2\pi f_0 t + \alpha(t)\}}\} \dots \quad (8.17)$$

The instantaneous frequency is defined, as usual, by

$$f_i(t) = f_0 + \frac{1}{2\pi} \frac{d\alpha(t)}{dt} \dots \quad (8.18)$$

A second equation derived using the stationary phase principle gives rise to,

$$\int_{-\infty}^{f_i} U_m^2(\xi) d\xi = \int_{-\infty}^t r^2(\eta) d\eta \dots \quad (8.19)$$

and according to Parseval's Theorem,

$$\int_{-\infty}^{\infty} U_m^2(f) df = \int_{-\infty}^{\infty} r^2(t) dt \dots \quad (8.20)$$

These three equations (8.18, 8.19 and 8.20) are sufficient to establish the necessary phase functions. Note that  $r(t)$  is a rectangular time envelope function and  $U_m(f)$  is the square root of the specified magnitude response over a band of frequencies. In this case the band of frequencies is the channel width which is 7MHz and the centre frequency is about 34.0MHz.



The various steps involved in calculating the phase functions  $\psi(f)$  and  $\{2\pi f_0 t + \alpha(t)\}$  so as to obtain the approximate achieved frequency response are described below.

The magnitude response according to equation (8.11f), can be written as

$$U_m^2(f) = K_2 |y_{21}(f)| \quad f_1 < f < f_2 \quad \dots \quad (8.21)$$

(where  $K_2$  is a constant and  $f$  is near  $f_0$ )

where  $(f_2 - f_1)$  is the channel width.


For uniform finger overlaps, a rectangular envelope function is assumed for  $r(t)$  and the complex phase function  $R(t)$  can be written as,

$$R(t) = r(t) e^{j\{2\pi f_0 t + \alpha(t)\}}$$

with

$$r(t) = \sqrt{B} \operatorname{rect} \left( \frac{t}{T} \right) = 1 \text{ for } 0 < t < T$$

$$= 0 \text{ elsewhere}$$



... (8.22)

where  $B$  is a constant and  $T$  is the duration of the source function.

Once the time interval is chosen, Parseval's Theorem sets up the constant 'B' in equation (8.22)

i.e.

$$B = \frac{1}{T} \int_{f_1}^{f_2} U_m^2(f) df \quad \dots \quad (8.23)$$

The relation between  $f_i$  and  $t$  can be found through the integrals in equation (8.19), i.e.

$$\int_{f_1}^{f_i} U_m^2(\xi) d\xi = Bt \quad \dots \quad (8.24)$$

Let

$$\begin{aligned}
 P_1(f_i) &= \int_{f_1}^{f_i} U_m^2(\xi) d\xi \\
 Q(t) &= Bt
 \end{aligned}
 \quad \left. \vphantom{\begin{aligned} P_1(f_i) \\ Q(t) \end{aligned}} \right\} \dots \quad (8.25)$$

Then the instantaneous frequency  $f_i(t)$  can be solved from equation (8.25).

This can be represented as

$$f_i(t) = P_1^{-1}(Q(t)) \quad \dots \quad (8.26)$$

Having obtained  $f_i(t)$ , the approximate phase function  $\alpha_1(t)$  for  $\alpha(t)$  is given by

$$\alpha_1(t) \approx 2\pi \int \{P_1^{-1}(Q(t))\} dt - 2\pi f_0 t + C_1 \quad \dots \quad (8.27)$$

The approximate phase function  $\psi_1(f)$  for  $\psi(f)$  is given by the following relation

$$\psi_1(f) \approx -2\pi \int Q^{-1}\{P_1(f)\} df + C_2 \quad \dots \quad (8.28)$$

Having obtained the approximate phase function  $\alpha_1(t)$  in time domain the approximate modulus function in frequency domain can be found through the Fourier transform relation, viz.,

$$|\mathcal{F}\{r(t) e^{j 2\pi f_0 t + \alpha_1(t)}\}| = U_{ma}(f) \quad \dots \quad (8.29)$$

where,

$$\begin{aligned}
 U_{ma}^2(f) &\approx U_m^2(f) = K_2 |y_{21}(f)| \\
 &\quad \text{for } f_1 < f < f_2
 \end{aligned}
 \quad \left. \vphantom{\begin{aligned} U_{ma}^2(f) \\ \text{for } f_1 < f < f_2 \end{aligned}} \right\} \dots \quad (8.29a)$$

The approximation of  $U_{ma}^2(f)$  to  $U_m^2(f)$  depends upon the extent to which the

phase functions are approximated to exact values, which in turn depend upon the Time-Bandwidth product of the filter and is discussed more clearly in Section (8.2.2).

The real time function which describes the transducer source function is obtained by taking the real part of  $r(t) e^{j\{2\pi f_0 t + \alpha_1(t)\}}$ . The finger locations are given by as pointed out earlier at the sampling points where the instantaneous phase changes its sign, i.e.

$$2\pi f_0 t_n + \alpha_1(t_n) = n\pi \quad \dots \quad (8.29b)$$

Since the time function has a rectangular envelope, the finger overlaps are all equal in magnitude and alternate in sign because of the above sampling procedure.

A diagrammatical representation of the various steps involved in arriving at the real FM function of one transducer, and locating the fingers on that transducer is illustrated in Figure 8.1. The filter is then fabricated by two such identical transducers and introducing the required separation, corresponding to the constant group delay between them.

### 8.2.1 Chirped Transducer Program

A computer illustration of the chirped transducer design for realizing the frequency response of Filter 1 is presented here. As mentioned earlier a constant time envelope function was chosen in order to have uniform finger overlaps in the transducer. The various steps necessary in the synthesis procedure are indicated below:

- (1) Assign arbitrary magnitude to  $U_m^2(f)$ . The amplitude of  $U_m^2(f)$  will have units of siemens (refer to equation 8.21).
- (2) Evaluate the constant 'B' using equation (8.23). The constant B will have units of siemens/sec<sup>2</sup>.
- (3) Obtain the relation between time versus instantaneous frequency using equation (8.25)

i.e. 
$$t = \frac{1}{B} P_1(f_i)$$

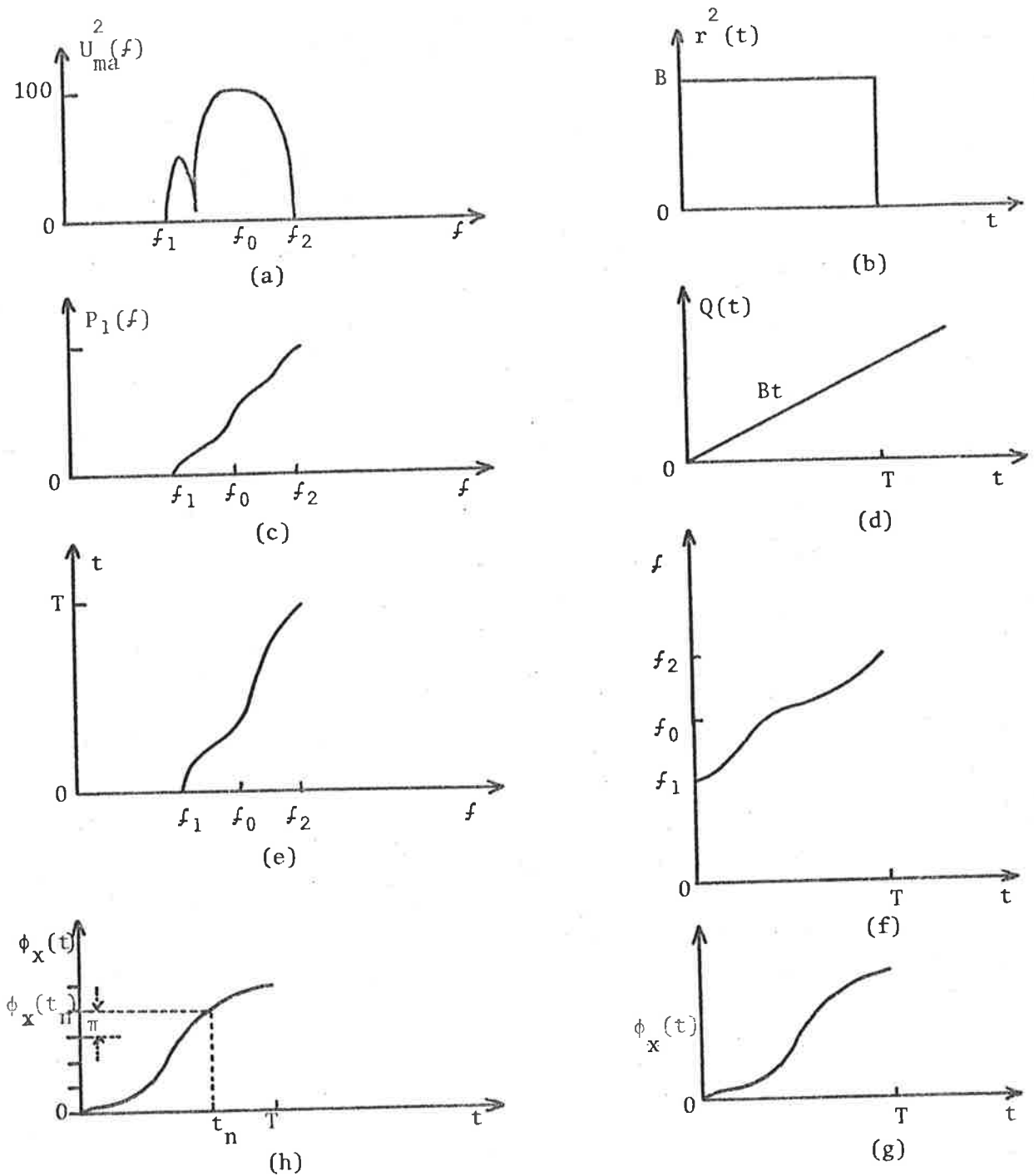


Figure 8.1 Schematic representation of chirped transducer design.

- (a) Magnitude response centred over the carrier frequency  $f_0$ .
- (b) Assumed time envelope function.
- (c) Integral representation of (a).
- (d) Integral representation of (b).
- (e) Solution for 't' from  $P_1(f)=Q(t)$ .
- (f) Inverting (e) i.e. solving for 'f'.
- (g) Integral representation of (f) (the phase function in time domain).
- (h) Locating finger positions in the transducer.

- (4) Solve for  $f_i(t)$  or invert the function  $P_1(f_i)$  to obtain the relation between instantaneous frequency versus time using equation (8.26)
- (5) Obtain the approximate phase function  $\alpha_1(t)$  using equation (8.27).
- (6) Evaluate the approximate magnitude response  $U_{ma}^2(f)$  using equation (8.29).
- (7) Compare  $U_{ma}^2(f)$  with  $U_m^2(f)$  and if the results are not close enough increase the time duration  $T$  to a new value and repeat the steps (2) to (7).
- (8) When a close agreement is obtained, the FM function in the time domain is used in evaluating the transducer geometry. The finger locations are given by the equation (8.29b) and the finger overlaps are calculated by introducing the appropriate constant of proportionality in equation (8.21).
- (9) Assign the same geometry to the other transducer introducing the required separation between the transducers.

A computer program was developed to carry out the various steps (1 to 8) described above and a listing of the program called CHIRPTR is given in the Appendix A7. The step number (9) is required in fabricating the device but is not necessary in the synthesis procedure. Calculation of phase function in the frequency domain and the number of finger locations in each transducer was also included in the program. The synthesis procedure evolved a time duration of 40 $\mu$ sec in order to achieve a good comparison with the specified response. The number of fingers in each transducer, according to the adopted sampling procedure are approximately 2720. The phase function of the transducer in the time domain was found to be fairly steep in certain regions. Hence, it was found that it is necessary to reduce the sampling interval in the time domain more than has been used in the previous filter examples. The FFT algorithm in the program operates with 4096 sampling points compared to 1024 sampling points in the previous examples. This enables us to increase the time resolution, but it was found that it is necessary to increase the frequency resolution also because of the inversion operation in step number (4). Hence, a choice of 10 $\mu$ sec periodic time

interval, operating with 4096 sampling points was found to be a suitable compromise, in frequency and time resolutions in this case. The theoretical results of the filter are presented in Figure 8.2. Even though the achieved response agrees well with the specified response, fabricating a SAW filter is not practicable for the reasons mentioned in the following section.

### 8.2.2 Discussion of the Results

The basic assumption in the design of chirped transducers using stationary phase approximation method is that the time-bandwidth (TW) product of FM function must be large compared to unity. Larger the TW product, better will be the approximation in the desired response. How large it must be is a question which depends upon the type of response to be realized. Fowle (8)<sup>16</sup> indicated that if both modulus (in time and frequency domains) are smooth, continuous and well behaved functions, then TW products of the order of three is sufficient to achieve the desired response. In the extreme case if both moduli have rectangular envelopes a TW product of the order 120 or more is necessary to achieve a reasonable agreement with the desired response. The importance of TW product is also discussed to some extent by Worley(8)<sup>15</sup>. In SAW devices the TW product will have an influence on the number of fingers which in turn determine the size of the substrate.

For the TV IF filter considered here the channel width is about 7MHz, but because of the unusual shape of the IF characteristic it was found that such large time durations (40 $\mu$ sec) are necessary to achieve a reasonable agreement with the desired response. In fact we are trying to achieve a response with a bandwidth corresponding to the bandwidth at the second carrier frequency where there is a trap in the IF passband. If we assume the width at the sound carrier is approximately equal to 0.15MHz (referring to the transmitted signal) the actual TW product is 6 and perhaps we may require even greater TW product (>6) which means we may require even

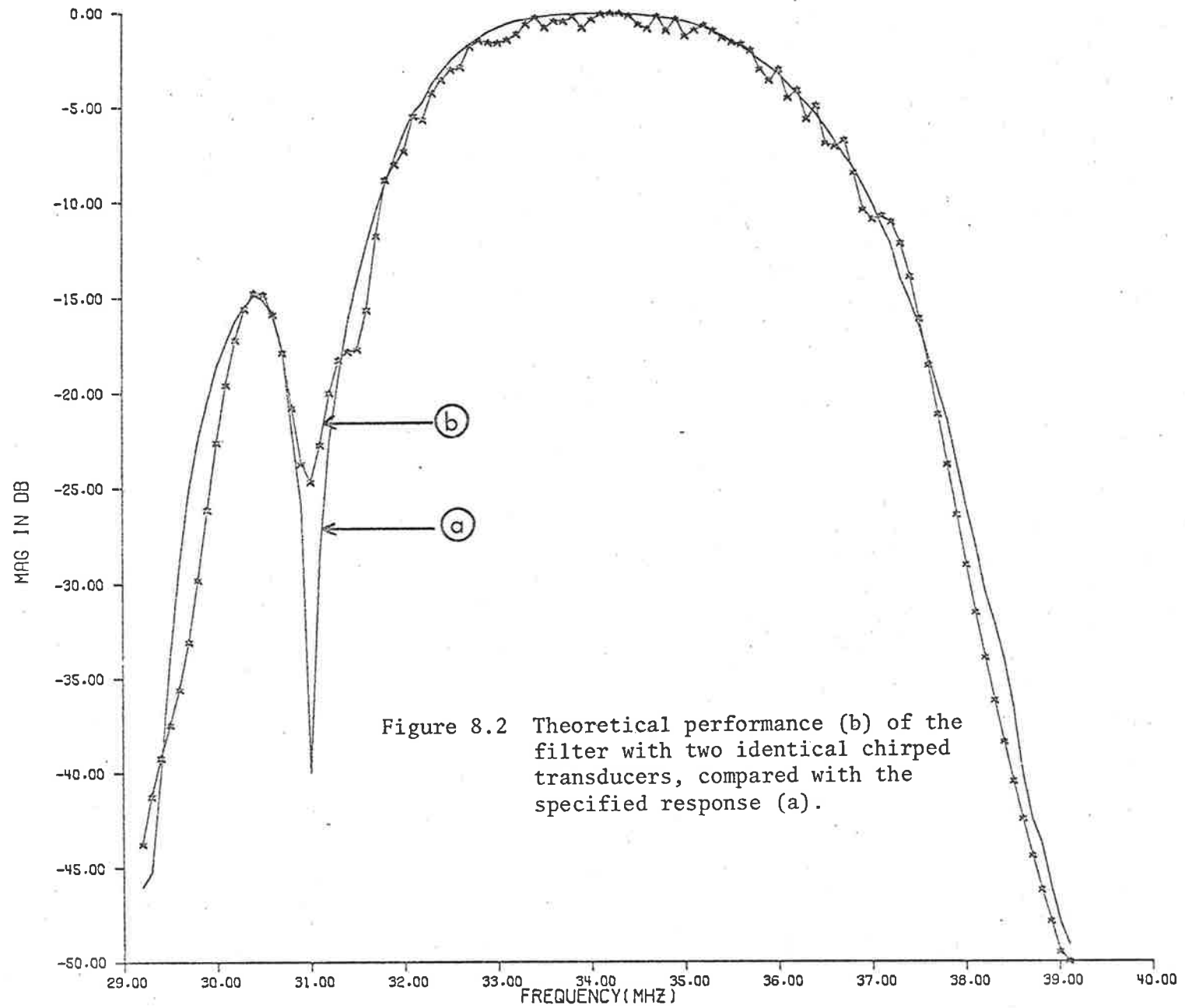


Figure 8.2 Theoretical performance (b) of the filter with two identical chirped transducers, compared with the specified response (a).

longer durations ( $>40\mu\text{sec}$ ) for better agreement in the results. In the designed filter each transducer is having 2720 fingers,  $40\mu\text{sec}$  duration corresponding to a length of approximately 12cm and this requires quite large substrates. This is highly undesirable especially when size and cost are of prime importance. Further, considerable difficulty arises in photofabrication with a large number of fingers. The number of fingers can, however, be reduced using the sampling method indicated by Atzeni (8)<sup>18</sup> i.e. instead of locating the fingers at multiples of  $\pi$  in the phase function, the fingers can be located at the multiples of  $K\pi$ , where  $K$  is an odd integer. This involves operating the transducer array at the  $K^{\text{th}}$  harmonic of the fundamental frequency and in the particular situation in order to reduce the number of fingers to a reasonable level 'K' must be of the order of 17. Working the transducer at  $17^{\text{th}}$  harmonic frequency, particularly with weak coupling substrates is again impracticable.

The observed ripples in the passband of Figure 8.2 arises due to sharp cut-off at the edges in the time envelope function and these can be removed or at least minimized by slightly tapering a few end electrodes in each transducer. Thus, even though we are able to synthesize the TV IF filter using chirped transducers, the result is not amenable to make a practical device, but the technique is quite simple and straightforward and is capable of designing any desired filter response. To test the validity of the technique a few other examples have been considered like rectangular passband, and a cosine shaped passband with the same  $f_0$  as that of TV IF filter and in both cases good agreement was obtained with the desired responses even with less time durations ( $<40\mu\text{sec}$ ). In case of a rectangular passband of 10MHz bandwidth, it was found that a time duration of  $10\mu\text{sec}$  ( $TW=100$ ) is necessary for good agreement in the results. In case of a cosine shaped passband with a 3dB bandwidth of 5MHz it was found that a time duration of  $1\mu\text{sec}$  ( $TW=5$ ) is enough to obtain a reasonable agreement in results and SAW filters can be easily fabricated, since they contain



only a small number of fingers in each transducer and occupy a length of about 6mm on the substrate.

An alternative method of designing TV IF filters using chirped transducers with less time durations is proposed in the next Section. Since the design with two identical chirped transducers does not give rise to practical realizations, it is intended to use one chirped transducer and the other is apodized to achieve the desired filter characteristic. It is hoped that the technique yields favourable results to implement in practice.

### 8.3 Synthesis Procedure with One Chirped and One Apodized Transducer

It is well known that wide bandwidths can be obtained using chirped (linear FM) transducers and now we are familiar in designing chirped (nonlinear FM) transducers for realizing any desired filter responses. In the early synthesis techniques (Chapter 3 and 5), the entire burden is placed on the apodized transducer in producing the desired IF characteristic and the input transducer contains only a small number of uniform fingers. If the burden is shared between the two transducers in producing the required IF passband, then the input transducer will have large number of fingers instead of only a small number and the problems associated with the filter having only a small number of fingers in the input transducers will be reduced to some extent. This is discussed more clearly in Section (3.3) when comparing the various finger weighting configurations. With the knowledge FM techniques (Section 8.1) it is possible to synthesize the input transducer to be a chirped transducer with a reasonable amount of time duration. The arbitrary response is taken to be the specified IF response while synthesizing the input transducer, thus allocating some burden to it in creating the IF passband. The required response is then obtained through the other apodized transducer. Since the input transducer is a chirped transducer with uniform finger overlaps, the transmittance model can still be used for the filter synthesis. Therefore, the filter

synthesis mainly consists of two parts. The first one is designing of a chirped transducer and the second one is designing of an apodized transducer. The chirped transducer is designed according to the stationary phase approximation as described in Section (8.2.1) and the apodized transducer is designed according to the four T's method as described in Section (3.4.3)

### 8.3.1 Computational Procedure

The computational procedure consists of a preliminary design of the chirped transducer, followed by the design of an apodized transducer. The preliminary synthesis is exactly the same as described in Section (8.2.1). Two identical chirped transducers are synthesized to realize the desired TV IF response, but with less time duration. The time duration is selected such that a practical SAW device can be fabricated. Typical time duration selected in this case for each transducer was 1μsec compared to 40μsec for the example considered in Section (8.2.1). Since the TW product is small the achieved response in the frequency domain departs far away from the desired response, but it will be similar in shape to some extent. One of the two identical transducers is taken as the required chirped transducer and then the apodized transducer is synthesized to meet the required specified response. If the chirped transducers have approximately the same desired IF characteristic, then we can expect the apodized transducer requires only a small amount of apodization with the same time duration as that of the chirped transducer. On the other hand, if the chirped transducer's response deviates considerably from the desired IF response, we can expect the apodized transducer may have a longer time duration than the chirped transducer and we have to search for an optimum duration to achieve the specified response.

A computer program was developed to synthesize one chirped transducer and one apodized transducer according to the procedure described above. The program is basically the same as given in Appendix A7 with

an extension of designing the apodized transducer as well. The chirped transducer was designed with a time duration of  $1\mu\text{sec}$ . which corresponds to about 68 fingers and the optimum length in the apodized transducer was found to be equal to  $1.9\mu\text{sec}$ . corresponding to about 108 fingers. The extra time duration of  $0.9\mu\text{sec}$ . was found to be necessary in order to produce sufficiently close level at the sound trap with the desired level and this is expected because of the reasons mentioned earlier. The apodization was found to be small compared to the apodization of other filters discussed in previous chapters, which indicates an improvement in the insertion and diffraction losses of the filter. One point to be remembered in this synthesis procedure is that a complex (complex in shape) phase response is associated with the chirped transducer which is inherent in the synthesis procedure itself and we have no control over it. Therefore the phase response of the apodized transducer, is to be compensated, in order to obtain a linear phase response of the TV IF filter. That means the phase response of the apodized transducer is equal to the linear phase response of the filter minus the complex phase response of the chirped transducer. Since the phase is nonlinear the response in the time domain is unsymmetrical and it was found that it is necessary to introduce a suitable group delay constant, so that the time domain is mainlobe centred with sidelobes falling on either side. An approximate group delay constant was found to be equal to half the periodic interval of the time response in the FFT algorithm. The results of  $1\mu\text{sec}$ . chirped-apodized transducer filter are shown in Figures 8.3, 8.4 and 8.5

### 8.3.2 Improvement in Admittance Parameters

It will be shown here that the admittance parameters of the filter (input, output as well as transfer admittance parameters) will increase as a result of chirped-apodized combination of the transducers, compared to a simple uniform-apodized combination of the transducers. The increase is mainly due to a large number of fingers required in the

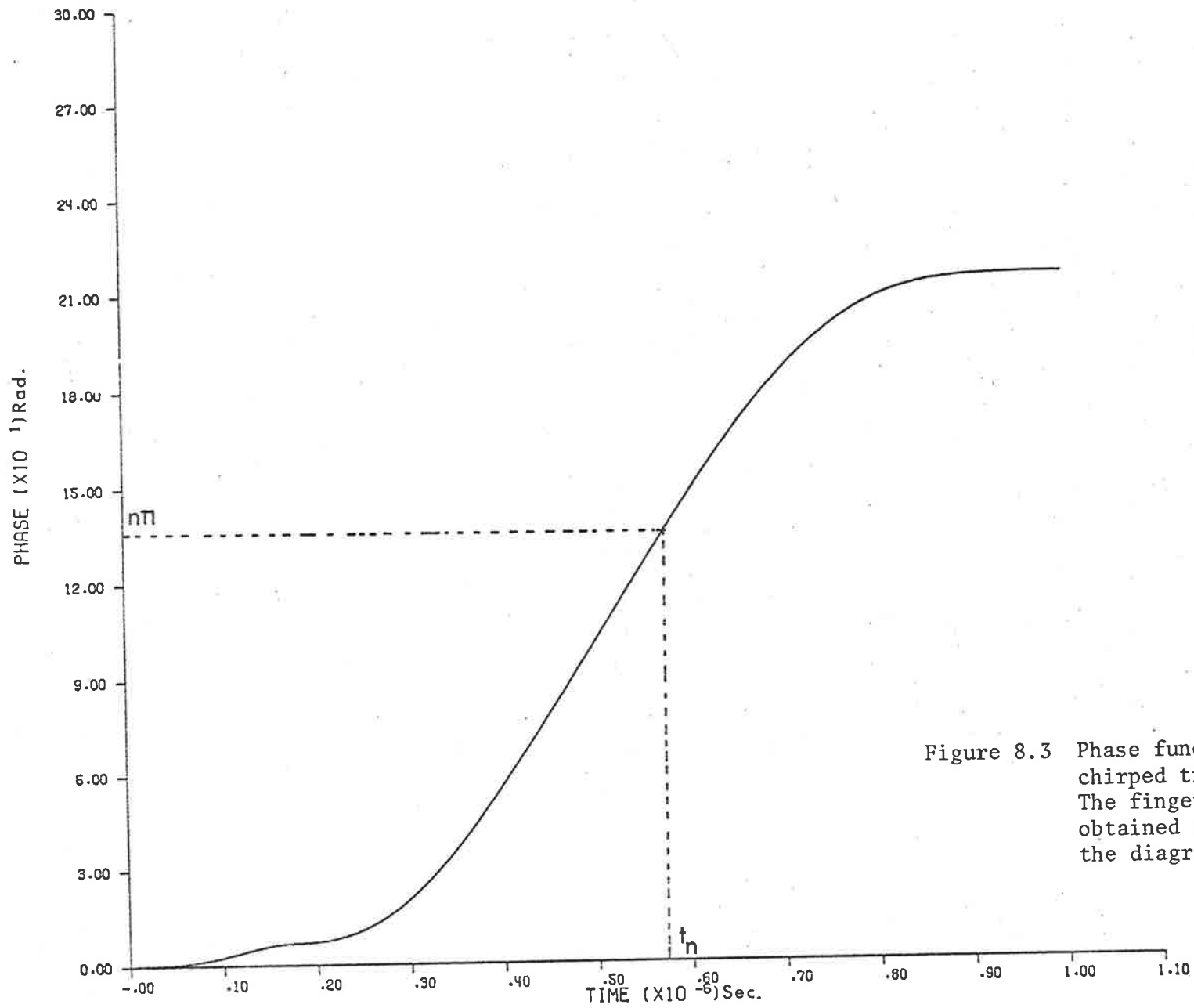


Figure 8.3 Phase function of the chirped transducer. The finger locations are obtained as indicated in the diagram.

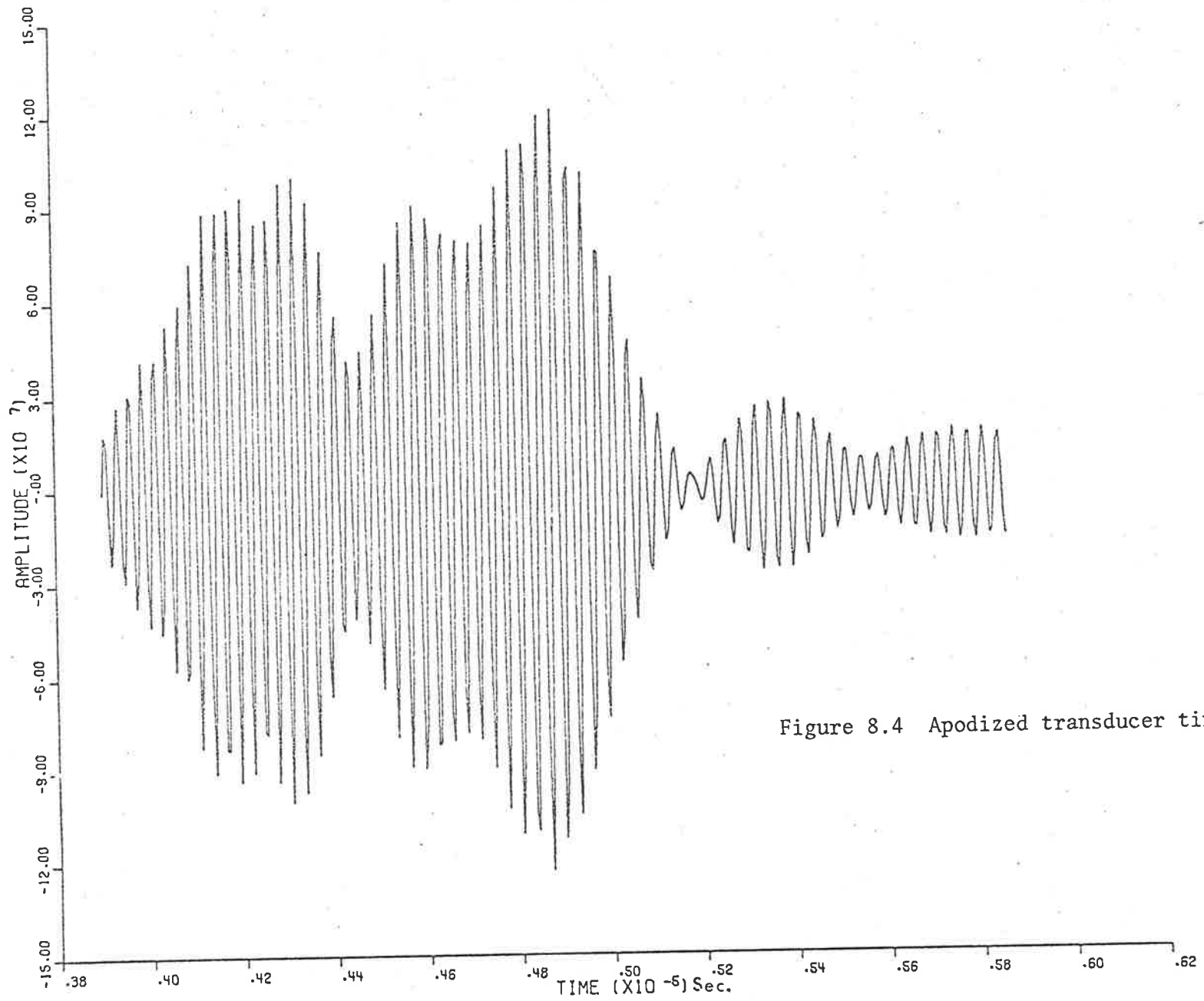
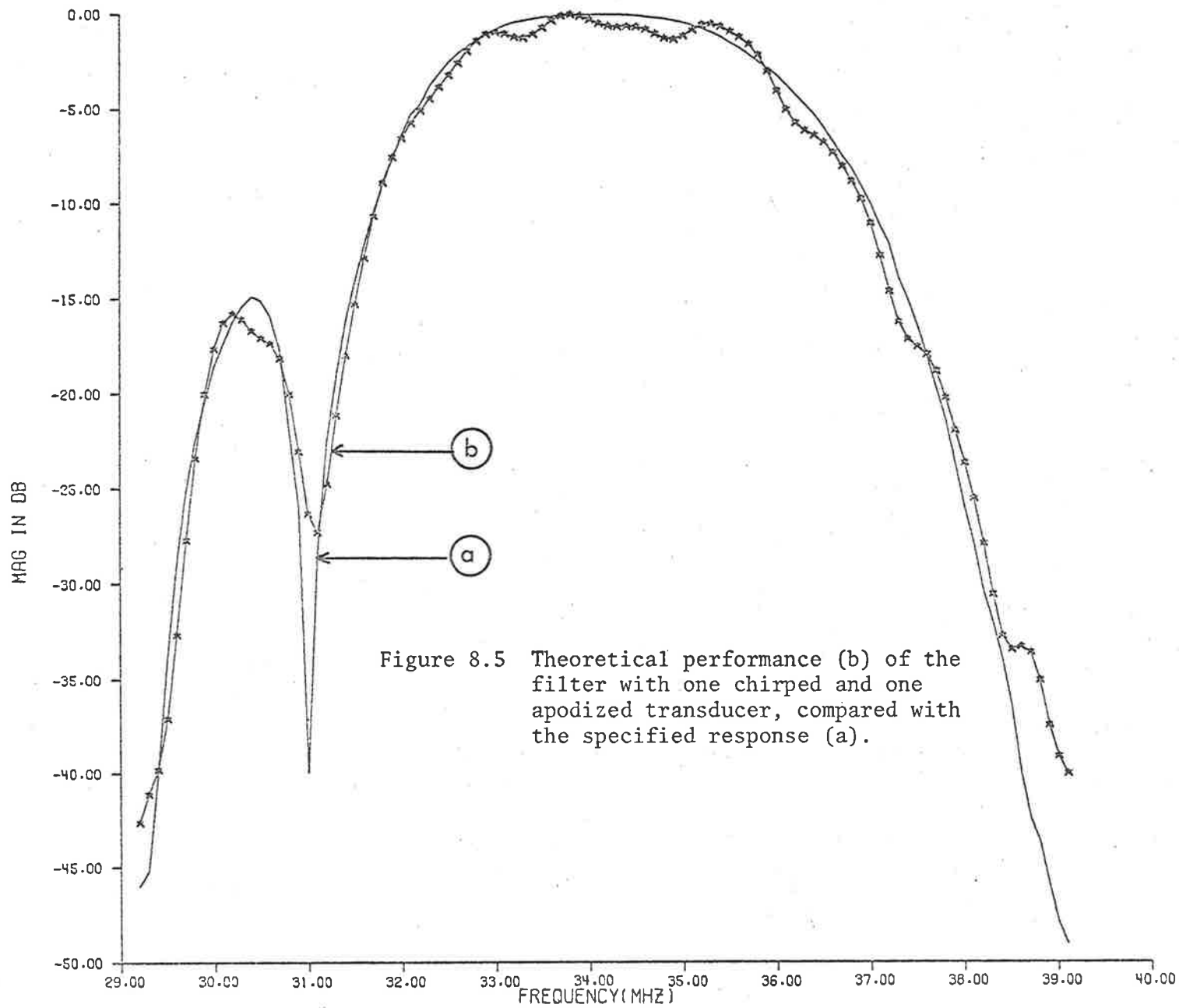


Figure 8.4 Apodized transducer time wave form.



chirped transducer in order to achieve the specified response. Increase in transadmittance indicates improvement in insertion-loss of the filter, while increase in input-output admittances indicates that it is much easier to select high impedance sources and loads to match the transducer admittances which in turn indicates further improvement in the insertion-loss of the filter. A very rough estimate in the improvement of the admittance parameters is presented, the absolute values can, however, be calculated using the computer programs developed for Filter 2.

#### Improvement in Transadmittance

We will compare the results of chirped-apodized transducer configuration with that of an unweighted-apodized configuration, with only a small number of fingers in the unweighted transducer. As an example let us compare the results with that of Filter 2 (Chapter 6). Let  $F_1(f)$  be the frequency response of uniform transducer. We have assumed it is of the form  $(\frac{\sin x}{x})$  response where  $x = \frac{N_1 \pi}{2} (\frac{f-f_0}{f_0})$ , in which  $N_1$  is the number of half wavelengths and  $f_0$  is the centre frequency of the filter. Let  $F(f)$  be the frequency response of the apodized transducer (after apodization). Therefore, the transadmittance is, neglecting the contribution due to  $|\omega|$  factor,

$$Y_{21}(f) = K F_1(f) F_2(f) \dots \quad (8.30)$$

where  $K$  is a constant of proportionality.

or in the time domain,

$$y_{21}(t) = K f_1(t) * f_2(t) \dots \quad (8.31)$$

where  $f_1(t)$  is the source function of uniform transducer and  $f_2(t)$  is the source function apodized transducer and '\*' indicates convolution.

Let  $A_1$  be the absolute magnitude of the peak amplitude in  $f_1(t)$  and  $B_1$  be the absolute peak amplitude in  $f_2(t)$ . Obviously, these two will not

be the same as we have assigned a certain magnitude to  $|y_{21}(f)|$  (units of siemens) and a different magnitude to  $|F_1(f)|$  (units of length) and obtained  $|F_2(f)|$  (units of length) according to the design procedure; but in device fabrication it is desirable to have  $|f_2(t)|_{\max} \leq |f_1(t)|_{\max}$ . We will consider the case for  $|f_2(t)|_{\max} = |f_1(t)|_{\max}$ , i.e. we scale the time response  $f_2(t)$  so that the peak amplitude in  $f_2(t)$  will have the same peak amplitude in  $f_1(t)$ .

$$\text{Let } f_2(t) = \frac{A_1}{B_1} f_1(t) \quad \dots \quad (8.32)$$

and the Fourier transform of  $f_2(t)$  be  $F_2(f)$

$$\text{i.e. } F_2(f) = \mathcal{F}\{f_2(t)\} = \frac{A_1}{B_1} \mathcal{F}\{f_1(t)\} = \frac{A_1}{B_1} F_1(f) \quad \dots \quad (8.33)$$

The transadmittance will also be scaled accordingly, and let the new value be equal to  $y_{21}(f)$

$$\text{i.e. } y_{21}(f) = K \frac{A_1}{B_1} F_1(f) F_2(f) \quad \left. \begin{array}{l} ) \\ ) \\ ) \\ ) \\ ) \\ ) \\ ) \\ ) \\ ) \\ ) \end{array} \right\} \quad (8.34)$$

but from equation (8.30),

$$y_{21}(f) = K \frac{A_1}{B_1} y_{21}(f) \quad \left. \begin{array}{l} ) \\ ) \\ ) \\ ) \\ ) \\ ) \\ ) \\ ) \\ ) \\ ) \end{array} \right\} \quad (8.34)$$

Now consider the chirped-apodized combination. This configuration is also designed to meet the same specification as that of Filter 2. Let  $F_x(f)$  be the frequency response of chirped transducer and let  $F_y(f)$  be the frequency response of the corresponding apodized transducer. Therefore, the transadmittance can be written as,



$$y_{21}(f) = K F_x(f) F_y(f) \quad \dots \quad (8.35)$$

or in the time domain,

$$y_{21}(t) = K f_2(t) * f_y(t) \quad \dots \quad (8.36)$$

where  $f_x(t)$  is the source function of the chirped transducer and  $f_y(t)$  is the source function of the corresponding apodized transducer.

Let  $A_x$  be the absolute peak amplitude in  $f_x(t)$  and  $B_x$  be the absolute peak amplitude in  $f_y(t)$  respectively. Once again these two will not be the same in general.

Now we scale  $f_x(t)$  in such a way that its peak magnitude is the same as  $f_1(t)$ .

i.e.

$$\text{Let } f_z(t) = \frac{A}{A_2} f_x(t) \quad \dots \quad (8.37)$$

Let its Fourier transform be  $F_z(f)$

$$\therefore F_z(f) = \mathcal{J}\{f_z(t)\} = \frac{A}{A_x} \mathcal{J}\{f_x(t)\} = \frac{A}{A_x} F_x(f) \quad \dots \quad (8.38)$$

Now we scale  $f_y(t)$  in such a way its peak amplitude is the same as that of  $f_z(t)$ .

i.e.

$$\text{Let } f_w(t) = \frac{A}{B_2} f_y(t) \quad \dots \quad (8.39)$$

Let its Fourier transform be  $F_w(f)$

i.e.

$$F_w(f) = \mathcal{J}\{f_w(t)\} = \frac{A}{B_x} \mathcal{J}\{f_y(t)\} = \frac{A}{B_x} F_y(f) \quad \dots \quad (8.40)$$

the transmittance will also be scaled accordingly and let the new value be  $y'_{21}(f)$

$$\begin{aligned} y'_{21}(f) &= K F_z(f) F_w(f) \\ &= K \frac{A}{A_x} \cdot \frac{A}{B_x} F_x(f) F_y(f) \end{aligned}$$

But from equation (8.35)

$$y''(f) = K \frac{A_1^2}{A_x B_x} y_{21}(f) \quad \dots \quad (8.41)$$

Therefore, the improvement in transadmittance is given by, from equations (8.34) and (8.41),

$$y_{21\text{IMP}} = \frac{y''_{21}(f)}{y'_{21}(f)} = \frac{A_1 B_1}{A_x B_x} \quad \dots \quad (8.42)$$

i.e. the improvement in transadmittance is given by the ratio of the product of the absolute peak amplitudes in the unweighted-apodized configuration to the product of the absolute peak amplitudes in the chirped-apodized configuration, provided these two configurations are designed to meet the same specified response with the same magnitude to  $|y_{21}(f)|$  in each case. For the same load admittance this ratio also represents the improvement in the insertion-loss of the filter.

The calculation  $A_1$  is simple. Once the number of fingers in the uniform broadband transducer is selected, the length of the transducer (duration) can be evaluated. Assigning arbitrary magnitude to  $|F_1(f)|$ , and considering at the centre frequency  $f_0$ ,  $A_1$  is given by the following relation: (spectral component at  $f = f_0$  equals the area of the uniform transducer),

$$A_1 = \frac{|F_1(f_0)|}{(\text{Transducer length})} \quad \dots \quad (8.43)$$

The peak magnitude  $B_1$  is automatically obtained while designing the apodized transducer.

The value of  $A_x$  is obtained while designing the chirped transducer and the value of  $B_x$  is automatically obtained while designing the respective apodized transducer. Thus knowing the values  $A_1$ ,  $B_1$ ,  $A_x$

and  $B_x$  we can estimate the improvement in the transmittance, (equation 8.42) and, therefore, the insertion-loss of the filter.

For the examples considered the following results were obtained.

$$\begin{aligned} \text{For Filter 2} \quad A_1 &= 8.85 \times 10^8 \quad (\text{units of velocity}) \\ B_1 &= 10.2 \times 10^6 \quad (\quad \quad \quad ) \end{aligned}$$

For the filter with two identical 40 $\mu$ sec. duration chirped transducers,  $A_x = B_x$  and from the computed results,

$$\frac{A_x B_x}{A_x^2} = \frac{B_x^2}{A_x^2} = 4 \times 1.145 \times 10^{13} \quad (\text{units of velocity}^2)$$

Had the filter been fabricated with similar fabrication considerations as Filter 2, the improvement in insertion-loss will be, substituting for  $A_1$ ,  $B_1$ ,  $A_x$  and  $B_x$

$$Y_{21\text{IMP}} \approx 197 \quad (\approx 46\text{dB}) \quad \dots \quad (8.44)$$

For Filter 2, the theoretical insertion-loss with a 50 $\Omega$  termination (voltage transfer ratio expressed in dB) was found to be (Chapter 7) approximately equal to -72dB, and, therefore, from equation (8.44) the insertion-loss for a 40 $\mu$ sec. identical chirped transducer filter will be, equal to -26dB.

For 1 $\mu$ sec. chirped-apodized transducer filter,

$$\begin{aligned} A_x &= 2.14 \times 10^7 \quad (\text{units of velocity}) \\ B_x &= 1.23 \times 10^8 \end{aligned}$$

and the improvement in insertion-loss will be from equation (8.42)

$$Y_{21\text{IMP}} = 3.43 \quad (10.7\text{dB}) \quad \dots \quad (8.45)$$

i.e. for the 1 $\mu$ sec. chirped-apodized transducer, the insertion-loss with the 50 $\Omega$  termination will be approximately equal to -61dB.

The synthesis procedure outlined in Section (8.3.1) was also carried on to a 2 $\mu$ sec. chirped transducer and the following results were obtained.

$$\begin{aligned} A_x &= 1.51 \times 10^7 \\ B_x &= 8.96 \times 10^7 \end{aligned} \quad \text{(units of velocity)}$$

and from equation (8.42),

$$y_{21_{\text{IMP}}} = 6.78 \quad (16.6\text{dB}) \quad \dots \quad (8.46)$$

i.e. the 2 $\mu$ sec. chirped-apodized transducer will have an insertion-loss with 50 $\Omega$  termination will be approximately equal to -55dB.

Thus we see the potential advantage in improving the insertion-loss of the filter by increasing the time durations in the chirped transducers (larger the time durations, larger the number of fingers in the transducer).

#### Improvement in Input-Output Admittance

We can also anticipate an improvement in the input-output admittances of the chirped-apodized combination compared to the simple unweighted-apodized combination of the transducers. Referring to Section (2.3) the input admittance of the filter (consisting of the admittance parameters of the chirped transducer) is given below:

$$y_{11}(f) = G_a(f) + j\{B_a(f) + 2\pi f C_{T_1}\} \quad \dots \quad (8.47)$$

where

$G_a(f)$  is the radiation conductance

$B_a(f)$  is the radiation susceptance

$C_{T_1}$  is the transducer static capacitance

The expressions for these three factors are given by,

$$\begin{aligned}
 G_a(f) &= \frac{-|\omega| \Delta \pi^2 (\epsilon_o - \epsilon_p)^2 |F_1(f)|^2}{W \times 1.854^2} \\
 B_a(f) &= H_i\{G_a(f)\} \\
 C_{T1} &= \frac{1}{2} W(N_1 - 1)(\epsilon_o + \epsilon_p)
 \end{aligned} \tag{8.48}$$

The notation used here being the same as introduced in Chapter 2  $F_1(f)$  is the frequency response of the chirped transducer. Unless otherwise the duration of the chirped transducer (in turn the number of fingers  $N_1$  in the chirped transducer) is sufficiently large so that  $\Delta N_1 \approx 1$ , the radiation conductance and susceptance, the two first terms in equation (8.47) are negligibly small compared to the static capacitive susceptance, the third term in equation (8.47). In the present case even for a 2 $\mu$ sec. chirped transducer ( $N_1 \approx 138$ ), and for quartz substrate ( $\Delta = 9.8 \times 10^{-4}$ ),  $N_1 \ll 1$  and the input admittance is predominantly given by static capacitive susceptance of the transducer, which is given by the third term in the equation (8.48). A similar conclusion can be drawn for the output admittance of the filter, i.e. the output admittance is essentially given by the static capacitive susceptance of the apodized transducer. In the case of an apodized transducer the static capacitance is given by

$$C_{T2} = \frac{1}{2} (\epsilon_o + \epsilon_p) \sum_{i=1}^{N_2} |L_i| \dots \tag{8.49}$$

where  $L_i$  are the overlap lengths of  $N_2$  half-wavelengths long and  $\epsilon_o$  and  $\epsilon_p$  are the material constants. Therefore, we compare the improvement in the static capacitances in both the cases and the associated Q factors with the same source and load impedances as used for Filter 2 (Section 7.4). Based on theoretical calculations, the results are summarized in Table 8.1. In all the cases the following quantities were assumed (Referring to Figure 7.6),

---

\*  $H_i$  denotes the Hilbert transform.

Filter Configuration	No. of Fingers in $T_1$	No. of Fingers in $T_1$	Input Capacitance $C_{T_1}$	Output Capacitance $C_{T_2}$	Input Q $Q_{T_1}$	Output Q $Q_{T_2}$
Filter 2	9	72	1.2pF	2.12pF	60.5	34.2
1 $\mu$ sec. chirped-apodized configuration	67	129	6.0pF	5.62pF	12.1	12.9
2 $\mu$ sec. chirped-apodized configuration	136	198	13.5pF	10.28pF	5.4	7.1

Table 8.1

centre frequency $f_o$	=	34.2MHz
source and load conductances	≈	15.6msiemens
YX-Quartz substrate with $\epsilon_o$	=	8.854pF/m
and $\frac{\epsilon_p}{\epsilon_o}$	=	4.55
maximum overlap length in each transducer	=	5mm

Thus we see the chirped-apodized configuration increases the input-output admittance and it is much easier to select suitable IC amplifiers to match these capacitances thereby improving considerably the insertion-loss of the filter. This is discussed more clearly in Chapter 9.

### 8.3.3 Discussion of the Results

The design of chirped-apodized transducer configuration for realizing TV IF filters, seems to be quite promising, especially in regard to the improvement in insertion-loss of the SAW filter (equation 8.33). The time wave form of the apodized transducer (Figure 8,3) varies uniformly containing about 3 to 4 sampling points in each half-cycle. However, on examination of the computer results (also Figure 8.3) showed that a skewed finger pattern might result if designed according to the method described for other filters (Section 3.4.4). The skewing effect can only be visualized after actually drawing the pattern and some conclusions can be drawn whether it is tolerable or some other alternative method has to be followed for representing the transducer geometry. Unfortunately, time did not permit to investigate further in the fabrication design and experimental verification of this filter. If a tolerable skewed pattern is obtained, the method is very attractive compared to the previous design techniques. The term tolerable is used in the sense that the pattern can be accomodated on a suitable substrate. Note that skewing in finger patterns does not influence the performance of the filter. A slight disadvantage might arise in photofabrication

of the chirped transducer, since the finger widths are graded from one end to the other resulting in narrow fingers on one side. However, with advent techniques in photolithography, this is not a serious problem, especially at IF frequencies. The only drawback in the method is that the phase response of the apodized transducer is nonlinear and hence the time response is unsymmetrical which in turn might produce a skewed finger pattern.

#### 8.4 Conclusions on Chirped Transducer Design

In general there are no restrictions in designing chirped transducers for realizing any passband characteristic provided the TW product is large as pointed out earlier. For this reason the chirped transducers are well suited at high frequencies in the UHF and UHF range where the bandwidths are usually large and hence only small time durations are needed in which case the SAW devices are quite practicable.

Two identical apodized transducers can also be realized using these FM techniques, once again provided that the TW product is large. The product form of the two integrals in the transadmittance formula (equation 2.7) can be used for the two identical apodized transducers under the strict conditions mentioned above i.e. large TW products. For example, for the case of TV IF filter we can assume a curved time envelope function, instead of a rectangular envelope (Section 8.2) in which case we end up with identical curved, apodized graded transducers. An obvious advantage with this configuration is that the ripples in the passband can be removed or minimized, but it was felt that we might encounter the same difficulty as with the chirped transducers, i.e. very long time durations, and hence, this method was not attempted. Moreover, the algebra becomes more complex, than with simple rectangular envelope functions.

The restrictions of large TW products can be relaxed using



one chirped and one apodized transducer and by far this weighting combination viz., chirped-apodized combination, is a very effective method of designing SAW TV IF filters, as pointed out in the last section.

Thus we conclude this chapter saying that the design of chirped-apodized transducer configuration constitutes a novel technique for designing SAW TV IF filters.

## CHAPTER 9

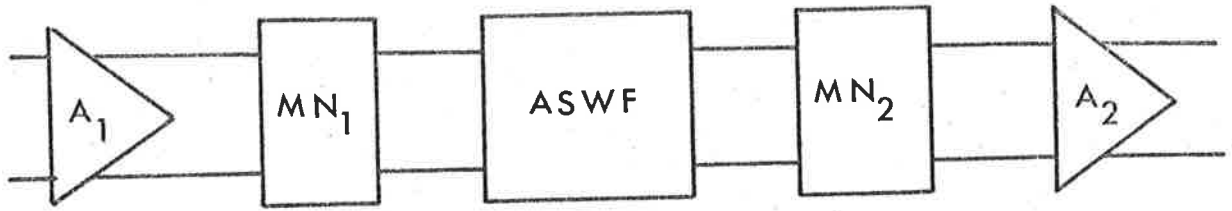
## SYNTHESIS OF A TV IF FILTER IN A HF LINEAR IC ENVIRONMENT

9.0 Introduction

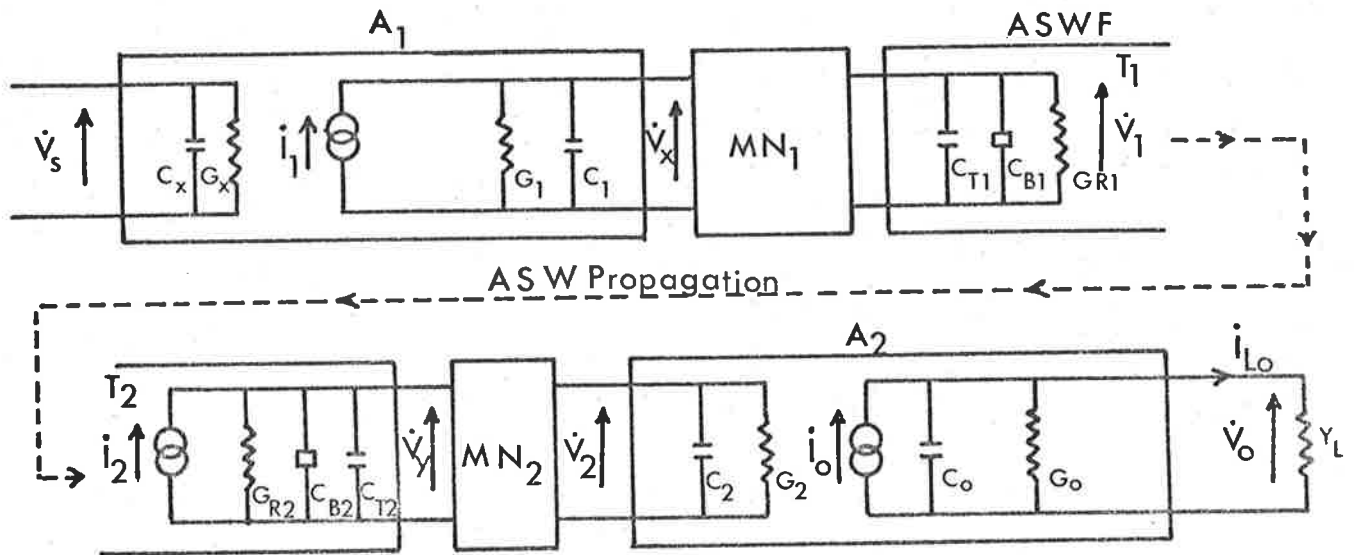
In the first chapter attention was drawn to the fact that SAW delay lines are very attractive for realizing TV IF filters and in later chapters (3, 5 and 8) several synthesis techniques had been developed for achieving the desired TV IF response. Although not all the theoretical responses have been tested as practical filters, the measured results on those have shown good agreement between the theoretical and experimental investigations. However, as pointed out in Chapter 7 the insertion-loss of the filter with  $50\Omega$  source and load impedances was found to be of the order of -70dB. The insertion-loss of the filter should be minimum in order to achieve good signal-to-noise ratio performance in the TV receiver, typically of the order of -10dB or so [9]<sup>1</sup>. It was pointed out in Section 7.4 that if we use high source and load impedances it is possible to improve the insertion-loss of the filter to some extent. In this chapter a synthesis procedure will be described to improve the insertion-loss by incorporating the HF linear IC amplifiers in the input-output side of the SAW delay line. If we consider the IF response to be the overall response of the amplifier-delay line-amplifier chain and design the filter accordingly, the filter may exhibit gain characteristic instead of insertion-loss, because of the presence of IC amplifiers and it may be possible to reduce the number of amplifiers in the receiver. This is the basic synthesis procedure followed in this chapter.

9.1 General Considerations

The type of system which we study is illustrated in Figure 9(a) and an equivalent circuit of such a combination is shown in Figure 9(b).



(a)



(b)

Figure 9. (a) Filter-amplifier assembly.  
(b) Equivalent circuit of (a).

In Figure 9(a), A1 and A2 are typical IC IF or HF amplifiers, MN1 and MN2 are passive matching networks and SAWF is the surface acoustic wave delay line. In the equivalent circuit of Figure 9(b),

$C_1, G_1$  are the output admittance parameters of Amplifier A<sub>1</sub>  
 $C_{T1}$  is the static capacitance of input transducer T<sub>1</sub>  
 $C_{B1}$  is the radiation susceptance of the input transducer T<sub>1</sub>  
 $G_{R1}$  is the radiation conductance of the input transducer T<sub>1</sub>  
 $G_{R2}$  is the radiation conductance of the output transducer T<sub>2</sub>  
 $C_{B2}$  is the radiation susceptance of the output transducer T<sub>2</sub>  
 $C_{T2}$  is the static capacitance of the output transducer T<sub>2</sub>  
 $C_2, G_2$  are the input admittance parameters of Amplifier A<sub>2</sub>  
 $C_0, G_0$  are the output admittance parameters of Amplifier A<sub>2</sub>  
 $Y_L$  is the load admittance.

The matters that are of interest in this study are:-

- (1) Suitable choice of IC amplifiers.
- (2) The definition of a suitable gain function for the above type of amplifier-delay line-amplifier chain. It will be shown later that it is defined as the voltage transfer ratio of the system considered.
- (3) The selection and detailed design of matching networks.
- (4) The synthesis procedure to achieve a prescribed overall response.

## 9.2 Choice of Suitable IC Amplifiers

Integrated circuit amplifiers are normally characterized by admittance parameters [9]<sup>3</sup>. The basic requirement in the choice of a suitable IC amplifier for the filter concerned is that the input (or output) admittance must match approximately the transducer admittance for improved insertion loss. In Figure 9(b) the transducer input (or output) admittance consists of a static capacitance, radiation conductance and

radiation susceptance  $[9]^4$ . In weak coupling materials the static capacitive admittance dominates the other two and hence they are usually neglected. This was clearly illustrated in Section 7.4. The measured values of the static capacitances for Filter 2 (Section 7.4) were found to be 2.5pf and 4pf for the input and output transducers respectively and this corresponds to susceptances of  $550\mu$  siemens and  $875\mu$  siemens at the centre frequency of approximately 35MHz. Very low admittances (conductances as well as susceptances) can usually be obtained with the help of Field Effect Transistors. In common source configuration, the FET exhibits low input admittance, high gain and a low noise figure. Hence, it was decided to use FET's for the two amplifiers A1 and A2. It is appropriate to select the amplifiers such that the input-output susceptances will approximately match the output-input static susceptances of the transducer and then choose a suitable load impedance as described in the following paragraph. Note that it is also possible to choose the amplifiers to match the radiation conductances, while tuning the capacitances with respective inductances, but such a perfect matching is not desirable as it will create more problems than improving the insertion loss of the filter (e.g. increased reflections in delay line which may cause ghost images in the TV receiver).

Let us consider some of the significant features of the Philips Silicon N-Channel Dual Insulated Gate FET, Type BFS28  $[9]^2$ , which we wish to use in our synthesis procedure. From the characteristics, in the 35MHz region, for a drain current of 10mA, the admittance parameters are:

$$\begin{aligned}
 y_{fs} &= g_{fs} - jb_{fs} = (13.0 - j2.0)\text{mA/v} \\
 y_{is} &= g_{is} + jb_{is} = (0.07 + j1.0)\text{mA/v} \\
 y_{os} &= g_{os} + jb_{os} = (60.0 + j500)\mu\text{A/v} \\
 y_{rs} &= g_{rs} - jb_{rs} \approx (0 - j1.57)\mu\text{A/v}
 \end{aligned}
 \tag{9.1}$$

An important question in the use of such amplifiers is how high a load impedance can be used before problems of stability, or excessive distortion of the passband response, can arise as a consequence of the internal feedback in these devices. This particular FET has a very low feedback capacitance ( $< 25\text{fF}$ ), however, we adopt as a rough criterion that the voltage gain  $A_0$  of the transistor, which is given approximately by  $|y_{fs}|/|Y_L|$ , should be limited to about (1/10) of the reverse voltage feedback ratio, which is given approximately by  $|y_{is}|/|y_{rs}|$ . From equation (9.1) we find that,

$$\left| \frac{y_{is}}{y_{rs}} \right| = 637.0$$

$$A_v \approx 63.7$$

... (9.2)

$$|Y_L| = \frac{|y_{fs}|}{A_v} \approx 0.2\text{m siemens}$$

or 
$$R_L = \frac{1}{|Y_L|} = 5\text{K}\Omega$$

Therefore, keeping voltage gain to about 63.7 and hence keeping the load impedance to less than  $5\text{K}\Omega$ , would be a sound policy. Under these conditions, the voltage gain of the stage is about 36dB and if more gain is required two stages may be used.

The Q-factors of the input and output circuits of the individual amplifiers, with the load impedances contemplated above, will be estimated as follows. For the input circuit without any added damping, we would consider Q to be given by,

$$Q_i = b_{is}/g_{is} \approx 14.0$$

... (9.3)

For the output circuit in which we have a load conductance of  $0.2\text{m A/v}$ , and negligible output conductance we consider the Q to be given by,

$$Q_o = b_{os} R_L = 2.5$$

... (9.4)

It is to be noted that the above calculations indicate as a guide to the order of magnitude of the impedances and bandwidths we expect to encounter in the matching circuits connecting the transducers to the amplifiers. We may have to offset the tuning\* of such circuits from band centre somewhat to compensate for the rather complex variation in frequency of the admittance parameters, and other complications brought about by attempts to match transducer and amplifier impedance may arise. Further considerations of tuning circuits may be found in the section dealing with the design of matching networks.

On observing the admittance parameters of the Field Effect Transistor Type BFS28 equation (9.1) we see that the input susceptance is nearly twice the output susceptance and from the measured results of the input-output capacitances of the experimental filters, we find that the static susceptance of the output transducer (apodized transducer) is nearly twice the static susceptance of the input transducer (uniform transducer), and also approximately same values as given in equation (9.1). Therefore, it is appropriate to choose the amplifiers in such a way that the output susceptance matches with that of the uniform transducer while the input susceptance matches with that of the apodized transducer.

### 9.3 Definition of a Gain Function

A synthesis procedure for a prescribed overall response can only be developed after we have given a clear definition of the gain function for which we wish to synthesize the response. The gain function may be defined in the following fashion, referring to Figure 9(b),

---

\* if any. There seems to be a good reason for omission of tuning networks because of the resulting simplicity of construction.

$$G_L = \frac{\dot{V}_O}{\dot{V}_S} = \frac{\dot{V}_X}{\dot{V}_S} \times \frac{\dot{V}_1}{\dot{V}_X} \times \frac{\dot{I}_2}{\dot{V}_1} \times \frac{\dot{V}_Y}{\dot{I}_2} \times \frac{\dot{V}_2}{\dot{V}_Y} \times \frac{\dot{V}_O}{\dot{V}_2} \quad \dots (9.5)$$

where

$$\frac{\dot{V}_X}{\dot{V}_S} = \dot{G}_{A1} \quad \text{is the voltage gain of the input Amplifier.}$$

$$\frac{\dot{V}_1}{\dot{V}_X} = H_{MN1} \quad \text{is the transfer function of the input matching network.}$$

$$\frac{\dot{I}_2}{\dot{V}_1} = \dot{y}_{21} \quad \text{forward transadmittance of the SAW delay line}$$

$$\frac{\dot{V}_Y}{\dot{I}_2} = \dot{z}_{22} \quad \text{The impedance across the output transducer.}$$

$$\frac{\dot{V}_2}{\dot{V}_Y} = H_{MN2} \quad \text{is the transfer function of the output matching network.}$$

$$\frac{\dot{V}_O}{\dot{V}_2} = \dot{G}_{A2} \quad \text{is the voltage gain of the output amplifier.}$$

With these definitions the gain function becomes,

$$G_L = \dot{G}_{A1} \dot{H}_{MN1} \dot{y}_{21} \dot{z}_{22} \dot{H}_{MN2} \dot{G}_{A2} \quad \dots (9.6)$$

Note that the voltage gains  $G_{A1}$  and  $G_{A2}$  are not the same even if we use identical input-output amplifiers because the operating conditions are different, in other words the source and load impedances are different in the two cases.

The exact calculation of  $G_{A1}$ ,  $G_{A2}$  and  $\dot{z}_{22}$  is complicated (largely as a result of the amplifiers  $A_1$  and  $A_2$  not completely being unilateral), and a very useful approximate understanding of the frequency behaviour of these factors can be obtained if we assume the load impedance



is low, and we neglect the internal feedback in the amplifiers. This approximate knowledge of the behaviour of these factors will then form a basis for the selection of the topology of the matching networks and perhaps also their circuit parameters. With these issues determined the more precise analysis can then be used to calculate the responses of the factors  $G_{A1}$ ,  $G_{A2}$  and  $\dot{z}_{22}$  so that appropriate allowance for the contributions of these responses to the overall response can be made in the synthesis for  $\dot{y}_{21}$ .

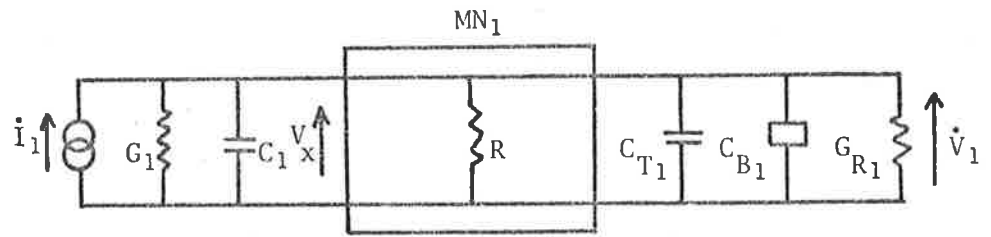
#### 9.4 Matching Networks

The network parameters of interest to us here are the transfer functions  $H_{MN1}$  and  $H_{MN2}$  for the input and output circuits respectively, as defined in the previous section. In principle a wide variety of choices, involving R,L,C elements and ideal transformers are possible for the tuning and matching networks. Some of them are discussed by Jones et al. [9]<sup>5</sup> for surface wave devices. Practical considerations, however, further limit the range of choices in this situation as discussed below.

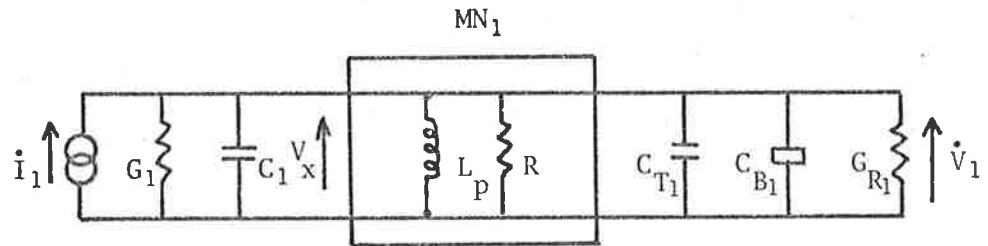
Considerations of space and geometry in planar IC-delay line configuration make transformers difficult to implement, so they will not be considered here.

##### 9.4.1 Input Matching Networks

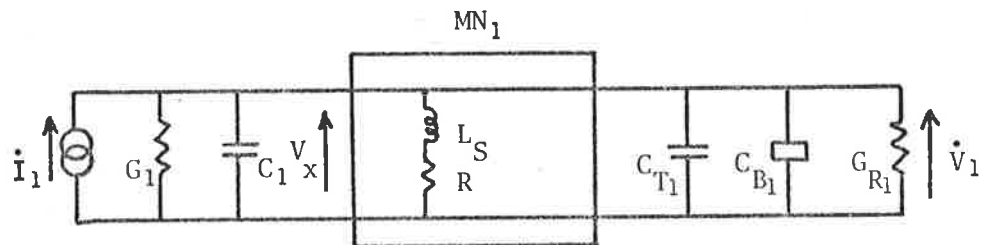
We recall that we have already decided that the maximum load impedance which should be presented to amplifier  $A_1$  is in the vicinity of  $5K\Omega$ . Since this impedance is much less than that provided by the transducer  $T_1$ , it must be provided either by extra parallel-connected elements or some form of impedance matching system. Four circuits are set forth in Figure 9.1 for examination.



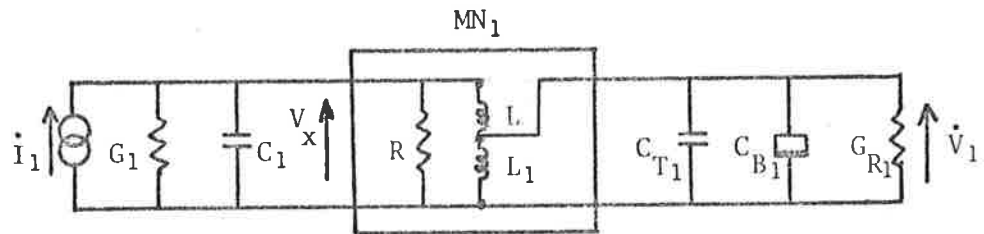
(1)



(2)



(3)



(4)

Figure 9.1 Some Configurations of Input Matching Circuits.

The simplest circuit we can use is (1), in which  $R$  is about  $5K\Omega$ . The conductances  $G_1$  and  $G_{R1}$  are negligible, and  $(C_1 + C_{T1})$  is much greater than  $C_{R1}$ . The time constant of  $R$  and  $(C_1 + C_{T1})$  is about 12.5 nsec, so this circuit has a low pass response with a simple high frequency time constant at about 13MHz. Hence, it is not a very suitable circuit.

In circuit No. (2), we make use of an inductor to produce peak bandpass response centred around 35MHz and following on either side of it. A resistor of about  $5K\Omega$  is still needed to keep the load presented to amplifier  $A_1$  to the value we decided was desirable for stable operation. However, a flat band response is desirable throughout the IF region and this may be achieved through circuit No. (3).

In circuit No. (3), we again make use of an inductor to provide a low  $Q$  resonance at high frequencies to improve and flatten the response in the frequency range of interest. The required inductance  $L_S$  is determined to give a good response shape, and thus is the circuit which we will use it in the synthesis procedure.

Circuit No. (4) differs from the above three circuits in that an attempt has been made, by the use of tapped inductor principle [9]<sup>6</sup> to step up the voltage  $\dot{V}_x$  at the amplifier output to a higher value  $\dot{V}_1$  across the transducer. However, this circuit has not been considered in detail since very large inductances are required than in circuit (2) or (3), moreover tapped inductor principle is useful if there is great mismatch between  $G_{R1}$  and the load conductance  $1/R$ .

Since a single shunt circuit is used in the input matching network,  $H_{MN1} = 1$ , but the effect of this response will be included in the calculation  $\dot{G}_L$ .

#### 9.4.2 Output Matching Networks

The network parameter of interest to us, here is the transfer function  $H_{MN2}$  as defined in Section 9.3. Again we must note that

practical considerations will limit the choice of tuning and matching networks to a few simple configurations. Before discussing these in detail we should note that the matching situation here has an essential difference from that studied in the previous section, in that the values of  $C_{T2}$ ,  $G_{R2}$  and  $C_{B2}$ , and their variation with frequency, will not be known until the synthesis procedure has been completed.

The simple circuit which can be used as output matching circuits are shown in Figure 9.2. Again we assume that no suitable transformers can be made for this application.

Circuit No. (1) has no matching circuits at all, a direct connection between the output of the transducer to the input of the amplifier. A considerable slope of the response would be expected across the passband, but this can be compensated for in the synthesis of the transducer response.

Circuit No. (2) would be expected to have higher gain, and by proper choice of  $L_p$  and introducing additional damping in the circuit we can achieve a substantially uniform response across the passband.

Circuit No. (3) will have a higher gain with a narrow bandwidth and is not particularly suitable.

Circuit No. (4) represents tapped inductor impedance matching and this is much more complex in design and used only for high degree of matching. In fact, a perfect impedance match is not desirable, as it would increase the extent to which the overall response depends on the detailed frequency dependence of  $G_{R2}$  and  $C_{B2}$ . Therefore, this circuit is also not suitable.

In the actual design we follow the circuit No. (2), and once again we ended up with a single shunt element in the output matching network and, therefore, the voltage transfer function  $\dot{H}_{MN2} = 1$ . With a damped resistor  $R$ , the  $Q$  of the circuit is approximately given by  $b_{is} R$  and for  $R = 5K\Omega$  it is equal to 4. The response due to this network will be taken into account while calculating the other parameters in  $G_L$ .

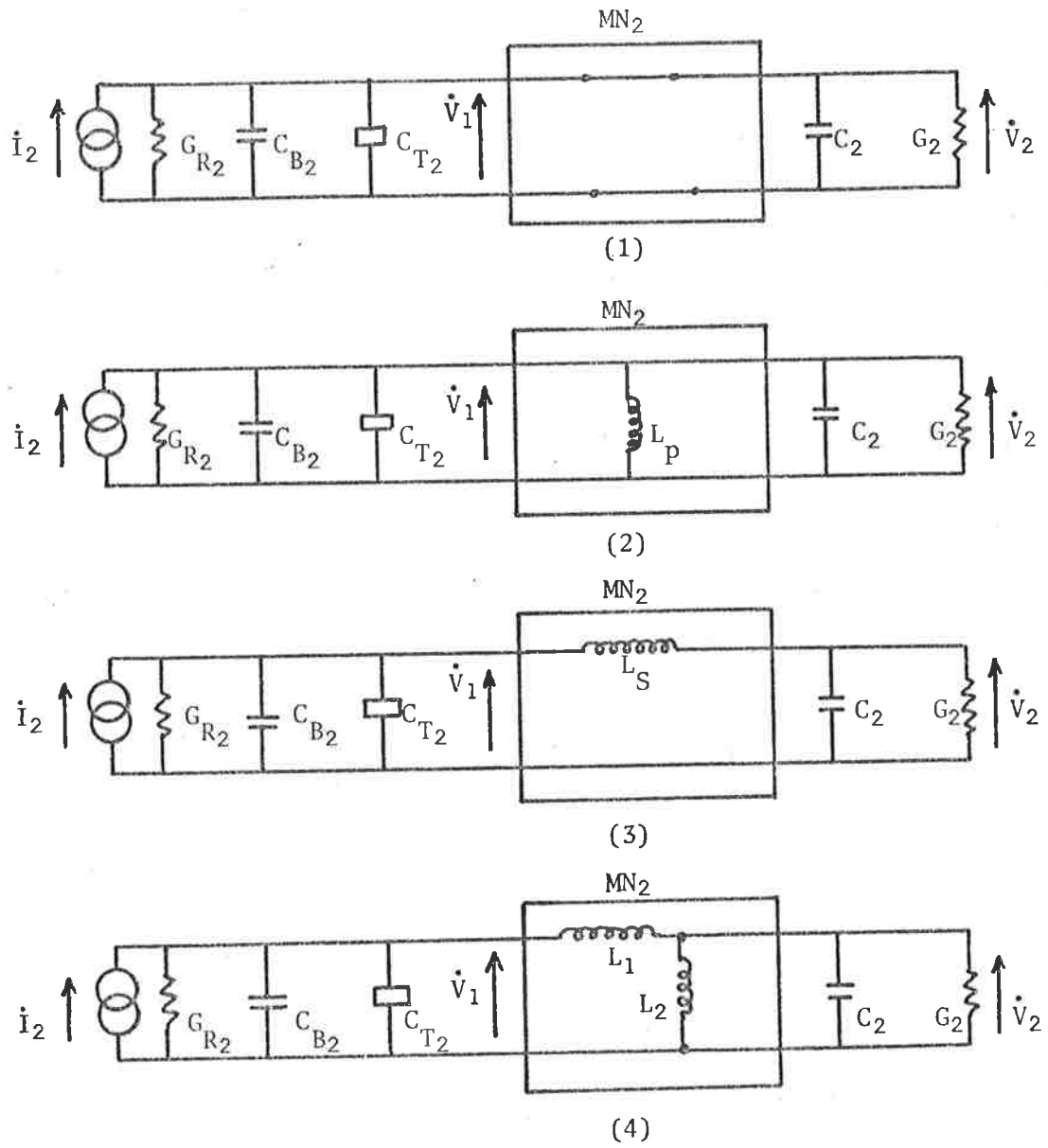


Figure 9.2 Some Configurations of Output Matching Circuits.

### 9.5 Analysis of the Gain Function

With the choice of matching networks the gain function defined in equation (9.6) becomes,

$$G_L = \dot{G}_{A1} \dot{y}_{21} \dot{z}_{22} \dot{G}_{A2} \quad \dots (9.7)$$

We present here some approximate formulae for the parameters  $\dot{G}_{A1}$ ,  $\dot{G}_{A2}$  and  $\dot{z}_{22}$ , which are all valid when the load impedance is small and the amplifiers can be regarded as unilateral, and the radiation admittances of the transducers are negligible. Referring to Figure 9.2(b) the impedance parameter  $\dot{z}_{22}$  is given by the parallel combination of  $C_{T2}$ ,  $L_p$ ,  $C_2$  and  $G_2$  i.e.

$$\frac{1}{\dot{z}_{22}(\omega)} \approx \dot{G}_2(\omega) + j(\omega C_{T2} + \omega C_2) + \frac{1}{R + \frac{1}{j\omega L_p}} \quad \dots (9.8)$$

The gain of the output amplifier is approximately given by,

$$\dot{G}_{A2}(\omega) \approx \frac{y_{fs}(\omega)}{G_0(\omega) + Y_L + j\omega C_0(\omega)} \quad \dots (9.9)$$

Similarly, the gain of the input amplifier is approximately given by,

$$\dot{G}_{A1}(\omega) \approx \frac{y_{fs}(\omega)}{G_1(\omega) + j\omega C_1(\omega) + j\omega C_{T1} + \frac{1}{R + j\omega L_S}} \quad \dots (9.10)$$

Let us now examine the calculation of  $\dot{G}_{A1}(\omega)$ ,  $\dot{z}_{22}(\omega)$  and  $\dot{G}_{A2}(\omega)$  in more detail. For the exact calculation of  $\dot{G}_{A1}(\omega)$ , the information required consists of the characteristics of amplifier  $A_1$  the parameters of the matching network,  $R$  and  $L_S$  and the input admittance (at least the static capacitance) of the uniform transducer. Once the number of fingers and the centre frequency is chosen, the input admittance can

be easily calculated. In the matching network, the value of  $R$  is chosen to be the value of the load impedance of the amplifier which was assumed to be of the order of  $5K\Omega$ . Knowing the input capacitance of the transducer the value of  $L_S$  can be determined and hence the calculation of  $G_{A_1}(\omega)$  presents no difficulty.

For the exact calculation  $G_{A_2}(\omega)$  the information required consists of the characteristics of amplifier  $A_2$  and the value of the load admittance these are already known and present no problem at all.

For the exact calculation of  $\dot{z}_{22}(\omega)$ , the information required consists of the characteristics of amplifier  $A_2$ , the parameter of the matching network  $L_P$  and the output admittance (at least the static capacitance) of the receiving (apodized) transducer. A problem arises here because this output admittance will not be known until after the synthesis for  $\dot{y}_{21}(\omega)$  has been performed. However, with the knowledge of previously designed filters (without IC amplifiers), approximate values of the output admittance parameters can be selected and hence the values of  $L_P$  can be calculated. The transadmittance function  $\dot{y}_{21}(\omega)$  is then synthesized and the actual values of the output admittance parameters are then calculated and compared with the approximately chosen values. If the results differ very much, a new set of values are selected and the synthesis procedure is repeated until a reasonable agreement is obtained. It is most likely that two or three iterations are enough to obtain the appropriate values for the output admittance parameters and hence the required apodization function for the output transducer.

The main concern in the design of the parameters,  $\dot{z}_{22}(\omega)$ ,  $\dot{G}_{A_1}(\omega)$  and  $\dot{G}_{A_2}(\omega)$  is that flat passband responses are desirable as far as possible so as to obtain a smooth apodization function, for realizing the transducer geometry.

9.6 Synthesis Procedure

We set forth here the detailed steps involved in the synthesis of TV IF filter using the gain function  $G_L$ , as defined in the previous section. Recall equation (9.7) and note that  $G_L$  is the voltage transfer function of the filter, hence we can represent the desired TV IF response by  $G_L$ .

$$G_L = \dot{G}_{A1} \dot{y}_{21} \dot{z}_{22} \dot{G}_A$$

- (1) Select suitable IC amplifiers and calculate maximum load impedances (refer to Section 9.2).
- (2) Calculate the elements of the input matching network, viz. R and  $L_S$ .
- (3) Select suitable number of fingers in the uniform transducer and calculate the input admittance parameters of this transducer.
- (4) Evaluate the gain of the input amplifier  $G_{A1}(\omega)$ , equation (9.10).
- (5) Evaluate the gain of the output amplifier  $G_{A2}(\omega)$ , (equation 9.9).
- (6) Calculate the inductance of the output matching network, viz.  $L_P$ .
- (7) Assume appropriate values of the admittance parameters of the output transducer.
- (8) Obtain the impedance parameter  $\dot{z}_{22}(\omega)$  (equation 9.8).
- (9) Divide the desired response  $G_L$  by the product  $\dot{G}_{A1}(\omega) \dot{z}_{22}(\omega) \dot{G}_{A2}(\omega)$  to obtain the required transadmittance  $\dot{y}_{21}(\omega)$ .
- (10) Synthesize the apodized transducer (output transducer) pattern to obtain the approximate  $y'_{21}(\omega)$  of  $\dot{y}_{21}(\omega)$ . Because of the truncation effect in the time response, we may have to use a suitable optimization technique developed in the previous chapters to bridge the gap between  $y'_{21}(\omega)$  and  $\dot{y}_{21}(\omega)$ .
- (11) Calculate the exact admittance parameters of the apodized transducer and the corresponding impedance parameter  $\dot{z}'_{22}(\omega)$



(equation 9.8).

- (12) Compare the value of  $\dot{z}'_{22}(\omega)$  with  $z_{22}(\omega)$  (step No. 8) and if unsatisfactory, select new values of the admittance parameters of transducer  $T_2$  and repeat the procedure from step (8).
- (13) Once a satisfactory value of  $\dot{z}'_{22}(\omega)$  is obtained, calculate the approximate gain function  $G'_L \approx G_L$  from equation (9.7), which represents the overall frequency response of the filter.
- (14) Examine the gain of the filter. If it is within the desired level the synthesis procedure completes at this stage if not, cascading the amplifiers or perhaps a new choice of IC amplifiers may be necessary to bring the gain to the desired level. Any change in the amplifier system requires the repetition of the entire synthesis procedure.

The synthesis procedure described above is a complete and detailed design of TV IF filters using IC amplifiers and requires most of the design techniques developed for various other filters described in the earlier chapters and unfortunately, time did not permit to carry out the complete synthesis procedure. However, the basic advantage of using IC amplifiers in the design of TV IF filters will be illustrated in the following way.

Assuming that we are able to design the matching networks MN1 and MN2 such that the gains  $\dot{G}_{A1}(\omega)$  and  $\dot{G}_{A2}(\omega)$  and the impedance parameter  $\dot{z}'_{22}(\omega)$  all have a flat band response at least over the IF range of interest, then the transadmittance parameter  $y'_{21}(\omega)$  represents the filter IF characteristic so also the gain function  $G'_L$ . Let us calculate the approximate gain function  $G'_L$  for a typical filter, Filter 2 under these conditions, with the known admittance parameters and with the chosen amplifiers, at the centre frequency  $\omega_0$ , we obtain the following quantities,

$$|y'_{21}(\omega_0)| \approx 3.9\mu \text{ siemens}$$

$$|z'_{22}(\omega_0)| \approx 1K\Omega$$

$$|G_{A2}(\omega_0)| \approx 22.6$$

$$|G_{A1}(\omega_0)| \approx 22.1$$

∴ From equation (9.7)

$$G'_L \approx 6\text{dB}$$

Thus we see that we shall be able to obtain apart from the desired IF characteristic, we also are able to obtain a gain of 6dB from the filter. If the exact synthesis procedure has been carried out we may be able to achieve even more gain than this figure. It is just to show the effectiveness of the filter design incorporating IC amplifiers. If we choose a more appropriate choice of IC amplifiers or by cascading a number of amplifiers and then design the filter according to the above synthesis procedure, we shall be able to obtain the required gain in the receiver thereby reducing considerable number of stages in the receiver. Note that designing the SAW TV IF filter first and then pre- or post-amplifying the signal is different from what has been described here. Even with high coupling materials the insertion loss of the filter is very high (< -10dB) and as pointed out by Van Raalte [9]<sup>1</sup> amplification after the IF filter cannot avoid the deterioration in noise performance, while amplification before the filter is limited by the desire for low cross modulation with adjacent channel signals. Therefore, it is preferable to design a TV IF filter with only a moderate amount of gain before channel separation filtering and only a moderate amount of gain after it. The design procedure described above is well suited in such applications.

## CHAPTER 10

## SUMMARY AND CONCLUSIONS

The synthesis of surface acoustic filters, in particular TV IF filters, have been successfully demonstrated. Several synthesis techniques have been developed, all of them are primarily based on the transadmittance formulation between a pair of acoustically-coupled interdigital transducers on a weak-coupling substrate. The main feature of this formulaism is that it not only provides explicit formulae for the input and transfer impedances between the transducer pairs but also enables us to predict the accurate behaviour of the device performance with considerably less computation effort than required with any of the earlier models (10)<sup>1,2,3,4</sup>.

Starting with a simple surface acoustic wave delay line configuration with one uniform broadband transducer with only a small number of fingers as the transmitting transducer, the receiving transducer is synthesized using the transadmittance formula for a typical TV IF specification as indicated by a major electronics industry in Australia. The synthesis gives rise to a finger length weighted (apodized) comb structure with nonuniform finger spacings (mainly in the sidelobe portions of the apodized comb). The initial design is concerned only with the search for an optimum transducer length. It is found that the sidelobes are the major contribution factors in creating the trap at the sound carrier frequency in the IF passband. Greater the number of sidelobes, deeper will be the trap, but large numbers of sidelobes will produce practical limitations in the device fabrications, hence the need for an optimum transducer length is necessary. In the synthesized pattern only one sidelobe is kept on either side of the mainlobe. A computer program

is then developed to generate this complicated pattern and the filter has been fabricated on a YX-Quartz crystal substrate with aluminium metal electrodes. The experimental results agree quite well with the predicted performance of the filter, thus providing a better footing for further investigation in the surface acoustic wave filter design. At this juncture a comment on the choice of a suitable substrate material for TV IF applications will be made.

There are very many important factors which must be considered for a proper choice of a material for TV IF applications. A few of them are listed below:

- (1) High  $K^2$  material for obtaining a broadband response with low insertion loss.
- (2) Stable and reproducible material (a) preferably zero temperature coefficient (b) aging of less than 0.5% per year (c) highly reproducible (errors in reproducibility should be less than 0.1%).
- (3) An homogenous polished surface to avoid acoustic scattering at frequencies above about 30MHz.
- (4) Relatively high dielectric constant for obtaining low impedance devices.
- (5) A material which produces zero or minimum spurious signals like reflections from the fingers, triple transit signals and other second or higher order responses all of which cause undue images on the TV receiver screen.
- (6) Above all it must be quite inexpensive in mass production.

Even though quartz has been selected for the experimental purpose for the reasons mentioned in Chapter 4, it is not the best material in view of the above requirements. There are a large number of new materials on which research has been done (10)<sup>5,6,7</sup>, but it has not been found so far a material which can achieve all of the above requirements simultaneously and hence, some trade-offs have to be made in the design process. For example, if we use a high  $K^2$  material for low insertio

loss, the triple transit signal apart from other spurious signals becomes a significant factor which produces a ghost image on the TV screen. This condition cannot be tolerated. There are many ways to remove or minimize the triple transit signal (10)<sup>8,9,18</sup>, but at the expense of additional complexity of the transducer structures. Hence, use of a low  $K^2$  material is highly desirable, especially in the TV IF applications. Apart from the triple transit signal being highly attenuated in a low  $K^2$  material the other problems like the second order responses associated with high  $K^2$  materials are greatly reduced in a low  $K^2$  material. However, to encompass the low insertion-loss it is necessary to use external tuning circuits, but the inductors inevitably increase the size and cost of the device package, but this is not necessarily disastrous as there is an added advantage with the extra selectivity, so introduced, it is possible to suppress the bulk wave responses. An overwhelmingly attractive method is to use high impedance, high frequency IC amplifiers in the filter design itself. This does not involve additional cost, as amplification of the signals before and after filtering are normally used in the receiver and if the amplifiers-SAW device assembly is designed in such a way so as to produce the required IF passband, we are in fact reducing some of the amplifier stages that are necessary in the TV receiver. This is demonstrated to some extent in Chapter 9.

Having indicated that low  $K^2$  materials are necessary for TV IF applications, it will be indicated here that some of the possible materials which can be produced in an inexpensive way.

The recent development of manufacturing techniques for the production of surface-wave transducers by depositing piezoelectric thin film materials like zinc oxide (10)<sup>10,11,12</sup> and cadmium sulphide (10)<sup>13,14</sup> onto nonpiezoelectric substrates creates the possibility of producing TV IF filters on inexpensive materials such as isopoustic glass (10)<sup>15</sup>. As it has been pointed out earlier that low  $K^2$  materials

are required to minimize second-order responses, it should be practical to use very thin layers of piezoelectric over the transducer metalization, thus minimizing the problem of frequency dispersion commonly associated with laminar structures.

It is also apparent that the cost for producing the transparencies for photolithography using conventional high resolution glass plates, would be prohibitive in large scale production of the filters, and an elegant method is to use a computer controlled electron beam unit to draw the required transducer configurations directly onto the photoresist for each filter unit.

Returning back to the synthesis procedure outlined above, although capable of providing an approximate representation of the desired response, deviates considerably from that of the actual specification as a result of truncating the time-domain response of the apodized transducer, and hence suitable optimization techniques have been developed to bridge the gap as closely as possible. The optimization technique followed here for achieving the best agreement between the specified response and the adopted response is the least square error criterion. The method is fairly simple and well formulated in the network design, but applying it to synthesize a surface acoustic wave TV IF filter using transmittance model constitutes a novel technique. This quadratic cost function optimization becomes even simpler for designing filters with linear phase responses, and is referred as OPTIM METHOD in this investigation (text). Apart from TV IF filters several other examples have been considered like rectangular passband and cosine shaped passband to test the validity of the OPTIM METHOD and in all cases good agreement is obtained between the achieved response and the specified response. Synthesis techniques have also been developed (Section 5.3) for filters with nonlinear phase responses and in this case they require large amount computing times if not prohibitive, compared to the OPTIM METHOD.

The same objective viz., the response in the frequency domain is made closer to the specified one, while maintaining the same finger locations but varying the overlaps in the apodized transducer, may be achieved with a successive truncating and weighting technique referred as zero-order successive iteration optimization method but with less computing effort, which seems to be a fortuitous method. All the synthesis techniques resulted in rather larger perturbations near the sidelobe region in the truncated time window, which shows once again that the sidelobes are responsible for creating as well as improving the trap at the sound carrier frequency in the IF passband characteristic.

Some remarks about the quadratic cost function optimization as applied to the SAW filters is worth mentioning at this point. As in any synthesis procedure, the designer is always faced with selecting a few design parameters, either empirically or by experience. In this situation selection of the cost-coefficients is a prominent design parameter. It is appropriate to select the same number of cost-coefficients in the frequency domain as there are the number of perturbations in the time-domain. However, with this notion, even though the frequency response was improved, a distorted time waveform was resulted which could not be represented by a suitable finger pattern for making the practical device. Eventually, it was found that it is necessary to assign cost-coefficients throughout the spectrum even though we consider a small number of perturbations in the time-domain. With this choice the method behaved very well, the response in the frequency domain improved to a great extent and the objective of making a practical filter was also achieved.

The optimization technique followed here is quite simple, straightforward and requires the solution of a set of linear equations, however, more powerful and elegant techniques, like dynamic programming (10)<sup>16</sup> may be used in minimizing the maximum deviations. Dynamic

programming is a general approach to the solution of sequential decision processes. Instead of optimizing a single function, optimization is performed on

$$\psi_i(\bar{x}) = \min_{\bar{x}_j} |f_i(\bar{x}) + \psi_{i-1}(\bar{x})| \quad i = 1, 2, \dots, N$$

where  $f_i(\bar{x})$  is the objective function for the  $i$ th stage defined over some range of interest and  $\bar{x}_j$  is the combination of  $(x_1, x_2, x_3 \dots x_N)$  that optimizes  $\psi_i(\bar{x})$ . The objective in the procedure is to determine the value of  $\bar{x}_j$  in the  $i$ th stage which optimizes  $\psi_i(\bar{x})$  with regard to the stage resulting from the  $(i-1)$ th decision. This decision process is performed  $N$  times to obtain the desired optimization. The reduced form obtained by techniques has a property like, 'monotonicity of convergence', and therefore, is well suited to problems like this - the SAW filter synthesis.

TV IF filters developed with various approaches have been constructed and tested using long-pulse CW-simulating measurements. The results agree quite well, within the experimental errors, to the theoretical predictions. However, the traps at the band edges are not as deep as the specified response, and also considerable amount of ripple, especially on low frequency band edge is found and we can postulate a number of reasons for this cause.

(1) The unweighted broadband uniform transducer might have caused the undesired rounding of the filter due to its  $\sin(x)/x$  frequency response. Deeper traps could be created by choosing the  $\sin(x)/x$  response in such a way that the first nulls will fall on the adjacent channel traps, which means by increasing the number of fingers in the uniform transducer. However, with larger number of fingers, the  $\sin(x)/x$  response becomes quite narrower and it is difficult to achieve the required trap at the sound carrier frequency. In fact, it was found that in the synthesis



procedure any attempt to improve the level at the band edges will deteriorate the level at the sound carrier frequency or vice versa, with this simple uniform-apodized configuration technique.

(2) As we have made no attempt in suppressing the bulk-waves, this bulk-wave response might have prevented filter from achieving high rejection at the band edges. Several techniques have been explored in the literature with some success to reduce bulk-wave response in IF filters. These include roughing the bottom surface, bonding the surface to a larger, lossy material or tilting the various crystal faces at an angle to deflect the generated bulk-waves; none of these techniques are fully adequate. Better means have been demonstrated, such as the use of multiple transducers so that surface waves are added in phase while bulk-waves cancel, or the steering of the surface waves along the surface to physically separate them from bulk-waves. These techniques are, however, more costly since they require considerably large substrates.

(3) The electrical response of the tuning inductor with the device static capacitance and the high-impedance capacitive probe on the input side might have degraded the sidelobe rejection at the low frequency band edge.

Further, in all the experimental filters it was found that there is a shift in frequency scale from that of the specified response and this is due to the limited facilities available in this laboratory for the prototype manufacture of the delay lines and considerable improvements are necessary for making an accurate device. Moreover, a prototype system is not expected to be an accurate device, but rather to function as a convenient vehicle for the examination of the general behaviour of the surface acoustic wave filter synthesized using the admittance formulation. However, by incorporating the possible errors occurred in the manufacturing process of the filter, a computer model revealed the exact shift in the frequency scale, thus ensuring that, apart from a slight shift in the frequency scale, the measured results agree quite well

with the theoretical ones.

A brief remark about the measurement system is that it is desirable to have a more elegant receiver system for measuring the output signals to detect the deep traps in the DF response than the simple (simulating long-pulse CW) measurement system followed here.

TV IF filters have also been synthesized using chirped transducers with stationary phase approximation method. With two identical chirped transducers it was found that enormous numbers of fingers are needed for achieving the desired response, and this restricts their use in practical situations. However, an alternative approach whereby, one transducer is chirped and the other apodized with reasonable amount of fingers in each transducer, for realizing the TV IF filters, once again using transadmittance model is presented. The various advantages with this configuration are fully discussed, the prime importance being, improvement in the admittance parameters compared to the simple uniform-apodized configuration and by far this is the most efficient and best synthesis technique for realising TV IF responses. Thus we can say the synthesis of chirped-apodized transducer configuration used in conjunction with the transadmittance formulation, constitutes a novel technique for the synthesis of surface acoustic wave TV IF filters. This technique does not require any computer iteration, does not require any optimization, produces results that are reasonably in good agreement with the specified response and hence saves considerable amount of computing time. The experimental investigation of this filter, though not undertaken due to lack of time, presents no problem at all in achieving the desired response, except it might take considerable amount of time in generating the art-work.

The last part of the study involves in the synthesis of TV IF filters using high frequency linear integrated circuit amplifiers. It is possible to improve the insertion-loss of the filter, considerably

using the IC amplifiers mainly due to the high impedance of the IC amplifiers can be nearly matched to the high impedances of the transducers. A complete synthesis procedure for this amplifier-delay line-amplifier configuration is presented, once again using the transadmittance formulation. The synthesis procedure mentioned herein requires most of design techniques developed for various other filters described in the earlier parts of the thesis, the most difficult one being the optimization technique for nonlinear phase responses. In addition it also requires the design of suitable IC amplifiers, and the appropriate matching networks, and unfortunately time did not permit to carry out the complete synthesis procedure. However, the basic advantage of using IC amplifiers in the design of TV IF filters is illustrated in a simpler way.

The filter synthesis concerned in this investigation is based on the transadmittance model. It will be indicated here that some of the improvements that are necessary to make it even more generalised formulation. The basic assumptions like weak-coupling approximation, neglecting the second or higher order responses, have been discussed in Chapter 2. Reflection from a shorted transducer (not the reflection due to the triple transit signals) is not included in the transadmittance model as it is assumed small enough to be neglected. This reflected signal may be regarded as being due to variation in the electromechanical impedance of the propagation path, presented to the surface-wave passing under the transducer, which may be due to either the mass loading of the fingers or the localized electric field-shorting effect of each electrode (10)<sup>17,18</sup>. Second or higher order responses have also not been included in the transadmittance formula once again assuming that their effects are negligibly small. However, these effects, second order as well as reflections from a shorted transducer have to be taken into account if an accurate performance of the device is required. The second and

higher order responses may be obtained in terms of the admittance parameters by binomial expansion of the voltage transfer function equations (2.2) and identifying the respective terms in the series. Even in the second order response all the admittance parameters are present and in the filter synthesis the transfer admittance and the output admittance are not known until after the synthesis is completed and a practical approach in such a situation is to adopt an iterative design procedure, similar to one described in Chapter 9 for the synthesis of filters incorporating IC amplifiers.

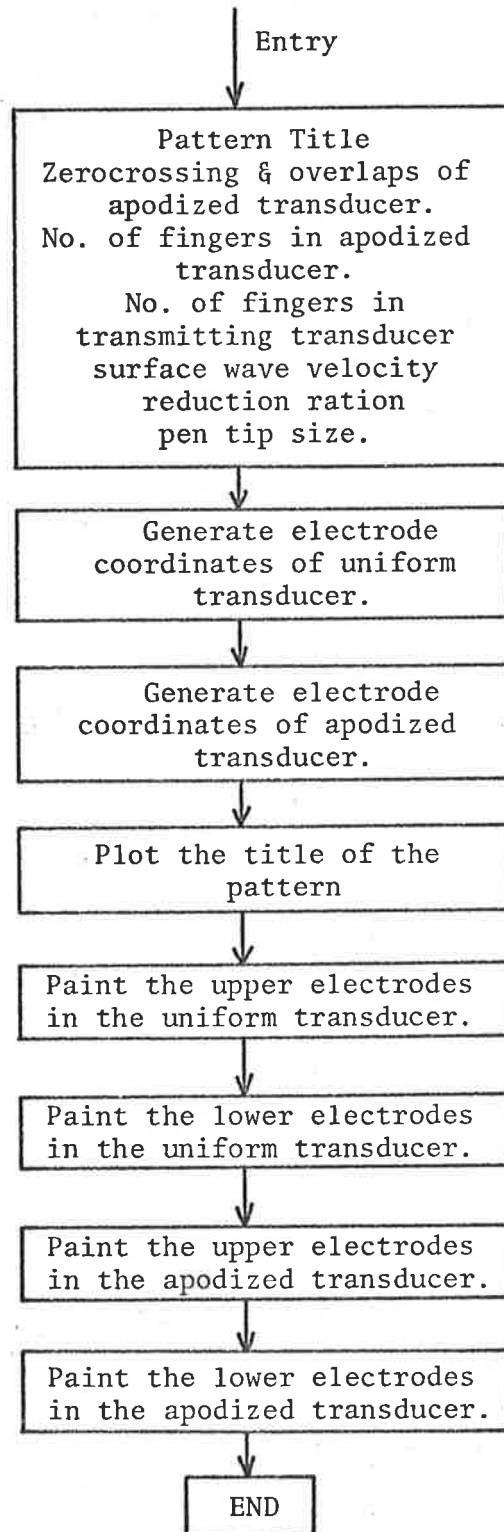
In conclusion we can say that the SAW filters can be designed with confidence using the transadmittance model. With this model as pointed out several times earlier, it is possible to predict the complete performance of the filter beforehand, and if any changes in the design parameters are needed, they can be amended in the synthesis procedure and after assuring ourselves that the predicted response is well within the specified limits, the filter is then fabricated for experimental purpose. The systematic computer design technique developed for SAW TV IF filters which have been constructed and tested may be briefly summarised as follows:

- (a) The first program takes the specified frequency response and produces a truncated time response which approximately satisfies the specification.
- (b) This is then fed into a second program which optimizes the truncated time response to improve the approximate specification in (a).
- (c) The truncated-optimized time response is then fed into a third program which designs a transducer structure and also calculates the expected response of this transducer structure. After comparison with the original specification, this produces a punched output (or tape) for drawing the art-work.
- (d) This is then fed into a fourth program, which drives the machine for producing the art-work.

(e) The filter is then fabricated with the standard photolithography, tested and the experimental readings are fed into a fifth program, which computes the frequency response with the given load conditions and compares with the original specification. If there is something wrong there is provision in the various programs to adjust suitable parameters for comparisons with the final result (e.g. frequency scaling).

A similar computer designed technique can be developed in case of TV IF filters incorporating linear HF IC amplifiers as pointed out in the closing remarks of Chapter 9.

## A1 PROGRAM ARTWORK: GENERATION OF TRANSDUCER PATTERN

A1.1 Flow Chart of ARTWORK

## A1.2 Listing of ARTWORK

```

PROGRAM ARTWORK(INPUT,OUTPUT)
*
C   THIS PROGRAM PRODUCES A BLACK AND WHITE ELECTRODE PATTERN SUITABLE
C   FOR PHOTOGRAPHY
C
C   PEN TIP WIDTH USED IS 0.3 MILLIMETRES
C   AVERAGE PEN TRACE OVERLAP = .15MM = .006 INCH
C   ALLOWANCE IS MADE FOR PEN TIP WIDTH
C
C   INPUT DATA REQUIRED =
*   NA = ANY NUMBER OF FINGERS IN THE TRANSDUCER UP TO 100
*   GA = SIZE OF FIRST GAP IN MILLIMETRES
*   XPA(1) = POSITION OF FIRST FINGER CENTRE IN MM.
*   XLA(1) = SIGNED MAGNITUDE OF FIRST OVERLAP IN MM.
*   AGA = RATIO OF SUCCESSIVE GAP WIDTHS
*   ALA = RATIO OF SUCCESSIVE OVERLAPS (UNSIGNED)
*   WNO = MINIMUM NON-OVERLAP LENGTH IN MM.
C   NOTE OVERLAP 1 IS BETWEEN FINGER 1 AND FINGER 1+1
*   REDR = TOTAL REDUCTION RATIO ((DEFINED GREATER THAN 1))
*   TITLE = IDENTIFYING NAME OF THE PATTERN
C   PROGRAM ASSUMES EACH GAP DIVIDED INTO QUARTERS AND RIGHT AND LEFT
C   QUARTERS METALLIZED
C   THE PROGRAM ASSUMES THE SUM OF THE SIGNED OVERLAPS IS SMALL
C
C   FURTHER COMMENTS
C   THE FIRST OVERLAP MUST BE POSITIVE
C   FOR UNIFORM TRANSDUCER THE OVERLAPS AND ZERO CROSSINGS ARE GENERATED
C   IN THE PROGRAM ITSELF
C   FOR APODIZED TRANSDUCER THEY ARE TO BE PROVIDED EXTERNALLY ACCORDING
C   TO THE FORMAT 1
C   TYPICAL DATA INCLUDED IS FOR FILTER4
C
C   DECLERATIONS
*
C   DIMENSION A1(100),B1(100),A(100),B(100),XR(400),YR(400)
C   DIMENSION XPA(100),XLA(100)
C   DIMENSION XPB(100),XLS(100),XT(400),YT(400)
C   REAL LAHDA
*
C   DATA TITLE/9HA/11/1/P2/
*
C   PTIP = 0.3
C   RECEIVING TRANSDUCER PLOTTING
C   PRINT 10
10  FORMAT (1H1,40X*RECEIVING TRANSDUCER PLOTTING PREPARATION*//)
C   XPA(1) = 1.0
C   WNO = 1.25
C   REDR = 25.2
C   VEL = 3.145E+06
C   FO = 34.0E+06
C   NA IS NO OF ZERO CROSSINGS
C   NA1 IS THE NO OF PEAKS (ONE LESS THAN NO OF ZERO CROSSINGS)
C   NA = 80
C   NA1=NA-1
*
C   READ THE DATA- A(I) ARE ZERO CROSSINGS AND B(I) ARE THE OVERLAPS
*
C   READ 1,(A1(I),I=1,NA)
C   READ 1,(B1(I),I=1,NA1)
1  FORMAT (5E16.8)
*
C   PRINT 2
2  FORMAT (1H0,10X*ZERO CROSSINGS AND OVERLAPS,THE PUNCHED OUTPUT FRO
C   CH THE PREVIOUS PROGRAM*//)
C   PRINT 3,(I,A1(I),B1(I),I=1,NA1)
3  FORMAT (15,5XE16.8,5XE16.8)
C   PRINT 4,(I,A1(I),I=NA,NA)
4  FORMAT (15,5XE16.8)
C
C   OMIT THE FIRST AND THE LAST ZERO CROSSINGS SINCE THIS GAVE AN ERROR THAT
C   LINE WIDTH LESS THAN PEN WIDTH
C   OMIT SO ALSO THE FIRST AND LAST OVERLAPS
*
C   DO 7 I = 2,79
C   A(I-1) = A1(I)
7  CONTINUE
C   DO 8 I = 2,78
C   B(I-1) = B1(I)
8  CONTINUE
C   NA = 80-2
C   NA1 = NA-1
C   PRINT 15
15  FORMAT (1H0,10X*ZERO CROSSINGS AND OVERLAPS AFTER OMITTING FIRST AN
C   CD LAST PAIRS*//)
C   PRINT 3,(I,A(I),B(I),I=1,NA1)
C   PRINT 4,(I,A(I),I=NA,NA)
*
C   GENERATE GAPS AND OVERLAPS IN MILLIMETERS
C   XYZ = 0.0
C   DO 9 I = 1,NA1

```

```

XYZ = AMAX1(ABS(B(I)),XYZ)
9 CONTINUE
DO 5 I = 1,NA1
X = A(I+1)-A(I)
II = I+1
XPA(II) = X*VEL+XPA(I)
XLA(II) = B(II)*5.0/XYZ
5 CONTINUE

C
C PRINT ELECTRODE POSITIONS AND OVERLAPS
PRINT 306
306 FORMAT (1H0,10X*ELECTRODE POSITIONS AND OVERLAPS IN HMS*/)
DO 307 J=1,NA1
PRINT 308,J,XPA(J),XLA(J)
307 CONTINUE
308 FORMAT (I10,E22.5,E16.5)
PRINT 6,(I,XPA(I),I=NA,NA)
6 FORMAT (I10,E22.5)

*
C TEST THE SIGN OF FIRST OVERLAP
C IF IT IS NEGATIVE ALTER THE SIGNS OF ALL OVERLAPS SO THAT THE
C FIRST ONE BECOMES POSITIVE
*
IF(XLA(1))11,11,12
11 DO 13 I = 1,NA1
XLA(I) = -XLA(I)
13 CONTINUE
PRINT 14
14 FORMAT (1H0,10X*SIGNS OF OVERLAPS HAVE BEEN CHANGED TO MAKE FIRST
COVERLAP POSITIVE*/)
12 CONTINUE
CALL COORD(XPA,XLA,NA,NA1,REDR,XR,YR,WNO)

*
C TRANSMITTING TRANSDUCER PLOTTING
PRINT 20
20 FORMAT (1H1,40X*TRANSMITTING TRANSDUCER PLOTTING PREPARATION*//)
LAMDA = VEL/FO
C NB IS NO OF FINGERS IN TRANSMITTING TRANSDUCER
NB = 11
NB1 = NB-1
BN = NB/2.0
NB2 = INT(BN)
C GENERATE GAPS AND OVERLAPS
C INCREASE OVERLAPS BY 25 PERCENT TO TAKE INTO DIFFRACTION EFFECTS
PRINT 21
21 FORMAT (1H0,10X*OVERLAPS INCREASED BY 25 PERCENT TO TAKE INTO DIFF
RACTION EFFECTS*/)
WNO = 1.57
XPB(1) = 1.0
DO 22 I = 1,NB1
II = I+1
XPB(II) = XPB(I)+LAMDA/2.0
22 CONTINUE
DO 23 I = 1, NB2
XLB(2*I-1) = 6.25
XLB(2*I) = -6.25
23 CONTINUE
C PRINT ELECTRODE POSITIONS AND OVERLAPS
PRINT 306
PRINT 309,(I,XPB(I),XLB(I),I=1,NB1)
PRINT 6,(I,XPB(I),I=NB,NB)
CALL COORD(XPB,XLB,NB,NB1,REDR,XT,YT,WNO)

*
C SUBROUTINE SETPLT CALLS THE PLOT ROUTINE AND PLOTS THE TITLE
CALL SETPLT(TITLE,REOR)
C PLOT THE TRANSMITTING TRANSDUCER
TRAVL = 20.0
CALL TRPLOT(XT,YT,NB,NB1,PTIP,TRAVL)
C PLOT THE RECEIVING TRANSDUCER
TRAVL = 20.0
CALL TRPLOT(XR,YR,NA,NA1,PTIP,TRAVL)
999 STOP
END

SUBROUTINE COORD (XPA,XLA,NA,NA1,REDR,X,Y,WNO)
*
* DIMENSION XPA(100),XLA(100),X(400),Y(400)
*
C SCALE UP TO ARTWORK SIZE (IN INCHES)
SCALE=REDR/25.4
WNO = WNO*SCALE
DO 309 I = 1,NA1
XPA(I)=XPA(I)*SCALE
309 XLA(I)=XLA(I)*SCALE
XPA(NA) = XPA(NA)*SCALE
C FIND THE MAXIMUM OVERLAP
XM=0
DO 400 I=1,NA1
XM = AMAX1(ABS(XLA(I)),XM)

```



```

400 CONTINUE
C   FIND TOTAL PATTERN WIDTH
   WT=XM*2*WNO
C   TEST PATTERN DOES NOT EXCEED 28 INCHES HIGH
   IF(WT.LT.28)GO TO 402
   PRINT 403
403 FORMAT(*1PATTERN TOO HIGH*)
   STOP

402 CONTINUE
C   GENERATE THE COORDINATES ACCORDING TO NA IS ODD OR EVEN
   AN = NA
   AN = AN/2.
   ANT = AN-AINT(AN)
   IF(ANT.EQ.0.0)GO TO 301
C   GENERATE PLOTTING COORDS - ELECTRODE 1
   CL = 14.0
   G3=(XPA(2)-XPA(1))/4
   X(1)=X(2)=XPA(1)-G3
   X(3)=X(4)=XPA(1)+G3
   YMAX=CL+WT/2
   YMIN=CL-WT/2
   Y(1)=Y(4)=YMAX
   Y(2)=Y(3)=CL-XLA(1)/2
C   GENERATE PLOTTING COORDS FOR REMAINING ELECTRODES
   DO 401 J = 2,NA1,2
   J4=4*J
   G1=G3
   G2=(XPA(J+1)-XPA(J))/4
   IF(J.EQ.NA1)GO TO 405
   G3=(XPA(J+2)-XPA(J+1))/4
   GO TO 404
405 G3 = G2
404 CONTINUE
   X(J4-3)=X(J4-2)=XPA(J)-G1
   X(J4-1)=X(J4)=XPA(J)+G2
   Y(J4-3)=Y(J4)=YMIN
   Y(J4-2)=Y(J4-1)=Y(J4-5)+XLA(J-1)
   X(J4+1)=X(J4+2)=XPA(J+1)-G2
   X(J4+3)=X(J4+4)=XPA(J+1)+G3
   Y(J4+1)=Y(J4+4)=YMAX
   Y(J4+2)=Y(J4+3)=Y(J4-1)+XLA(J)
401 CONTINUE
   GO TO 302
*
301 CONTINUE
C   GENERATE PLOTTING COORDS - ELECTRODE 1
   CL = 14.0
   G3=(XPA(2)-XPA(1))/4
   X(1)=X(2)=XPA(1)-G3
   X(3)=X(4)=XPA(1)+G3
   YMAX=CL+WT/2
   YMIN=CL-WT/2
   Y(1)=Y(4)=YMAX
   Y(2)=Y(3)=CL-XLA(1)/2
C   GENERATE PLOTTING COORDS FOR REMAINING ELECTRODES
   DO 601 J = 2,NA1,2
   J4=4*J
   G1=G3
   G2=(XPA(J+1)-XPA(J))/4
   G3=(XPA(J+2)-XPA(J+1))/4
   X(J4-3)=X(J4-2)=XPA(J)-G1
   X(J4-1)=X(J4)=XPA(J)+G2
   Y(J4-3)=Y(J4)=YMIN
   Y(J4-2)=Y(J4-1)=Y(J4-5)+XLA(J-1)
   X(J4+1)=X(J4+2)=XPA(J+1)-G2
   X(J4+3)=X(J4+4)=XPA(J+1)+G3
   Y(J4+1)=Y(J4+4)=YMAX
   Y(J4+2)=Y(J4+3)=Y(J4-1)+XLA(J)
601 CONTINUE
*
C   GENERATE PLOTTING COORDINATES FOR THE LAST ELECTRODE
*
   J4 = 4*NA1
   X(J4+1) = X(J4+2) = XPA(NA) - (XPA(NA) - XPA(NA1))/4.
   X(J4+3) = X(J4+4) = XPA(NA) + (XPA(NA) - XPA(NA1))/4.
   Y(J4+1) = Y(J4+4) = YMIN
   Y(J4+2) = Y(J4+3) = Y(J4-1) + XLA(NA1)
*
C   PRINT OUT COORDINATES
302 PRINT 502
502 FORMAT(35X*PLOTTING COORDINATES (IN INCHES)*/// ELECTRODE*6X*X1*8X
C*Y1*12X*X2*8X*Y2*12X*X3*8X*Y3*12X*X4*8X*Y4*//)
   DO 503 I=1,NA
   I4=4*I
   PRINT 504, I, X(I4-3), Y(I4-3), X(I4-2), Y(I4-2), X(I4-1), Y(I4-1), X(I4),
   CY(I4)
504 FORMAT (I6.4(F14.3,F10.3))
503 CONTINUE
C

```

RETURN  
END

SUBROUTINE SETPLT(TITLE,REDR)

CALL PLOT30(11HNEBP6BOX142,11)  
CALL PAUPLOT(28HBLANKPAPER,0.3MHPEN,BLACKINK,28)  
CALL XLIMIT(60.)

PLOT PATTERN DATA  
CALL SYMBOL(0.,26.,0.3,9HPATTERN =,0.,9)  
CALL SYMBOL(3.0,25.,0.3,TITLE,0.,10)  
CALL SYMBOL(0.,25.,0.3,17HREDUCTION RATIO =,0.,17)  
CALL NUMBER(5.,25.,0.3,REDR,0.,4HF6.2)  
CALL PLOT(10.,0.,-3)  
RETURN  
END

SUBROUTINE TRPLOT(X,Y,NA,NA1,PTIP,TRAVL)

DIMENSION X(400),Y(400)

NOTE DIMENSIONS NOW IN INCHES  
P = PTIP/25.4  
P2=P/2  
OLAP=0.006

PLOT THE ELECTRODE PATTERN

PLOT THE PATTERN ACCORDING AS NA IS ODD OR EVEN

AN = NA  
AN = AN/2.  
ANT = AN-AINT(AN)  
IF(ANT.EQ.0.0)GO TO 300

PLOT UPPER HALF OF PATTERN

DO 601 I=1,NA,2  
J=4\*I

IS LINE WIDTH LESS THAN PEN TIP WIDTH

IF((X(J)-X(J-3)).LT.P)602,603

PRINT 604

FORMAT(\*ILINE WIDTH LESS THAN PEN WIDTH\*)

STOP

603 XD=X(J-3)+P2

YD=Y(J-3)

CALL PLOT(XD,YD,3)

YD=Y(J-2)

CALL PLOT(XD,YD,2)

YD=Y(J)

CALL PLOT(XD,YD,1)

IS THERE ROOM FOR A FULL STROKE DOWN

CONTINUE

IF((X(J)-(XD+P2-OLAP)).LT.P)606,607

606 XD=X(J)-P2

CALL PLOT(XD,YD,1)

YD=Y(J-1)

CALL PLOT(XD,YD,1)

YD=Y(J)

CALL PLOT(XD,YD,1)

GO TO 601

607 XD=XD+P-OLAP

CALL PLOT(XD,YD,1)

YD=Y(J-1)

CALL PLOT(XD,YD,1)

YD=Y(J)

CALL PLOT(XD,YD,1)

GO TO 608

601 CONTINUE

PLOT THE LOWER HALF OF THE PATTERN

CALL PLOT(0.,YD,3)

CALL PLOT(0.,Y(5),3)

DO 610 I=2,NA1,2

J=4\*I

XD=X(J-3)+P2

YD=Y(J-3)

CALL PLOT(XD,YD,3)

YD=Y(J-2)

CALL PLOT(XD,YD,2)

YD=Y(J)

CALL PLOT(XD,YD,1)

```

C      IS THERE ROOM FOR A FULL STROKE DOWN
618  CONTINUE
      IF((X(J)-(XD+P2-OLAP)).LT.P)616,617
616  XD=X(J)-P2
      CALL PLOT(XD,YD,1)
      YD=Y(J-1)
      CALL PLOT(XD,YD,1)
      YD=Y(J)
      CALL PLOT(XD,YD,1)
      GO TO 610
617  XD=XD+P-OLAP
      CALL PLOT(XD,YD,1)
      YD=Y(J-1)
      CALL PLOT(XD,YD,1)
      YD=Y(J)
      CALL PLOT(XD,YD,1)
      GO TO 618
610  CONTINUE
      GO TO 299
*
* 300 CONTINUE
*
      DO 301 I = 1,NA1,2
      J=4*I
C      IS LINE WIDTH LESS THAN PEN TIP WIDTH
      IF((X(J)-X(J-3)).LT.P)302,303
302  PRINT 304
304  FORMAT(*1LINE WIDTH LESS THAN PEN WIDTH*)
      STOP
303  XD=X(J-3)+P2
      YD=Y(J-3)
      CALL PLOT(XD,YD,3)
      YD=Y(J-2)
      CALL PLOT(XD,YD,2)

      YD=Y(J)
      CALL PLOT(XD,YD,1)

C
C      IS THERE ROOM FOR A FULL STROKE DOWN
303  CONTINUE
      IF((X(J)-(XD+P2-OLAP)).LT.P)306,307
306  XD=X(J)-P2
      CALL PLOT(XD,YD,1)
      YD=Y(J-1)
      CALL PLOT(XD,YD,1)
      YD=Y(J)
      CALL PLOT(XD,YD,1)
      GO TO 301
307  XD=XD+P-OLAP
      CALL PLOT(XD,YD,1)
      YD=Y(J-1)
      CALL PLOT(XD,YD,1)
      YD=Y(J)
      CALL PLOT(XD,YD,1)
      GO TO 308
301  CONTINUE
$
C      PLOT THE LOWER HALF OF THE PATTERN
C
      CALL PLOT(0.,YD,3)
      CALL PLOT(0.,Y(5),3)
      DO 310 I = 2,NA,2
      J=4*I
      XD=X(J-3)+P2
      YD=Y(J-3)
      CALL PLOT(XD,YD,3)
      YD=Y(J-2)
      CALL PLOT(XD,YD,2)

      YD=Y(J)
      CALL PLOT(XD,YD,1)

C
C      IS THERE ROOM FOR A FULL STROKE DOWN
318  CONTINUE
      IF((X(J)-(XD+P2-OLAP)).LT.P)316,317
316  XD=X(J)-P2
      CALL PLOT(XD,YD,1)
      YD=Y(J-1)
      CALL PLOT(XD,YD,1)
      YD=Y(J)
      CALL PLOT(XD,YD,1)
      GO TO 310
317  XD=XD+P-OLAP
      CALL PLOT(XD,YD,1)
      YD=Y(J-1)
      CALL PLOT(XD,YD,1)
      YD=Y(J)
      CALL PLOT(XD,YD,1)
      GO TO 318

```

310 CONTINUE  
299 CALL PLOT (TRAVL,0.0,-3)

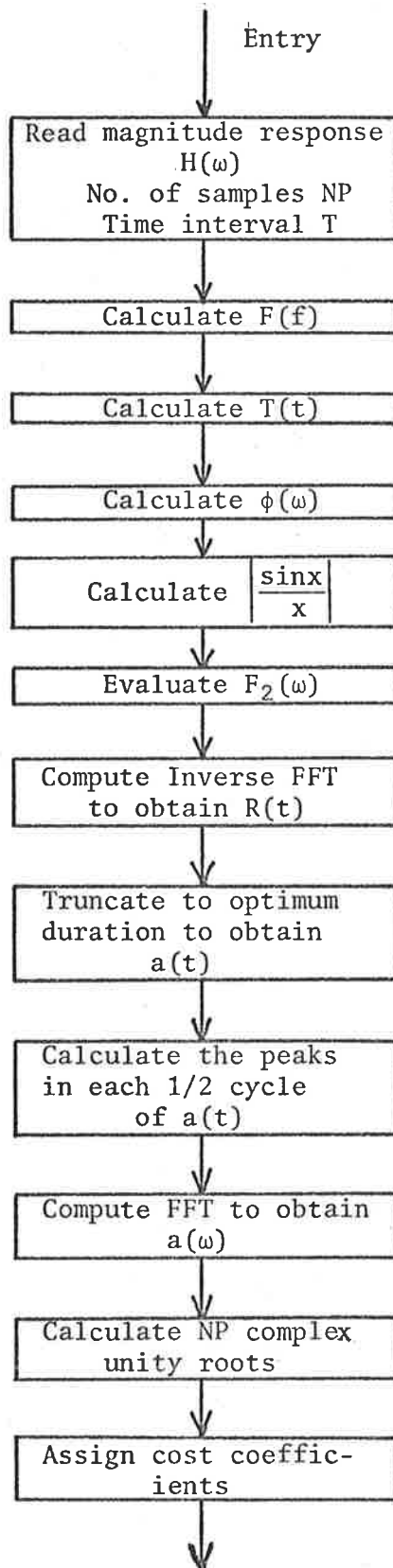
\*  
\* RETURN  
\* END

\*  
\* C DATA

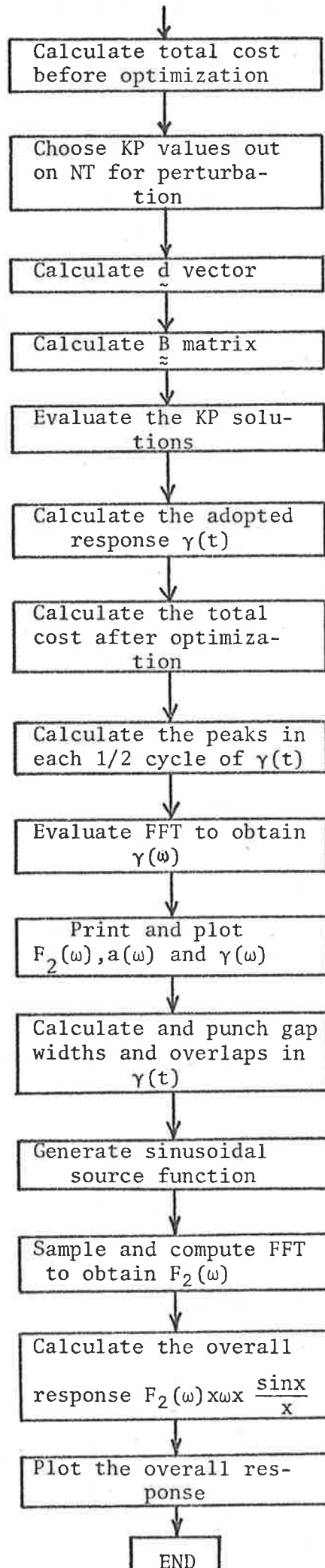
1.88512372E-06	1.89313488E-06	1.91876156E-06	1.93447697E-06	1.94985352E-06
1.96543983E-06	1.98185117E-06	2.00060391E-06	2.01591231E-06	2.02756200E-06
2.03879326E-06	2.05276495E-06	2.06747384E-06	2.08260876E-06	2.10756904E-06
2.12465599E-06	2.13977361E-06	2.15473762E-06	2.16962513E-06	2.18449391E-06
2.19933883E-06	2.21417214E-06	2.22894409E-06	2.24358746E-06	2.25788862E-06
2.27182227E-06	2.28586487E-06	2.31565768E-06	2.33051129E-06	2.34525509E-06
2.35997700E-06	2.37469657E-06	2.38941991E-06	2.40414893E-06	2.41883391E-06
2.43362430E-06	2.44836956E-06	2.46311843E-06	2.47785999E-06	2.49262315E-06
2.50737685E-06	2.52213001E-06	2.53688157E-06	2.55163044E-06	2.56637561E-06
2.58111609E-06	2.59585107E-06	2.61058009E-06	2.62530343E-06	2.64002300E-06
2.65474491E-06	2.66940871E-06	2.68434232E-06	2.71413513E-06	2.72817773E-06
2.74211138E-06	2.75641260E-06	2.77105591E-06	2.78582786E-06	2.80066117E-06
2.81550609E-06	2.83037487E-06	2.84526238E-06	2.86022139E-06	2.87534401E-06
2.89243096E-06	2.91719124E-06	2.93252616E-06	2.94723505E-06	2.96120674E-06
2.97243800E-06	2.98408719E-06	2.99939609E-06	3.01814883E-06	3.03456017E-06
3.05014648E-06	3.06552303E-06	3.08123844E-06	3.10686512E-06	3.11487628E-06
2.75535048E-03	-9.43871007E-03	8.96734137E-03	-8.47820581E-03	6.29943532E-03
-3.75882770E-03	1.98178834E-03	-1.02809836E-03	5.16117817E-04	-6.14024825E-04
1.35822219E-03	-2.01028413E-03	2.09570070E-03	-1.74732224E-03	2.73184471E-03
-5.05163922E-03	7.23430220E-03	-8.79953521E-03	9.53723730E-03	-9.31626295E-03
8.30056661E-03	-6.71360538E-03	4.98353474E-03	-3.46502319E-03	2.57139736E-03
-2.46273405E-03	4.84569429E-03	-4.61165751E-03	8.04001867E-03	-1.18323067E-02
1.59011937E-02	-2.01341206E-02	2.43962544E-02	-2.85365629E-02	3.23958900E-02
-3.58163244E-02	3.86510924E-02	-4.07741565E-02	4.20887074E-02	-4.27962510E-02
4.20887074E-02	-4.07741565E-02	3.86510924E-02	-3.58163244E-02	3.23958900E-02
-2.85365629E-02	2.43962544E-02	-2.01341206E-02	1.59011937E-02	-1.18323067E-02
8.04001867E-03	-4.61165751E-03	4.84569429E-03	-2.46273405E-03	2.57139736E-03
-3.46502319E-03	4.98353474E-03	-6.71360538E-03	8.30056661E-03	-9.31626295E-03
9.53723730E-03	-8.79953521E-03	7.23430220E-03	-5.05163922E-03	2.73184471E-03
-1.74732224E-03	2.09570070E-03	-2.01028413E-03	1.35822219E-03	-6.14024825E-04
5.16117817E-04	-1.02809836E-03	1.98178834E-03	-3.75882770E-03	6.29943532E-03
-8.47820581E-03	8.96734137E-03	-9.43871007E-03	2.75535048E-03	

A2 PROGRAM FILTER 2: OPTIMIZATION OF FILTER 1  
USING OPTIM METHOD

A2.1 Flow Chart



A9



## A2.2 Listing of FILTER 2

1

```

PROGRAM FILTER2(INPUT,OUTPUT,PUNCH)
PROGRAM P/09/1/P2
*
C   IN THE OPTIMIZATION PROCEDURE THE TOTAL COST T IS GIVEN BY,
C    $T = P \cdot B \cdot P + 2D \cdot P + K$ , WHERE P IS THE PERTURBATION VECTOR
C   THE ELEMENTS OF B MATRIX ARE EVALUATED THROUGH THE USE OF COMPLEX
*   ROOTS OF UNITY WHILE THE ELEMENTS OF D VECTOR ARE EVALUATED BY THE FFT
*   ROUTINE
*
C   NOTATION
*
C   NF NUMBER OF FINGERS IN APODISED TRANSDUCER, 70.
C   NP TOTAL NUMBER OF POINTS IN DISCRETE FOURIER TRANSFORM, 1024.
C   TIME TOTAL PERIODIC TIME 5 MICRO SECONDS.
C   DT SAMPLING TIME INCREMENT APROX. 5 NSEC.
C   DF SAMPLING FREQUENCY INCREMENT, 200 KHZ.
C   IFI INITIAL INDEX OF SPECIFIED FREQUENCY RESPONSE, 148; CORRESPONDING TO
*   29.4 MHZ.
C   IFF FINAL INDEX OF SPECIFIED FREQUENCY RESPONSE, 197 CORRESPONDING 39.2
*   MHZ.
C   ITI INITIAL INDEX OF ADOPTED TIME RESPONSE, 400, CORRESPONDING TO APROX 2
*   MICROSEC.
C   ITF FINAL INDEX OF ADOPTED TIME RESPONSE, 626. CORRESPONDING TO APROX 3
*   MICROSEC.
C   FO CENTRE FREQUENCY OF UNIFORM TRANSDUCER, APPROX 34.1 MHZ.
C   F2F SIGN FOR TRANSFORMING TIME TO FREQUENCY, -1.0
C   F2T SIGN FOR TRANSFORMING FREQUENCY TO TIME, +1.0
C   DIR, DIRECTION IN WHICH THE TRANSFORMATION IS CARRIED OUT, F2T OR T2F
C   DEL TIME OR FREQUENCY INCREMENT DEPENDING ON DIR IS T2F OR F2T
C   ZF(I) COMPLEX ARRAY USED TO TRANSFORM IN EITHER DIRECTION T2F OR F2T
C   MAG(I) MAGNITUDE RESPONSE OF THE FILTER.
C   MAGDB(I) MAGNITUDE RESPONSE IN DBS OF THE FILTER.
C   PHAS(I) PHASE RESPONSE OF APODISED TRANSDUCER.
C   XY(I) MAGNITUDE RESPONSE OF UNIFORM TRANSDUCER.
C   Y(I) MAGNITUDE RESPONSE OF APODIZED TRANSDUCER.
C   DBI(I) THE OVERALL MAGNITUDE RESPONSE OF THE FILTER
C   RT(I), TIME DOMAIN RESPONSE OF SPECIFIED RESPONSE
C   T(I) UNIFORM SAMPLED TIME ARRAY
C   FREQ(I) FREQUENCY SCALE OF THE SPECIFIED RESPONSE 29.4 MHZ TO 39.2 MHZ.
*
C   NOTATION FOR OPTIMIZATION PROCESS.
*
C   ZFI(I) SPECIFIED INPUT RESPONSE IN FREQUENCY DOMAIN 27.4 MHZ TO 41.2 MHZ.
C   ZFT(I) ADOPTED RESPONSE IN FREQUENCY DOMAIN 27.4 MHZ TO 41.2 MHZ.
C   C(I) COST COEFFICIENTS ASSIGNED IN THE FREQUENCY DOMAIN
C   NC NUMBER OF POINTS IN FREQUENCY DOMAIN USED IN THE OPTIMIZATION PROCEDURE
*   EQUAL TO OR GREATER THAN NF.
C   IP(I) TIME INDEX OF PEAK POINT ON ITH FINGER.
C   KP THE NUMBER OF PERTURBATIONS USED IN THE ADOPTED TIME RESPONSE
C   WN(I) THE NP COMPLEX ROOTS OF UNITY
C   IQ(I) AN ARRAY IN TIME DOMAIN WITH LOCATIONS WHERE THE PERTURBATION ARE
*   APPLIED
C   PT(I) THE PERTURBATION VECTOR
C   IF1 INITIAL INDEX IN FREQUENCY DOMAIN.
C   IF2 FINAL INDEX IN FREQUENCY DOMAIN.
C   B(I,J) A REAL (KP*KP) MATRIX ASSOCIATED WITH QUADRATIC TERMS OF THE
*   PERTURBATION IN THE QUADRATIC COST FUNCTION.
C   D(I) A REAL ONE DIMENSIONAL VECTOR OF KP ELEMENTS ASSOCIATED WITH FIRST
*   ORDER TERMS OF THE PERTURBATION IN THE QUADRATIC COST FUNCTION.
*
C   THIS PROGRAM IS MODIFIED TO PERTURB ANY NO OF POINTS WITH ANY NO
C   OF GIVEN COST COEFFICIENTS
C   SUBROUTINE LSSS IS USED IN OBTAINING THE SOLUTION
*   SUBROUTINE BMAT IS MODIFIED
C   * *****
C   * THIS PROGRAM ALSO REQUIRES SUBROUTINE PLT GIVEN IN APPENDIX A8 *
C   * *****
C   DECLARATIONS
*
C   DIMENSION DBI(100)
C   DIMENSION T(650)
C   DIMENSION IP(100),D(100),PT(100),IQ(100),KF(100),B(4000)
C   DIMENSION C(513)
C   DIMENSION WN(1024)
C   DIMENSION Y(50),XY(50)
C   DIMENSION MAG(50),MAGDB(52),PHAS(50),RT(1024)
C   DIMENSION FREQ(52)
C   COMPLEX ZF(1024)
C   DIMENSION ZFI(513),ZFT(513)
C   COMMON ZF,ZFI,ZFT,FREQ
C   REAL MAG ,MAGDB
*
C   BASIC PARAMETERS
*
C   NP = 1024
C   NQ = 50
C   TIME = 5.0E-06
C   IFI = 148
C   IFF = 197

```

```

ITI = 400
NF = 71
ITA = 1+(NP/2)
F2T = +1.0
T2F = -1.0
PI = 4.0*ATAN2(1.,1.)
SF = 1.0E+08
PAMP = 1.0
*
C DERIVED PARAMETERS
*
ITF = NP*2-ITI
DT = TIME/NP
DF = 1./TIME
FO = 1./(6.*DT)
DW = 2.*PI*CF
IF1 = 1
IF2 = 513
IFN = IF2-IF1+1
NF1 = NF+1
NC = IF2-IF1+1
*
C INPUT OF SPECIFIED RESPONSE
READ 1,(MAG(I),I=1,NQ)
1 FORMAT (8F10.5)
C FREQUENCY SCALE (29.4MHZ TO 39.2MHZ, CORRESPONDING TO 50 SAMPLING
C POINTS)
DO 2 I = 1,NQ
FREQ(I) = DF*(I+146)
2 CONTINUE
*
C CALCULATE THE TIME SAMPLES WHICH ARE NECESSARY IN PUNCHING ZERICROSSINGS
C AND OVERLAPS
DO 11 I = 1,650
T(I) = DT*(I-1)
11 CONTINUE
*
C CALCULATE THE RESPONSE IN DB SCALE
DO 3 I = 1,NQ
MAGDB(I) = 20.*ALOG10(0.01*MAG(I)) + 1.0
3 CONTINUE
C ASSUME ALINEAR PHASE RELATION
C PHAS = CONSTANT*OMEGA
DO 16 I = 1,NQ
PHAS(I) = -2.5E-06*DW*I
16 CONTINUE
C PRINT THE INPUT DATA
PRINT 4
4 FORMAT (1H1,40X*INPUT DATA*//6X*INDEX* 8X*FREQUENCY*11X*MAGNITUDE*
*8X*MAGNITUDE IN DB*13X*PHASE*//)
PRINT 18,(I,FREQ(I),MAG(I),MAGDB(I),PHAS(I),I=1,NQ)
18 FORMAT (110,4E20.5)
*
C PUNCH THE INPUT SPECIFIED RESPONSE
CALL DBPUNCH(NQ,FREQ,MAG)
*
DO 5 I = 1,NP
ZF(I) = CHPLX(0.,0.)
5 CONTINUE
C ASSUME A 9 FINGER TRANSDUCER AND CALCULATE IT'S RESPONSE USING
C SIN(X)/X FORMULA
C NO OF FINGERS = 2.*F+1, AND FOR 15 FINGERS F = 7
C CALCULATE THE MAXIMUM AMPLITUDES CORRESPONDING TO TO+ONE DB
C AMPLITUDES ARE CALCULATED IN THE SUBROUTINE SINEX AS FOLLOWS
C AMPLITUDE = 100.0*PAMP*SIN(X)/X
C F = 4.0
CALL SINEX(NQ,F,PAMP,FO,XY)
C CALCULATE THE RECEIVING TRANSDUCER RESPONSE BY DIVIDING INPUT
C SPECIFIED RESPONSE BY THE TRANSMITTING TRANSDUCER RESPONSE
C AND ALSO BY OMEGA FACTOR AND PRESCALE THE RESPONSE BY A FACTOR OF 10**8
DO 6 I = 1,NQ
Y(I) = MAG(I)/(XY(I)*DW*(I+146)*1.0E-08)
ZF(147+I) = CHPLX(Y(I)*COS(PHAS(I)),Y(I)*SIN(PHAS(I)))
IT = I+147
ZF(NP*2-IT) = CONJG(ZF(IT))
6 CONTINUE
C NOTE THAT FROM HERE ONWARDS FOR THE SYNTHESIS PURPOSE THIS RESPONSE
C WILL BE TAKEN AS THE SPECIFIED INPUT RESPONSE
DO 10 I = 1,NC
ZFI(I) = REAL(ZF(I+IF1-1))
10 CONTINUE
C PLOT THE SPECIFIED RESPONSE USING SUBROUTINE TRANS
ENTRY = 10.0
CALL TRANS2(IT,ITF,NP,NQ,PAMP,TIME,ENTRY,RT)
C TRANSFORM TO TIME DOMAIN
DEL = DF
DIR = F2T
CALL BFAST(ZF,10,DIR,DEL)
C NOTE THAT DEL HAS BEEN NOW CHANGED TO DT AND
C ALSO ZF NOW CONTAINS TRANSFORMED TIME DOMAIN RESPONSE

```



```

DO 9 I = 1, NP
RT(I) = REAL(ZF(I))
9 CONTINUE
*
C CALCULATE THE PEAKS OF THE ADOPTED TIME RESPONSE
CALL PEAKS3(ITI, ITF, NF, RT, IP)
*
*
C PRINT OF TIME DOMAIN TRANSFORM OF SPECIFIED RESPONSE
PRINT 101
101 FORMAT (1H1, 42X, *TIME DOMAIN TRANSFORM OF SPECIED RESPONSE*//)
CALL TPRINT(ITI, ITF, RT)
*
PUNCH 555, (RT(I), I=ITI, ITF)
555 FORMAT (6E13.3)
*
C EFFECT OF TRUNCATING THE TIME FUNCTION
*
ENTRY = 0.0
CALL TRANS2(ITI, ITF, NP, NQ, PAMP, TIME, ENTRY, RT)
*
*
C STORE THE FREQUENCY RESPONSE OF ADOPTED TIME RESPONSE IN ZFT(I)
DO 397 I = 1, NC
ZFT(I) = REAL(ZF(I+IFI-1))
397 CONTINUE
PRINT 398
398 FORMAT (1X, /40X*FREQUENCY RESPONSE OF ADOPTED TIME RESPONSE*//
*5X*INDEX*8X*FREQUENCY(MHZ)*8X*REAL PART*/)
PRINT 399, (I, FREQ(I), ZFT(I+IFI-1), I=1, NQ)
399 FORMAT (18, 2E20.5)
C CALCULATE THE OVERALL RESPONSE OF THIS TRUNCATED TIME FILTER
DO 556 I = 1, NQ
DBI(I) = REAL(ZF(I+147))*XY(I)*DW*(I+146)*1.0E-08
556 CONTINUE
CALL DBPUNCH(NQ, FREQ, DBI)
*
*
*****
* OPTIMIZATION PROCESS STARTS FROM HERE *
*****
*
PRINT 400
400 FORMAT (1H1, /50X*OPTIMIZATION PROCESS STARTS FROM HERE*//)
*
C SUBROUTINE CUNITY CALCULATES 1024 REAL PARTS OF OF COMPLEX UNITY ROOTS
CALL CUNITY(NP, WN)
*
*
C SELECT SUITABLE COST COEFFICIENTS
*
C COFF1 ARE THE VALUES OF COSTS BETWEEN IF1 AND IFI
C COFF2 ARE THE VALUES OF COSTS BETWEEN IFF AND IF2
COFF1 = 0.01
COFF2 = 0.01
CALL COST2(COFF1, COFF2, IF1, IFI, IFF, IF2, NC, C)
C CALCULATE THE TOTAL COST BEFORE OPTIMIZATION
CALL TCOST(NF, IF1, NC, C, T1)
*
*
KP = 86
*
DO 401 I = 1, 85
IQ(I) = ITI+I-1
401 CONTINUE
IQ(KP) = ITA
DO 402 I = 1, KP
IPI = IQ(I)
D(I) = RT(IPI)
402 CONTINUE
PRINT 403
403 FORMAT (1H0, 10X*RESPONSE AT WHICH THE PERTURBATIONS IS APPLIED*//)
PRINT 404, (I, IQ(I), D(I), I=1, KP)
404 FORMAT (5(2I6, E12.3))
DF = 1./TIME
C SUBROUTINE DVCT2 CALCULATES THE D ELEMENTS USING FFT ROUTINE
*
CALL DVCT2(KP, NP, NC, IF1, IF2, TIME, IQ, C, SF, D)
*
*
C SUBROUTINE BMAT CALCULATES THE ELEMENTS OF B USING FT ALGORITHMAM
DT = TIME/NP
KP1 = KP+1
CALL BMAT(KP, KP1, NP, IF1, IF2, IQ, C, WN, DT, NC, SF, B)
*
*
C SUBROUTINE SOLU CALCULATES THE SOLUTION USING SYMMETRIC MATRIX SUBROUTINE
LSSS
CALL SOLU2(KP, KF, D, B, SF, PT)
C RECONSTRUCTION OF RT(I)
DO 823 I = 1, KP
IPI = IQ(I)
RT(IPI) = RT(IPI)+PT(I)
RT(NP+2-IPI) = RT(IPI)
823 CONTINUE

```

```

      PRINT 824
824  FORMAT(1H1, /40X*TOTAL TIME RESPONSE AFTER ADDING PERTURBATIONS*//)
      CALL TPRINT(ITI,ITF,RT)
*
C    CHECK THE FREQUENCY RESPONSE WITH THIS PERT TIME FUNCTION
      ENTRY = 0.0
      CALL TRANS2(ITI,ITF,NP,NQ,PAMP,TIME,ENTRY,RT)
*
C    CALCULATE THE TOTAL FREQUENCY RESPONSE OF THE OPTIMIZED FILTER
      DO 558 I = 1,NQ
      DBI(I) = REAL(ZF(I+147))*XY(I)*DW*(I+146)*1.0E-08
558  CONTINUE
      CALL DBPUNCH(NQ,FREQ,DBI)
*
C    CALCULATE THE PEAKS OF THIS NEW TIME RESPONSE
      CALL PEAKS3(ITI,ITF,NF,RT,IP)
*
C    CALCULATE THE TOTAL COST AFTER OPTIMIZATION
      DO 829 I = 1,NC
      ZFT(I) = REAL(ZF(I+IF1-1))
829  CONTINUE
      CALL TCOST(NF,IF1,NC,C,I2)
*
      X = I2/T1
      X = 100.0*(1.0-X)
      PRINT 997,X
997  FORMAT (1H0,10X*PERCENTAGE REDUCTION IN COST =*F5.2)
*
C    GENERATE GAP FUNCTION FROM THIS OPTIMIZED TIME FUNCTION
*
C    ADD ONE FINGER ON EITHER SIDE TO ENSURE THAT THE END PERTURBATIONS ARE
C    INCLUDED IN THE ADOPTED RESPONSE
      ITI = ITI-3
      ITF = ITF+3
C    CALCULATE THE PEAKS IN THIS NEW LIMITS
      CALL PEAKS3(ITI,ITF,NF,RT,IP)
*
C    IF PINCH IS LESS THAN ONE THE ZERO CROSSINGS AND THE OVERLAPS ARE NOT
C    PUNCHED OTHERWISE THEY ARE
      PINCH = 2.0
*
      CALL PATERN(ITI,ITF,NP,NF,IP,RT,TIME,T,PINCH,NQ,PAMP)
*
C    OBTAIN OVERALL RESPONSE BY MULTIPLYING BY TRANSMITTING TRANSDUCER
C    RESPONSE , OMEGA FACTOR AND BY SCALE FACTOR
      DO 996 I = 1,NQ
      ZF(I+147) = ZF(I+147)*XY(I)*DW*(I+146)*1.0E-08
996  CONTINUE
      PRINT 995
995  FORMAT (1H1,10X*EXPECTED OVERALL RESPONSE OF THE FILTER*//)
C    PLOT THE RESPONSE USING TRANS2
      ENTRY = 10.0
      CALL TRANS2(ITI,ITF,NP,NQ,PAMP,TIME,ENTRY,RT)
*
998  STOP
      END

      SUBROUTINE DBPUNCH(NQ,FREQ,X)
*
      DIMENSION FREQ(2),X(2),Y(100),YY(100)
*
      XYZ = 0.0
      DO 1 I = 1,NQ
      XYZ = AMAX1(XYZ,ABS(X(I)))
1    CONTINUE
      DO 2 I = 1,NQ
      YY(I) = 100.*ABS(X(I))/XYZ
2    CONTINUE
      DO 3 I = 1,NQ
      Y(I) = 20.*ALOG10(0.01*YY(I))
3    CONTINUE
      PRINT 4
4    FORMAT (1H0,10X*FREQUENCY RESPONSE IN DB SCALE*//)
      PRINT 5,(I,FREQ(I),YY(I),Y(I),I=1,NQ)
5    FORMAT (110,3E20,3)
      PUNCH 6,(Y(I),I=1,NQ)
6    FORMAT (6E13,3)
      CALL PLT(NQ,1,Y)
*
      RETURN
      END

      SUBROUTINE LSSS(N,NS,A,B,IB,IC)
      DIMENSION A(1),B(1B,NS),H3(3),H1(5,2),IC(N)
      DOUBLE PRECISION Y
      DATA H1/100H LSSS ARRAYS DIMEN. INCORRECTLY OR INDICES.LE.0 LSS
      IS SINGULAR SYSTEM. NO UNIQUE SOLUTION. /

```

```

DATA H3/50M LSSS NEAR SINGULAR SYSTEM. CALC. CONTINUED. /
DATA EPS/1.E-15/
ID=1
IF(N,LE,0.OR,NS,LE,0.OR,N,GT,18) GO TO 41
NR=2
ND=N
5 NP=ID
J=ID
K=ND
X=ABS(A(ID))
L=ID+1
IC(NR)=0.
DO 6 I=NR,N
J=J+K
K=K-1
IF(X,GE,ABS(A(J))) GO TO 6
X=ABS(A(J))
IC(NR)=I
NP=L
6 L=L+1
IF(X,EQ,0.0) GO TO 40
IF(NP,EQ,ID) GO TO 7
II=1
32 IF(NR,EQ,2) GO TO 34
L=IC(NR)
J=NR-1
K=N-1
DO 33 I=3,NR
X=A(J)
A(J)=A(L)
A(L)=X
L=L+K
J=J+K
33 K=K-1
34 J=IC(NR)
DO 35 I=1,NS
X=B(NR-1,I)
B(NR-1,I)=B(J,I)
35 B(J,I)=X
L=NP
NP=L+1
IF(ND,LE,1) GO TO 38
NP=NP-1
J=ID
K=ND
DO 37 I=1,ND
X=A(J)
A(J)=A(L)
A(L)=X
K=K-1
J=J+1
IF(J,GT,NP) K=1
37 L=L+K
38 X=A(ID)
A(ID)=A(NP)
A(NP)=X
IF(II,EQ,2) GO TO 29
7 LL=ND
N1=ID+ND
J=N1+ND-2
K=ID+1
DO 10 NP=NR,N
L=K
X=A(K)/A(ID)
DO 8 I=N1,J
A(I)=A(I)-X*A(L)
8 L=L+1
DO 9 I=1,NS
9 B(NP,I)=B(NP,I)-X*B(NR-1,I)
LL=LL-1
N1=N1+LL
J=N1+LL-2
10 K=K+1
ID=ID+ND
ND=ND-1
NR=NR+1
IF(NR,LE,N) GO TO 5
X=A(ID)
IF(ABS(X).LT,EPS) CALL LABRT(1,H3,0)
NR=N
N1=N-1
11 LL=N-NR
IF(LL,EQ,0) GO TO 14
DO 13 K=1,NS
J=ID+1
Y=DBLE(B(NR,K))
DO 12 I=NR,N1
Y=Y-DBLE(A(J))*DBLE(B(I+1,K))
12 J=J+1
13 B(NR,K)=SNGL(Y)

```

```

14 X=A(ID)
DO 15 I=1,NS
15 B(NR,I)=B(NR,I)/X
NR=NR-1
ND=ND+1
ID=ID-ND
IF(NR.GT.0) GO TO 11
ID=(N*(N+1))/2-2
ND=2
NR=N
DO 30 N1=2,N
IF(IC(NR).EQ.0) GO TO 29
L=IC(NR)
NP=ID+L-NR+1
II=2
GO TO 32
29 ND=ND+1
ID=ID-ND
30 NR=NR-1
RETURN
40 ID=2
41 CALL LABRT(1,H1(1,ID),0)
RETURN
END
SUBROUTINE LABRT(ISW,LHOL,INX)
DIMENSION LHOL(5)
LOGICAL PS,TS
IF((ISW.EQ.0).OR.(ISW.GT.5))RETURN
GOTO(1,2,3,4,5),ISW
DATA NP/10/,PS/.TRUE./,TS/.FALSE./
1 IF(PS.AND.(NP.GT.0)) PRINT 27,LHOL,INX
27 FORMAT(1H0,9X,5A10,3X,06)
NP=NP-1
IF(TS) CALLEXIT
RETURN
2 PS=.FALSE.
RETURN
3 PS=.TRUE.
NP=INX
RETURN
4 TS=.TRUE.
RETURN
5 TS=.FALSE.
RETURN
END

SUBROUTINE SINEX(NQ,F,PAMP,FO,XY)
*
* SUBROUTINE SINEX CALCULATES TRANSMITTING TRANSDUCER FREQUENCY RESPONSE
* WITH CENTRE FREQUENCY FO AND FOR A UNIFORM NO FINGERS EQUAL TO 2.*F+1.
*
DIMENSION XY(50),XZ(50)
DIMENSION FREQ(52)
DIMENSION ZFI(513),ZFT(513)
COMPLEX ZF(1024)
COMMON ZF,ZFI,ZFT,FREQ

PRINT 1
1 FORMAT (1H1,40X*FREQUENCY RESPONSE OF TRANSMITTING TRANSDUCER*//)
PI = 4.0*ATAN2(1.,1.)
MF = 2.*F+1.
PRINT 3,MF
3 FORMAT (1H0,10X*NUMBER OF FINGERS =*15/)
PRINT 4,FO
4 FORMAT (1H0,10X*CENTRE FREQUENCY IN HZ =*E10.2/)
DO 17 I = 1,NQ
X = F*PI*((FREQ(I)-FO)/FO)
IF(X.EQ.0.0)X = 100.0*PAMP
XY(I) = 100.0*PAMP*SIN(X)/X
17 CONTINUE
XYZ = 0.0
DO 18 I = 1,NQ
XYZ = AMAX1(ABS(XY(I)),XYZ)
18 CONTINUE
DO 19 I = 1,NQ
XZ(I) = 20.*ALOG10(ABS(XY(I))/XYZ)+1.0
19 CONTINUE
PRINT 20
20 FORMAT (6X*INDEX*8X*FREQUENCY*11X*MAGNITUDE*8X*MAGNITUDE IN DB*//)
PRINT 21,(I,FREQ(I),XY(I),XZ(I),I=1,NQ)
21 FORMAT (110,JE20.5)
CALL PLT(NQ,1,XY)
PRINT 22
22 FORMAT (1H0,10X*FREQUENCY RESPONSE IN LINEAR SCALE*//)
RETURN
END

SUBROUTINE TRANS2(ITI,ITF,NP,NQ,PAMP,TIME,ENTRY,RT)

```

```

*
C   SUBROUTINE TRANS DOES THE FOLLOWING OPERATIONS
*
C   (1) CALCULATES THE ADOPTED RESPONSE BY TRUNCATING THE IMPULSE
C   RESPONSE TO THE DESIRED LIMITS, IT1,ITF.
*
C   (2) CALCULATES THE FREQUENCY RESPONSE OF THIS TRUNCATED TIME
C   RESPONSE USING FFT ROUTINE
*
C   (3) CALCULATES THE RELATIVE MAGNITUDE AND PHASE RESPONSES IN THE
C   SPECIFIED RANGE OF FREQUENCY LIMITS.
*
C   (4) PLOTS THE FREQUENCY RESPONSE IN RELATIVE SCALE AND IN DB SCALE
*
C   (5) IF ENTRY IS EQUAL TO ZERO IT TRANSFORMS THE GIVEN TIME RESPONSE
C   TO FREQUENCY RESPONSE AND THEN PLOTS IN LINEAR SCALE AS WELL AS IN DBSCALE
*
C   (6) IF ENTRY IS NOT EQUAL TO ZERO IT PLOTS ONLY THE GIVEN FREQUENCY
C   RESPONSE IN LINEAR SCALE AS WELL AS IN DB SCALE
*
C   PAMP IS THE FACTOR BY WHICH MAXIMUM AMPLITUDES IN LINEAR SCALE
C   WOULD REPRESENT ABOVE 100 UNITS
*
DIMENSION RT(1024)
DIMENSION ZTA(52),ZT1(52),ZT2(52),ZT3(52)
DIMENSION FREQ(52)
COMPLEX ZF(1024)
DIMENSION ZF1(513),ZFT(513)
COMMON ZF,ZF1,ZFT,FREQ
*
DT = TIME/NP
T2F = -1.0
F2T = +1.0
IF(ENTRY)499,488,499
488 CONTINUE
DO 500 I = 1,NP
ZF(I) = CMPLX(0.,0.)
500 CONTINUE
DO 503 I = IT1,ITF
ZF(I) = CMPLX(RT(I),0.)
503 CONTINUE
C   TRANSFORM TO FREQUENCY DOMAIN
DEL = DT
DIR = T2F
CALL BFAST(ZF,10,DIR,DEL)
C   NOTE THAT DEL HAS NOW BEEN CHANGED TO DF
C   ALSO ZF NOW CONTAINS TRANSFORMED FREQUENCY DOMAIN RESPONSE
499 PRINT 5
5   FORMAT(1X,/,40X*FREQUENCY RESPONSE IN COMPLEX FORM*//
*5X*INDEX*8X*FREQUENCY(MHZ)*8X*REAL PART*11X*IMAG PART*//)
PRINT 4,(I,FREQ(I),ZF(I+147)),I=1,NQ)
4   FORMAT (18,3E20.5)
XYZ = 0.0
DO 504 I = 1,NQ
ZTA(I) = CABS(ZF(I+147))
XYZ = AMAX1(ZTA(I),XYZ)
504 CONTINUE
DO 505 I = 1,NQ
ZT1(I) = 20.*ALOG10(ZTA(I)/XYZ)+1.0
ZT2(I) = 100.0*PAMP*ZTA(I)/XYZ
X1 = REAL(ZF(I+147))
X2 = AIMAG(ZF(I+147))
ZT3(I) = ATAN2(X2,X1)
505 CONTINUE
PRINT 623
623 FORMAT (1H1,20X*FREQUENCY RESPONSE IN THE DESIRED RANGE 29.4 TO 39
*.2 MHZ*//
C5X*5.NQ*7X*FREQUENCY*7X*RELATIVE MAGNITUDE*3X*MAGNITUDE IN DB*10X*
CPHASE*//)
PRINT 624,(I,FREQ(I),ZT2(I),ZT1(I),ZT3(I)),I=1,NQ)
624 FORMAT (18,4(E15.3,5X))
DO 625 I = 1,NQ
IF(ZT1(I).LE.-50.)ZT1(I)=-49.5
625 CONTINUE
CALL PLT(NQ,1,ZT2)
PRINT 626
626 FORMAT (1X,/,40X*PLOT OF FREQUENCY VS RELATIVE MAGNITUDE*//)
CALL PLT(NQ,1,ZT1)
PRINT 627
627 FORMAT (1X,/,40X*PLOT OF FREQUENCY VS MAGNITUDE IN DBS*//)
RETURN
END

SUBROUTINE PEAKS3(IT1,ITF,NF,RT,IP)
*
C   SUBROUTINE PEAKS CALCULATES THE + AND - PEAKS IN EACH HALF CYCLE
C   OF THE TRUNCATED TIME RESPONSE. IT ALSO CALCULATES THE MAGNITUDE
C   OF THESE PEAKS, NORMALISED WITH RESPECT TO THE MAXIMUM PEAK VALUE
C   OF 100 UNITS

```

```

      DIMENSION IP(NF),RT(2)
      DIMENSION P(100),D(100)

      PRINT 820
820  FORMAT (1X/X*PEAK AMPLITUDES AND THEIR LOCATIONS IN THE ADOPTED T
      *IME RESPONSE*/)
      M = 0
      I = 1
      J = 1
      3  X = RT(I)*RT(I+1)
      IF(X)1,1,2
      2  I = I+1
      IF(1.GE.I*TF)GO TO 1
      GO TO 3
      1  K = I
      Y = 0.0
      DO 4 L = J,K
      Y = AMAX1(Y,ABS(RT(L)))
      4  CONTINUE
      DO 5 L = J,K
      IF(Y.EQ.ABS(RT(L)))GO TO 6
      5  CONTINUE
      6  M = M+1
      IP(M) = L
      D(M) = RT(L)
      IF(1.GE.I*TF)GO TO 814
      I = I+1
      J = I
      GO TO 3
814  CONTINUE
C    NORMALIZE THE PEAK AMPLITUDES
      XYZ = 0.0
      DO 816 I = 1,M
      XYZ = AMAX1(ABS(D(I)),XYZ)
816  CONTINUE
      DO 817 I = 1,M
      P(I) = 100.*D(I)/XYZ
817  CONTINUE
      PRINT 818
818  FORMAT (8X,*PEAK*5X,*PEAK*12X,*PEAK*8X,*NORMALISED*/
      *8X,*INDEX*4X,*POINT*9X,*MAGNITUDE*5X,*PEAK MAGNITUDE*/)
      PRINT 815,(I,IP(I),D(I),P(I),I=1,M)
815  FORMAT(2I10,E20.5,F15.5)
      NF = M
      RETURN
      END

```

```

SUBROUTINE COST2(COFF1,COFF2,IF1,IF1,IFF,IF2,NC,C)

```

```

*
C    ARBITRARY CHOICE OF COST COEFFICIENTS ARE MADE IN THIS SUBROUTINE
*
      DIMENSION C(NC)
      DIMENSION FREQ(52)
      COMPLEX ZF(1024)
      DIMENSION ZFI(513),ZFT(513)
      COMMON ZF,ZFI,ZFT,FREQ

      DO 1 I = IF1,IF1
      C(I+1-IF1) = COFF1
      1  CONTINUE
      DO 2 I = IFF,IF2
      C(I+1-IF1) = COFF2
      2  CONTINUE
      DO 3 I = IF1,IFF
      X = ZFI(I)
      X = ABS(X)
      X = X**0.65
      IF(X.EQ.0.)X=0.04
      C(I+1-IF1) = 1./X
      3  CONTINUE
      6  PRINT 826
826  FORMAT (1X,/55X*COST COEFFICIENTS ARE*/)
      CALL TPRINT(1,NC,C)
      RETURN
      END

```

```

SUBROUTINE TCOST(NF,IF1,NC,C,TAU)

```

```

*
C    SUBROUTINE TCOST CALCULATES THE TOTAL COST ASSOCIATED WITH AN
C    ADOPTED RESPONSE AND THE SPECIFIED RESPONSE WITH AN ARBITRARY
C    GIVEN COST COEFFICIENTS
*
C    THE VARIABLES NEEDED ARE
C    C, THE COST COEFFICIENTS ASSOCIATED WITH THE NF FINGERS
C    ZFI, SPECIFIED INPUT RESPONSE
C    ZFT, ADOPTED RESPONSE
C    TAU, THE TOTAL COST

```

```

DIMENSION C(NC)
DIMENSION FREQ(52)
COMPLEX ZF(1024)
DIMENSION ZFI(S13),ZFT(S13)
COMMON ZF,ZFI,ZFT,FREQ

DATA TB/1.0/

SUM = 0.0
DO 7 I = 1,NC
X = ZFT(I-1+IF1)-ZFI(I-1+IF1)
SUM = SUM + (X*X)*C(I)
7 CONTINUE
TAU = SUM
TB = TB+1.0
IF(TB.EQ.2.0)GO TO 2
GO TO 4
2 PRINT 3,TAU
3 FORMAT (1X,/5X,*TOTAL COST BEFORE OPTIMIZATION =*E16.8)
GO TO 6
4 PRINT 5,TAU
5 FORMAT (1X,/5X,*TOTAL COST AFTER OPTIMIZATION =*E16.8)
6 RETURN
END

```

```

SUBROUTINE DVCT2(NF,NP,NC,IF1,IF2,TIME,IP,C,SF,D)
DIMENSION D(NF)
DIMENSION IP(NF)
DIMENSION C(NC)
DIMENSION FREQ(52)
COMPLEX ZF(1024)
DIMENSION ZFI(S13),ZFT(S13)
COMMON ZF,ZFI,ZFT,FREQ

ITA = 1*NP/2
IF(IF1.GT.1)GO TO 7
DO 1 I = 1,IF1
X = ZFT(I)-ZFI(I)
ZF(I) = CMPLX(X,0.0)
1 CONTINUE
DO 5 I = IF2,ITA
X = ZFT(I)-ZFI(I)
ZF(I) = CMPLX(X,0.0)
5 CONTINUE
DO 2 I = IF1,IF2
X = C(I+1-IF1)*(ZFT(I)-ZFI(I))
ZF(I) = CMPLX(X,0.0)
2 CONTINUE
DO 6 I = 2,ITA
ZF(NP+2-I) = ZF(I)
6 CONTINUE
GO TO 8
7 DO 9 I = 1,NP
ZF(I) = (0.,0.)
9 CONTINUE
DO 10 I = IF1,IF2
ZF(I) = C(I+1-IF1)*(ZFT(I)-ZFI(I))
ZF(NP+2-I) = ZF(I)
10 CONTINUE
8 CONTINUE
DF = 1./TIME
CALL BFAST(ZF,10,+1.,DF)
DF = 1./TIME
DT = TIME/NP
X = SF*DT/(2.*SF)
DO 3 I = 1,NF
IPI = IP(I)
D(I) = X*(REAL(ZF(IPI)))
3 CONTINUE
PRINT 4
4 FORMAT (1H0,14X*THE ELEMENTS OF D VECTOR ARE GIVEN BY*/
SCALE UPWARDS THE ELEMENTS OF D BY A FACTOR OF SF
CALL TPRINT(1,NF,0)
RETURN
END

```

```

SUBROUTINE CUNITY(NP,WN)
DIMENSION WN(1024)
COMPLEX WX
COMPLEX W
COMPLEX ROOTS OF UNITY
PI = 4.0*ATAN2(1.,1.)
DO 816 I = 1,256
W = CMPLX(0.,-2.*PI*(I-1)/NP)
WX = CEXP(W)
WR = REAL(WX)
WI = AIMAG(WX)

```





```

COMMON /TAB/TC(10),TS(10)
PI=4.0*ATAN2(1.0,1.0)
DOL1=1,M
TC(1)=COS(PI/(2**(I-1)))
TS(1)=SIN(PI/(2**(I-1)))
1 RETURN
END
SUBROUTINE CON(M)
INTEGER A,T
COMMON /PERM/ A(1024)
N=2**M
NV2=N/2
NM1=N-1
J=1
DOL1=1,N
1 A(I)=I
DO 7 I=1,NM1
IF(I.GE.J)GOTO5
T=A(J)
A(J)=A(I)
A(I)=T
5 K=NV2
6 IF(K.GE.J)GOTO7
J=J-K
K=K/2
GOTO 6
7 J=J+K
RETURN
END

SUBROUTINE BMAT(NF,NF1,NP,IF1,IF2,IP,C,WN,DT,NC,SF,B)
DIMENSION WN(1024)
DIMENSION B(2)
DIMENSION IP(NF)
DIMENSION C(NC)
C CALCULATE THE MATRIX ELEMENTS
XNP = NP
ST = SF*DT
ST = ST*ST*2.0
C MULTIPLY THE B ELEMENTS BY 2 FOR SYMMETRY REASONS
IJ = 0
DO 817 I = 1,NF
DO 818 J = I,NF
IJ = IJ+1
X = IP(I)-1
Y = IP(J)-1
A = 0.
IF(X.EQ.Y)GO TO 1
DO 819 K = IF1,IF2
Z = K-1
CALL ARGU(XNP,X,Z,IP1)
CALL ARGU(XNP,Y,Z,IP2)
A = A + WN(IP1)*WN(IP2)*C(K-IF1+1)
819 CONTINUE
B(IJ) = ST*A
GO TO 818
1 DO 2 K = IF1,IF2
Z = K-1
CALL ARGU(XNP,X,Z,IP1)
A = A + WN(IP1)*WN(IP1)*C(K-IF1+1)
2 CONTINUE
B(IJ) = A*ST
818 CONTINUE
817 CONTINUE
C SCALE UPWARDS THE ELEMENTS OF H BY A FACTOR OF SF*SF
PRINT 815 ,IJ
815 FORMAT (1H0,10X*NO OF UPPER TRIANGULAR ELEMENTS IN B =*110/)
RETURN
END
SUBROUTINE ARGU(XNP,R,S,IPK)
XX = (R*S)/XNP
YY = INT(XX)
ZZ = (XX-YY+5.0E-07)*XNP
IPK = INT(ZZ)+1
RETURN
END

SUBROUTINE SOLU2(NF,NF1,D,B,SF,PT)
DIMENSION D(NF),PT(NF)
DIMENSION R(2)
DIMENSION NF1(NF)
*
C PRINT FIRST ROW OF TRIANGULAR MATRIX B
PRINT 1
1 FORMAT(1H0,10X*FIRST ROW OF B MATRIX=/)
CALL TPRINT(1,NF,B)

```

```

11
TABL 20
TABL 30
TABL 40
TABL 50
TABL 60
TABL 70
TABL 80
CON 10
CON 20
CON 30
CON 40
CON 50
CON 60
CON 70
CON 80
CON 90
CON 100
CON 110
CON 120
CON 130
CON 140
CON 150
CON 160
CON 170
CON 180
CON 190
CON 200
CON 210
CON 220

```

```

C   CALCULATE THE SOLUTION USING SUBROUTINE LSSS
C   SUBROUTINE LSSS REQUIRES ONLY THE TRIANGULAR ELEMENTS OF THE
C   SYMMETRIC MATRIX
*
*   CALL LSSS(NF,1,B,D,NF,NF1)
*
C   THE INPUT MATRIX B IS DESTROYED
C   NOTE THE SOLUTION IS RETURNED IN D
*
DO 3 I = 1,NF
PT(I) = -SF*D(I)
3 CONTINUE
C   MULTIPLY THE LAST SOLUTION BY 2 FOR SYMMETRY REASONS
PT(NF) = 2.0*PT(NF)
C   NOTE THE SOLUTION ALSO NEED TO BE SCALED UPWARDS BY A FACTOR OF SF
*
PRINT 4
4 FORMAT (1H0,10X*SOLUTION OF PERTURBATION VECTOR IS GIVEN BY*/)
CALL TPRINT(1,NF,PT)
RETURN
END

SUBROUTINE TPRINT(N1,N2,RT)
DIMENSION VOP(10)
DIMENSION RT(N2)
DO 104 I = N1,N2,10
DO 102 J = 1,10
VOP(J) = 0.0
IF((I+J-1).LE.N2)VOP(J) = RT(I+J-1)
102 CONTINUE
PRINT 103,I,(VOP(J),J=1,10)
103 FORMAT (1X,I4,3X,10E12.3)
104 CONTINUE
RETURN
END

SUBROUTINE PATERN(ITI,ITF,NP,NF,IP,RT,TIME,T,PINCH,NQ,PAMP)
*
C   SUBROUTINE PATERN CALCULATES THE GAP FUNCTION FROM THE ZERO CROSSINGS
C   AND THE PEAK AMPLITUDES
*
DIMENSION IP(NF),RT(2),T(2)
DIMENSION OV MID(100)
DIMENSION ZRCR(100),ZRCM(100),DIFF(100)
DIMENSION FREQ(52)
COMPLEX ZF(1024),ZFI(50),ZFT(50)
COMMON ZF,ZFI,ZFT,FREQ
COMMON/SUB/ZRCR,ZRCM,DIFF
*
PRINT 6
6 FORMAT (1H1,40X*GENERATION OF GAP FUNCTION STARTS FROM HERE*/)
*
C   CALCULATES THE ZEROCROSSINGS OF THE ADOPTED RESPONSE IN THE INTERVAL
C   ITI AND ITF
C   ALSO CALCULATE THE GAP WIDTHS AND THE MIDDLE POINTS OF THESE GAPWIDTHS
*
CALL ZEROCR(ITI,ITF,NP,NF,RT,T)
*
C   CALCULATES THE OVERLAPS OF THE GAP FUNCTION
C   OVERLAPS ARE PROPORTIONAL TO THE AREA OF GAPWIDTH MULTIPLIED BY PEAK
C   AMPLITUDE IN THAT GAP AND THE ACTUAL
C   THE PEAK AMPLITUDE IS CALCULATED BY A PARABOLIC CURVE FITTING
*
DT = TIME/NP
CALL AREA1(RT,DT,OV MID,PINCH)
C   VERIFY THE FREQUENCY RESPONSE OF THIS GAP FUNCTION USING APPROXIMATE
C   ANALYSIS METHOD
CALL ANALYSE(ITI,ITF,NP,NF,TIME,OV MID,RT,NQ,PAMP)
622 RETURN
END

SUBROUTINE ZEROCR(ITI,ITF,NP,NF,RT,T)
*
DIMENSION RT(2),T(2)
DIMENSION ZRCR(100),ZRCM(100),DIFF(100)
DIMENSION FREQ(52)
COMPLEX ZF(1024)
DIMENSION ZFI(513),ZFT(513)
COMMON ZF,ZFI,ZFT,FREQ
COMMON/SUB/ZRCR,ZRCM,DIFF
*
IZ = 0
DO 600 I = ITI,ITF
IF(I.GE.ITF)GO TO 603
X = RT(I)*RT(I+1)
IF(X)601,601,600
601 SLOP = (RT(I+1)-RT(I))/(T(I+1)-T(I))

```

```

CONST = RT(I)-SLOP*T(I)
IZ = IZ+1
ZRCR(IZ) = -CONST/SLOP
600 CONTINUE
603 CONTINUE
PRINT 602, IZ, NF
602 FORMAT (1H0, 10X*NO OF ZERO CROSSINGS =*15, 10X*NO OF PEAKS =*15//)
*
C   CALCULATE THE GAPWIDTHS BETWEEN THE FINGERS
C   THAT IS THE DIFFERENCE BETWEEN THE ZERO CROSSINGS
*
LSTZ = IZ
JSTZ = LSTZ-1
DO 702 I = 1, JSTZ
DIFF(I) = ZRCR(I+1)-ZRCR(I)
702 CONTINUE
C   LOCATE MID POINTS OF ZERO CROSSINGS
DO 605 I = 1, JSTZ
ZRCM(I) = (ZRCR(I)+ZRCR(I+1))/2.
605 CONTINUE
RETURN
END

SUBROUTINE AREA1(RT, NF, DT, OVMID, PINCH)
*
C   SUBROUTINE AREA1 CALCULATES THE OVERLAPS ASSUMING THAT OVERLAPS ARE
C   PROPORTIONAL TO THE TRIANGULAR AREA BETWEEN THE ZERO CROSSINGS AND ALL THE
C   SAMPLING POINTS BETWEEN THESE ZERO CROSSINGS
*
DIMENSION RT(2)
DIMENSION OVMID(100), YNOR(100)
DIMENSION ZRCR(100), ZRCM(100), DIFF(100)
DIMENSION FREQ(52)
COMPLEX ZF(1024)
DIMENSION ZFI(513), ZFT(513)
COMMON ZF, ZFI, ZFT, FREQ
COMMON /SUB/ZRCR, ZRCM, DIFF
*
NFL = NF-1
NFM = NF-2
DO 1 I = 1, NFM
AREA = 0.0
IFP = 2+INT(ZRCR(I)/DT)
LFP = 1+INT(ZRCR(I+1)/DT)
AREA = AREA + (DT*(IFP-1)-ZRCR(I))*RT(IFP)/2.0
AREA = AREA + (ZRCR(I+1)-DT*(LFP-1))*RT(LFP)/2.0
IF(IFP.EQ.LFP)GO TO 3
M1 = IFP
M2 = M1+1
2 AREA = AREA + (RT(M1)+RT(M2))*DT/2.0
M1 = M1+1
M2 = M2+1
IF(M1.EQ.LFP)GO TO 3
GO TO 2
3 OVMID(I) = AREA
1 CONTINUE
*
C   NORMALISE THE OVERLAPS WITH RESPECT TO THE PEAK AMPLITUDES
XYZ = 0.0
DO 8 I = 1, NFM
XYZ = AMAX1(XYZ, ABS(OVMID(I)))
8 CONTINUE
DO 9 I = 1, NFM
YNOR(I) = 100.0*OVMID(I)/XYZ
9 CONTINUE
*
PRINT 4
4 FORMAT(1H0* INDEX*9X*ZERO CROSSINGS*13X*GAPWIDTHS*17X*OVERLAPS*10X
C*NOR. OVERLAPS*/)
PRINT 5, (I, ZRCR(I), DIFF(I), OVMID(I), YNOR(I), I=1, NFM)
5 FORMAT (15, 3E25.8, F16.2)
PRINT 6, NFL, ZRCR(NFL)
6 FORMAT (15, E25.8)
IF(PINCH.LT.1.0)GO TO 10
PUNCH 7, (ZRCR(I), I=1, NFL)
PUNCH 7, (OVMID(I), I=1, NFM)
7 FORMAT (5E16.8)
10 RETURN
END

SUBROUTINE ANALYSE(ITI, ITF, NP, NF, TIME, OVMID, RT, NQ, PAMP)
*
C   SUBROUTINE ANALYSE CALCULATES THE FREQUENCY RESPONSE OF THE GAP FUNCTION
C   USING APPROXIMATE ANALYSIS METHOD
*
DIMENSION RT(2)
DIMENSION OVMID(100), GAP(300), OVLAP(100)
DIMENSION ZRCR(100), ZRCM(100), DIFF(100)

```

```

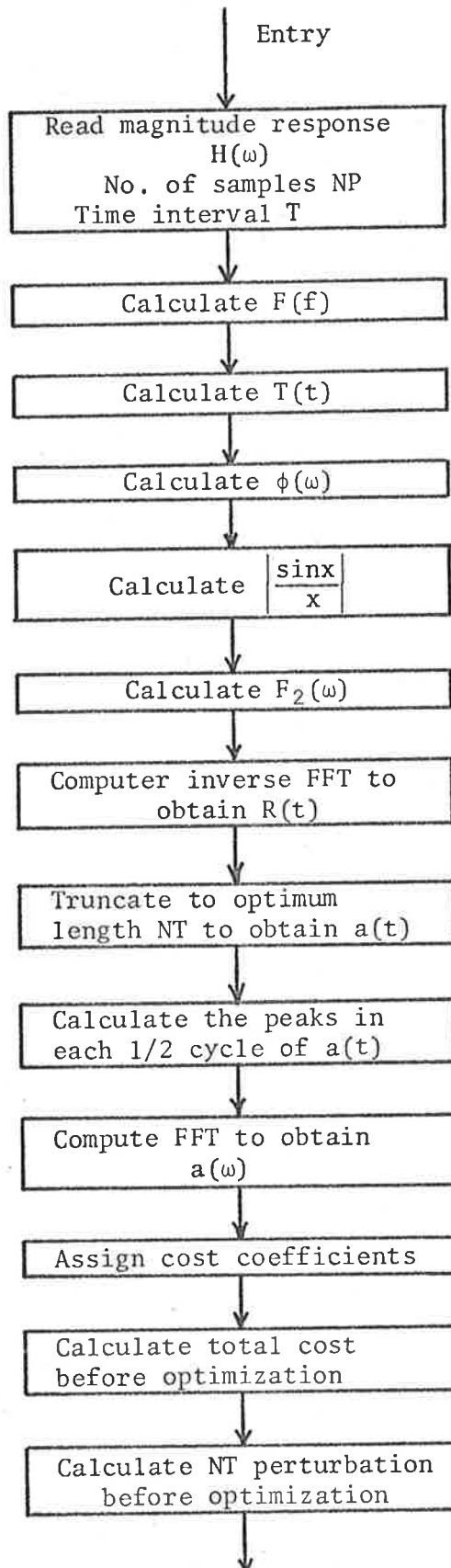
DIMENSION FREQ(52)
COMPLEX ZF(1024)
DIMENSION ZFI(513),ZFT(513)
COMMON ZF,ZFI,ZFT,FREQ
COMMON/SUB/ZRCR,ZRCM,DIFF
*
PI = 4.0*ATAN2(1.,1.)
DT = TIME/NP
NFL = NF-1
NFM = NF-2
C   CALCULATE THE PEAK AMPLITUDES BY DIVIDING OVERLAPS BY GAPWIDTHS
*
DO 620 I = 1,NFM
OVLAP(I) = OVMIID(I)/DIFF(I)
620 CONTINUE
*
C   LOCATE THESE PEAK AMPLITUDES AT THE MIDDLE OF THE GAPWIDTHS AND FIT
C   QUARTER SINE WAVE BETWEEN THE ZERO CROSSINGS AND THE PEAK AMPLITUDES
C   AND CALCULATE THE AMPLITUDES AT THE SAMPLING POINTS OF DT
*
M = ZRCR(1)/DT
MM = 0
DO 613 I = 1,NFM
614 M = M+1
Z = M*DT
IF(Z.LE.ZRCR(I))GO TO 614
IF(Z.GE.ZRCR(I+1))GO TO 615
MM = MM+1
ARG = PI*(Z-ZRCR(I))/DIFF(I)
GAP(MM) = OVLAP(I)*SIN(ARG)
GO TO 614
615 M = M-1
613 CONTINUE
LVAL = MM
PRINT 619
619 FORMAT (1H0,40X*SAMPLED RESPONSE OF THE GAP FUNCTION*//)
CALL TPRINT(1,LVAL,GAP)
C   MAP ON THE SAMPLES IN THE INTERVAL ITI TO ITF
C   CALCULATE ITI AND NOTE THAT TO GET RIGHT SIDE SAMPLING POINT WE HAVE TO
C   ADD 2 TO THE INTEGER RESULT BECAUSE OF THE FACT T(I) = DT*(I-1)
ITI = 2+INT(ZRCR(1)/DT)
DO 616 I = 1,LVAL
RT(I+ITI-1) = GAP(I)
616 CONTINUE
ITF = ITI+LVAL-1
C   PRINT THE SAMPLED TIME RESPONSE IN THE INTERVAL ITI ITF
PRINT 617
617 FORMAT (1H0,10X*TIME RESPONSE OF ANALISED GAP FUNCTION SHIFTED IN
CTIME SO THAT IT IS SYMMETRICAL OVER T/2*//)
CALL TPRINT(ITI,ITF,RT)
C   CALCULATE THE FREQUENCY RESPONSE USING FFT ROUTINE
ENTRY = 0.0
CALL TRANS2(ITI,ITF,NP,NQ,PAMP,TIME,ENTRY,RT)
RETURN
END

*
C   DATA
*
1.00    3.5    7.5    11.5    14.5    18.0    16.0    7.5
1.0     8.0    15.5   24.5   35.5   48.0    59.0    70.0
79.0   86.0   91.5   95.5   97.5   99.0   100.0   100.0
100.0  99.5   98.5   97.0   95.0   91.5   87.0    81.5
75.0   69.0   61.0   54.0   46.0   39.0   31.5   24.5
17.5   12.5   8.5    5.0    3.0    2.0    1.0    0.5
0.5    0.5

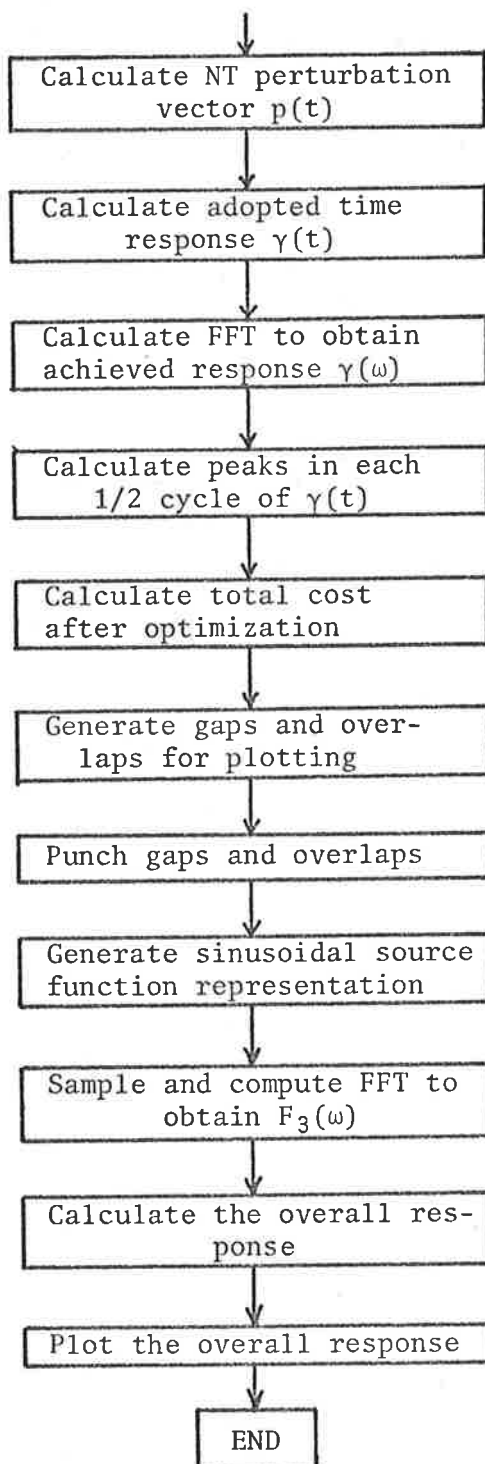
```

A3 PROGRAM FILTER 3: OPTIMIZATION OF FILTER 1  
 USING ZERO-ORDER ITERATION METHOD

A3.1 Flow Chart



A25



## A3.2 Listing of FILTER 3

```

PROGRAM FILTER3(INPUT,OUTPUT,PUNCH)
C PROGRAM FOR DESIGNING A FILTER WITH ZERO ORDER SUCCESSIVE ITERATION
* PROCESS
*
C CLASSIFICATION OF PROGRAM F/09/0/T1 (FFT ROUTINE THROUGHOUT)
C ONLY 50 COST COEFFICIENTS ARE USED
C OMEGA FACTOR IS TAKEN INTO CONSIDERATION
C USED IN PUNCHING DATA FOR PLOTTING ON 4TH DECEMBER,1973.
*
C DECLARATIONS
C * *****
C * THIS PROGRAM ALSO REQUIRES SUBROUTINE PL1 GIVEN IN APPENDIX A8 *
C * *****
*
DIMENSION DBI(60)
DIMENSION T(650)
DIMENSION QT(230)
DIMENSION C(50)
DIMENSION IP(100)
DIMENSION Y(50),XY(50)
DIMENSION MAG(50),MAGDB(52),PHAS(50),RT(1024)
DIMENSION FREQ(52)
COMPLEX ZF(1024),ZF1(50),ZFT(50)
COMMON ZF,ZF1,ZFT,FREQ
REAL MAG ,MAGDB
INTEGER FP
*
C BASIC PARAMETERS
IFI = 148
IFF = 197
ITI = 400
NF = 71
NQ = 50
*
F2T = +1.0
T2F = -1.0
NP = 1024
TIME = 5.0E-06
PI = 4.0*ATAN2(1.,1.)
*
C DERIVED PARAMETERS
*
ITF = NP+2-ITI
DT = TIME/NP
DF = 1./TIME
FO = 1./(6.*DT)
DW = 2.*PI*DF
IFN = IFF-IFI+1
NF1 = NF+1
IF1 = IFI
IF2 = IFF
NC = IF2-IF1+1
*
C INPUT OF SPECIFIED RESPONSE
C A MAXIMUM AMPLITUDE OF 100 UNITS IS ASSUMED
READ 1,(MAG(I),I=1,NQ)
1 FORMAT (8F10.5)
C FREQUENCY SCALE(29.4MHZ TO 39.2MHZ, CORRESPONDING TO 50 SAMPLING
C POINTS)
DO 2 I = 1,NQ
FREQ(I) = DF*(I+146)
2 CONTINUE
DO 11 I = 1,650
T(I) = DT*(I-1)
11 CONTINUE
C CALCULATE THE RESPONSE IN DW SCALE WITH REFERENCE TO + ONE DB.
DO 3 I = 1,NQ
MAGDB(I) = 20.0*ALOG10(0.01*MAG(I))+1.0
3 CONTINUE
C ASSUME ALINEAR PHASE RELATION
C PHAS = CONSTANT*OMEGA
DO 16 I = 1,NQ
PHAS(I) = -2.5E-06*DW*I
16 CONTINUE
C PRINT THE INPUT DATA
PRINT 4
4 FORMAT (1H1,40X*INPUT DATA//6X*INDEX* 8X*FREQUENCY*11X*MAGNITUDE*
*8X*MAGNITUDE IN DB*1)X*PHASE*//)
PRINT 18,(I,FREQ(I),MAG(I),MAGDB(I),PHAS(I),I=1,50)
18 FORMAT (110,4E20.5)
*
C PUNCH THE INPUT SPECIFIED RESPONSE
CALL DBPUNCH(NQ,FREQ,MAG)
*
DO 5 I = 1,NP
ZF(I) = CNPLX(0.,0.)
5 CONTINUE
C ASSUME A 9 FINGER TRANSDUCER AND CALCULATE IT'S RESPONSE USING
C SIN(X)/X FORMULA
C NO OF FINGERS = 2.0*F + 1.0

```

```

C      ASSUME A MAXIMUM AMPLITUDE OF 100 UNITS
C      AMPLITUDES ARE CALCULATED IN THE SUBROUTINE SINEX AS FOLLOWS
C      AMPLITUDE = 100.0*PAMP*SIN(X)/X
C      F = 4.0
C      PAMP = 1.0
C      CALL SINEX(NQ,F,PAMP,FO,XY)
*
C      CALCULATE THE RECEIVING TRANSDUCER RESPONSE BY DIVIDING INPUT
C      SPECIFIED RESPONSE BY THE TRANSMITTING TRANSDUCER RESPONSE
C      AND ALSO BY OMEGA FACTOR
C      DO 6 I = 1,NQ
C      Y(I) = MAG(I)/(XY(I)*DW*(I+146))
C      ZF(I+1) = CMPLX(Y(I)*COS(PHAS(I)),Y(I)*SIN(PHAS(I)))
C      IT = I+147
C      ZF(NP+2-IT) = CONJG(ZF(IT))
6     CONTINUE
C      NOTE THAT FROM HERE ONWARDS FOR THE SYNTHESIS PURPOSE THIS RESPONSE
C      WILL BE TAKEN AS THE SPECIFIED INPUT RESPONSE
C      DO 10 I = 1,NC
C      ZFI(I) = ZF(I+IF1-1)
10    CONTINUE
C      PLOT THE SPECIFIED RESPONSE USING SUBROUTINE TRANS
C      ENTRY = 10.0
C      CALL TRANS2(ITI,ITF,NP,NQ,PAMP,TIME,ENTRY,RT)
C      TRANSFORM TO TIME DOMAIN
C      DEL = DF
C      DIR = F2T
C      CALL BFAST(ZF,10,DIR,DEL)
C      NOTE THAT DEL HAS BEEN NOW CHANGED TO DT AND
C      ALSO ZF NOW CONTAINS TRANSFORMED TIME DOMAIN RESPONSE
C      DO 9 I = 1,NP
C      RT(I) = REAL(ZF(I))
9     CONTINUE
C      PRINT OF TIME DOMAIN TRANSFORM OF SPECIFIED RESPONSE
C      PRINT 101
101   FORMAT (1H1,42X,*TIME DOMAIN TRANSFORM OF SPECIED RESPONSE*//)
C      CALL TPRINT(ITI,ITF,RT)
*
C      CALCULATE THE PEAKS OF THE ADOPTED TIME RESPONSE
C      NOTE THAT THE ACTUAL NO FINGERS IS CALCULATED IN SUBROUTINE PEAKS3
C      CALL PEAKS3(ITI,ITF,NF,RT,IP)
*
C      PRINT 109,ITI,ITF
109   FORMAT(1H0,10X*INITIAL TIME INDEX =*14,10X*FINAL TIME INDEX =*14//)
*
C      STORE THE ADOPTED RESPONSE IN QT(I)
*
C      IT = ITF-ITI+1
*
C      DO 105 I = 1,IT
C      QT(I) = RT(I+ITI-1)
105   CONTINUE
C      EFFECT OF TRUNCATING THE TIME FUNCTION
C      ENTRY = 0.0
C      CALL TRANS2(ITI,ITF,NP,NQ,PAMP,TIME,ENTRY,RT)
*
C      STORE THE FREQUENCY RESPONSE OF ADOPTED TIME RESPONSE IN ZFT(I)
C      DO 397 I = 1,NC
C      ZFT(I) = ZF(I+IF1-1)
397   CONTINUE
C      PRINT 398
398   FORMAT (1X, /40X*FREQUENCY RESPONSE OF ADOPTED TIME RESPONSE*//
*5X*INDEX*8X*FREQUENCY (MHZ)*8X*REAL PART*11X*IMAG PART*//)
C      PRINT 399, (I,FREQ(I),ZFT(I), I=1,NQ)
399   FORMAT (1B,3E20.5)
*
C      CALCULATE THE FREQUENC F RESPONSE OF TRUNCATED APODISED FILTER
*
C      DO 556 I = 1,NQ
C      DBI(I) = REAL(ZF(I+IF1-1))*XY(I)*DW*(I+146)
556   CONTINUE
C      CALL DBPUNCH(NQ,FREQ,DBI)
*
C      PROGRAM FILTER1 CAN ALSO BE CALCULATED FROM THIS PROGRAM
*
C      *****
C      * OPTIMIZATION PROCESS STARTS FROM HERE *
C      *****
C      PRINT 400
400   FORMAT (1H1, /50X*OPTIMIZATION PROCESS STARTS FROM HERE*//)
*
C      SELECT SUITABLE COST COEFFICIENTS
C      Y IS THE EXPONENT TO WHICH THE INVERSE ABSOLUTE SPECIFIED FREQUENCY
C      TERMS ARE RAISED
C      Y = 0.65
C      CALL COST(IF1,IFI,IFF,IF2,NC,C,Y)
*
C      CALCULATE THE TOTAL COST BEFORE OPTIMIZATION
C      CALL TCOST(NF,NF1,NC,C,T1,S1)
*

```



```

C      SUBROUTINE DVCT2 CALCULATES THE D ELEMENTS USING FFT ROUTINE
C      CALL DVCT2(NC,NP,C,TIME,ITI,ITF,IF1,RT)
C      NOTE HERE RT(I) IS NOT THE TIME DOMAIN TRANSFORM OF SPECIFIED RESPONSE
*
C      THE SOLUTION OF THE PERTURBATION VECTOR IS CALCULATED IN THE
C      SUBROUTINE SOLUIT USING FFT ROUTINES ONLY
C      CALL SOLUIT(NP,NC,ITI,ITF,TIME,IF1,C,RT)
C      NOTE THE ELEMENTS OF D ARE TRANSFERED THROUGH RT AND ALSO THE SOLUTION
C      IS RETURNED VIA RT
*
C      RECONSTRUCTION OF RT(I)
      DO 823 I = 1,IT
      QT(I) = QT(I)+RT(I+ITI-1)
823 CONTINUE
C      MAP ON TO RT(I) VECTOR
      DO 830 I = 1,IT
      RT(I+ITI-1) = QT(I)
830 CONTINUE
*
      PRINT 824
824 FORMAT(1H1,/,40X*TOTAL TIME RESPONSE AFTER ADDING PERTURBATIONS*//)
      CALL TPRINT(ITI,ITF,RT)
*
C      CHECK THE FREQUENCY RESPONSE WITH THIS PERT TIME FUNCTION
      ENTRY = 0.0
      CALL TRANS2(ITI,ITF,NP,NQ,PAMP,TIME,ENTRY,RT)
*
C      CALCULATE THE FFEQUENCY RESPONSE OF OPTIMIZED FILTER
      DO 558 I = 1,NQ
      DBI(I) = REAL(ZF(I+IF1-1))*XY(I)*DW*(I+146)
558 CONTINUE
      CALL DBPUNCH(NQ,FREQ,DBI)
*
C      CALCULATE THE PEAKS OF THIS NEW TIME RESPONSE
      CALL PEAKS3(ITI,ITF,NF,RT,IP)
*
C      CALCULATE THE TOTAL COST AFTER OPTIMIZATION
      DO 829 I = 1,NC
      ZFT(I) = ZF(I+IF1-1)
829 CONTINUE
      CALL TCOST(NS,NF1,NC,C,T2,S2)
      X = T2/T1
      X = 100.0*(1.0-X)
      PRINT 997,X
997 FORMAT (1H0,10X*PERCENTAGE REDUCTION IN COST =*F5.2)
C      GENERATE THE GAP FUNCTION FROM THIS OPTIMIZED TIME FUNCTION
*
      299 CONTINUE
*
      PINCH = 0.1
C      IF PINCH IS LESS THAN ONE THE ZERO CROSSINGS AND THE OVERLAPS ARE NOT
C      PUNCHED, OTHERWISE THEY ARE
      CALL PATERN(ITI,ITF,NP,NF,IP,RT,TIME,T,PINCH,NQ,PAMP)
*
C      OBTAIN THE OVERALL RESPONSE BY MULTIPLYING BY TRANSMITTING TRANSDUCER
C      RESPONSE AND BY OMEGA FACTOR
      DO 401 I = 1,NQ
      ZF(I+147) = ZF(I+147)*XY(I)*DW*(I+146)
401 CONTINUE
      DO 559 I = 1,NQ
      DBI(I) = REAL(ZF(I+147))
559 CONTINUE
      CALL DBPUNCH(NQ,FREQ,DBI)
      PRINT 402
402 FORMAT (1H1,10X*EXPECTED OVERALL RESPONSE OF THE FILTER*//)
C      PLOT THE RESPONSE USING SUBROUTINE TRANS2
      ENTRY = 10.0
      CALL TRANS2(ITI,ITF,NP,NQ,PAMP,TIME,ENTRY,RT)
998 STOP
      END

      SUBROUTINE DBPUNCH(NQ,FREQ,X)
*
      DIMENSION FREQ(2),X(2),Y(100),YY(100)
*
      XYZ = 0.0
      DO 1 I = 1,NQ
      XYZ = AMAX1(XYZ,ABS(X(I)))
1 CONTINUE
      DO 2 I = 1,NQ
      YY(I) = 100.*ABS(X(I))/XYZ
2 CONTINUE
      DO 3 I = 1,NQ
      Y(I) = 20.*ALOG10(0.01*YY(I))
3 CONTINUE
      PRINT 4
4 FORMAT (1H0,10X*FREQUENCY RESPONSE IN DB SCALE*//)
      PRINT 5,(I,FREQ(I),YY(I),Y(I),I=1,NQ)
8 FORMAT (110,3E20.3)

```

```

PUNCH 6,(Y(I),I=1,NQ)
6 FORMAT (6E13.3)
CALL PLT(NQ,1,Y)

*
RETURN
END

SUBROUTINE BFAST(Y,M,SIGN,DXY)
*
*
* SUBROUTINE FOR THE CALCULATION OF EITHER THE FORWARD OR
* INVERSE FOURIER TRANSFORM OF A COMPLEX SEQUENCE Y USING THE
* FAST FOURIER TRANSFORM (FFT) ALGORITHM.
*
*
* Y IS A COMPLEX ARRAY OF DIMENSION 2M AND IS BOTH THE INPUT
* AND OUTPUT SEQUENCE OF THE SUBROUTINE.
*
* PRESENT DIMENSIONS LIMIT=2**10
*
* DXY = THE SAMPLE SPACING FOR THE INPUT ARRAY Y. THE CORRES-
* PONDING SAMPLE SPACING IN THE TRANSFORM DOMAIN IS OUTPUT IN DXY
*
* FOR TIME TO FREQUENCY TRANSFORMATION, SIGN = -1.0
* FOR FREQUENCY TO TIME TRANSFORMATION, SIGN = +1.0
*
* FOR FOURIER ANALYSIS, DXY = DT = 1.0/(2**M)
* FOR FOURIER SYNTHESIS, DXY = DF = 1.0
*
* SUBROUTINE CON SETS UP A CONVERSION TABLE TO REARRANGE THE
* INPUT ARRAY FOR PROCESSING.
*
* SUBROUTINE TABLE SETS UP A TABLE OF ALL SINES AND COSINES
* USED IN SUBROUTINE FAST.
*
* SUBROUTINE BFAST IS MODIFIED VERSION OF SUBROUTINE FAST WRITTEN
* ON 2 MAY 1972
*
*
* COMPLEX A,U,W,T,Y
* DIMENSION A(1024),Y(2)
* COMMON /PERM/MM(1024)
* COMMON /TAB/TC(10),TS(10)
* DATA MSET/0/
*
* IF (MSET.EQ.M) GOTO 1
* CALL TABLE(M)
* CALL CON(M)
* MSET=M
* N=2**M
* CONTINUE
*
* DO 7 I=1,N
* J=MM(I)
* A(I)=Y(J)
*
* DO 20 L=1,M
* LE=2**L
* LE1=LE/2
* U=(1,0,0.0)
* W=CHPLX(TC(L),TS(L)*SIGN)
* DO 20 J=1,LE1
* DO 10 I=J,N,LE
* IP=I+LE1
* T=A(IP)*U
* A(IP)=A(I)-T
* A(I)=A(I)+T
* CONTINUE
* U=U*W
* CONTINUE
*
* DO 30 I=1,N
* Y(I)=A(I)*DXY
* CONTINUE
*
* DXY=1./(DXY*N)
*
* RETURN
* END BFAST
* SUBROUTINE TABLE(M)
* COMMON /TAB/TC(10),TS(10)
* PI=4,0*ATAN2(1.0,1.0)
* DO 1 I=1,M
* TC(I)=COS(PI/(2**(I-1)))
* TS(I)=SIN(PI/(2**(I-1)))
* RETURN
* END
* SUBROUTINE CON(M)
* INTEGER A,T

```

4

FAST 20  
FAST 30  
FAST 40  
FAST 50  
FAST 60  
FAST 70  
FAST 90  
FAST 100  
FAST 280  
FAST 110  
FAST 140  
FAST 150  
FAST 160  
FAST 180  
FAST 190  
FAST 200  
FAST 210  
FAST 220  
FAST 230  
FAST 260  
FAST 270  
FAST 290  
FAST 330  
FAST 340  
FAST 350  
FAST 360  
FAST 370  
FAST 380  
FAST 430  
FAST 400  
FAST 390  
FAST 470  
FAST 480  
FAST 490  
FAST 500  
FAST 510  
FAST 520  
FAST 530  
FAST 540  
FAST 550  
FAST 560  
FAST 570  
FAST 580  
FAST 590  
FAST 600  
FAST 610  
FAST 620  
FAST 660  
FAST 680  
FAST 170  
FAST 700  
FAST 690  
FAST 760  
TABL 10  
TABL 30  
TABL 40  
TABL 50  
TABL 60  
TABL 70  
TABL 80  
CON 10  
CON 20

```

COMMON /PERM/ A(1024)
N=2**M
NV2=N/2
NM1=N-1
J=1
DO 1 I=1,N
1 A(I)=I
DO 7 I=1,NM1
IF(I.GE.J)GOTO5
T=A(J)
A(J)=A(I)
A(I)=T
5 K=NV2
6 IF(K.GE.J)GOTO7
J=J-K
K=K/2
GOTO 6
7 J=J+K
RETURN
END
SUBROUTINE SINEX(NQ,F,PAMP,FO,XY)
*
C SUBROUTINE SINEX CALCULATES TRANSMITTING TRANSDUCER FREQUENCY RESPONSE
C WITH CENTRE FREQUENC F0 AND FOR A UNIFORM NO FINGERS EQUAL TO 2.*F+1.
*
DIMENSION XY(50),XZ(50)
DIMENSION FREQ(52)
COMPLEX ZF(1024),ZFI(50),ZFT(50)
COMMON ZF,ZFI,ZFT,FREQ
*
PRINT 1
1 FORMAT (1H1,40X*FREQUENCY RESPONSE OF TRANSMITTING TRANSDUCER*//)
PI = 4.0*ATAN2(1.,1.)
MF = 2.*F+1.
PRINT 3,MF
3 FORMAT (1H0,10X*NUMBER OF FINGERS =*I5/)
PRINT 4,F0
4 FORMAT (1H0,10X*CENTRE FREQUENCY IN HZ =*E10.2/)
DO 17 I = 1,NQ
X = F*PI*((FREQ(I)-F0)/F0)
IF(X.EQ.0.0)X = 100.0*PAMP
XY(I) = 100.0*PAMP*SIN(X)/X
17 CONTINUE
XYZ = 0.0
DO 18 I = 1,NQ
XYZ = AMAX1(ABS(XY(I)),XYZ)
18 CONTINUE
DO 19 I = 1,NQ
XZ(I) = 20.*ALOG10(ABS(XY(I))/XYZ)+1.0
19 CONTINUE
PRINT 20
20 FORMAT (6X*INDEX*8X*FREQUENCY*11X*MAGNITUDE*8X*MAGNITUDE IN DB*//)
PRINT 21,(I,FREQ(I),XY(I),XZ(I),I=1,NQ)
21 FORMAT (110,3E20,5)
CALL PLT(NQ,1,XY)
PRINT 22
22 FORMAT (1H0,10X*FREQUENCY RESPONSE IN LINEAR SCALE*//)
RETURN
END

SUBROUTINE PEAKS3(ITI,ITF,MF,RT,IP)
*
C SUBROUTINE PEAKS CALCULATES THE + AND - PEAKS IN EACH HALF CYCLE
C OF THE TRUNCATED TIME RESPONSE. IT ALSO CALCULATES THE MAGNITUDE
C OF THESE PEAKS, NORMALISED WITH RESPECT TO THE MAXIMUM PEAK VALUE
C OF 100 UNITS
*
DIMENSION IP(MF),RT(2)
DIMENSION P(100),D(100)
*
PRINT 820
820 FORMAT (1X/X*PEAK AMPLITUDES AND THEIR LOCATIONS IN THE ADOPTED T
*IME RESPONSE*//)
M = 0
I = ITI
J = I
3 X = RT(I)*RT(I+1)
IF(X)1,1,2
2 I = I+1
IF(I.GE.ITF)GO TO 1
GO TO 3
1 K = 1
Y = 0.0
DO 4 L = J,K
Y = AMAX1(Y,ABS(RT(L)))
4 CONTINUE
DO 5 L = J,K
IF(Y.FQ.ABS(RT(L)))GO TO 6
5 CONTINUE

```

```

6 M = M+1
  IP(M) = L
  D(M) = RT(L)
  IF(I.GE.1TF)GO TO 814
  I = I+1
  J = I
  GO TO 3
814 CONTINUE
C NORMALIZE THE PEAK AMPLITUDES
  XYZ = 0.0
  DO 816 I = 1,M
  XYZ = AMAX1(ABS(D(I)),XYZ)
816 CONTINUE
  DO 817 I = 1,M
  P(I) = 100.*D(I)/XYZ
817 CONTINUE
  PRINT 818
818 FORMAT (8X,*PEAK*5X,*PEAK*12X,*PEAK*8X,*NORMALISED*/
  *8X,*INDEX*4X,*POINT*9X,*MAGNITUDE*5X,*PEAK MAGNITUDE*/)
  PRINT 815,(I,IP(I),D(I),P(I),I=1,M)
815 FORMAT(2110,E20.5,F15.5)
  NF = M
  RETURN
  END

```

SUBROUTINE COST(IF1,IFI,IFF,IF2,NC,C,Y)

```

*
C ARBITRARY CHOICE OF COST COEFFICIENTS ARE MADE IN THIS SUBROUTINE
*
  DIMENSION C(NC)
  DIMENSION FREQ(52)
  COMPLEX ZF(1024),ZFI(50),ZFT(50)
  COMMON ZF,ZFI,ZFT,FREQ
*
  DO 801 I = 1,NC
  X = REAL(ZFI(I))
  X = ABS(X)
  X = X**Y
  IF(X.EQ.0.)X=0.04
  C(I) = 1./X
801 CONTINUE
  PRINT 826
826 FORMAT (1X,/55X*COST COEFFICIENTS ARE*/)
  PRINT 820,(I,C(I),I=1,NC)
820 FORMAT (8(15,E11.3))
  RETURN
  END

```

SUBROUTINE TCOST(NF,NF1,NC,C,TAU,TAU2)

```

*
C SUBROUTINE TCOST CALCULATES THE TOTAL COST ASSOCIATED WITH AN
C ADOPTED RESPONSE AND THE SPECIFIED RESPONSE WITH AN ARBITRARY
C GIVEN COST COEFFICIENTS
*
C THE VARIABLES NEEDED ARE
C C, THE COST COEFFICIENTS ASSOCIATED WITH THE NF FINGERS
C ZFI, SPECIFIED INPUT RESPONSE
C ZFT, ADOPTED RESPONSE
C TAU, THE TOTAL COST
*
  DIMENSION C(NC)
  DIMENSION FREQ(52)
  COMPLEX ZF(1024),ZFI(50),ZFT(50)
  COMMON ZF,ZFI,ZFT,FREQ
*
  DATA TB/1.0/
*
  SUM = 0.0
  DO 7 I = 1,NC
  X = REAL(ZFT(I)-ZFI(I))
  Y = AIMAG(ZFT(I)-ZFI(I))
  SUM = SUM + (X*X+Y*Y)*C(I)
7 CONTINUE
  TAU = SUM
  TB = TB*1.0
  IF(TB.EQ.2.0)GO TO 2
  GO TO 4
2 PRINT 3,TAU
3 FORMAT (1X,/5X,*TOTAL COST BEFORE OPTIMIZATION =*F16.8)
  GO TO 6
4 PRINT 5,TAU
5 FORMAT (1X,/5X,*TOTAL COST AFTER OPTIMIZATION =*E16.8)
6 RETURN
  END

```

SUBROUTINE DVCT2(NC,NP,C,TIME,ITI,ITF,IF1,D)

```

DIMENSION D(2)
DIMENSION C(NC)
DIMENSION FREQ(52)
COMPLEX ZF(1024),ZFI(50),ZFT(50)
COMMON ZF,ZFI,ZFT,FREQ
*
DO 1 I = 1, NP
ZF(I) = CMPLX(0.,0.)
1 CONTINUE
IN = 1
IF(IF1.EQ.1) IN = 2
ZF(IF1) = C(1)*(ZFT(1)-ZFI(1))
DO 2 I = IN, NC
IT = I+IF1-1
ZF(IT) = C(I)*(ZFT(I)-ZFI(I))
ZF(NP+2-IT) = CONJG(ZF(IT))
2 CONTINUE
DF = 1./TIME
CALL BFAST(ZF,10,+1.,DF)
DF = 1./TIME
DO 3 I = 1, NP
D(I) = REAL(ZF(I))
3 CONTINUE
C WE HAVE CALCULATED NC VALUES OF THE D VECTOR
RETURN
END

SUBROUTINE SOLUIT(NP,NC,ITI,ITF,TIME,IF1,C,RT)
*
DIMENSION C(NC)
DIMENSION RT(2)
DIMENSION FREQ(52)
COMPLEX ZF(1024),ZFI(50),ZFT(50)
COMMON ZF,ZFI,ZFT,FREQ
*
F2T = +1.0
T2F = -1.0
DF = 1./TIME
DT = TIME/NP
*
DO 1 I = 1, NP
ZF(I) = CMPLX(0.,0.)
1 CONTINUE
DO 2 I = 1, NP
ZF(I) = CMPLX(RT(I),0.)
2 CONTINUE
C TRANSFORM TO FREQUENCY DOMAIN
DEL = DT
DIR = T2F
CALL BFAST(ZF,10,DIR,DEL)
DO 3 I = 1, NC
ZFT(I) = ZF(I+IF1-1)/C(I)
3 CONTINUE
DO 4 I = 1, NP
ZF(I) = CMPLX(0.,0.)
4 CONTINUE
IN = 1
IF(IF1.EQ.1) IN = 2
ZF(IF1) = ZFT(1)
DO 5 I = IN, NC
IT = I+IF1-1
ZF(IT) = ZFT(I)
ZF(NP+2-IT) = CONJG(ZF(IT))
5 CONTINUE
*
C TRANSFORM TO FREQUENCY DOMAIN
DEL = DF
DIR = F2T
CALL BFAST(ZF,10,DIR,DEL)
*
DO 6 I = 1, NP
RT(I) = -REAL(ZF(I))
6 CONTINUE
PRINT 7
7 FORMAT(1H0,10X*THE SOLUTION OF PERTURBATION VECTOR IS GIVEN BY*/)
CALL TPRINT(ITI,ITF,RT)
RETURN
END

SUBROUTINE TPRINT(N1,N2,RT)
DIMENSION RT(N2),VOP(10)
DO 104 I = N1,N2,10
DO 102 J = 1,10
VOP(J) = 0.0
IF((I+J-1).LE.N2)VOP(J) = RT(I+J-1)
102 CONTINUE
PRINT 103,1,(VOP(J),J=1,10)
103 FORMAT(1X,14,3X,10E12.3)

```

```
104 CONTINUE
RETURN
END
```

```
SUBROUTINE TRANS2(ITI,ITF,NP,NQ,PAMP,TIME,ENTRY,RT)
```

```
*
C SUBROUTINE TRANS DOES THE FOLLOWING OPERATIONS
*
C (1) CALCULATES THE ADOPTED RESPONSE BY TRUNCATING THE IMPULSE
C RESPONSE TO THE DESIRED LIMITS, ITI,ITF.
*
C (2) CALCULATES THE FREQUENCY RESPONSE OF THIS TRUNCATED TIME
C RESPONSE USING FFT ROUTINE
*
C (3) CALCULATES THE RELATIVE MAGNITUDE AND PHASE RESPONSES IN THE
C SPECIFIED RANGE OF FREQUENCY LIMITS.
*
C (4) PLOTS THE FREQUENCY RESPONSE IN RELATIVE SCALE AND IN DB SCALE
*
C (5) IF ENTRY IS EQUAL TO ZERO IT TRANSFORMS THE GIVEN TIME RESPONSE
C TO FREQUENCY RESPONSE AND THEN PLOTS IN LINEAR SCALE AS WELL AS IN DBSCALE
*
C (6) IF ENTRY IS NOT EQUAL TO ZERO IT PLOTS ONLY THE GIVEN FREQUENCY
C RESPONSE IN LINEAR SCALE AS WELL AS IN DB SCALE
*
C PAMP IS THE FACTOR BY WHICH MAXIMUM AMPLITUDES IN LINEAR SCALE
C WOULD REPRESENT ABOVE 100 UNITS
*
DIMENSION RT(1024)
DIMENSION ZTA(52),ZT1(52),ZT2(52),ZT3(52)
DIMENSION FREQ(52)
COMPLEX ZF(1024),ZFI(50),ZFT(50)
COMMON ZF,ZFI,ZFT,FREQ
*
DT = TIME/NP
T2F = -1.0
F2T = +1.0
IF(ENTRY)499,488,499
488 CONTINUE
DO 500 I = 1,NP
ZF(I) = CMPLX(0.,0.)
500 CONTINUE
DO 503 I = 1,ITF
ZF(I) = CMPLX(RT(I),0.)
503 CONTINUE
C TRANSFORM TO FREQUENCY DOMAIN
DEL = DT
DIR = T2F
CALL RFAST(ZF,10,DIR,DEL)
C NOTE THAT DEL HAS NOW BEEN CHANGED TO DF
C ALSO ZF NOW CONTAINS TRANSFORMED FREQUENCY DOMAIN RESPONSE
499 PRINT 5
5 FORMAT(1X, /40X*FREQUENCY RESPONSE IN COMPLEX FORM*//
*5X*INDEX*8X*FREQUENCY(MHZ)*8X*REAL PART*11X*IMAG PART*//)
PRINT 4,(I,FREQ(I),ZF(I+147)),I=1,NQ)
4 FORMAT (18,3E20.5)
XYZ = 0.
DO 504 I = 1,NQ
ZTA(I) = CABS(ZF(I+147))
XYZ = AMAX1(ZTA(I),XYZ)
504 CONTINUE
DO 505 I = 1,NQ
ZT1(I) = 20.*ALOG10(ZTA(I)/XYZ)+1.0
ZT2(I) = 100.0*PAMP*ZTA(I)/XYZ
X1 = REAL(ZF(I+147))
X2 = AIMAG(ZF(I+147))
ZT3(I) = ATAN2(X2,X1)
505 CONTINUE
PRINT 623
623 FORMAT (1H1,20X*FREQUENCY RESPONSE IN THE DESIRED RANGE 9.4 TO 39
*.2 MHZ*//
CSX*5,NO*7X*FREQUENCY*7X*RELATIVE MAGNITUDE*3X*MAGNITUDE IN DB*10X*
CPHASE*//)
PRINT 624,(I,FREQ(I),ZT2(I),ZT1(I),ZT3(I)),I=1,NQ)
624 FORMAT (18,4(E15.3,5X))
DO 625 I = 1,NQ
IF(ZT1(I).LE.-50.)ZT1(I)=-49.5
625 CONTINUE
CALL PLT(NQ,1,ZT2)
PRINT 626
626 FORMAT (1X, /40X*PLOT OF FREQUENCY VS RELATIVE MAGNITUDE*//)
CALL PLT(NQ,1,ZT1)
PRINT 627
627 FORMAT (1X, /40X*PLOT OF FREQUENCY VS MAGNITUDE IN DB*//)
RETURN
END
```

```
SUBROUTINE PATERN(ITI,ITF,NP,NF,IP,RT,TIME,T,PINCH,NQ,PAMP)
```

```

*
C   SUBROUTINE PATERN CALCULATES THE GAP FUNCTION FROM THE ZERO CROSSINGS
C   AND THE PEAK AMPLITUDES
*
      DIMENSION IP(NF),RT(2),T(2)
      DIMENSION OVHID(100)
      DIMENSION ZRCR(100),ZRCM(100),DIFF(100)
      DIMENSION FREQ(52)
      COMPLEX ZF(1024),ZFI(50),ZFT(50)
      COMMON ZF,ZFI,ZFT,FREQ
      COMMON/SUB/ZRCR,ZRCM,DIFF
*
      PRINT 6
6   FORMAT (1H1,40X*GENERATION OF GAP FUNCTION STARTS FROM HERE*//)
*
C   CALCULATES THE ZEROCROSSINGS OF THE ADOPTED RESPONSE IN THE INTERVAL
C   ITI AND ITF
C   ALSO CALCULATE THE GAP WIDTHS AND THE MIDDLE POINTS OF THESE GAPWIDTHS
*
      CALL ZEROCR(ITI,ITF,NP,NF,RT,T)
*
C   CALCULATES THE OVERLAPS OF THE GAP FUNCTION
C   OVERLAPS ARE PROPORTIONAL TO THE AREA OF GAPWIDTH MULTIPLIED BY PEAK
C   AMPLITUDE IN THAT GAP AND THE ACTUAL
C   THE PEAK AMPLITUDE IS CALCULATED BY A PARABOLIC CURVE FITTING
*
      DT = TIME/NP
      CALL AREA1(RT,NF,DT,OVHID,PINCH)
C   VERIFY THE FREQUENCY RESPONSE OF THIS GAP FUNCTION USING APPROXIMATE
C   ANALYSIS METHOD
      CALL ANLYSE(ITI,ITF,NP,NF,TIME,OVHID,RT,NQ,PAMP)
622  RETURN
      END
*
      SUBROUTINE ZEROCR(ITI,ITF,NP,NF,RT,T)
*
      DIMENSION RT(2),T(2)
      DIMENSION ZRCR(100),ZRCM(100),DIFF(100)
      DIMENSION FREQ(52)
      COMPLEX ZF(1024),ZFI(50),ZFT(50)
      COMMON ZF,ZFI,ZFT,FREQ
      COMMON/SUB/ZRCR,ZRCM,DIFF
*
      IZ = 0
      DO 600 I = ITI,ITF
      IF(I,GE,ITF)GO TO 603
      X = RT(I)*RT(I+1)
      IF(X)601,601,600
601  SLOP = (RT(I+1)-RT(I))/(T(I+1)-T(I))
      CONST = RT(I)-SLOP*T(I)
      IZ = IZ+1
      ZRCR(IZ) = -CONST/SLOP
600  CONTINUE
603  CONTINUE
      PRINT 602,IZ,NF
602  FORMAT (1H0,10X*NO OF ZERO CROSSINGS =*15,10X*NO OF PEAKS =*15//)
*
C   CALCULATE THE GAPWIDTHS BETWEEN THE FINGERS
C   THAT IS THE DIFFERENCE BETWEEN THE ZERO CROSSINGS
*
      LSTZ = IZ
      JSTZ = LSTZ-1
      DO 702 I = 1,JSTZ
      DIFF(I) = ZRCR(I+1)-ZRCR(I)
702  CONTINUE
C   LOCATE MID POINTS OF ZERO CROSSINGS
      DO 605 I = 1,JSTZ
      ZRCM(I) = (ZRCR(I)+ZRCR(I+1))/2.
605  CONTINUE
      RETURN
      END
*
      SUBROUTINE AREA1(RT,NF,DT,OVHID,PINCH)
*
C   SUBROUTINE AREA1 CALCULATES THE OVERLAPS ASSUMING THAT OVERLAPS ARE
C   PROPOTIONAL TO THE TRIANGULAR AREABETWEEN THE ZERO CROSSINGS AND ALL THE
C   SAMPLING POINTS BETWEEN THESE ZERO CROSSINGS
*
      DIMENSION RT(2)
      DIMENSION OVHID(100),YNOR(100)
      DIMENSION ZRCM(100),ZRCR(100),DIFF(100)
      DIMENSION FREQ(52)
      COMPLEX ZF(1024),ZFI(50),ZFT(50)
      COMMON ZF,ZFI,ZFT,FREQ
      COMMON /SUB/ZRCR,ZRCM,DIFF
*
      NFL = NF-1
      NFM = NF-2

```

```

DO 1 I = 1,NFM
AREA = 0.0
IFP = 2*INT(ZRCR(I)/DT)
LFP = 1+INT(ZRCR(I+1)/DT)
AREA = AREA + (DT*(IFP-1)-ZRCR(I))*RT(IFP)/2.0
AREA = AREA + (ZRCR(I+1)-DT*(LFP-1))*RT(LFP)/2.0
IF(IFP.EQ.LFP)GO TO 3
M1 = IFP
M2 = M1+1
2 AREA = AREA + (RT(M1)+RT(M2))*DT/2.0
M1 = M1+1
M2 = M2+1
IF(M1.EQ.LFP)GO TO 3
GO TO 2
3 OVMID(I) = AREA
1 CONTINUE
*
C NORMALISE THE OVERLAPS WITH RESPECT TO THE PEAK AMPLITUDES
XYZ = 0.0
DO 8 I = 1,NFM
XYZ = AMAX1(XYZ,ABS(OVMID(I)))
8 CONTINUE
DO 9 I = 1,NFM
YNOR(I) = 100.0*OVMID(I)/XYZ
9 CONTINUE
*
PRINT 4
4 FORMAT(1H0* INDEX*9X*ZERO CROSSINGS*13X*GAPWIDTHS*17X*OVERLAPS*10X
C*NOR, OVERLAPS*/)
PRINT 5,(I,ZRCR(I),DIFF(I),OVMID(I),YNOR(I),I=1,NFM)
5 FORMAT (15,3E25.8,F16.2)
PRINT 6,NFL,ZRCR(NFL)
6 FORMAT (15,E25.8)
IF(PINCH.LT.1.0)GO TO 10
PUNCH 7,(ZRCR(I),I=1,NFL)
PUNCH 7,(OVMID(I),I=1,NFM)
7 FORMAT (5E16.8)
10 RETURN
END
*
SUBROUTINE ANALYSE(ITI,ITF,NP,NF,TIME,OVMID,RT,NQ,PAMP)
*
C SUBROUTINE ANALYSE CALCULATES THE FREQUENCY RESPONSE OF THE GAP FUNCTION
C USING APPROXIMATE ANALYSIS METHOD
*
DIMENSION RT(2)
DIMENSION OVMID(100),GAP(300),OVLAP(100)
DIMENSION ZRCR(100),ZRCM(100),DIFF(100)
DIMENSION FREQ(52)
COMPLEX ZF(1024),ZFI(50),ZFT(50)
COMMON ZF,ZFI,ZFT,FREQ
COMMON/SUB/ZRCR,ZRCM,DIFF
*
PI = 4.0*ATAN2(1.,1.)
DT = TIME/NP
NFL = NF-1
NFM = NF-2
C CALCULATE THE PEAK AMPLITUDES BY DIVIDING OVERLAPS BY GAPWIDTHS
*
DO 620 I = 1,NFM
OVLAP(I) = OVMID(I)/DIFF(I)
620 CONTINUE
*
C LOCATE THESE PEAK AMPLITUDES AT THE MIDDLE OF THE GAPWIDTHS AND FIT
C QUARTER SINE WAVE BETWEEN THE ZERO CROSSINGS AND THE PEAK AMPLITUDES
C AND CALCULATE THE AMPLITUDES AT THE SAMPLING POINTS OF DT
*
M = ZRCR(1)/DT
MM = 0
DO 613 I = 1,NFM
614 M = M+1
Z = M*DT
IF(Z.LE.ZRCR(I))GO TO 614
IF(Z.GE.ZRCR(I+1))GO TO 615
MM = MM+1
ARG = PI*(Z-ZRCR(I))/DIFF(I)
GAP(MM) = OVLAP(I)*SIN(ARG)
GO TO 614
615 M = M-1
613 CONTINUE
LVAL = MM
PRINT 619
619 FORMAT (1H0,40X*SAMPLED RESPONSE OF THE GAP FUNCTION*/)
CALL TPRINT(I,LVAL,GAP)
C MAP ON THE SAMPLES IN THE INTERVAL ITI TO ITF
C CALCULATE ITI AND NOTE THAT TO GET RIGHT SIDE SAMPLING POINT WE HAVE TO
C ADD 2 TO THE INTEGER RESULT BECAUSE OF THE FACT I(I) = DT*(I-1)
ITI = 2+INT(ZRCR(1)/DT)
DO 616 I = 1,LVAL

```



```

RT(I,ITI-1) = GAP(I)
616 CONTINUE
ITF = ITI*LVAL-1
C PRINT THE SAMPLED TIME RESPONSE IN THE INTERVAL ITI ITF
PRINT 617
617 FORMAT (1H0,10X*TIME RESPONSE OF ANALISED GAP FUNCTION SHIFTED IN
CTIME SO THAT IT IS SYMMETRICAL OVER T/2*//)
CALL TPRINT(ITI,ITF,RT)
C CALCULATE THE FREQUENCY RESPONSE USING FFT ROUTINE
ENTRY = 0.0
CALL TRANS2(ITI,ITF,NP,NO,PAMP,TIME,ENTRY,RT)
RETURN
END

```

```

*

```

```

C DATA

```

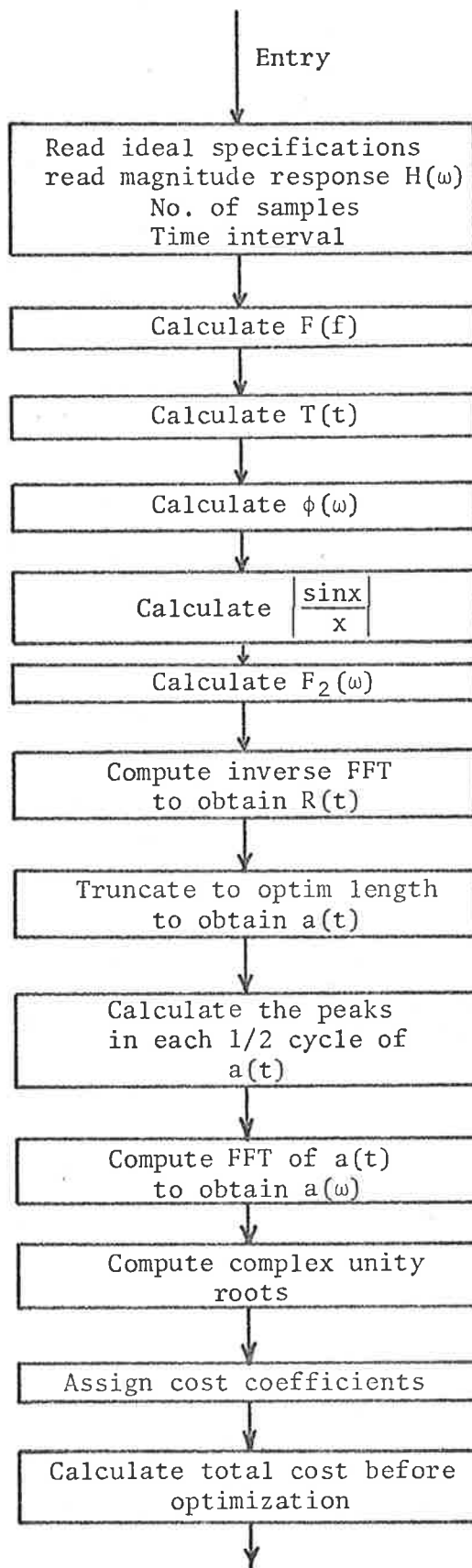
```

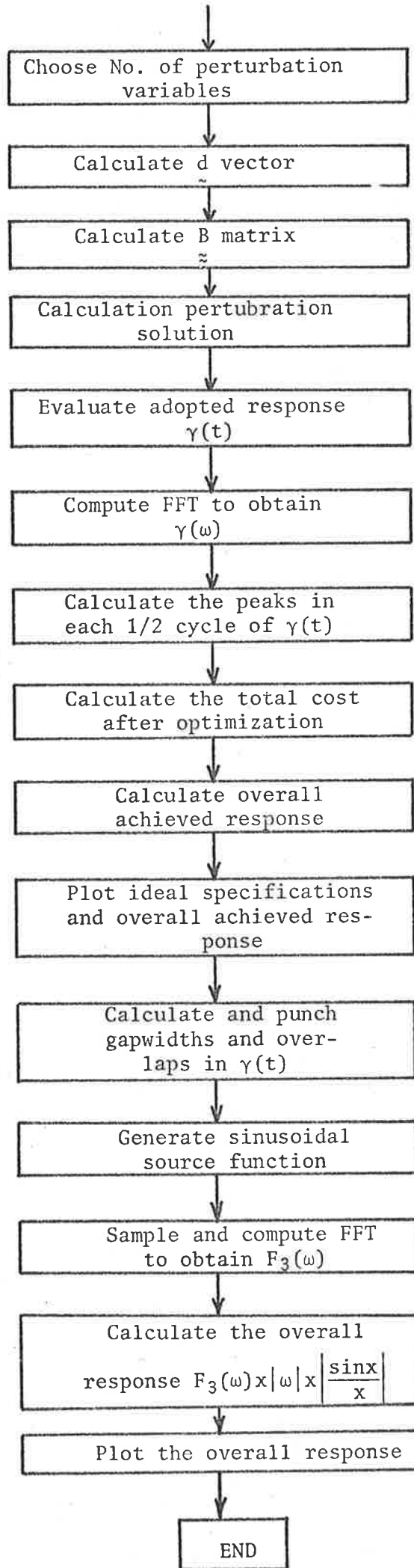
*
1.00 3.5 7.5 11.5 14.5 18.0 16.0 7.5
1.0 8.0 15.5 24.5 35.5 48.0 59.0 70.0
79.0 86.0 91.5 95.5 97.5 99.0 100.0 100.0
100.0 99.5 98.5 97.0 95.0 91.5 87.0 81.5
75.0 69.0 61.0 54.0 46.0 39.0 31.5 24.5
17.5 12.5 8.5 5.0 3.0 2.0 1.0 0.5
0.5 0.5

```

A4 PROGRAM FILTER 4: SYNTHESIS OF A FILTER WITH GIVEN IDEAL  
SPECIFICATIONS USING OPTIM METHOD

A4.1 Flow Chart





A4.2 Listing of FILTER 4

```

PROGRAM FILTER4(INPUT,OUTPUT,PUNCH)
C CLASSIFICATION OF PROGRAM A/11/1/P2
C PROGRAM FOR DESIGNING A FILTER WITH IDEAL SPECIFICATIONS
C 513 COSTS ARE USED
C OMEGA FACTOR IS TAKEN INTO CONSIDERATION
C NOTATION IS VERY MUCH SAME AS THAT USED IN PROGRAM FOR FILTER2
C DECLARATIONS
C
DIMENSION DBI(100)
DIMENSION SPEC1(65),SPEC2(65),ORD(63)
DIMENSION T(650)
DIMENSION IP(100),D(100),PT(100),IQ(100),KF(100),B(4000)
DIMENSION C(513)
DIMENSION WN(1024)
DIMENSION Y(50),XY(50)
DIMENSION MAG(50),MAGDB(52),PHAS(50),RT(1024)
DIMENSION FREQ(52)
COMPLEX ZF(1024)
DIMENSION ZFI(513),ZFT(513)
COMMON ZF,ZFI,ZFT,FREQ
REAL MAG ,MAGDB
C BASIC PARAMETERS
C
IFI = 148
IFF = 192
ITI = 388
NF = 71
C
F2T = +1.0
T2F = -1.0
NP = 1024
NQ = 45
TIME = 5.0E-06
PI = 4.0*ATAN2(1.,1.)
SF = 1.0E+08
FO = 34.0E+06
F = 5
PAMP = 10.0**(1./20)
C DERIVED PARAMETERS
C
ITA = 1+(NP/2)
ITF = NP+2-ITI
DT = TIME/NP
DF = 1./TIME
DW = 2.*PI*DF
IFN = IFF-IFI+1
NF1 = NF+1
IF1 = 1
IF2 = 513
NC = IF2-IF1+1
C INPUT OF SPECIFIED LIMITS
READ 1,(SPEC1(I),I=1,61)
READ 1,(SPEC2(I),I=1,61)
DO 300 I = 1,61
ORD(I) = DF*(I+139)
300 CONTINUE
C PRINT THE IDEAL SPECIFICATION LIMITS
PRINT 269
269 FORMAT (1H1,10X*IDEAL SPECIFICATION LIMITS ARE*/)
PRINT 270,(I,ORD(I),SPEC1(I),SPEC2(I),I=1,61)
270 FORMAT (I10,3E20.3)
C PLOT THE SPECIFIED LIMITS OF THE FREQUENCY RESPONSE
CALL PLT(60,2,SPEC1,SPEC2)
C INPUT OF SPECIFIED RESPONSE IN DB SCALE
READ 1,(MAGDB(I),I=1,NQ)
1 FORMAT (3F10.5)
C FREQUENCY SCALE(29.4MHZ TO 39.2MHZ, CORRESPONDING TO 50 SAMPLING
C POINTS)
DO 2 I = 1,NQ
FREQ(I) = DF*(I+146)
2 CONTINUE
C CALCULATE THE TIME SAMPLES WHICH ARE NECESSARY FIR PUNCHING ZEROCROSSINGS
C AND OVERLAPS
C
DO 11 I = 1,650
T(I) = DT*(I-1)
11 CONTINUE
C CALCULATE THE RESPONSE IN LINEAR SCALE
DO 3 I = 1,NQ
POWER = MAGDB(I)/20.0

```

```

MAG(I) = 100.0*10.**POWER
3 CONTINUE
CALL PLT(NQ,1,MAGDB)
CALL PLT(NQ,1,MAG)
C ASSUME A LINEAR PHASE RELATION
C PHAS = CONSTANT*OMEGA
DO 16 I = 1,NQ
PHAS(I) = -2.5E-06*DW*I
16 CONTINUE
C PRINT THE INPUT DATA
PRINT 4
4 FORMAT (1H1,40X*INPUT DATA*//6X*INDEX* 8X*FREQUENCY*11X*MAGNITUDE*
*8X*MAGNITUDE IN DB*13X*PHASE*//)
PRINT 18,(I,FREQ(I),MAG(I),MAGDB(I),PHAS(I),I=1,NQ)
18 FORMAT (110,4E20.5)
DO 5 I = 1,NP
ZF(I) = CHPLX(0.,0.)
5 CONTINUE
*
C ASSUME A 11 FINGER TRANSDUCER AND CALCULATE ITS RESPONSE USING SIN(X)/X
C FORMULA
C CENTRE FREQUENCY = 34.0 MHZ
C NO OF FINGERS = 2.*F+1. , AND FOR 15 FINGERS F = 7
C CALCULATE THE MAXIMUM AMPLITUDES CORRESPONDING TO 10 DB
C AMPLITUDES ARE CALCULATED IN THE SUBROUTINE SINEX AS FOLLOWS
C AMPLITUDE = 100.0*PAMP*SIN(X)/X
CALL SINEX(NQ,F,PAMP,FO,XY)
*
C PLOT THE OVERALL RESPONSE AND THE SINE(X)/X RESPONSE
CALL PLT(NQ,2,MAG,XY)
*
C CALCULATE THE RECEIVING TRANSDUCER RESPONSE BY DIVIDING INPUT
C SPECIFIED RESPONSE BY THE TRANSMITTING TRANSDUCER RESPONSE
C AND ALSO BY OMEGA FACTOR AND PRESCALE THE RESPONSE BY A FACTOR OF 10**8
DO 6 I = 1,NQ
Y(I) = MAG(I)/(XY(I)*DW*(I+146)*1.0E-08)
ZF(147+I) = CHPLX(Y(I)*COS(PHAS(I)),Y(I)*SIN(PHAS(I)))
IT = I+147
ZF(NP+2-IT) = CONJG(ZF(IT))
6 CONTINUE
C NOTE THAT FROM HERE ONWARDS FOR THE SYNTHESIS PURPOSE THIS RESPONSE
C WILL BE TAKEN AS THE SPECIFIED INPUT RESPONSE
DO 10 I = 1,NC
ZFI(I) = REAL(ZF(I+IF1-1))
10 CONTINUE
C PLOT THE SPECIFIED RESPONSE USING SUBROUTINE TRANS
ENTRY = 10.0
CALL TRANS2(ITI,ITF,NP,NQ,PAMP,TIME,ENTRY,RT)
*
C TRANSFORM TO TIME DOMAIN
DEL = DF
DIR = F2T
CALL BFAST(ZF,10,DIR,DEL)
C NOTE THAT DEL HAS BEEN NOW CHANGED TO DT AND
C ALSO ZF NOW CONTAINS TRANSFORMED TIME DOMAIN RESPONSE
DO 9 I = 1,NP
RT(I) = REAL(ZF(I))
9 CONTINUE
C PRINT OF TIME DOMAIN TRANSFORM OF SPECIFIED RESPONSE
PRINT 101
101 FORMAT (1H1,42X,*TIME DOMAIN TRANSFORM OF SPECIFIED RESPONSE*//)
CALL YPRINT(ITI,ITF,RT)
*
C CALCULATE THE PEAKS OF THE ADOPTED TIME RESPONSE
C THE ACTUAL NO OF PEAKS IS READJUSTED FROM THAT OF THE GIVEN NUMBER IN
C THE SUBROUTINE PEAKS3 AND RETURNED THROUGH THE PARAMETER NF
CALL PEAKS3(ITI,ITF,NF,RT,IP)
*
PRINT 109,ITI,ITF
109 FORMAT(1H0,10X*INITIAL TIME INDEX =*I4,10X*FINAL TIME INDEX =*I4/)
*
C EFFECT OF TRUNCATING THE TIME FUNCTION
ENTRY = 0.0
CALL TRANS2(ITI,ITF,NP,NQ,PAMP,TIME,ENTRY,RT)
*
C STORE THE FREQUENCY RESPONSE OF ADOPTED TIME RESPONSE IN ZFT(I)
DO 397 I = 1,NC
ZFT(I) = ZF(I+IF1-1)
397 CONTINUE
PRINT 398
398 FORMAT (1X,40X*FREQUENCY RESPONSE OF ADOPTED TIME RESPONSE*//
*5X*INDEX*8X*FREQUENCY(MHZ)*8X*REAL PART*//)
PRINT 399,(I,FREQ(I),ZFT(I+IF1-1),I=1,NQ)
399 FORMAT (18,2E20.5)
C CALCULATE THE OVERALL RESPONSE OF THIS TRUNCATED TIME FILTER
DO 556 I = 1,NQ
DBI(I) = REAL(ZF(I+147))*XY(I)*DW*(I+146)*1.0E-08
556 CONTINUE
CALL DBPUNCH(NQ,FREQ,DBI)
*

```

```

* *****
C * OPTIMIZATION PROCESS STARTS FROM HERE *
* *****
*
PRINT 400
400 FORMAT (1H1, /50X*OPTIMIZATION PROCESS STARTS FROM HERE*/)
*
C SUBROUTINE CUNITY CALCULATES 1024 REAL PARTS OF OF COMPLEX UNITY ROOTS
CALL CUNITY(NP,WN)
*
C SELECT SUITABLE COST COEFFICIENTS
*
C COFF1 ARE THE VALUES OF COSTS BETWEEN IF1 AND IF1
C COFF2 ARE THE VALUES OF COSTS BETWEEN IFF AND IF2
C COFF1 = 0.01
C COFF2 = 0.01
CALL COST2(COFF1,COFF2,IF1,IFI,IFF,IF2,NC,C)
C CALCULATE THE TOTAL COST BEFORE OPTIMIZATION
CALL TCOST(NF,IF1,NC,C,T1)
*
* KP = 86
*
DO 401 I = 1,85
IQ(I) = 1TI+I-1
401 CONTINUE
IQ(KP) = ITA
DO 402 I = 1,KP
IPI = IQ(I)
D(I) = RT(IPI)
402 CONTINUE
PRINT 403
403 FORMAT (1H0,10X*RESPONSE AT WHICH THE PERTURBATIONS IS APPLIED*///)
PRINT 404,(I,IQ(I),D(I),I=1,KP)
404 FORMAT (5(2I6,E12.3))
DF = 1./TIME
C SUBROUTINE DVCT2 CALCULATES THE D ELEMENTS USING FFT ROUTINE
*
CALL DVCT2(KP,NP,NC,IF1,IF2,TIME,IQ,C,SF,D)
*
C SUBROUTINE BMAT CALCULATES THE ELEMENTS OF B USING FT ALGORITHM
DT = TIME/NP
KP1 = KP+1
CALL BMAT(KP,KP1,NP,IF1,IF2,IQ,C,WN,DT,NC,SF,B)
*
C SUBROUTINE SOLU CALCULATES THE SOLUTION USING SYMMETRIC MATRIX SUBROUTINE
C LSSS
CALL SOLU2(KP,KF,D,B,SF,PT)
C RECONSTRUCTION OF RT(I)
DO 823 I = 1,KP
IPI = IQ(I)
RT(IPI) = RT(IPI)+PT(I)
RT(NP+2-IPI) = RT(IPI)
823 CONTINUE
*
PRINT 824
824 FORMAT(1H1, /40X*TOTAL TIME RESPONSE AFTER ADDING PERTURBATIONS*///)
CALL TPRINT(ITI,ITF,RT)
*
C CHECK THE FREQUENCY RESPONSE WITH THIS PERT TIME FUNCTION
ENTRY = 0.0
CALL TRANS2(ITI,ITF,NP,NQ,PAMP,TIME,ENTRY,RT)
*
C CALCULATE THE TOTAL FREQUENCY RESPONSE OF THE OPTIMIZED FILTER
DO 558 I = 1,NQ
DBI(I) = REAL(ZF(I+147))*XY(I)*DW*(I+146)*1.0E-08
558 CONTINUE
CALL DBPUNCH(NQ,FREQ,DBI)
*
C CALCULATE THE PEAKS OF THIS NEW TIME RESPONSE
CALL PEAKS3(ITI,ITF,NF,RT,IP)
*
C CALCULATE THE TOTAL COST AFTER OPTIMIZATION
DO 829 I = 1,NC
ZFT(I) = REAL(ZF(I+IF1-1))
829 CONTINUE
CALL TCOST(NF,IF1,NC,C,T2)
*
X = T2/T1
X = 100.0*(1.0-X)
PRINT 997,X
997 FORMAT (1H0,10X*PERCENTAGE REDUCTION IN COST =*F5.2)
*
C GENERATE GAP FUNCTION FROM THIS OPTIMIZED TIME FUNCTION
*
C ADD ONE FINGER ON EITHER SIDE TO ENSURE THAT THE END PERTURBATIONS ARE
C INCLUDED IN THE ADOPTED RESPONSE
ITI = ITI-3
ITF = ITF+3
C CALCULATE THE PEAKS IN THIS NEW LIMITS
CALL PEAKS3(ITI,ITF,NF,RT,IP)

```

```

*
C   IF PINCH IS LESS THAN ONE THE ZERO CROSSINGS AND THE OVERLAPS ARE NOT
C   PUNCHED OTHERWISE THEY ARE
C   PINCH = 2.0
*
      CALL PATERN(ITI,ITF,NP,NF ,IP,RT,TIME,T,PINCH,NQ,PAMP)
*
C   OBTAIN OVERALL RESPONSE BY MULTIPLYING BY TRANSMITTING TRANSDUCER
C   RESPONSE , OMEGA FACTOR AND BY SCALE FACTOR
      DO 996 I = 1,NQ
      ZF(I+147) = ZF(I+147)*XY(I)*DW*(I+146)*1.0E-08
996  CONTINUE
      PRINT 995
995  FORMAT (1H1,10X*EXPECTED OVERALL RESPONSE OF THE FILTER*/ )
C   PLOT THE RESPONSE USING TRANS2
      ENTRY = 10.0
      CALL TRANS2(ITI,ITF,NP,NQ,PAMP,TIME,ENTRY,RT)
*
998  STOP
      END

```

```

      SUBROUTINE DBPUNCH(NQ,FREQ,X)
*
      DIMENSION FREQ(2),X(2),Y(100),YY(100)
*
      XYZ = 0.0
      DO 1 I = 1,NQ
      XYZ = AMAX1(XYZ,ABS(X(I)))
1   CONTINUE
      DO 2 I = 1,NQ
      YY(I) = 100.*ABS(X(I))/XYZ
2   CONTINUE
      DO 3 I = 1,NQ
      Y(I) = 20.*ALOG10(0.01*YY(I)) + 1.0
3   CONTINUE
      PRINT 4
4   FORMAT (1H0,10X*FREQUENCY RESPONSE IN DB SCALE*/ )
      PRINT 5,(I,FREQ(I),YY(I),Y(I),I=1,NQ)
5   FORMAT (110,3E20.3)
      PUNCH 6,(Y(I),I=1,NQ)
6   FORMAT (6E13.3)
      CALL PLT(NQ,1,Y)
*
      RETURN
      END

```

```

*
C   SAME
C   SUBROUTINES
C   USED
C   IN
C   PROGRAM
C   FILTER2
*

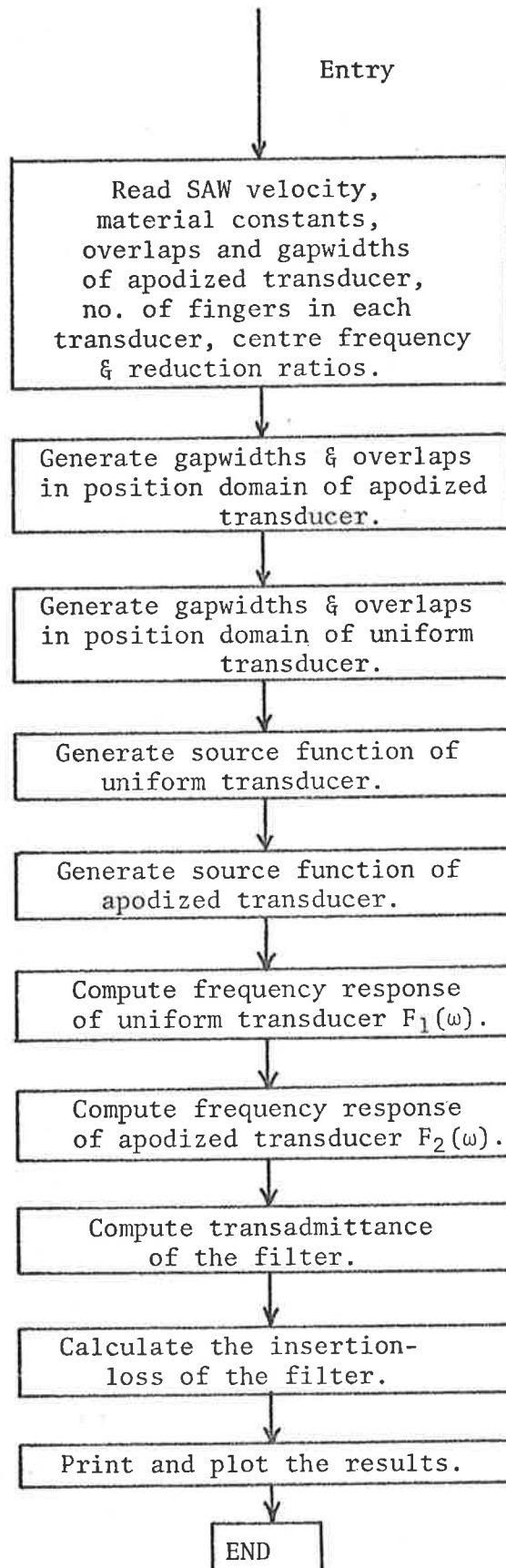
```

DATA

-59.5	-59.5	-59.5	-59.5	-59.5	-59.5	-59.5	-59.5
-59.5	-59.5	-59.5	-28.0	-27.75	-27.25	-26.75	-26.5
-23.0	-19.25	-15.75	-12.25	-8.75	-5.25	-1.75	0.0005
0.0	0.0	0.0	0.0	0.0	0.0	0.0	0.0
0.0	0.0	0.0	0.0	0.0	0.0	-0.75	-1.75
-3.0	-4.25	-5.45	-20.0	-50.0	-59.5	-59.5	-59.5
-59.5	-59.5	-59.5	-59.5	-59.5	-59.5	-59.5	-59.5
-59.5	-59.5	-59.5	-59.5	-59.5	-59.5	-59.5	-59.5
-59.5	-40.0	-40.0	-40.0	-40.0	-40.0	-40.0	-43.5
-43.5	-40.0	-20.0	-20.0	-20.0	-20.0	-20.0	-22.0
-17.5	-12.5	-7.5	-2.5	2.0	2.0	2.0	2.0
2.0	2.0	2.0	2.0	2.0	2.0	2.0	2.0
2.0	2.0	2.0	2.0	2.0	2.0	2.0	2.0
2.0	-1.5	-4.5	-9.5	-16.0	-23.0	-30.0	-36.5
-41.0	-43.0	-45.0	-43.0	-41.0	-40.0	-40.0	-41.5
-41.0	-40.0	-40.0	-40.0	-59.5	-59.5	-59.5	-59.5
-59.5	-54.5	-40.0	-25.0	-22.0	-20.0	-20.5	-22.5
-25.0	-19.5	-14.0	-8.0	-3.0	+0.5	1.0	1.0
1.0	1.0	1.0	1.0	1.0	1.0	1.0	1.0
1.0	1.0	1.0	1.0	1.0	1.0	1.0	1.0
0.5	0.0	-2.0	-4.5	-12.5	-16.25	-23.0	-30.0
-36.0	-42.5	-48.0	-55.0	-59.5	-59.5	-59.5	-59.5

## A5 PROGRAM Y21FIL: TRANSADMITTANCE OF THE FILTER

A5.1

Flow Chart



## A5.1 Listing of Y21FIL

```

PROGRAM Y21FIL(INPUT,OUTPUT)
*
C   THIS PROGRAM COMPUTES THE TRANSADMITTANCE Y21(W) BETWEEN A PAIR OF
C   TRANSDUCERS AND CALCULATES THE INSERTIONLOSS OF THE DELAY LINE WITH
C   GIVEN LOAD CONDITIONS
C   THE BASIC EXCITATION CELL FOR THE TRANSDUCERS IS ASSUMED TO BE THE GAP
C   BETWEEN A PAIR OF ELECTRODES.
C   THE CELL INCLUDES AN ELECTRODE HALF WIDTH ON EACH SIDE SET EQUAL TO A
C   QUARTER CELL WIDTH.
C   THE REQUIRED INPUT DATA ARE=
*   XPA(I)= POSITION OF ELECTRODE I IN TRANSDUCER A (IN MILLIMETRES)
*   XPB(I)= DITTO TRANSDUCER B
*   XLA(I)= OVERLAP LENGTH OF CELL I (IN MILLIMETRES)
*   XLB(I)= DITTO TB
*   NA = NUMBER OF GAPS IN TA
*   NB = DITTO TB
*   VSAW= SURFACE VELOCITY (IN MM/SEC)
*   GA = INITIAL GAP WIDTH (IN MM) TA
*   GB = DITTO FOR TB
*   TINC = SAMPLING TIME INTERVAL
*   M = LOG(BASE 2) OF NUMBER OF SAMPLES
C   TITLE= IDENTIFIER OF THE PARTICULAR DELAY LINE
*
C   ETA = CHARACTERISTIC IMPEDANCE OF FREE SPACE IN OHMS
S   EPSI = DIELECTRIC CONSTANT OF FREE SPACE
C   STEP = SPATIAL SAMPLING INTERVAL = TINC*VSAW
S   VT = INPUT PULSE TO DELAY LINE IN VOLT-SECONDS
*
C   TYPICAL DATA INCLUDED IS FOR FILTER2
C   * *****
C   * THIS PROGRAM ALSO REQUIRES SUBROUTINE PLT GIVEN IN APPENDIX A8 *
C   * *****
*
C   DECLARATIONS
*
C   DIMENSION FREQA(60),FREOB(60)
C   DIMENSION RMAG(60)
C   DIMENSION FREQ(60)
C   DIMENSION ZRCR(100),OVLAP(100)
C   DIMENSION XPA(100),XLA(100),XPB(100),XLB(100)
C   COMPLEX A(1026),B(1026),Y(60)
C   REAL C(60),D(60),GD(60)
C   REAL MAGDB(60)
C   REAL LAMDA
C   REAL LOSS(60)
C   COMMON /A,B,Y
*
C   READ 777,TITLE,NA,NB,FO,REDRE,REDRA
777 FORMAT (A9,2I2,E9.2,2F10.2)
*
C   BASIC PARAMETERS
C   PI=3.141592653589793
C   ETA = 337.
C   EPSI=8.85E-12
C   EPSQ=39.21E-12
C   DELTA=-9.3E-4
C   Z=0
C   VSAW = 3.159E+06
C   TIME = 5.0E-06
C   M = 10
*
C   DERIVED PARAMETERS
*
C   N=2.*M
C   TINC = TIME/N
C   NA1 = NA+1
C   NB1 = NB+1
C   STEP=TINC*VSAW
C   CORRECTION NEEDED IN REDUCTION RATIO
C   REDRC = REDRE/REDRA
*
C   PRINT 103,TITLE,NA,NB,FO,REDRE,REDRA
103 FORMAT (I11,44X*CLASSIFICATION OF PROGRAM *A10/
145X*NO OF OVERLAPS IN TRANSDUCER A **I3/
245X*NO OF OVERLAPS IN TRANSDUCER B **I3/
345X*CENTR FREQUENCY OF TRANSDUCER A = *E10.2/
445X*ESTIMATED REDUCTION RATIO =*F5.2/
545X*ACTUAL REDUCTION RATIO *F5.2//)
C   CALCULATE THE FREQUENCY IN THE DESIRED RANGE (29.4MHZ TO 39.2MHZ)
C   DF = 1./TIME
C   DO 30 I = 1,50
C   FREQ(I) = DF*(I+146)
30 CONTINUE
*
C   GENERATE ELECTRODE POSITIONS AND OVERLAPS FOR TRANSDUCER B
*
C   READ 1,(ZRCR(I),I=1,NB1)
1 FORMAT (5E16.8)
C   READ 1,(OVLAP(I),I=1,NB)
C   PRINT 2

```

```

2 FORMAT (1H0,10X*ZEROCROSSINGS AND OVERLAPS ,THE PUNCHED OUTPUT FRO2
CM THE PREVIOUS PROGRAM*/)
3 FORMAT (15,5XE16.8,5XE16.8)
PRINT 3,(I,ZRCR(I),OVLAP(I),I=1,NB)
PRINT 4,(I,ZRCR(I),I=NB1,NB1)
4 FORMAT (15,5XE16.8)
C CALCULATE ELECTRODE POSITIONS IN HMS
XPB(1) = 300./REDRC
XPB(I) = REDRC*XPB(1)
DO 5 I = 1,NB
XPB(I+1) = XPB(I)+VSAW*(ZRCR(I+1)-ZRCR(I))*REDRC
5 CONTINUE
C CALCULATE OVERLAPS IN HMS CORRESPONDING TO A MAXIMUM OVERLAP OF 5HMS
XYZ = 0.0
DO 6 I = 1,NB
XYZ = AMAXI(ABS(OVLAP(I)),XYZ)
6 CONTINUE
DO 7 I = 1,NB
XLB(I) = ABS(OVLAP(I))*5.0*REDRC/XYZ
7 CONTINUE
C PRINT ELECTRODE POSITIONS AND OVERLAPS
PRINT 8
8 FORMAT (1H0,10X*ELECTRODES POSITIONS AND OVERLAPS IN HMS OF TRANSD
CUCER B*/)
DO 9 I = 1,NB
PRINT 10,I,XPB(I),XLB(I)
10 FORMAT (I10,E22.5,E16.5)
9 CONTINUE
PRINT 11 ,(I,XPB(I),I=NB1,NB1)
11 FORMAT (I10,E22.5)
*
C GENERATE ELECTRODE POSITIONS AND OVERLAPS FOR TRANSDUCER A
C OVERLAPS A ARE INCREASED BY 25 PERCENT OF THE MAXIMUM OVERLAP IN B
C TO TAKE INTO DIFFRACTION EFFECTS
C THE ELECTRODE POSITIONS ARE SO CHOSEN SO THAT THE TIME FUNCTION IS
C SYMMETRICAL OVER T/2
*
DO 20 I = 1,NA
XLA(I) = 6.25*REDRC
20 CONTINUE
LAMDA = VSAW/FO
XPA(1) = 25.2/REDRE
DO 21 I = 1,NA
XPA(I+1) = XPA(I)+REDRC*LAMDA/2.
21 CONTINUE
PRINT 22
22 FORMAT (1H0,10X*ELECTRODE POSITIONS AND OVERLAPS IN HMS OF TRANSDU
CCER A*/)
DO 23 I = 1,NA
PRINT 10,I,XPA(I),XLA(I)
23 CONTINUE
PRINT 11,(I,XPA(I),I=NA1,NA1)
*
C ASSUME THAT THE SIGN OF THE FIELD ALTERNATES IN EACH GAP AND THAT THE
C FIRST GAP HAS POSITIVE ELECTRIC FIELD
C ASSUME THAT THE GAP FUNCTION IS FORM SIN(PI/2) TO SIN(3PI/2)
C THE FFT OPERATES ON 2**M POINTS
SIGN=-1
NSTEP = XPA(1)/STEP
DO 600 NS=1,NSTEP
A(NS)=(0.,0.)
ACON = PI*(EPSQ+EPSI)/(EPS1*1.854)
DO 601 I=1,NA
SIGN=-1.*SIGN
NSTEP=XPA(I+1)/STEP-NS
NSS=NS+1
NSE=NS+NSTEP
GA=XPA(I+1)-XPA(I)
AMP=ACON*XLA(I)/GA
DO 602 NS=NSS,NSE
ARG = (NS*STEP-XPA(I))*PI/GA
AR=AMP*COS(ARG)*SIGN
A(NS)=CMPLX(AR,Z)
602 CONTINUE
601 CONTINUE
NSS=NS+1
DO 603 NS=NSS,N
A(NS)=(0.,0.)
603 PRINT GAP FUNCTION A
C PRINT 650
650 FORMAT(*0AMPITUDE FUNCTION A*/)
NSTEP = XPA(1)/STEP
DO 651 I = NSTEP,NSS,4
PRINT 652,I,(A(I+J-1),J=1,4)
652 FORMAT(15,8E15.3)
651 CONTINUE
C GAP FUNCTION FOR TRANSDUCER B
SIGN=-1
NSTEP = XPB(1)/STEP
NSR=NSTEP

```

```

DO 700 NS=1,NSTEP
700 B(NS)=(0.,0.)
DO 701 I=1,N8
SIGN=-1*SIGN
NSTEP=XPB(I+1)/STEP-NS
NSS=NS+1
NSE=NS*NSTEP
GB=XPB(I+1)-XPB(I)
BMP=ACON*ALB(I)/GB
DO 702 NS=NSS,NSE
BRG = (NS*STEP-XPB(I))*PI/GB
BR=BMP*SIGN*COS(BRG)
B(NS)=CMPLX(BR,Z)
702 CONTINUE
701 CONTINUE
NSE1=NSE+1
DO 703 NS=NSE1,N
703 B(NS)=(0.,0.)
C PRINT GAP FUNCTION B
PRINT 750
750 FORMAT(*0AMPLITUDE FUNCTION B**/)
DO 751 I=NS8,NSE1,4
PRINT 752,I,(B(I+J-1),J=1,4)
752 FORMAT(I5,8E15.3)
751 CONTINUE
C COMPUTE INTEGRAL TRANSFORM OF TRANSDUCER A
DXY=STEP
CALL BFAST(A,M,+1.,DXY)
FINC=DXY*VSAW
PRINT 800
800 FORMAT (1H1,40X*FREQUENCY RESPONSE OF TRANSDUCER A**/
*5X*INDEX*8X*FREQUENCY(MHZ)*8X*REAL PART*11X*IMAG PART**/)
PRINT 801,(I,FREQ(I),A(I+147),I=1,50)
801 FORMAT (I8,3E20.5)
C PLOT THE FREQUENCY RESPONSE OF TRANSDUCER A IN RELATIVE SCALE
XYZ = 0.0
DO 803 I = 1,50
XYZ = AMAX1(XYZ,CABS(A(I+147)))
803 CONTINUE
DO 804 I = 1,50
FREQA(I) = 100.*CABS(A(I+147))/XYZ
804 CONTINUE
CALL PLT(50,1,FREQA)
PRINT 805
805 FORMAT (1H0,10X*PLOT OF FREQUENCY RESPONSE OF TRANSDUCER A**/)
*
C COMPUTE INTEGRAL TRANSFORM OF TRANSDUCER B
DXY=STEP
CALL BFAST(B,M,-1.,DXY)
FINC=DXY*VSAW
PRINT 900
900 FORMAT (1H1,40X*FREQUENCY RESPONSE OF TRANSDUCER B**/
*5X*INDEX*8X*FREQUENCY(MHZ)*8X*REAL PART*11X*IMAG PART**/)
PRINT 801,(I,FREQ(I),B(I+147),I=1,50)
C PLOT THE FREQUENCY RESPONSE OF TRANSDUCER B IN RELATIVE SCALE
XYZ = 0.0
DO 901 I = 1,50
XYZ = AMAX1(XYZ,CABS(B(I+147)))
901 CONTINUE
DO 902 I = 1,50
FREQB(I) = 100.*CABS(B(I+147))/XYZ
902 CONTINUE
CALL PLT(50,1,FREQB)
PRINT 903
903 FORMAT (1H0,10X*PLOT OF FREQUENCY RESPONSE OF TRANSDUCER B**/)
C COMPUTE TRANSMITTANCE Y(I) MHOS
PRINT 1000
1000 FORMAT(*1DELAY LINE TRANSMITTANCE** FREQUENCY*10X*COMPLEX Y(I)*
CSX*MAGNITUDE*5X*PHASE*9X*GROUP DELAY*5X*MAGNITUDE*)
PRINT 1004
1004 FORMAT(5X*HERTZ*7X*REAL*8X*IMAG*8X*MHOS*6X*DEGREES*7X*SECONDS*9X*D
*ECIBELS**/)
DELF= 2.*PI*FINC
RADTDEG=180./PI
CONKK=-PI*(EPS1**2)*DELTA/(XLA(1))*(EPS1+EPSQ)
CONKK=CONKK*2./1000.
*
C APPLY THE CORRECTION DUE TO (2F/F+FO) WHICH HAS NOT BEEN TAKEN INTO
C ACCOUNT IN THE SYNTHESIS PROSEFURE BUT FFT GIVES RISE TO THIS FACTOR
C THAT IS MULTIPLY Y21 BY (F+FO/2F)
*
DO 1001 I = 1,50
Y(I) = -(FO*DF*(I+146))*CONKK*A(I+147)*B(I+147)/2.
C(I) = CABS(Y(I))
XX=REAL(Y(I))
YY=AIMAG(Y(I))
D(I)=ATAN2(YY,XX)*RADTDEG
1001 CONTINUE
DO 1002 I = 2,50

```

```

GO(I-1) = (D(I-1)-D(I))/(DELTA*PI*DEG)
1002 CONTINUE
XYZ = 0.0
DO 1006 I = 1,50
XYZ = AMAX1(C(I),XYZ)
1006 CONTINUE
DO 1007 I = 1,50
MAGDB(I) = 20.*ALOG10(C(I)/XYZ)
RMAG(I) = 100.*C(I)/XYZ
1007 CONTINUE
PRINT 1003 ,(FREQ(I),Y(I),C(I),D(I),GD(I),MAGDB(I),I=1,49)
1003 FORMAT (5E12.3,E15.3,E16.3)
PRINT 1005,(FREQ(I),Y(I),C(I),D(I),MAGDB(I),I=50,50)
1005 FORMAT (5E12.3,E31.3)
CALL PLT(50,1,MAGDB)
CALL PLT(50,1,RMAG)

C
*
C
ESTIMATE THE EXPECTED INSERTIONLOSS OF THE FILTER WHEN THE APODISED
TRANSUCER IS TERMINATED IN A KNOWN ADMITTANCE LOAD
*
CALL INLOSS(50,FREQ,C,LOSS,TITLE)
*
C
PLOT THE RESPONSE IN DB SCALE
*
STOP
END

SUBROUTINE INLOSS(N,FREQ,Y21,LOSS,TITLE)
*
C
SUBROUTINE INLOSS CALCULATES THE INSERTIONLOSS,KNOWING THE TRANSADMITTANCE
AND THE LOAD ADMITTANCE CONNECTED ACROSS THE APODISED TRANSUCER
C
C
USE THE FORMULA INLOSS = 20.*ALOG10(Y21/YLOAD)
C
C
YLOAD IS CALCULATED ESTIMATING THE VARIOUS CIRCUIT ELEMENTS AND MEASURING
C
C
THE INPUT ADMITTANCE OF THE PREAMPLIFIER TERMINATING IT WITH A 50 OHM LOAD
*
C
THE EFFECT OF STRAY INDUCTANCES WERE NEGLECTED
C
C
C2 CAPACITANCE OF APODISED TRANSUCER + CAPACITANCES OF CONNECTING WIRES
C
C
+ CAPACITANCE OF BNC CONNECTORS AND THE COAXIAL CABLE UPTO THE INPUT OF
C
C
THE PREAMPLIFIER
C
C
THE INPUT ADMITTANCE OF THE PREAMPLIFIER WAS TAKEN TO BE CONSTANT
C
C
OF CONDUCTANCE OF 16.0 MILLIMHOS AND A SUSPECTANCE CORRESPONDING TO A
C
C
CAPACITANCE OF -5 PICOFARADS
C
C
NOTE THAT THE BRIDGE BALANCES THE INDUCTIVE REACTANCE AS THE NEGATIVE
C
C
OF THE CAPACITIVE REACTANCE
C
C
THE EQUIVALENT CIRCUIT CONSISTS OF A CURRENT GENERATOR I, IN PARALLEL
C
C
WITH TOTAL CAPACITANCE C2,IN PARALLEL WITH TOTAL INDUCTANCE L2,AND THE
C
C
INPUT ADMITTANCE YIN CONNECTED ACROSS L2 AND C2.
*
C
NOTE THE PRE AMPLIFIER WAS ACTUALLY CONNECTED TO THE FILTER GIJ WITH A
C
C
SHORT CABLE OF 21 CM LONG INSTEAD OF A MALE TO MALE BNC CONNECTOR,
C
C
HENCE THE LARGE VALUES OF TOTAL CAPICITANCE C2
C
C
INPUT DATA REQUIRED IS,MEASURED INPUT AND OUTPUTVOLTAGES AND THE
C
C
CAPACITANCE AND CONDUCTANCE OF THE PRE AMPLIFIER
*
C
CLASSIFICATION OF PROGRAM          P/09/1/P2
*
C
DECLARATIONS
*
REAL L2
DIMENSION DB(60)
REAL LOSS(60)
DIMENSION FREQ(2),Y21(2)
DIMENSION G(60),C(60),YL(60)
COMPLEX Y(60),A(60)
COMPLEX S,Z
*
C
INPUT ADMITTANCE OF THE AMPLIFIER IN HILLIMHOS AND PICOFARADS
DO 1 I = 1,N
G(I) = 16.65
C(I) = 3.5
1 CONTINUE
C
INDUCTANCE IN MICROHENRIES AND CAPACITANCE IN PICOFARADS
*
L2 = 0.055
C2 = 26.5
PY = 4.0*ATAN2(1.,1.)
*
C
CONVERT THE QUANTITIES INTO PROPER SI UNITS
L2 = L2*1.E-06
C2 = C2*1.E-12
DO 2 I = 1,N
G(I) = G(I)*1.E-03
C(I) = C(I)*1.0E-12
2 CONTINUE
*
C
CALCULATE THE INPUT ADMITTANCE OF THE AMPLIFIER
DO 50 I = 1,N
R = 2.*PY*FREQ(I)

```

```

C(I) = -C(I)*R
Y(I) = CMPLX(G(I),C(I))
50 CONTINUE
*
C   CALCULATE THE LOAD ADMITTANCE OF THE FILTER
DO 51 I = 1,N
R = 2.*PY*FREQ(I)
S = CMPLX(0.,R)
A(I) = L2*C2*Y(I)*S*S + C2*S + Y(I)
YL(I) = CABS(A(I))
51 CONTINUE
*
*
PRINT 54
54 FORMAT (1H1,6X*INDEX*9X*FREQUENCY*8X*INPUT ADMITTANCE OF AMPLIFIER
1(MHOS)*5X*LOAD ADMITTANCE OF THE FILTER(MHOS)*4X*ABS LOAD ADMIT*/
223X*(HZ)*13X*REAL PART*11X*IMAG PART*11X*REAL PART*11X*IMAG PART*1
32X*(MHOS)*//)
PRINT 20,(I,FREQ(I),Y(I),A(I),YL(I),I=1,N)
20 FORMAT (I10,6E20.3)
*
C   CALCULATE THE INSERTION LOSS BY DIVIDING Y2I BY A
*
DO 5 I = 1,N
LOSS(I) = 20.*ALOG10(Y2I(I)/YL(I))
5 CONTINUE
*
XYZ = -1.0E+10
DO 4 I = 1,N
XYZ = AMAX1(XYZ,LOSS(I))
4 CONTINUE
DO 6 I = 1,N
DB(I) = LOSS(I)-XYZ
6 CONTINUE
PRINT 19
19 FORMAT (1H1,6X*INDEX*9X*FREQUENCY*4X*ABS TRANSFER ADMIT*2X*ABS LO
1AD ADMITTANCE*7X*INSERTION LOSS*/23X*(HZ)*14X*(MHOS)*14X*(MHOS)*14
3X*(DB)*//)
PRINT 3,(I,FREQ(I),Y2I(I),YL(I),LOSS(I),DB(I),I=1,N)
3 FORMAT (I10,5E20.3)
CALL PLT(N,1,DB)
CALL PLOT10(5HNEBP6,5)
CALL GRAPH(TITLE,FREQ,DB,N)
RETURN
END

SUBROUTINE GRAPH(TITLE,X,Y,NQ)
*
C   SUBROUTINE GRAPH PLOTS THE FREQUENCY RESPONSE IN DB SCALE WITH REFERENCE
C   ZERO LEVEL AND -50 DB BELOW
*
DIMENSION X(2),Y(2)
*
C   PLOT THE TITLE OF THE PATTERN
CALL SYMBOL(0.,0.,0.2,9HPATTERN =,0.,9)
CALL SYMBOL(2.,0.,0.2,TITLE,0.,9)
CALL PLOT(10.,0.,-3)
*
C   SELECT ONE LAST EXTRA POINT FOR SUITABLE SCALE
TIME = 5.0E-06
DF = 1./TIME
NQ1 = NQ+1
X(NQ1) = X(NQ)+DF
Y(NQ1) = -50.0
C   ARRANGE THE RESPONSE LESS THAN 50 DB
DO 1 I = 1,NQ
IF(Y(I).LE.-50.)Y(I) = -50.0
1 CONTINUE
C   SELECT THE X AND Y AXIS SCALES
CALL SCALE(X,11.0,NQ1,1)
CALL SCALE(Y,10.0,NQ1,1)
C   PLOT THE AXIS
CALL AXIS(0.0,0.0,9HFREQUENCY,-9,11.0,0.0,X(NQ1+1),X(NQ1+2),0)
CALL AXIS(0.,0.,19HY2I,DB('THEORETICAL'),+19*10.,90.,Y(NQ1+1),Y(NQ1+
12),-1)
C   RESTORE THE AXIS AND SCALE FACTOR IN THE LAST BUT BUT ONE ARRAY
X(NQ+1) = X(NQ1+1)
X(NQ+2) = X(NQ1+2)
Y(NQ+1) = Y(NQ1+1)
Y(NQ+2) = Y(NQ1+2)
C   PLOT THE NQ POINTS BY JOINING THEM IN STRIGHT LINES
CALL LINE(X,Y,NQ,1,0,0)
C   RESET THE ORIGIN TO (0,0)
CALL PLOT(15,0.,-3)
RETURN
END

```

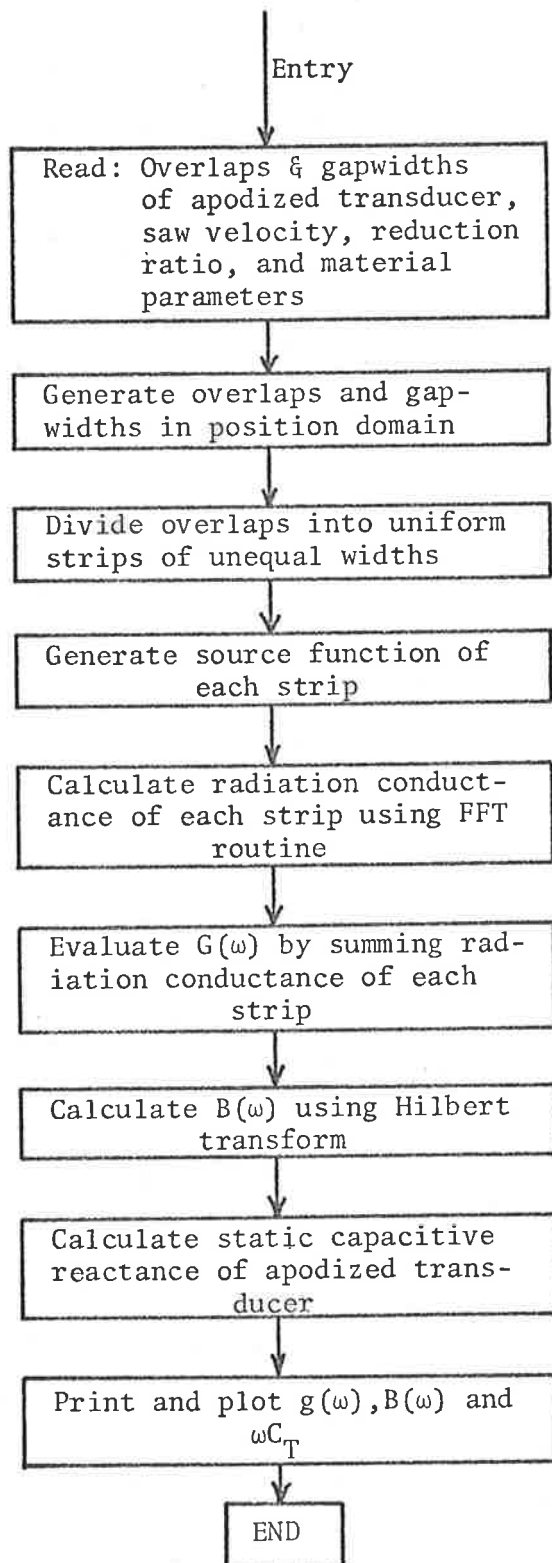


```

DO 7 I=1,NH1
IF(I,GE,J)GOTO5
T=A(J)
A(J)=A(I)
A(I)=T
5 K=NV2
6 IF(K,GE,J)GOTO7
J=J-K
K=K/2
GOTO 6
7 J=J+K
RETURN
END
*
C DATA
*
P/09/1/P2097134.20E+06 25.2 25.40
1.94354258E-06 1.95475119E-06 1.98077672E-06 1.99676531E-06 2.01302754E-06
2.03224573E-06 2.05198707E-06 2.06779797E-06 2.08306581E-06 2.09797703E-06
2.11246387E-06 2.11506609E-06 2.12852221E-06 2.14341508E-06 2.17040220E-06
2.18646887E-06 2.20180337E-06 2.21701049E-06 2.23252043E-06 2.24864718E-06
2.26766455E-06 2.28626938E-06 2.30231209E-06 2.31770779E-06 2.33294482E-06
2.34789831E-06 2.36062622E-06 2.37560815E-06 2.39017968E-06 2.40477428E-06
2.41939012E-06 2.43402377E-06 2.44867147E-06 2.46332963E-06 2.47799499E-06
2.49266454E-06 2.50733546E-06 2.52200501E-06 2.53667037E-06 2.55132853E-06
2.56597623E-06 2.58060988E-06 2.59522572E-06 2.60982032E-06 2.62439185E-06
2.63937378E-06 2.65210169E-06 2.66705518E-06 2.68229221E-06 2.69768791E-06
2.71373062E-06 2.73233545E-06 2.75135282E-06 2.76747957E-06 2.78293951E-06
2.79819663E-06 2.81353113E-06 2.82959780E-06 2.85658492E-06 2.87147779E-06
2.88493391E-06 2.88753613E-06 2.90202297E-06 2.91693419E-06 2.93220203E-06
2.94801293E-06 2.96775427E-06 2.98697246E-06 3.00323469E-06 3.01922328E-06
3.04524881E-06 3.05645742E-06
1.04201507E-02 -1.12722360E-02 9.91714911E-03 -8.88984749E-03 6.02847900E-03
-4.99233013E-03 5.27702943E-03 -4.78411253E-03 3.03438495E-03 -1.01680096E-03
1.63802469E-05 -7.88514009E-04 1.46603170E-03 -1.59909721E-03 2.51320089E-03
-4.56063397E-03 5.85360130E-03 -6.27833231E-03 5.52453913E-03 -4.58817900E-03
4.65853502E-03 -6.03726382E-03 6.93396254E-03 -7.10267166E-03 6.36436215E-03
-4.96352437E-03 1.27201982E-02 -1.61029247E-02 1.99400226E-02 -2.39359564E-02
2.78809952E-02 -3.15429913E-02 3.46890610E-02 -3.71081676E-02 3.86321131E-02
-3.98202359E-02 3.86321131E-02 -3.71081676E-02 3.46890610E-02 -3.15429913E-02
2.78809952E-02 -2.39359564E-02 1.99400226E-02 -1.61029247E-02 1.27201982E-02
-4.96352437E-03 6.36436215E-03 -7.10267166E-03 6.93396254E-03 -6.03726382E-03
4.65853502E-03 -4.58817900E-03 5.52453913E-03 -6.27833231E-03 5.85360130E-03
-4.56063397E-03 2.51320089E-03 -1.59909721E-03 1.46603170E-03 -7.88514009E-04
1.63802469E-05 -1.01680096E-03 3.03438495E-03 -4.78411253E-03 5.27702943E-03
-4.99233013E-03 6.02847900E-03 -8.88984749E-03 9.91714911E-03 -1.12722360E-02
1.04201507E-02
-4.000E+01 -2.912E+01 -2.250E+01 -1.879E+01 -1.677E+01 -1.489E+01
-1.592E+01 -2.250E+01 -4.000E+01 -2.194E+01 -1.619E+01 -1.222E+01
-8.995E+00 -6.375E+00 -4.583E+00 -3.098E+00 -2.047E+00 -1.310E+00
-7.716E-01 -3.999E-01 -2.199E-01 -8.730E-02 0. 0.
0. -4.354E-02 -1.313E-01 -2.646E-01 -4.455E-01 -7.716E-01
-1.210E+00 -1.777E+00 -2.499E+00 -3.223E+00 -4.293E+00 -5.352E+00
-6.745E+00 -8.179E+00 -1.003E+01 -1.222E+01 -1.514E+01 -1.806E+01
-2.141E+01 -2.602E+01 -3.046E+01 -3.398E+01 -4.000E+01 -4.602E+01
-4.602E+01 -4.602E+01
-3.285E+01 -2.534E+01 -2.108E+01 -1.863E+01 -1.752E+01 -1.757E+01
-1.860E+01 -2.022E+01 -2.135E+01 -2.034E+01 -1.711E+01 -1.320E+01
-9.658E+00 -6.792E+00 -4.607E+00 -3.019E+00 -1.928E+00 -1.226E+00
-8.050E-01 -5.613E-01 -4.069E-01 -2.822E-01 -1.637E-01 -6.049E-02
-6.172E-14 -1.136E-02 -1.132E-01 -3.098E-01 -5.937E-01 -9.543E-01
-1.397E+00 -1.900E+00 -2.517E+00 -3.273E+00 -4.206E+00 -5.355E+00
-6.748E+00 -8.408E+00 -1.035E+01 -1.258E+01 -1.511E+01 -1.798E+01
-2.127E+01 -2.507E+01 -2.960E+01 -3.512E+01 -4.199E+01 -5.013E+01
-5.594E+01 -5.463E+01

```

## A6 PROGRAM Y22APOD: INPUT ADMITTANCE OF APODIZED TRANSDUCER

A6.1 Flow Chart



## A6.2 Listing of Y22APOD

```

PROGRAM Y22APOD(INPUT,OUTPUT,PUNCH)
C      THIS PROGRAM COMPUTES THE INPUT ADMITTANCE OF A GIVEN TRANSDUCER
C      SPECIFIED BY IT OVERLAPS AND ZERO CROSSINGS
C      THIS IS APPLICABLE FOR EITHER UNIFORM TRANSDUCERS OR APODISED
C      TRANSDUCER
C      THE OVERLAPS ARE DIVIDED INTO UNIFORM STRIPS BUT WITH UNEQUAL WIDTHS
C
C      THE BASIC EXCITATION CELL FOR THE TRANSDUCERS IS ASSUMED TO BE THE GAP
C      BETWEEN A PAIR OF ELECTRODES.
C      THE CELL INCLUDES AN ELECTRODE HALF WIDTH ON EACH SIDE SET EQUAL TO A
C      QUARTER CELL WIDTH.
C      THE REQUIRED INPUT DATA ARE=
*      XPA(I)= POSITION OF ELECTRODE I IN TRANSDUCER A (IN MILLIMETRES)
*      XLA(I)= OVERLAP LENGTH OF CELL I (IN MILLIMETRES)
*      NA = NUMBER OF GAPS IN TA
*      VSAW= SURFACE VELOCITY (IN MM/SEC)
*      GA = INITIAL GAP WIDTH (IN MM) TA
*      TINC = SAMPLING TIME INTERVAL
*      M = LOG(BASE 2) OF NUMBER OF SAMPLES
C      TITLE= IDENTIFIER OF THE PARTICULAR DELAY LINE
C
C      ETA = CHARACTERISTIC IMPEDANCE OF FREE SPACE IN OHMS
C      EPSI = DIELECTRIC CONSTANT OF FREE SPACE
C      STEP = SPATIAL SAMPLING INTERVAL = TINC*VSAW
C
C      TYPICAL DATA INCLUDED IS FOR FILTER
C
C      * *****
C      * THIS PROGRAM ALSO REQUIRES SUBROUTINE PLT GIVEN IN APPENDIX A8 *
C      * *****
C
C      DECLARATIONS
C
C      DIMENSION B1(50)
C      COMPLEX B(2048)
C      DIMENSION Y11(50,36)
C      DIMENSION FREQ(60)
C      DIMENSION ZRCR(100),OVLAP(100)
C      DIMENSION G(50)
C      DIMENSION ST(100),L(100)
C      DIMENSION XPB(100),XLB(100)
C      REAL MAGDB(60)
C      REAL LAMDA
C      COMMON B,Y11
C
C      *
C      READ 777,TITLE,NA,NB,FO,REDRE,REDRA
777 FORMAT (A9,2I2,E9.2,2F10.2)
C
C      *
C      BASIC PARAMETERS
C      PI=3.141592653589793
C      ETA = 337.
C      EPSI=8.85E-12
C      EPSQ=39.21E-12
C      DELTA=-9.3E-4
C      Z=0
C      VSAW = 3.175E+06
C      TIME = 5.0E-06
C      M = 10
C
C      *
C      DERIVED PARAMETERS
C
C      N=2.*M
C      TINC = TIME/N
C      NA1 = NA+1
C      NB1 = NB+1
C      STEP=TINC*VSAW
C      Y11CON = 2.*PI*(EPSI**2)*DELTA/(1000.*(EPSI+EPSQ))
C      SFCON = PI*(EPSQ*EPSI)/(1.854*EPSI)
C      CORRECTION NEEDED IN REDUCTION RATIO
C      REDRC = REDRE/REDRA
C
C      PRINT 103,TITLE,NA,NB,FO,REDRE,REDRA
103 FORMAT (1H1,44X*CLASSIFICATION OF PROGRAM *A10/
145X*NO OF OVERLAPS IN TRANSDUCER A =*I3/
245X*NO OF OVERLAPS IN TRANSDUCER B =*I3/
345X*CENTR FREQUENCY OF TRANSDUCER A = *E10.2/
445X*ESTIMATED REDUCTION RATIO =*F5.2/
545X*ACTUAL REDUCTION RATIO *F5.2//)
C      CALCULATE THE FREQUENCY IN THE DESIRED RANGE (29.4MHZ TO 39.2MHZ)
C      DF = 1./TIME
C      DO 30 I = 1,50
C      FREQ(I) = DF*(I+146)
30 CONTINUE
C
C      *
C      GENERATE ELECTRODE POSITIONS AND OVERLAPS FOR TRANSDUCER B
C
C      READ 1,(ZRCR(I),I=1,NB1)
1 FORMAT (SE14.8)
C      READ 1,(OVLAP(I),I=1,NB)
C      PRINT 2

```

```

2 FORMAT (1H0,10X*ZEROCROSSINGS AND OVERLAPS ,THE PUNCHED OUTPUT FRO
CM THE PREVIOUS PROGRAM*/
3 FORMAT (15,5XE16.8,5XE16.8)
PRINT 3,(I,ZRCR(I),OVLAP(I),I=1,NB)
PRINT 4,(I,ZRCR(I),I=NB1,NB1)
4 FORMAT (15,5XE16.8)
C CALCULATE ELECTRODE POSITIONS IN MMS
XPB(1) = 254./REDRE
XPB(I) = REDRC*XPB(1)
DO 5 I = 1,NB
XPB(I+1) = XPB(I)+VSAW*(ZRCR(I+1)-ZRCR(I))*REDRC
5 CONTINUE
C CALCULATE OVERLAPS IN MMS CORRESPONDING TO A MAXIMUM OVERLAP OF 5MMS
XYZ = 0.0
DO 6 I = 1,NB
XYZ = AMAX1(ABS(OVLAP(I)),XYZ)
6 CONTINUE
DO 7 I = 1,NB
XLB(I) = ABS(OVLAP(I))*5.0*REDRC/XYZ
7 CONTINUE
C PRINT ELECTRODE POSITIONS AND OVERLAPS
PRINT 8
8 FORMAT (1H0,10X*ELECTRODES POSITIONS AND OVERLAPS IN MMS OF TRANSD
CUCER B*/
DO 9 I = 1,NB
PRINT 10,I,XPB(I),XLB(I)
10 FORMAT (I10,E22.5,E16.5)
9 CONTINUE
PRINT 11 ,(I,XPB(I),I=NB1,NB1)
11 FORMAT (I10,E22.5)
*
C CONSIDER THE OVERLAPS ONLY OVER THE HALF RANGE
NMID = NB1/2
NMID1 = NMID+1
XLB(NMID1) = 0.0
DO 300 I = 1,NMID1
ST(I) = XLB(I)
300 CONTINUE
C ARRANGE THE OVERLAPS IN ASCENDING ORDER
CALL STRIP(NMID1,ST,XLB,L)
PRINT 301
301 FORMAT (1H0,10X*OVERLAPS ARRANGED IN ASCENDING ORDER AND THEIR LOC
*ATIONS IN THE GIVEN ARRAY ARE*/
PRINT 302,(I,ST(I),L(I),I=1,NMID1)
302 FORMAT (I10,F10.5,I10)
C ASSUME ODD NO OF OVERLAPS IN THE TRANSDUCER
EORO = +1.0
CALL UNIWID(NMID1,XLB,ST,L,EORO,XPB,FREQ,STEP,SFCON,-Y11CON,NTAL)
*
C SUM UP THE RADIATION CONDUCTANCE OF ALL THE STRIPS
DO 304 J = 1,50
SUM = 0.0
DO 303 I = 1,NTAL
SUM = SUM + Y11(J,I)
303 CONTINUE
G(J) = SUM
304 CONTINUE
PRINT 305
305 FORMAT (1H1,10X*INPUT CONDUCTANCE OF APOISED TRANSDYCYER IS*/
PRINT 306,(I,FREQ(I),G(I),I=1,50)
306 FORMAT (I10,E15.2,E15.5)
CALL ANORM(50,G)
C CALCULATE THE RADIATION SUSCEPTANCE
CALL RADSUS(50,N,FREQ,G,B1)
*
STOP
END

SUBROUTINE STRIP(N,A,B,IL)
*
C SUBROUTINE STRIP CALCULATES THE GIVEN ABSOLUTE OVERLAPS IN THE ASCENDING
C ORDER STORES THEM IN THE ARRAY A(I) AND THEIR LOCATIONS WHICH ARE STORED
C IN THE ARRAY IL(I)
*
DIMENSION A(2),IL(2),B(2)
*
DO 1 I = 1,N
DO 1 J = I,N
IF(A(J).GE.A(I))GO TO 1
TEMP = A(J)
A(J) = A(I)
A(I) = TEMP
1 CONTINUE
*
C LOCATE THE POSITION OF OVERLAPS IN THE SUPPLIED ARRAY
*
DO 3 I = 1,N
DO 4 J = 1,N
IF(B(J).EQ.0.)GO TO 5

```

```

XYZ = A(I)/B(J)
IF(XYZ.EQ.1.)GO TO 5
GO TO 4
5 IL(I) = J
GO TO 3
4 CONTINUE
3 CONTINUE
*
RETURN
END

SUBROUTINE UNIWID(N,OV,ST,L,EORO,XPB,FREQ,STEP,SFCON,Y11CON,NTAL)
*
C SUBROUTINE UNIWID CALCULATES THE UNIFORM WIDTH OVERLAPS IN EACH STRIP
*
C EORO = +1.0 IF THE TOTAL NO OF OVERLAPS IS ODD IN THE TRANSDUCER
C EORO = -1.0 IF THE TOTAL NO OF OVERLAPS IS EVEN IN THE TRANSDUCER
*
COMPLEX B(2048)
DIMENSION Y11(50,10)
DIMENSION Y(50)
DIMENSION XPB(2),FREQ(2)
DIMENSION XLA(100)
DIMENSION OV(2),ST(2),L(2)
COMMON B,Y11
*
NP = 1024
PI = 4.*ATAN2(1.,1.)
IF(EORO.EQ.+1.0)GO TO 8
IF(EORO.EQ.-1.0)GO TO 9
8 M = 2*N-1
GO TO 10
9 M = 2*N
GO TO 10
10 CONTINUE
PRINTS
5 FORMAT (1H0,10X*UNIFORM-OVERLAPS IN EACH STRIP ARE*/)
NTAL = 0
DO 1 J = 2,N
JJ = J-1
IF(ST(J).EQ.ST(JJ))GO TO 1
NTAL = NTAL + 1
DO 2 I = 2,N
XLA(I-1) = 0.0
XLA(M-I) = 0.0
XLA(2*N-I) = 0.0
2 CONTINUE
IJ = L(J)
DO 3 K = 2,N
IF(OV(IJ).LE.OV(K-1))GO TO 4
GO TO 3
4 XLA(K-1) = ST(J)-ST(JJ)
XLA(M-K) = XLA(K-1)
3 CONTINUE
MM = M-2
PRINT 803
803 FORMAT(40X*GAP WIDTHS ARE*/)
PRINT 6,(I,XLA(I),I=1,MM)
6 FORMAT (8(15,E10.2))
*
* COMPUTE THE RADIATION CONDUCTANCE OF EACH STRIP
*
C ASSUME THAT THE SIGN OF THE FIELD ALTERNATES IN EACH GAP AND THAT THE
C FIRST GAP HAS POSITIVE ELECTRIC FIELD
C ASSUME THAT THE GAP FUNCTION IS FORM SIN(PI/2) TO SIN(3PI/2)
C THE FFT OPERATES ON 2*M POINTS
C GAP FUNCTION FOR EACH STRIP
SIGN=-1
NSTEP = XPB(1)/STEP
NSB=NSTEP
DO 700 NS=1,NSTEP
700 B(NS)=(0.,0.)
DO 701 II = 1,MM
SIGN=-1*SIGN
NSTEP = XPB(II+1)/STEP-NS
NSS=NS+1
NSE=NS+NSTEP
GB = XPA(II+1)-XPA(II)
BMP = SFCON*XLA(II)/GB
DO 702 NS=NSS,NSE
BRG = (NS*STEP-XPB(II))*PI/GB
BR=BMP*SIGN*COS(BRG)
B(NS) = CMPLX(BR,0.)
702 CONTINUE
701 CONTINUE
NSE1=NSE+1
DO 703 NS = NSE1,NP
703 B(NS)=(0.,0.)
C PRINT GAP FUNCTION B

```

```

*
C      COMPUTE THE INTEGRAL TRANSFORM OF EACH STRIP
      DXY=STEP
      CALL BFAST(B,10,-1.0,DXY)
C      CALCULATE THE INPUT ADMITTANCE OF EACH STRIP
      DO 1001 I = 1,50
      Y(I) = Y11CON*FREQ(I)*B(I+147)*CONJG(B(I+147))/(ST(J)-ST(JJ))
1001  CONTINUE
      PRINT 900,NTAL
      900  FORMAT (1H1,40X*INPUT CONDUCTANCE OF STRIP =*15/)
      PRINT 801 ,(I,FREQ(I),Y(I),I=1,50)
      801  FORMAT (110,E15.2,E15.5)
*
      DO 802 IK = 1,50
      Y11(IK,NTAL) = Y(IK)
      802  CONTINUE
C      STORE THE TOTAL NO OF STRIPS
      1  CONTINUE
      7  CONTINUE
      RETURN
      END

      SUBROUTINE ANORM(NQ,Y)
      DIMENSION Y(NQ),X(50)
      XYZ = 0.0
      DO 1 I = 1,NQ
      XYZ = AMAX1(XYZ,ABS(Y(I)))
      1  CONTINUE
      DO 2 I = 1,NQ
      X(I) = ABS(Y(I))/XYZ
      2  CONTINUE
      CALL PLT(NQ,1,X)
      PRINT 3
      3  FORMAT (1H0,10X*NORMALISED RADIATION CONDUCTANCE IN LINEAR SCALE
      *MAXIMUM AMPLITUDE IS 100 UNITS*/)
      RETURN
      END

      SUBROUTINE RADSUS(NQ,NP,FREQ,G,B1)
*
C      SUBROUTINE RADSUS CALCULATES THE RADIATION SUSCEPTANCE KNOWING THE
C      RADIATION CONDUCTANCE. THIS IS OBTAINED BY JUST TAKING THE HILBERT
C      TRANSFORM OF THE RADIATION CONDUCTANCE.
*
C      HILBERT TRANSFORM IS PERFORMED RATHER IN AN INDIRECT WAY
*
      DIMENSION FREQ(2),G(2),B1(2)
      COMPLEX B(2048)
      DIMENSION Y11(50,50)
      COMPLEX Z
      COMMON B,Y11
*
      TIME = 5.0E-06
      DT = TIME/NP
      DF = 1./TIME
      N1 = NP/2
      N2 = N1+1
      NS = 2*NP
*
      DO 10 I = 1,NS
      B(I) = (0.,0.)
      10  CONTINUE
      DO 4 I = 1,NQ
      IT = I+147
      B(IT) = CMPLX(G(I),0.0)
      B(NS+2-IT) = CONJG(B(IT))
      4  CONTINUE
      DXY = DF
C      TRANSFORM TO A Z PLANE FOR EXAMPLE TO GET THE EVEN FUNCTION OF Z
      CALL BFAST(B,11,+1.0,DXY)
      Z = CMPLX(0.,-1.0)
      DO 5 I = 2,NP
      B(I) = Z*B(I)
      B(NS+2-I) = CONJG(B(I))
      5  CONTINUE
      B(1) = Z*B(1)
      B(NP+1) = -Z*B(NP+1)
*
      DT = TIME/NS
      DXY = DT
      CALL BFAST(B,11,-1.0,DXY)
      PRINT 7
      7  FORMAT (1H1,40X*RADIATION SUSCEPTANCE B(W) IS*/)
      PRINT 8,(I,FREQ(I),B(I+147),I=1,NQ)
      8  FORMAT (110,3E15.3)
      DO 11 I = 1,NQ
      B1(I) = REAL(B(I+147))
      11  CONTINUE

```



```

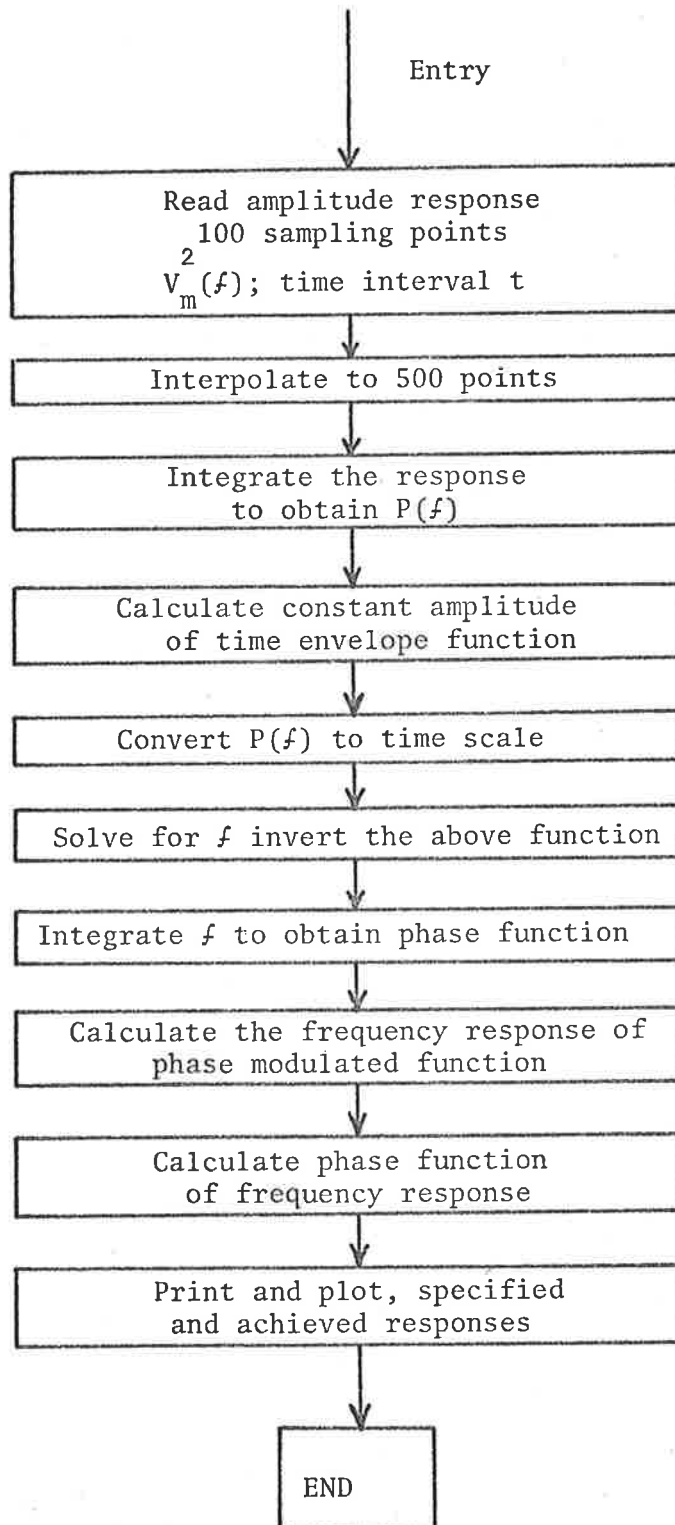
*
*          6
*          FAST 170
*
*          DXY=1./(DXY*N)
*
*          RETURN
*          END BFAST
*          SUBROUTINE TABLE(M)
*          COMMON /TAB/TC(11),TS(11)
*          PI=4.0*ATAN2(1.0,1.0)
*          DO 1 I=1,M
*          TC(I)=COS(PI/(2*(I-1)))
*          TS(I)=SIN(PI/(2*(I-1)))
*          RETURN
*          END
*          SUBROUTINE CON(M)
*          INTEGER A,T
*          COMMON /PERM/A(2048)
*          N=2**M
*          NV2=N/2
*          NM1=N-1
*          J=1
*          DO 1 I=1,N
*          A(I)=I
*          DO 7 I=1,NM1
*          IF(I.GE.J)GOTO5
*          T=A(J)
*          A(J)=A(I)
*          A(I)=T
*          K=NV2
*          IF(K.GE.J)GOTO7
*          J=J-K
*          K=K/2
*          GOTO 6
*          J=J+K
*          RETURN
*          END
*
*          CON 700
*          CON 690
*          CON 760
*          CON 10
*
*          CON 30
*          CON 40
*          CON 50
*          CON 60
*          CON 70
*          CON 80
*          CON 10
*          CON 20
*
*          CON 40
*          CON 50
*          CON 60
*          CON 70
*          CON 80
*          CON 90
*          CON 100
*          CON 110
*          CON 120
*          CON 130
*          CON 140
*          CON 150
*          CON 160
*          CON 170
*          CON 180
*          CON 190
*          CON 200
*          CON 210
*          CON 220

```

C DATA

		25.40			
P/09/1/P2087134.20E+06	25.2				
1.94354258E-06	1.95475119E-06	1.98077672E-06	1.99676531E-06	2.01302754E-06	
2.03224573E-06	2.05198707E-06	2.06779797E-06	2.08306581E-06	2.09797703E-06	
2.11246387E-06	2.11506609E-06	2.12852221E-06	2.14341508E-06	2.17040220E-06	
2.18646887E-06	2.20180337E-06	2.21701049E-06	2.23252043E-06	2.24864718E-06	
2.26766455E-06	2.28626938E-06	2.30231209E-06	2.31770779E-06	2.33294482E-06	
2.34789831E-06	2.36062622E-06	2.37560815E-06	2.39017968E-06	2.40477428E-06	
2.41939012E-06	2.43402377E-06	2.44867147E-06	2.46332963E-06	2.47799499E-06	
2.49266454E-06	2.50733546E-06	2.52200501E-06	2.53667037E-06	2.55132853E-06	
2.56597623E-06	2.58060988E-06	2.59522572E-06	2.60982032E-06	2.62439185E-06	
2.63937378E-06	2.65210169E-06	2.66705518E-06	2.68229221E-06	2.69768791E-06	
2.71373062E-06	2.73233545E-06	2.75135282E-06	2.76747957E-06	2.78298951E-06	
2.79819663E-06	2.81353113E-06	2.82959780E-06	2.85658492E-06	2.87147779E-06	
2.88493391E-06	2.88753613E-06	2.90202297E-06	2.91693419E-06	2.93220203E-06	
2.94801293E-06	2.95775427E-06	2.98697246E-06	3.00323469E-06	3.01922328E-06	
3.04524881E-06	3.05645742E-06				
1.04201507E-02	-1.12722360E-02	9.91714911E-03	-8.88984749E-03	6.02847900E-03	
-4.99233013E-03	5.27702943E-03	-4.78411253E-03	3.03438495E-03	-1.01680096E-03	
1.63802469E-05	-7.88514009E-04	1.46603170E-03	-1.59909721E-03	2.51320089E-03	
-4.56063397E-03	5.85360130E-03	-6.27833231E-03	5.52453913E-03	-4.58817900E-03	
4.65853502E-03	-6.03726382E-03	6.93396254E-03	-7.10267106E-03	6.36436215E-03	
-4.96352437E-03	1.27201982E-02	-1.61029247E-02	1.99400226E-02	-2.39359564E-02	
2.78809952E-02	-3.15429913E-02	3.46890610E-02	-3.71081676E-02	3.86321131E-02	
-3.98202359E-02	3.86321131E-02	-3.71081676E-02	3.46890610E-02	-3.15429913E-02	
2.78809952E-02	-2.39359564E-02	1.99400226E-02	-1.61029247E-02	1.27201982E-02	
-4.96352437E-03	6.36436215E-03	-7.10267106E-03	6.93396254E-03	-6.03726382E-03	
4.65853502E-03	-4.58817900E-03	5.52453913E-03	-6.27833231E-03	5.85360130E-03	
-4.56063397E-03	2.51320089E-03	-1.59909721E-03	1.46603170E-03	-7.88514009E-04	
1.63802469E-05	-1.01680096E-03	3.03438495E-03	-4.78411253E-03	5.27702943E-03	
-4.99233013E-03	6.02847900E-03	-8.88984749E-03	9.91714911E-03	-1.12722360E-02	
1.04201507E-02					

## A7 PROGRAM CHIRPTR: FILTER SYNTHESIS USING CHIRPED TRANSDUCERS

A7.1 Flow Chart

## A7.2 Listing of CHIRPTR

```

PROGRAM CHIRPTR(INPUT,OUTPUT,PUNCH)
*
C THIS PROGRAM CALCULATES THE NECESSARY PHASE FUNCTION FOR DESIGNING CHIRPED
C TRANSDUCERS WITH A GIVEN FREQUENCY RESPONSE.
C TYPICAL FREQUENCY RESPONSE CHOOSEN IS THAT OF A TV IF FILTER.
C * *****
C * THIS PROGRAM ALSO REQUIRES SUBROUTINE PLT GIVEN IN APPENDIX A8 *
C * *****
*
C DECLARATIONS
*
REAL MAG(100)
DIMENSION FX(500),YX(500),T(500),PHAS(500)
DIMENSION AMAGDB(100),FREQ(100),XNORM(100)
DIMENSION YY(4100),XX(2)
COMPLEX C(4100)
COMMON XX,YY,PHAS,C,FX,YX,T,AMAGDB
*
PI = 4.*ATAN2(1.,1.)
NQ = 100
TIME = 10.0E-06
DF = 1./TIME
TTOTAL = 40.0E-06
*
C CHOOSE AN ARBITRARY MAXIMUM AMPLITUDE OF 100 UNITS
READ 10,(MAG(I),I=1,NQ)
10 FORMAT (8F10.5)
DO 20 I = 1,NQ
FREQ(I) = DF*(I+291)
20 CONTINUE
PRINT 21
21 FORMAT (1H1,10X*INPUT OF SPECIFIED RESPONSE IS*/)
CALL ANORM(NQ,FREQ,MAG,XNORM)
*
DO 22 I = 1,NQ
AMAGDB(I) = 20.*ALOG10(XNORM(I))-40.
22 CONTINUE
CALL PLT(NQ,1,MAG)
CALL PLT(NQ,1,AMAGDB)
C ASSUME Y21 IS PROPORTIONAL TO THE GIVEN MAGNITUDE RESPONSE SQUARED
*
C LINEAR INTERPOLATE THE RESPONSE TO NR POINTS
NR = 500
CALL LININT(NQ,NR,FREQ,MAG,FX,YX,MT)
*
C INTEGRATE THE RESPONSE
CALL QTFG(FX,YX,T,MT)
*
C T IS THE FUNCTION OBTAINED AFTER INTEGRATION
C VERTICAL AXIS REPRESENTS TIME AND HORIZONTAL AXIS REPRESENTS FREQUENCY
*
PRINT 33
33 FORMAT (1H0,10X*INTEGRATED RESPONSE OF THE GIVEN MODULUS SQUARED
*FUNCTION IS*/)
CALL QIKPLT(FX,T,MT,1,11H*FREQUENCY*,10H*UFSQUARE*)
*
C USE PARSEVALS THEOREM TO DETERMINE THE MAGNITUDE OF TIME FUNCTION
AMAG = T(MT)/TTOTAL
PRINT 34,AMAG
34 FORMAT (1H0,10X*UETSQUARE =*E15.5/)
C CONVERT INTO ACTUAL TIME SCALE
DO 40 I = 1,MT
T(I) = T(I)/AMAG
40 CONTINUE
*
C PLOT THE INTERGRATED RESPONSE
PRINT 32
32 FORMAT (1H0,10X*INTERGRATED RESPONSE CONVERTED INTO TIME SCALE IS
1*/)
*
CALL QIKPLT(FX,T,MT,1,11H*FREQUENCY*,6H*TIME*)
C INVERT THE FUNCTION BY CHANGING INDIPENDENT VARIABLE INTO DEPENDENT
C VARIABLE AND DEPENDENT VARIABLE INTO INDEPENDENT VARIABLE
*
PRINT 41
41 FORMAT (1H0,10X*INVERTING THE FUNCTION */)
*
CALL QIKPLT(T,FX,MT,1,6H*TIME*,11H*FREQUENCY*)
C INTEGRATE THE INVERTED FUNCTION TO GIVE RISE TO PHASE FUNCTION
*
CALL QTF0(T,FX,PHAS,MT)
*
DO 60 I = 1,MT
PHAS(I) = 2.*PI*PHAS(I)
60 CONTINUE
*
PRINT 59
59 FORMAT (1H0,10X*PHASE FUNCTION IS*/)
CALL PLT(MT,1,PHAS)
PRINT 61,MT,PHAS(MT)

```



```

61 FORMAT (1H0,10X*INDEX*110,10X*NO OF RADIANS IN PHASE FUNCTION ARE
1*E15.5)
*
C   CALCULATE THE FOURIER TRANSFORM OF THIS MAGNITUDE-PHASE FUNCTION
*
C   CALL FOURIER(MT,FREQ,XNORM,AMAG,NQ,TTOTAL)
*
C   CALCULATE THE FREQUENCY PHASE FUNCTION
*
C   CALL FREOPHS(NQ,MT,FREQ)
*
STOP
END

SUBROUTINE FINPOS(NQ,T,PHAS,FLOC,PHASE,NFING)
DIMENSION GAP(100)
DIMENSION T(2),PHAS(2)
DIMENSION PHASE(2),FLOC(2)
PI = 4.*ATAN2(1.,1.)
NQ1 = NQ-1
XMIN = PI
*
C   DIVIDE THE PHASE FUNCTION INTO MINIMUM INTEGRALS OF 2 PI
C   ASSUME A LINEAR RELATION BETWEEN PHASE AND TIME BETWEEN ANY TWO
C   CONSEQUETIVE INTERVALS
*
J = 0
DO 30 I = 1,NQ1
IF(XMIN.GT.PHAS(I+1))GO TO 30
SLOP = (PHAS(I+1)-PHAS(I))/(T(I+1)-T(I))
CONST = PHAS(I+1)-SLOP*T(I+1)
41 J = J+1
XYZ = J*XMIN
IF(XYZ.LE.PHAS(I+1))GO TO 40
J = J-1
GO TO 30
40 FLOC(J) = (XYZ-CONST)/SLOP
PHASE(J) = XYZ
GO TO 41
30 CONTINUE
C   STORE THE LAST FINGER LOCATION
NFING = J
MFING = NFING-1
C   PRINT THE FINGER LOCATIONS
DO 52 I = 1,MFING
GAP(I) = FLOC(I+1)-FLOC(I)
52 CONTINUE
PRINT 50
50 FORMAT (1H1,10X*FINGER LOCATIONS AND THEIR PHASES AT THE MULTIPLES
* OF PI*/)
PRINT 51,(I,FLOC(I),PHASE(I),GAP(I),I=1,MFING)
51 FORMAT (I10,3E15.5)
PRINT 53,(NFING,FLOC(NFING),PHASE(NFING))
53 FORMAT (I10,2E15.5)
PRINT 70,(PHASE(I),I=1,NFING)
70 FORMAT (6E13.5)
RETURN
END

SUBROUTINE QTFG(X,Y,Z,NDIM)
*DECK D1053
C
C
C   .....
C
C   SUBROUTINE QTFG
C
C   PURPOSE
C   TO COMPUTE THE VECTOR OF INTEGRAL VALUES FOR A GIVEN
C   GENERAL TABLE OF ARGUMENT AND FUNCTION VALUES.
C
C   USAGE
C   CALL QTFG (X,Y,Z,NDIM)
C
C   DESCRIPTION OF PARAMETERS
C   X - THE INPUT VECTOR OF ARGUMENT VALUES.
C   Y - THE INPUT VECTOR OF FUNCTION VALUES.
C   Z - THE RESULTING VECTOR OF INTEGRAL VALUES. Z MAY BE
C       IDENTICAL WITH X OR Y.
C   NDIM - THE DIMENSION OF VECTORS X,Y,Z.
C
C   REMARKS
C   NO ACTION IN CASE NDIM LESS THAN 1.
C
C   SUBROUTINES AND FUNCTION SUBPROGRAMS REQUIRED
C   NONE
C
C   METHOD
C   BEGINNING WITH Z(1)=0, EVALUATION OF VECTOR Z IS DONE BY

```

```

C          MEANS OF TRAPEZOIDAL RULE (SECOND ORDER FORMULA).
C          FOR REFERENCE, SEE
C          F.B.HILDEBRAND, INTRODUCTION TO NUMERICAL ANALYSIS,
C          MCGRAW-HILL, NEW YORK/TORONTO/LONDON, 1956, PP.75.

```

```

C          SOURCE   /IBM
C          .....

```

```

C          DIMENSION X(1),Y(1),Z(1)
C
C          SUM2=0.0
C          IF(NDIM-1)4,3,1
C
C          INTEGRATION LOOP
C          1 DO 2 I=2,NDIM
C            SUM1=SUM2
C            SUM2=SUM2+0.5*(X(I)-X(I-1))*(Y(I)+Y(I-1))
C          2 Z(I-1)=SUM1
C          3 Z(NDIM)=SUM2
C          4 RETURN
C          END

```

```

*          SUBROUTINE PARINT(NQ,NP,X,Y,ORD,ABSA,NT)
*
*          DIMENSION X(2),Y(2),ABSA(2),ORD(2)
*
*          NQ1 = NQ-1
*          XINCR = (X(NQ)-X(1))/NP
*          XMIN = X(1)
*          J = 0
*          DO 30 I = 1,NQ1
*            IF(XINCR.GT.X(I+1))GO TO 30
*            SLOP = (Y(I+1)-Y(I))/(X(I+1)**2-X(I)**2)
*            CONST = Y(I)-SLOP*X(I)**2
*          41 J = J+1
*            XYZ = J*XINCR+XMIN
*            IF(XYZ.LE.X(I+1))GO TO 40
*            J = J-1
*            GO TO 30
*          40 Z = SLOP*XYZ**2+CONST
*            ABSA(J) = Z
*            GO TO 41
*          30 CONTINUE
C          STORE THE LAST INTERPOLATION POINT
C          NT = J
C          PRINT 59,NT
*          59 FORMAT (1H0,10X*TOTAL NO OF INTERPOLATION POINTS ARE*110)
*          ORD(1) = XINCR
*          ORD(2) = XYZ - XINCR
*
*          PRINT 60,ORD(1),ABSA(1)
*          60 FORMAT (1H0,10X*FIRST INTERPOLATION POINT IS*2E20.8)
*          PRINT 61,ORD(2),ABSA(NT)
*          61 FORMAT (1H0,10X*LAST INTERPOLATION POINT IS*2E15.5)
*
*          RETURN
*          END

```

```

*          SUBROUTINE LININT(NQ,NP,X,Y,ORD,ABSA,NT)
*
*          DIMENSION X(2),Y(2),ABSA(2),ORD(2)
*
*          NQ1 = NQ-1
*          XINCR = (X(NQ)-X(1))/NP
*          XMIN = X(1)
*          J = 0
*          DO 30 I = 1,NQ1
*            IF(XINCR.GT.X(I+1))GO TO 30
*            SLOP = (Y(I+1)-Y(I))/(X(I+1)-X(I))
*            CONST = Y(I+1)-SLOP*X(I+1)
*          41 J = J+1
*            XYZ = J*XINCR+XMIN
*            IF(XYZ.LE.X(I+1))GO TO 40
*            J = J-1
*            GO TO 30
*          40 Z = SLOP*XYZ+CONST
*            ABSA(J) = Z
*            ORD(J) = XYZ
*            GO TO 41
*          30 CONTINUE
C          STORE THE LAST INTERPOLATION POINT
C          NT = J
C          PRINT 59,NT
*          59 FORMAT (1H0,10X*TOTAL NO OF INTERPOLATION POINTS ARE*110)
*
*          PRINT 60,ORD(1),ABSA(1)

```

```

60 FORMAT (1H0,10X*FIRST INTERPOLATION POINT IS*2E15.5)
   PRINT 61,ORO(NT),ABSA(NT)
61 FORMAT (1H0,10X*LAST INTERPOLATION POINT IS*2E15.5)
*
   RETURN
   END

SUBROUTINE ANORM(NQ,FREQ,Y,X)
DIMENSION FREQ(2),Y(2),X(2)
XYZ = 0.0
DO 1 I = 1,NQ
XYZ = AMAX1(XYZ,ABS(Y(I)))
1 CONTINUE
DO 2 I = 1,NQ
X(I) = 100.*ABS(Y(I))/XYZ
2 CONTINUE
PRINT 4,(I,FREQ(I),Y(I),X(I),I=1,NQ)
4 FORMAT (I10,3E20.5)
PRINT 3
3 FORMAT (1H0,10X*NORMALISED MAGNITUDE GRAPH IN LINEAR SCALE OF MAXI
1MUM AMPLITUDE 100 UINTS*//)
RETURN
END

SUBROUTINE FREOPHS(NQ,MT,FREQ)
*
DIMENSION AMAGDB(100)
DIMENSION FREQ(100)
DIMENSION FX(500),YX(500),T(500),PHAS(500)
DIMENSION YY(4100),XX(2)
COMPLEX C(4100)
COMMON XX,YY,PHAS,C,FX,YX,T,AMAGDB
*
PI = 4.*ATAN2(1.,1.)
C
CALCULATE THE FREQUENCY PHASE FUNCTION
PRINT 20
20 FORMAT (1H0,10X*FREQUENCY PHASE FUNCTION IS*//)
*
CALL QTFG(FX,T,YX,MT)
*
C
CALCULATE THE PHASE AT THE REQUIRED FREQUENCY INCREMENTS
DO 10 I = 1,MT
YX(I) = -2.*PI*YX(I)
10 CONTINUE
DO 30 I = 1,NQ
II = 5*I
PRINT 40,I,FREQ(I),YX(II)
30 CONTINUE
40 FORMAT (I10,2E15.3)
CALL PLT(NQ,I,YX)
*
RETURN
END

SUBROUTINE FOURIER(NT,FREQ,XNORM,AMAG,NQ,TTOTAL)
*
DIMENSION AMAGDB(100)
COMPLEX C(4100)
DIMENSION YY(4100),XX(2)
DIMENSION FX(500),YX(500),T(500),PHAS(500)
DIMENSION ADB(100),Z(100)
DIMENSION FREQ(2),XNORM(2)
COMMON XX,YY,PHAS,C,FX,YX,T,AMAGDB
*
TIME = 40.0E-06
PI = 4.*ATAN2(1.,1.)
M = 12
NP = 2**M
DT = TIME/NP
DF = 1./TIME
*
CALL PARINT(NT,NP,T,PHAS,XX,YY,MT)
*
DO 20 I = 1,NP
C(I) = (0.,0.)
20 CONTINUE
DO 21 I = 1,MT
X = YY(I)
C(I) = CMPLX(COS(X),SIN(X))
21 CONTINUE
DXY = DT
*
CALL RFAST(C,M,-1.,DXY)
*
C
CALCULATE THE FREQUENCY RESPONSE IN THE RANGE OF INTEREST AT THE
INCREMENTS OF 100 KHZ
DO 50 I = 1,NQ

```



```

*
*      DXY=1./(DXY*N)
*
RETURN
END BFAST
SUBROUTINE TABLE(M)
COMMON /TAB/TC(12),TS(12)
PI=4.0*ATAN2(1.0,1.0)
DO I=1,M
1   TC(I)=COS(PI/(2*(I-1)))
    TS(I)=SIN(PI/(2*(I-1)))
RETURN
END
SUBROUTINE CON(M)
INTEGER A,T
COMMON /PERM/ A(4096)
N=2**M
NV2=N/2
NM1=N-1
J=1
DO I=1,N
1   A(I)=I
    DO 7 I=1,NM1
        IF(I.GE.J)GOTO5
        T=A(J)
        A(J)=A(I)
        A(I)=T
5     K=NV2
6     IF(K.GE.J)GOTO7
        J=J-K
        K=K/2
        GOTO 6
7     J=J+K
RETURN
END

```

	6		
	FAST	170	
	FAST	700	
	FAST	690	
	FAST	760	
	TABL	10	
	TABL	30	
	TABL	40	
	TABL	50	
	TABL	60	
	TABL	70	
	TABL	80	
	CON	10	
	CON	20	
	CON	40	
	CON	50	
	CON	60	
	CON	70	
	CON	80	
	CON	90	
	CON	100	
	CON	110	
	CON	120	
	CON	130	
	CON	140	
	CON	150	
	CON	160	
	CON	170	
	CON	180	
	CON	190	
	CON	200	
	CON	210	
	CON	220	

```

*
C      DATA
*
0.5      0.55      1.0      2.0      3.5      5.5      7.5      9.5
11.75    13.5     15.5     17.0     18.0     17.5     16.0     13.0
8.0      5.0       1.0      3.75    7.5      11.0     15.5     19.75
24.5     30.0     35.5     41.5     48.0     54.5     58.0     65.0
70.0     75.0     79.0     82.75   86.0     89.25   91.5     93.75
95.5     96.5     97.5     98.5     99.0     99.5     99.75   100.0
100.0    100.0    99.85    99.75   99.5     99.0     98.5     97.75
97.0     96.0     95.0     93.5     91.5     89.5     87.0     84.0
81.5     78.25    75.0     72.0     69.0     65.0     61.0     57.5
54.0     50.0     46.0     42.0     39.0     35.0     31.5     27.5
24.5     20.0     17.5     15.0     12.5     10.25    8.5      6.5
5.0      4.0      3.0      2.5     2.0     1.5      1.0      0.75
0.65     0.5      0.4      0.35    0.25

```



	IF (NPOINTS.GT.60.AND.NPOINTS.LE.128) GOTO 221	2	
	PRINT99		PLOT 790
	GOTO 222		PLOT 800
			PLOT 810
			PLOT 820
221	CONTINUE		PLOT 840
	PRINT 93		PLOT 850
	PRINT94		PLOT 860
			PLOT 870
222	CONTINUE		PLOT 880
	PRINT23,FMIN,FMAX		PLOT 890
23	FORMAT( 5X,E10.2,35X,40H(1) *** (2) *** (3) XXX (4) ??? ,		
	A35X,E10.2/10X,***,119X,***)		
			PLOT 910
			PLOT 920
30	K=1		
	D0311=2,120		
31	L(I)=1H-		PLOT 940
	D0321=1,121,10		
32	L(I)=1H:		PLOT 960
	L(LZERO)=1H:		
	N=1		PLOT1000
	II=(K-1)*NDIV+1		
	GOTO (304,303,302,301) NF		
301	M=F(A4(II))		
	L(M)=B(N,4)		
302	M=F(A3(II))		
	L(M)=B(N,3)		
303	M=F(A2(II))		
	L(M)=B(N,2)		
304	M=F(A1(II))		
	L(M)=B(N,1)		
	PRINT33,II,L		PLOT1010
	IF (K.NE.1) GOTO 36		PLOT1020
			PLOT1030
	D03121=1,121		PLOT1050
312	L(I)=1H		PLOT1070
	L(LZERO)=1H:		
	L(1)=L(121)=1H:		
	NP1=NPOINTS-1		PLOT1080
			PLOT1090
			PLOT1100
			PLOT1170
	D0351=2,NP1		
	II=(I-1)*NDIV+1		
	D034N=1,2		
	GOTO (324,323,322,321) NF		
321	M=F(A4(II))		
	L(M)=B(N,4)		
322	M=F(A3(II))		
	L(M)=B(N,3)		
323	M=F(A2(II))		
	L(M)=B(N,2)		
324	M=F(A1(II))		
	L(M)=B(N,1)		
	IF (N.EQ.2) GOTO 34		
	PRINT33,II,L		
33	FORMAT(15, 5X,121A1)		PLOT1200
34	CONTINUE		
	L(1)=L(121)=1H:		PLOT1220
	L(LZERO)=1H:		PLOT1230
35	CONTINUE		PLOT1240
			PLOT1250
			PLOT1260
	K=NPOINTS		
	GOTO 30		
C			
36	CONTINUE		PLOT1280
	RETURN		PLOT1290
			PLOT1300
			PLOT1310
93	FORMAT(1H2)		PLOT1320
94	FORMAT(1H1/31(1H0/))		PLOT1330
99	FORMAT(1H1)		PLOT1340
			PLOT1350
	END		

## APPENDIX B

PHOTOFABRICATION TECHNIQUES

The experimental facilities for the prototype manufacture of surface acoustic wave delay lines are entirely developed by the research students who worked\*or are working (the author himself) in the Department under the supervision and collaboration of Dr. P.H. Cole. The author has contributed in calibrating the optical system, i.e. the two cameras for the various reduction ratios and developed an optimum procedure for producing the final transparencies. The various steps followed in the manufacture of delay lines are briefly given below.

B1. Preparation of the Artwork

Preparation of the artwork is discussed to a great extent in Section 4.3.1. Simple patterns can be directly cut onto the Rubylith sheet by hand and more complex patterns can be generated by a computer. Therefore, the essential features of the artwork are,

Hand-cut drafting mask	..	Rubylith D3R 40" wide rolls
	OR	
XY-Plotter	..	30" Calcom drum-plotter with increamental drive at 250 steps per inch
Drawing surface	..	Matte Cellulose Triacetate
Drawing ink	..	Calcomp GP1 black ink
Copy-board working area	..	30" x 40"
Illumination	..	6 apple-green 48" flourescent tubes
Filter	..	Kodak Yellow Sheetting
Diffuser	..	¼" White Opalescent Perspex 4" behind glass
Screen	..	3/8" glass plate

B2. First Stage Reduction Camera

Lens	..	Wray 12" f/10 process copying optimized for 4 to 1
Reduction range	..	2½X to 5X
Film size	..	10" x 8"

\* Dr. P.V.H. Sabine and Dr. A.S. Burgess



Film type	..	Kodalith Ortho Type 3 on a 0.007" ester base
Film support	..	Vacuum hold-down
Working area	..	9" x 7"

The first-stage reduction camera mounted on the carriage and the copy-board is shown in Figure B1.

### Processing

The processing indicated here is suitable for patterns drawn on the 30" Matte Cellulose Triacetate paper with the Calcom GP1 black ink.

Cleaning the film	..	Gas blast from 50 p.s.i. filtered dry nitrogen supply
Expose	..	1 second at f32
Develop	..	5 min. in Kodak D19 Developer at 68° F
Stop	..	30 sec. in Kodak Stop Bath
Fix	..	2 min. in Kodak Fixer
Rinse	..	5 min. in running water
Clearing agent	..	2 min. in Kodak Hypo Clearing Agent
Rinse	..	5 min. in running water
Wetting agent	..	30 sec. in Kodak Photoflo
Dry	..	dry suspended in laminar- flow clean cabinet

### Contact Printing

For contact printing the same set-up is used viz., the first stage reduction camera and the copy-board illumination. The same size and type of film is used with the emulsion side facing with that of the transparency, vacuum held in the camera and then exposed to 1 sec. at f/11, with bare illumination of the copyboard. The exposed film is then processed according to the instructions mentioned in 'Processing' step.

### B3. Second Stage Reduction Camera

Lens	..	Wray 3" f4 processing copying optimized for 25 to 1
------	----	--

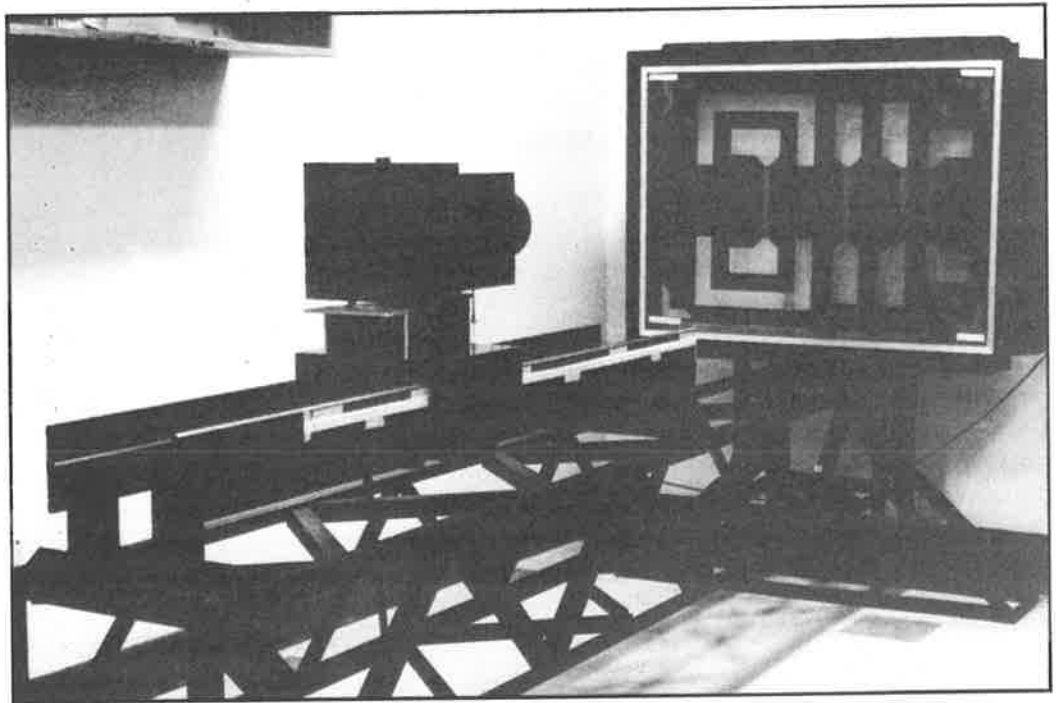


Figure B1 Optical bench system and first-stage reduction camera.

## B3

Reduction range	..	20X to 35X
Plate size	..	2" x 2" glass plates
Type of plates	..	Kodak High Resolution Plates
Plate support	..	Spring pressure against 3-point support studs defining image plane
Working area	..	$\frac{3}{8}$ " x $\frac{3}{8}$ "

The second stage camera mountable on the same carriage board is shown in Figure B2.

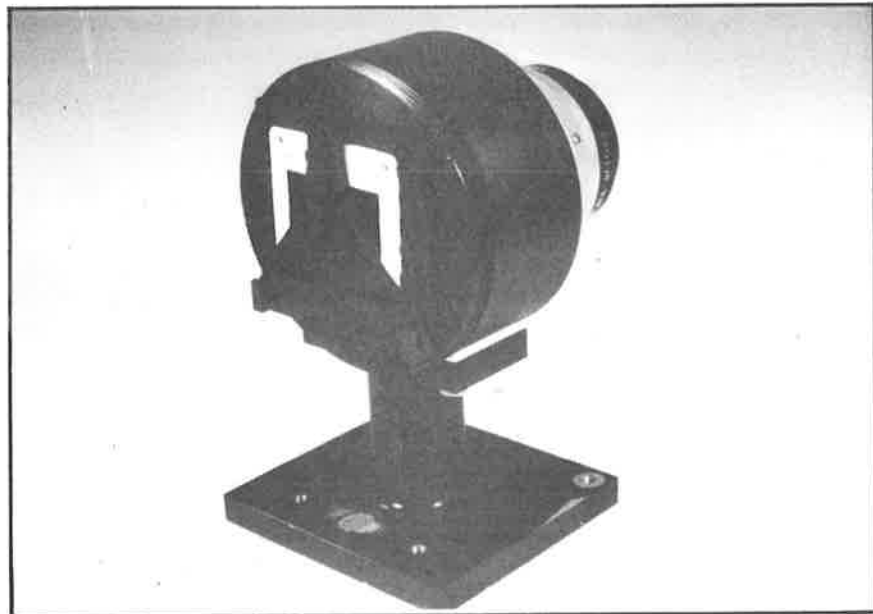
Processing

Clean plates	..	Gas blast from 50 p.s.i. dry nitrogen supply
Expose	..	120 sec. at f5.6
Filtration	..	All chemicals vacuum filtered through No. 1 paper
Soaking	..	Soak exposed film in distilled water for 2 min. at 68°F
Develop	..	5 min. in Kodak D19 Developer at 68°F
Stop	..	30 sec. in Kodak Stop Bath
Fix	..	45 sec. in Kodak Fixer
Wash	..	30 sec. in running distilled water
Clear	..	1½ min. in Hypo Clearing Agent
Rinse	..	5 min. in running distilled water
Wetting agent	..	30 sec. in Kodak Photoflo
Dry	..	Air dry standing vertical in laminar-flow clean cabinet

If the pattern is designed to a single stage reduction ratio, then the exposure timing is different than that presented here. Typical value in such case was found to be equal to 40 sec. at f5.6. Note that no reversal process (contact printing) is necessary in this situation and this saves considerable amount of time in photographic process.



(a)



(b)

Figure B2 Second stage reduction camera (a) front view, and  
(b) rear view.

#### B4. Substrate Preparation

Polished crystals were obtained from Sawyer Research Products, Inc., (U.S.A.), however, clean dust free surfaces are necessary for good adhesion of the aluminium metalization to the substrate and the cleaning procedure adopted here is as follows:

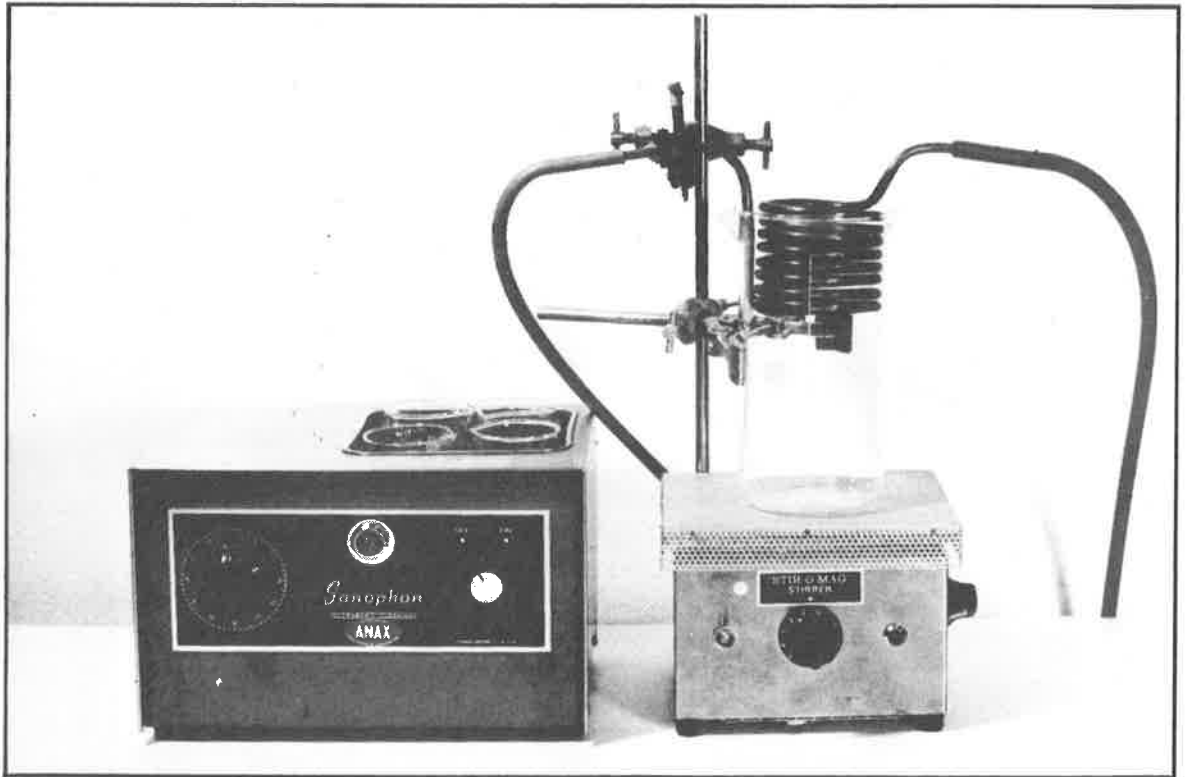
1st cleaning	..	2 min. ultrasonic cleaning with Trichlorethylene
2nd cleaning	..	2 min. ultrasonic cleaning with Decon 75 detergent solution
3rd cleaning	..	2 min. ultrasonic cleaning with distilled water
4th cleaning	..	2 min. ultrasonic cleaning with isopropyl alcohol
5th cleaning	..	2 min. ultrasonic cleaning with Analar Diethyl Ether
final cleaning	..	Immersion in a vapour bath

The ultrasonic cleaning bath and the vapour degreasing bath used for this purpose are shown in Figure B3. It is to be noted that two or three repetitions in the final cleaning, i.e. in the vapour degreasing bath, may be necessary for obtaining a fairly clean surface.

#### B5. Metal Coating

After final cleaning in the vapour degreasing bath, the crystals are then transferred on the substrate heater block, which has been previously arranged in the vacuum coating unit. The required amount of metalization is estimated and the tungsten filament is loaded accordingly before transferring the substrate onto the heater block and then the vacuum chamber is sealed carefully. The metalization apparatus arranged in the vacuum coating unit is shown in Figure B4. The coating of the specimens is as follows:

- (1) Pump down to less than 0.2 torr. with the rotary pump, switch on the diffusion pump, and maintain this pressure with a gas inlet valve.
- (2) The crystal surfaces are further cleaned by applying an ionic glow discharge, obtained by applying a high voltage (3kV at 8mA) between high-purity aluminium electrodes. The glow discharge is run for about 10 minutes.
- (3) Heat the crystals to 200°C. The heater upon which the crystals are placed, contains 4 quartz iodide lamps each rated 100W and run at 10V, 15A DC. The block temperature is monitored using a chrome-alumel thermocouple.



(a)

(b)

Figure B3 Substrate cleaning apparatus (a) ultrasonic cleaning bath and (b) vapour degreasing bath.

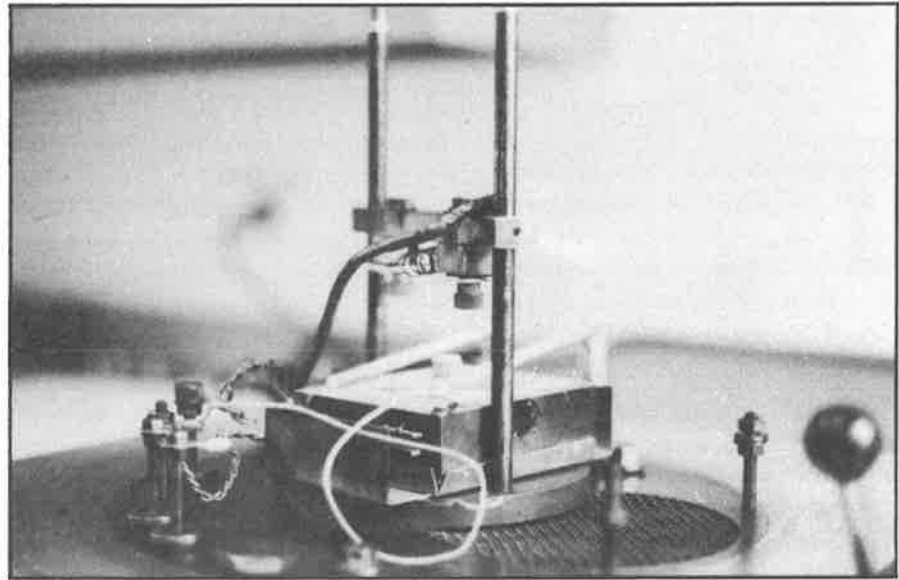


Figure B4 Metalization apparatus arranged in the vacuum coating unit.

- (4) Close the gas inlet and evacuate to less than  $5 \times 10^{-4}$  torr.
- (5) The tungsten filament is heated slowly, so that the aluminium wire warped around the filament is melted.
- (6) Evaporate the aluminium quickly (to avoid grain growth) using 25A for about 10 seconds.
- (7) Switch off the unit and open the flap valve to let the air in for cooling the substrates.
- (8) Transfer the crystals into the laminar-flow clean cabinet for photofabrication.

## B6. Photoetching

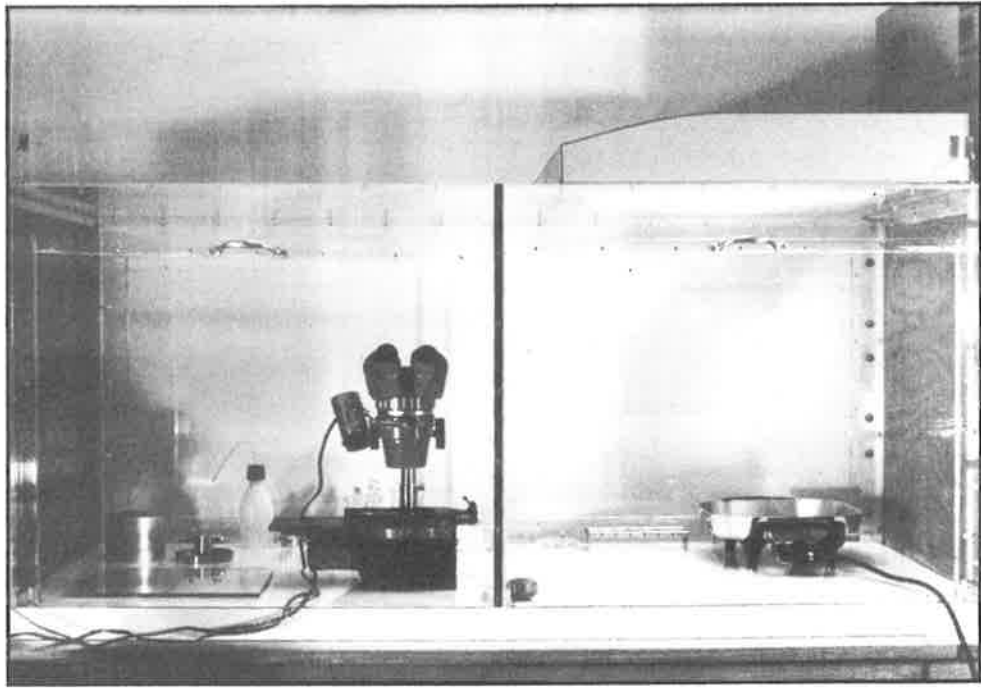
The method used to produce the electrode patterns on the substrates involves contact-printing the transparency onto a thin film of photoresist spread over the metalized substrate, and then immersing the developed resist image in a chemical etching solution for removing the undesired portions of the metal film. Most of the work is carried out in a laminar-flow clean cabinet which is shown in Figure B5(a).

### B6.1 Photoresist Coating

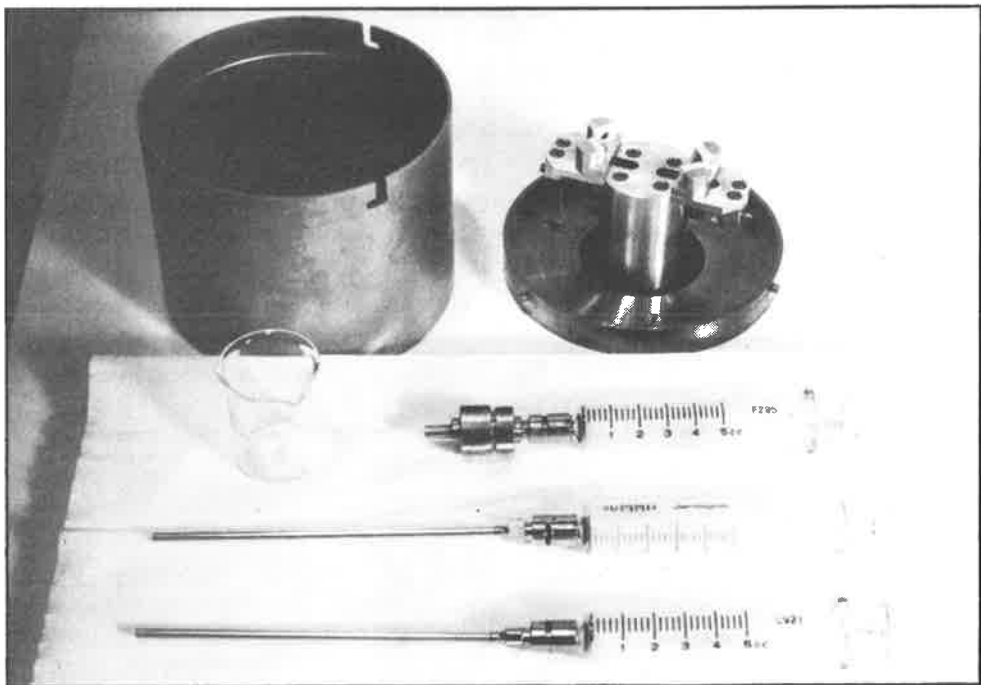
The first part in photoetching process is applying the photoresist coating. The various steps followed are indicated below:

- (1) Dilute one volume of Kodak Thin Film Resist (KTFR) with two volumes of KTFR Thinner and mix thoroughly.
- (2) Assemble a carefully cleaned stainless steel 13 mm. Swinney filter-holder by placing, in order, upon the stainless steel support screen a  $1.2\mu\text{m}$  Gelman Acropor filter membrane (AN-1200), a  $10\mu\text{m}$  Millipore Mitex filter (LCWPO 1300) and a Millipore glass prefilter (AP2501300). The micronrange filter assembly is then fitted to a glass syringe.
- (3) The diluted solution is poured into the syringe and some portion of it is ejected out into waste to make sure that there are no air bubbles in the syringe.
- (4) The metal coated substrate is clamped to the spinner head (see Figure B5(b)), the resist is then ejected on to the surface from the syringe, making sure that the whole surface is covered fully with the resist.
- (5) Fit the safety cover, run the spinner for 30 seconds, wait for it to stop and remove the cover.
- (6) Unclamp the substrate, transfer it to a hot-plate and bake for 20 min. at  $82^{\circ}\text{C}$  ( $180^{\circ}\text{F}$ ). The temperature is controlled through a thermostat and monitored through a thermocouple probe.
- (7) Allow the substrate to cool.





(a)



(b)

Figure B5 Laminar-flow clean cabinet for photoresist work  
(a) clean cabinet with inlet filter at right, outlet filter at left, safe light housing at the top and the alignment microscope in the left foreground, and (b) a closer view of the syringes fitted with micronrange filter assembly and the spinner assembly for the substrates.

### B6.2 Exposing to UV Source

The second part in the photoetching process consists of exposing the photoresist-coated surface with the photographically reduced transparency to the UV source. The exposure jig and the lamp-house are shown in Figure B6. The jig is first loaded with the 2" x 2" glass transparency (emulsion side up) and then the resist coated substrate is placed face down onto the glass transparency, aligning carefully with the pattern. The jig is closed and evacuated through a non-returning valve. The exposure jig is then placed over the exposure aperture in the lamp-house and exposed to 50 sec. and then returned to the clean cabinet. After releasing the vacuum from the jig, the crystal is removed and allowed to cool.

Note that if the transparency is produced from a computer plotted pattern designed for a single stage reduction ratio, longer exposure timings are necessary than 50 sec. and typical exposure timing in this case was found to be equal to 1 min. 30 sec.

### B6.3 Developing Exposed Photosensitive Resist Coatings

The third part in the photoetching process consists of developing the exposed photoresist in the proper developer. The various steps followed are indicated below:

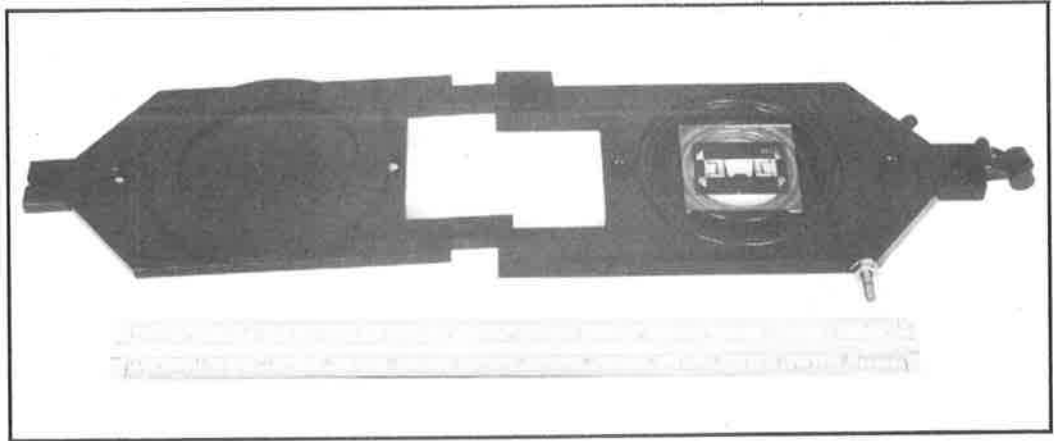
- (1) The KTRF developer of appropriate quantity is taken into two clean beakers and the substrate is immersed sequentially into the two beakers for 20 sec. with continuous agitation in each beaker.
- (2) Immediately after development in the second beaker, the crystal is taken out and a thorough flow of KTRF Rinse from a squeeze bottle or syringe is applied.
- (3) Allow the substrate to dry and examine the resist image under a microscope.
- (4) If not satisfactory, the resist pattern is removed from the substrate (by immersing in a JL1 stripper) and the entire process is repeated from B5.1, i.e. starting from a fresh photoresist coating.

### B6.4 Etching

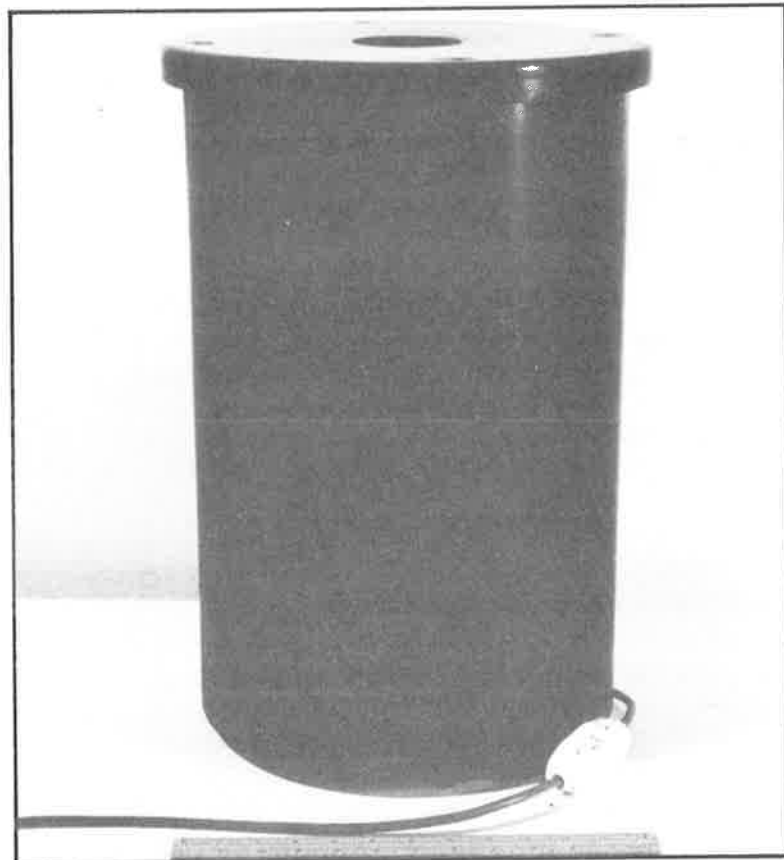
The final part in the photoetching process is etching or removing the unwanted metal from the substrate. The steps followed for this process are indicated below:

- (1) Postbake the crystal on hot-plate to remove all traces of the solvents at 120°C (250°F) for 10 minutes and allow to cool.
- (2) Make up etch solution (for aluminium) using

16 parts	concentrated $H_3PO_4$
2 parts	glacial $CH_3COOH$
1 part	concentrated $HNO_3$



(a)



(b)

Figure B6 Contact printing apparatus (a) contact printing jig, and (b) the lamp house containing UV source.

1 part H<sub>2</sub>O

- (3) Immerse the substrate in the etchant warmed to 90°F and agitate steadily.
- (4) Observe the crystal surface carefully and withdraw immediately as soon as a clear pattern has appeared on the surface and rinse under running distilled water. Note that if this is not followed, further etching will produce undercutting of the pattern beneath the resist, resulting in a damaged SAW device.
- (5) Dry in the clean cabinet.
- (6) A further post-baking or allowing the crystal to dry sufficiently (preferably overnight) is necessary for removing the photoresist on the pattern. Immerse the substrate in the resist-stripping bath warmed to 90°F (50°C) and agitate gently for 2 mins.
- (7) Remove the substrate from the solution and rinse under running distilled water.
- (8) Dry the substrate in the clean cabinet. The device is ready for mounting in the jig for experimental purpose.

REFERENCESCHAPTER 1

1. RAYLEIGH, LORD., *"On waves propagated along the plane surfaces of an elastic solid"*, Proc. London Math. Soc., Vol. 17, 1885, pp. 4-11.
2. RAYLEIGH, LORD., *"The theory of sound"*, Vol. 1,2, Dower Press, New York, 1896.
3. STONELY, R., *"Elastic waves at the surface of separation of two solids"*, Proc. Roy. Soc., Vol. A106, 1924, pp. 416 - 428.
4. BREKHOVSKIKH, L.M., *"Waves in Layered media"*, Moscow: Acad. Sciences, USSR Press, 1957.
5. SEZAW, K., *"Dispersion of elastic waves propagated on the surface of stratified bodies and on curved surfaces"*, Bull. Earthquake Res. Inst. Tokyo, Vol. 3, 1927, pp. 1 - 18.
6. BREKHOVSKIKH, L.M., *"Surface waves confined to the curvature of the boundary in solids"*, Soviet Physics - Acoustics, Vol. 13, No. 4, April-June, 1968, pp. 462 - 472.
7. EWING, W.M., JARDENTZKY, W.S. and PRESS, F., *"Elastic waves in layered media"*, McGraw-Hill, New York, 1957.
8. COOK, E.G. and VAN VALKENBURG, H.E., *"Surface waves at ultrasonic frequencies"*, ASTM Bulletin, May 1954, pp. 81 - 84.
9. CARLIN, B., *"Ultrasonics"*, McGraw Hill, New York, 2nd Edition, Chapter 8, 1960.
10. VIKTOROV, I.A., *"Investigation of methods for exciting Rayleigh waves"*, Soviet Physics - Acoustics, Vol. 7, No. 3, Jan - March, 1962, pp. 236 - 244.
11. \_\_\_\_\_ *"Rayleigh and Lamb waves"*, Plenum Press, New York, 1967.

12. WHITE, R.M. and VOLTNER, F.W., "*Diletric piezoelectric coupling to surface elastic waves*", Appl. Phys. Lett., Vol. 7, 1965, pp. 314 - 316.  
(MORTLEY, W.S., "*Pulse compression by dispersive gratings on crystals quartz*", Marconi Rev., Vol. 28, 1965, pp. 273 - 290 )
13. ARMSTRONG, D.B., "*Surface wave transducers for delay application in the low microwave frequency range*", Paper A-3, IEEE Ultrasonics symp. New York, 1968.
14. STONELY, R., "*The propogation of surface eleastic waves in a cubic crystal*", Proc. Roy. Soc. (London), Vol. A232, 1955, pp. 447 - 458.
15. GOLD, L., "*Rayleigh wave propogation on anisotropic (cubic) media*", Phys. Rev., vol. 104, No. 6, Dec. 1956, pp. 1532 - 1536.
16. GAZIS, D.C., HERMAN, R and WALLIS, R.F., "*Surface elastic waves in cubic crystals*", Phys. Rev., vol. 119, No. 2, July 1960, pp. 533 - 544.
17. BUCHWALD, V.T., "*Rayleigh waves in anisotropic media*", Quart. Jrnl. Mech. Appl. Maths., vol. 14, pt. 4, 1961, pp. 461 - 469.
18. BUCHWALD, V.T. and DAVIS, A., "*Surface waves in elastic media with cubic symmetry*" *ibid*, vol. 16, pt.3, Aug. 1963, pp. 283 - 294.
19. PRESS, F and HEALY, J., "*Absorption of Rayleigh waves in low loss media*", J. Appl. Rhy. vol. 28, 1957, pp. 1323 - 1325.
20. LAMB, J., REDWOOD, M and SHTEINSHLEIFER, Z., "*Absorption of compressional waves in solids from 100 to 1000 Mc/sec*", Phys. Rev. Lett., vol. 3, 1959, pp. 28 - 29.
21. VINOGRADOV, K.N. and UL'YANOV, K.G., "*Measurement of the velocity and attenuation of ultrasonic surface waves in hard materials*", Soviet Phys. Acoustics, vol. 5, 1960, pp. 296 - 299.

22. DERESIEWICH, H and MINDLIN, R.D., "*Waves on the surface of a crystal*", *Phy. Rev.* vol. 104, 1956, pp. 1532 - 1536.
23. TSENG, C.C., "*Elastic surface waves on free and metalized surfaces of Cds, Zno and P2T-4*", *Jrnl. Appl. Phys.*, Vol. 38, No. 11, Oct. 1967, pp. 4281 - 4284.
24. TSENG, C.C. and WHITE, R.M., "*Propagation of piezoelectric and elastic surface waves on basal plane of hexagonal piezoelectric crystals*", *ibid*, vol. 38, no. 11, Oct. 1967, pp. 4274 - 4280.
25. COQUIN, G.A. and TIERSTEN, H.F., "*Analysis of the excitation and detection of piezoelectric surface waves on quartz by means of surface electrodes*", *JASA*, Vol. 41, No.4, Pt. 2, 1967, pp. 921 - 939.
26. CAMPBELL, J.J. and JONES, W.R., "*A method for estimating optimal crystal cuts and propagation directions for excitation of piezoelectric surface waves*", *IEEE, Trans. sonics and ultrasonics*, vol. SU-15, No. 4, Oct. 1968, pp. 209 - 217.
27. TIERSTEN, H.F., "*Linear piezoelectric plate vibrations*", Plenum Press, New York, 1969.
28. BREKHOVSKIKH, L.M., "*Waves in layered media*", Academic Press, New York, 1960.
29. WHITE, J.E., "*Seismic waves, Radiation, Transmission and Attenuation*", McGraw Hill Book Co., New York, 1965.
30. HOLLAND, R and EERNISSE, E.P., "*Design of resonant piezoelectric devices*", Research Monograph No. 56, The MIT Press, Cambridge, Mass., 1969.
31. MUSGRAVE, M.J.P., "*Crystal acoustics*", Holden-Day, San Francisco, 1970.
32. MASON, L.P., "*Physical acoustics*", Academic Press, New York and London, Vol. 6, ch. 3, 1970.

33. MASON, W.P., "*Physical acoustics*", Academic Press, New York and London, vol. 7, ch. 4, 1970.
34. REDWOOD, H., "*Mechanical waveguides*", Pergamon, Oxford, 1960.
35. LOVE, A.E.H., "*Some problems in Geodynamics*", Cambridge University Press, Cambridge, 1926.
36. LOVE, A.E.H., "*On mathematical theory of elasticity*", Cambridge University Press, London and New York (Also Dover Publications, New York, ch. 7, 1944.)
37. LIM, T.C. and MUSGRAVE, M.J.P., "*On elastic waves at crystalline interfaces*", Math. Dept., Imp. College of sci and tech., Univ. of London, 1969.
38. AULD, B.A., "*Acoustic fields and waves in solids*", A Wiley-Interscience Publication, New York, London, Sydney, Toronto, Vol. 1 and vol. 2, 1973.
39. BROERS, A.N., LEAN, E.G. and HATZAKIS, J., "*1.75 MHz acoustic surface wave transducer by electron beam*", Appl. Phys. Lett., Vol. 15, No. 3, Aug. 1969, pp. 98 - 101.
40. LEAN, E.G. and BROERS, A.N., "*2.5 GHz interdigital wave transducers fabricated by electron beam*", IEEE Ultrasonics Symposium, St. Lavius, Sept., 1969.
41. ADKINS, L.R. and HUGHES, A.J., "*Long delay lines employing surface acoustic wave guidance*", Jrnl. Appl. Phys., vol. 42, No. 5, April 1971, pp. 1819 - 1822.
42. LEWIS, M.F. and PATTERSON, E., "*Novel helical path surface wave delay line*", Appl. Phys. Letters, vol. 18, No. 6, Feb. 1971, pp. 143 - 145.
43. BOND, W.L., REEDER, T.M. and SHAW, H.J., "*Warp around surface wave delay lines*", Electronics Letters, Vol. 7, No. 3, Feb. 1971, pp. 79 - 80.



44. QUILICI, S.L. and SHAW, H.J., "*Helical surface acoustic wave delay line*", *ibid*, vol. 8, 1972, pp. 625 - 626.
46. REEDER, T.M., SHAW, H.J. and WESTBROOK, E.M., "*Multimillisecond time delays with wrap-around surface-acoustic-wave delay lines*", *ibid*, vol. 8, 1972, pp. 356 - 358.
47. CHO, F.Y., HUNSINGER, W.J. and LAWSON, R.L., "*Surface waves circulating on piezoelectric substrates*", *Appl. Phys. Letters*, vol. 18, No. 7, April 1971, pp. 298 - 301.
48. VAN DER VAART, H. and SCHISLER, L.R., "*Acoustic surface wave recirculating memory*" *Electronics Letters*, vol. 8, 1972, pp. 333 - 334.
49. COSTANZA, S.T., MAGON, P.J. and MACNEVIN, L.A., "*Analog matched filters using tapped acoustic surface wave delay lines*", *IEEE Trans. Microwave Theory and Tech.*, vol. MTT-17, No. 11, Nov. 1969, pp. 1042 - 1043.
50. SQUIRE, W.D., WHITEHOUSE, H.J. and ALSUP, J.H., "*Linear signal processing and ultrasonic transversal filters*", *ibid*, vol. MTT-17, No. 11, Nov, 1969, pp. 1020 - 1040.
51. MARTIN, T.A., "*The IMCON pulse compression filter and its applications (invited paper)*", *ibid*, Vol. MTT-21, No. 4, April, 1973, pp. 186 - 194.
52. BELL, Jr. D.T., HOLMES, J.D. and RIDINGS, R.V., "*Application of acoustic surface wave technology to spread spectrum communications (invited paper)*", *ibid*, vol. MTT-17, No. 4, April, 1973, pp. 263 - 271.
53. BURNSWEIG, J and WOOLDRIDGE, J., "*Ranging and data Transmission using digital encoded-FM-chirp surface acoustic wave filters*", *ibid*, vol. MTT-17, No. 4, April 1973, pp. 272 - 278.

54. HAGON, P.J. and DYAL, L., "*Wideband U.H.F. compression filters using AIN on sapphire*", IEEE Ultrasonics Symposium Proc., 1972, pp. 274 - 275.
55. HUNSINGER, W.J. and FRANK, A.R., "*Programmable surface - wave tapped delay line*" IEEE Trans. Sonics and Ultrasonics, Vol. SU-18, 1971, pp. 152 - 154.
56. O'CLOCK, Jun, GRASSE, G.D. and GANDOLFO, D.A., "*Switchable acoustic - surface - wave sequence generator*", IEEE. Proc., Vol. 59, 1971, pp. 58 - 60.
57. WRIGLEY, C.Y, HAGON, P.J. and SEYMOUR, R.N., "*Programmable s.a.w. matched filters for phase cooled waveforms*", IEEE Ultrasonics Symposium Proc, 1972, pp. 226 - 228.
58. FISHER, T.S., PATTERSON, E. and SCOTTER, D.G., "*Surface wave correlator with inclined transducer*" Electronics Letters, Vol. 9, 1973, pp. 35.
59. LUUKKALA, M, and KINO, G.S., "*Convolution and time inversion using parametric interaction of acoustic surface waves*", Appl. Phy. Lett., vol. 18, 1971, pp. 393 - 394.
60. BONGIANNI, W.L., "*Pulse compression using nonlinear interaction in a surface acoustic wave convolver*", IEEE, Proc, Vol. 59, 1971, pp. 713 - 714.
61. GRASSE, C.L. and GANDOLFO, D.A., "*Acoustic surface wave dispersive delay lines as high frequency discriminators*", IEEE, Ultrasonics Symposium Proc., 1972, pp. 233 - 236.
62. JOHNSON, J.N., "*Dispersive subsystem for pulse compression radar using s.a.w. devices*", Microwave Conference Proc., 1973, pp. 460 - 464.
63. MICROWAVE ACOUSTICS, special issue of IEEE Trans. on Microwave Theory and Techniques MTT-17, Nov., 1969.

64. COLLINS, J.H. and HAGON, P.J., *"Tapping microwave acoustics for better signal processing"*, Electronics, November 19, 1969, pp. 94 - 96.
65. \_\_\_\_\_ *"Applying surface wave acoustics"*, ibid, November 19, 1969, pp. 97 - 103.
66. \_\_\_\_\_ *"Amplifying acoustic surface waves"*, ibid, December 8, 1969, pp. 102 - 111.
67. \_\_\_\_\_ *"Surface wave delay lines promise filters for radar, flat tubes for television, and faster computers"*, ibid, January 19, 1970, pp. 111 - 122.
68. MASON, P. and THURSTON, R.N., *"Physical acoustics"*, Vol. 7, Chp. 4 and Ch. 5, Academic Press, New York and London, 1970.
69. COLLINS, J.H., *"The 70's the decade of microwave acoustic engineering?"* Microwave Journal, Vol. 13, No. 3, March, 1970, pp. 46 - 49.
70. OLSON, F.A., *"Today's microwave acoustic (Bulk wave) delay lines"*, ibid, vol. 13, No. 3, March, 1970, pp. 67 - 76.
71. KINO, G.S. and REEDER, T.M., *"Microwave acoustic amplifiers"*, ibid, vol. 13, No. 3, March, 1970, pp. 79 - 85.
72. ADKINS, L.R., BRISTOL, T.W., HAGON, P.J. and HUGES, A.J., *"Surface acoustic waves - device applications and signal routing techniques for VHF and UHF"*, Vol. 13, No. 3, March, 1970, pp. 87 - 94.
73. LEAN, E.G. and BROERS, A.N., *"Microwave surface acoustic delay lines"*, ibid, vol. 13, No. 3, March, 1970, pp. 97 - 101.
74. WHITE, R.M., *"Surface elastic waves"*, Proc. of IEEE, Vol. 58, No. 8, Aug, 1970, pp. 1238 - 1276.
75. KLERK de, J., *"Ultrasonic transducers"*, Ultrasonics, Jan. 1971, pp. 35 - 48.
76. SABINE, H. and COLE, P.H. *"Acoustic surface wave devices: A survey"*, Presented at 13th National Conference of IREE, Melb. (Aust.) May, '71

77. \_\_\_\_\_ *"Surface acoustic waves in communications engineering"*, Ultrasonics, April 1971, pp. 103 - 113.
78. KINO, G.S., and MATTHEWS, H., *"Signal processing in acoustic surface wave devices"*, IEEE Spectrum, Aug. 1971, pp. 22 - 35.
79. KALLARD, T., *"Acoustic surface wave and acousto-optic devices"*, Optosonic Press, New York, Sept. 1971.
80. COLLINS, J.H. and GRANT, P.M., *"The role of surface acoustic wave technology in Communication systems"*, Ultrasonics, March, 1972, pp. 59 - 71.
81. MORGAN, D.P., *"Surface acoustic wave devices and applications. 1. Introductory review"*, Ultrasonics, May, 1973, pp. 121 - 131.
82. MAINES, D.J. and JOHNSTON, J.N., *"Surface acoustic wave devices and applications. 2. Pulse compression systems"*, *ibid*, Sept. 1973, pp. 211 - 217.
83. HUNSINGER, B.J., *"Surface acoustic wave devices and applications. 3. Spread spectrum processors"*, *ibid*, Nov. 1973, pp. 254 - 262.
84. MITCHELL, R.F., *"Surface acoustic wave devices and applications. 4. Band pass filters"*, *ibid*, Jan. 1974, pp. 29 - 35.
85. MORGAN, D.P., *"Surface acoustic wave devices and applications. 5. Signal processing using programmable non-linear convolvers"*, *ibid*, March 1974, pp. 74 - 83.
86. LEWIS, M.F., *"Surface acoustic wave devices and applications. 6. Oscillators - the next successful surface acoustic wave devices?"* *ibid*, May 1974, pp. 115 - 123.
87. MAINES, J.D., *"Surface acoustic wave components, devices and applications"*, Proc. IEE, Vol. 120, No. 10R, Oct. 1973, IEE, Reviews, pp. 1078 - 1110.
88. Microwave acoustic signal processing, special issue of IEEE Trans. Microwave Theory and Technology MTT-21, April, 1973.

89. MORSCH, W., *"Technology forecasting and assessment in ultrasonics"*,  
IEEE Ultrasonics symposium Proc. 1973, pp. 579 - 582.
90. Special issue on microwave acoustic signal processing, IEEE Trans.  
on Sonics and Ultrasonics, Vol. SU-20, No. 2, April, 1973.
91. BRISTOL, T.W., *"Acoustic surface - wave - device - Applications"*,  
Microwave Journal, Jan, 1974, pp. 25 - 27 and 63.
92. ASH, E.A. and MORGAN, D.P., *"Realization of microwave circuit  
functions using acoustic surface waves"*, Electronics Letters,  
Vol. 3, Oct, 1967, pp. 462 - 463.
93. ASH, E.A., De La RUE, R.M. and HUMPHRYES, R.F., *"Microsound  
surface wave guides"*, IEEE Trans. Microwave Theory and  
Techniques, Vol. MTT-17, Nov. 1969, pp. 882 - 892.
94. LAKIN, K.M. and SHAW, H.J., *"Surface wave delay line amplifiers"*,  
IEEE Trans. Microwave Theory and Tech., vol. MTT-17, No. 11,  
Nov. 1969, pp. 912 - 920.
95. WHITE, R.M., *"Surface elastostatic wave propagation and ampli-  
fication"*, IEEE Trans. Electron Devices, Vol. ED-14, No. 4,  
April, 1967, pp. 181 - 189.
96. ADKINS, L.R. and HUGHES, A.J., *"Investigations of surface acoustic  
wave directional couplers"*, IEEE Trans. Sonics and Ultrasonics,  
vol. SU-19, No. 1, Jan. 1972, pp. 45 - 58.
97. BURKE, B.E., *"An electronically variable surface acoustic wave  
phase shifter"*, Paper IV-4, IEEE International Microwave  
Symposium, Washington, May, 1971.
98. DUZER van, T., *"Lenses and Graded Films for focusing and guiding  
acoustic surface waves"*, IEEE Proc. Vol. 58, no. 8, Aug.  
1970, pp. 1230 - 1237.
99. STERN, E., *"Microsound components, circuits and applications"*,  
IEEE Trans. Microwave Theory and Tehc., vol. MTT-17, No. 11,  
Nov. 1969, pp. 835 - 844.

100. ENGAN, H, HANEBREKKE, H., INGEBRIGTSEN, K.A. and JERGAN, E.,  
*"Numerical calculation of surface waves in piezoelectrics"*,  
Appl. Phys. Lett. Vol. 15, Oct 15, 1969, pp. 239 - 241.
101. INGEBRIGTSEN, K.A., *"Surface waves in piezoelectrics"*, J. Appl.  
Phys. Vol.40, June, 1969, pp. 2681 - 2688.
102. INGEBRIGTSEN, K.A., *"Elastic surface waves in crystals"*, Phys.  
Rev. Vol. 184, Aug, 1969, pp. 942 - 951.
103. KALLMAN, H.E., *"Transversal filters"*, Proc. IRE, Vol. 28,  
July, 1940, pp. 302 - 310.
104. JEFFERY, M.S. and WHITEHOUSE, H.J., *"Surface wave transducer  
array design using transversal filter concepts"*, Acoustic  
Surface wave and Acousto-optic devices, Edited by Thomas  
Kallard, Optosonic Press, New York, 1971, pp. 81 - 90.
105. ATZENI, C., and MASOTTI, L., *"Acoustic surface wave transversal  
filters"*, ibid, Edited by Thomas Kallard, Optosonic  
Press, New York, 1971, pp. 68 - 80.
106. DIEULESAINT, E. and HARTMAN, P., *"Surface acoustic wave filters"*,  
Ultrasonics, Jan. 1973, pp. 24 - 30.
107. SITTING, E.K. and COQUIN, G.A., *"Filters and dispersive delay lines  
using repetitively mismatched ultrasonic transmission lines"*,  
IEEE Trans. Sonics and Ultrasonics, vol. SU-15, 1968, pp. 111 -  
119.
108. TANCERELL, R.H. and HOLLAND, M.G., *"Acoustic surface wave filters"*,  
Proc. IEEE, Vol.59, No. 3, March 1971, pp. 393 - 409.
109. TANCERELL, R.H., *"Analytic design of surface wave bandpass filters"*,  
IEEE Trans. on Sonics and Ultrasonics, vol. SU-21, No. 1,  
Jan. 1974, pp. 12 - 22.
110. CLAIBORNE, L.T., HARTMAN, C.S., HAYS, R.M. and ROSENFELD, R.C.,  
*"VHF/UHF bandpass filters using SAW device technology"*, Microwave  
Journal, May 1974, pp. 35 - 38, 40.

111. MILSON, R.F. and REDWOOD, M., "*The interdigital piezoelectric Rayleigh wave transducer: An improved equivalent circuit*", Electronics Letters, Vol. 7, 1971, pp. 217 - 218.
112. EMTAGE, P.R., "*Self consistent theory of interdigital transducers*", IEEE, Ultrasonics Symposium Proc., 1972, pp. 397 - 402.
113. INGEBRIGTSEN, K.A., "*Analysis of interdigital transducers*", *ibid*, 1972, pp. 408-412.
114. DANIEL, M.R., EHTAGE, P.R. and DE KLERK, J., "*Acoustic radiation by interdigitated grids on  $LiNbO_3$* ", *ibid*, 1972, pp. 408 - 412.
115. MITCHELL, R.F., WILLIS, W. and REDWOOD, M., "*Electrode interactions in acoustic surface wave transducers*", Electronics Letters, Vol. 5, 1969, pp. 456 - 457.
116. JONES, W.S., HARTMAN, C.S. and STURDIVANT, T.D., "*Second order effects in surface wave devices*", IEEE Trans. Sonics and Ultrasonics, Vol. SU-19, 1972, pp. 368 - 377.
117. AULD, B.A., "*Application of microwave concepts to the theory of acoustic fields and waves in solids*", IEEE Trans. Microwave Theory and Tech. Vol. MTT-17, No. 11, Nov, 1969, pp. 808 - 811.
118. \_\_\_\_\_ "*Surface wave theory - invited Proceedings of 1970*", IEEE Ultrasonics Symposium, (L.W. Kessler Ed.), IEEE, New York, 1971, pp. 1 - 15.
119. AULD, B.A. and KINO, G.S., "*Normal mode theory for acoustic waves and its application to the interdigital transducers*", IEEE Trans. Electron Devices, Vol. ED-18, No. 10, Oct, 1971, pp. 898 - 908.
120. SMITH, W.R., GERRARD, H.M., COLLINS, J.H., REEDER, T.M. and SHAW, H.J., "*Analysis of interdigital surface wave transducers by the use of an equivalent circuit model*", IEEE Trans. Microwave Theory and Techniques, Vol. MTT-17, No. 11, Nov. 1969, pp. 856 - 864.

121. \_\_\_\_\_ *"Design of surface wave delay lines with interdigital transducers"*, *ibid*, vol. MTT-17, No. 11, Nov, 1969, pp. 865 - 873.
122. HARTMAN, C.S., BELL, D.T. and ROSENFELD, R.C., *"Impulse model design of acoustic surface-wave filters"*, *IEEE Trans. Sonics and Ultrasonics*, Vol. SU-20, No. 2, April, 1973, pp. 80 - 93.
123. ATZENI, C. and MASOTTI, L., *"Design of interdigital arrays for acoustic surface wave filters"*, *IEEE Ultrasonics Symposium Proc.* 1972, pp. 241 - 252.
124. ATZENI, C., MANES, G. and MASOTTI, L., *"Synthesis of amplitude - modulated SAW filters with constant-finger lengths,"**ibid*, 1973, pp. 414 - 418.
125. ATZENI, C., *"Sensor number minimization in acoustic surface wave matched filters"*, *IEEE Trans. Sonics and Ultrasonics*, Vol. SU-18, No. 4, Oct. 1971, pp. 193 - 201.
126. MITCHELL, R.F., PRATT, R.G., SINGELTON, J.S. and WILLS, W., *"Surface wave filters"*, *Mullard Technical Communications*, No. 108, No. 1970, pp. 175 - 181.
127. MITCHELL, R.F., *"Acoustic surface wave filters"*, *Philips Tech. Rev.* 32, No. 6/7/8, 1971, pp. 179 - 189.
128. \_\_\_\_\_ *"Generation and detection of sound by distributed piezoelectric sources"*, *Philips Res. Repts. Suppl.* No. 3, 1972.
129. GANGULY, A.K. and VASSEL, M.O., *"Frequency response of acoustic surface wave filter I"*, *J. Appl. Phys.* Vol. 44, No. 3, March, 1973, pp. 1072 - 1085.
130. ZUCKER, J. and GANGULY, A.K., *"Frequency response of acoustic surface wave filters II"*, *ibid*, vol.44, No. 3, March, 1973, pp. 1086 - 1089.
131. BURGESS, A.S. and COLE, P.H., *"Design of acoustic surface-wave devices using an admittance formalism"*, *IEEE Trans. Microwave Theory and Tech.*, Vol MTT-21, No. 10, Oct. 1973, pp. 611 - 618.



132. KRISHNAMACHARYULU, N.C.V. and COLE, P.H., "*Synthesis of surface acoustic wave filters for Australian TV IF standards*", IREE (Aust.) Convention Digest, 1973, pp. 130 - 131.
133. TANCRELL, R.H. and ENGAN, H., "*Design considerations for SAW filters*", IEEE Ultrasonics Symposium, Proc., 1972, pp. 419 - 422.
134. MARSHALL, F.G., NEWTON, C.O. and PAIGE, E.G.C., "*Surface acoustic wave multistrip components and their applications*", IEEE Trans. Microwave Theory and Techniques, Vol. MTT-21, No. 4, April, 1973, pp. 216-224.
135. \_\_\_\_\_ "*Theory and design of surface acoustic wave multistrip coupler*", *ibid*, vol. MTT-21, No.4, April, 1973, pp. 206 - 215.
136. VASILE, C.G., "*A numerical Fourier transform technique and its application to acoustic surface wave bandpass filter synthesis and design*", *ibid*, vol. SU-21, No.1, Jan, 1974, pp. 7 - 11.
137. GERARD, H.M., SMITH, W.R., JONES, W.R., and HARRINGTON, J.B., "*The design and applications of highly dispersive acoustic surface wave filters*", *ibid*, vol. SU-20, No.2, April, 1973, pp. 94 - 104.
138. GERARD, H.M., JONES, W.R., SMITH, W.R. and SNOW, P.B. "*Development of a broadband, loco loss 1000: 1 dispersive filter*", IEEE Ultrasonics Symposium, Proc. Oct. 1972, pp. 253 - 262.
139. WORLEY, J.C., "*Bandpass filters using non linear F.M. surface wave transducers*", IEEE Trans. Sonics and Ultrasonics, April, 1973, pp. 220 - 221.
140. MORGAN, D.P., "*Log-periodic transducers for acoustic surface waves*", Proc. IEE, Vol. 119, No.1, Jan, 1972, pp. 53 - 60.
141. BUBREAU, A.J. and CARR, P.H., "*Narrow band surface wave filters at 1GHz*", IEEE Ultrasonics Symposium Proc., Oct. 1972, pp. 218 - 220.

142. HARTEMANN, P., "Narrow bandwidth Rayleigh wave filters", *Electronics Letters*, vol. 8, 1971, pp. 674 - 675.
143. LEWIS, H.F., "Surface acoustic wave filters employing symmetric phase-weighted transducers", *ibid*, vol. 9, no. 6, 1973, pp. 138 - 140.
144. SPEISER, J.M. and WHITEHOUSE, H.J., "Surface wave transducer array design using transversal filter concepts", *Optosonic Press*, 1971, pp. 81 - 90.
145. DeVRIES, A.J., DIAS, J.F., RYPKEMA, J.N. and WOJCIK, T.J., "Characteristics of surface-wave integratable filters (SWIFS)", (Jrnl. not known).
146. DeVRIES, A.J., ADLER, R., DJAS, J.F. and WOJCIK, T.J., "Realization of a 40 MHz colour Television IF Response using surface wave transducers on Lead Zirconate Titanate", Paper G-5, IEEE Ultrasonics Symposium St. Louis, Missouri, Sept. 1969.
147. CHAUVIN, D, COUSSO T.G. and DIEULESAINT, E., "Acoustic surface wave television filters", *Electronics Letters*, Vol. 7, No.17, Aug. 1971, pp. 491 - 492.
148. LEWIS, M.F., "Surface acoustic wave devices", *GEC Journal of Science and Technology*, Vol. 39, No. 4, 1972, pp. 156 - 162.
149. HIGHWAY, J and DEACON, J.M., "A continuous phase analysis of dispersive A.S.W. transducers" *IEEE Ultrasonics Symposium Prac.*, Oct. 1972, pp. 384 - 387.
150. RAALTE van, J.A., "Surface acoustic wave filter for television intermediate frequencies", *RCA Engineer*, Vol. 20, No. 1, June-July, 1974, pp. 15 - 19.

13. SLOBODNIK, A.J., "A review of material tradeoffs in the design of acoustic surface wave devices at VHF and microwave frequencies", IEEE Trans. Sonics and Ultrasonics, Vol. SU-20, No.4, Oct.1973, pp. 315 - 323.
14. SLOBODNIK, A.J. and CONLAY, E.D., "Microwave acoustics Handbook, Vol. 1: Surface wave velocities", USAF Cambridge Res. Labs, Bedford, Mass., Physical science Research Paper 414, March, (1970), (unpublished).
15. SLOBODNIK, A.J. and SZABO, T.L., "Design data for microwave acoustic surface wave devices", Monday, May 17, 1971 (1400 - 1700) pp. 52 - 53.
16. BECHMANN, R., "Elastic and piezoelectric constants of Alpha quartz", Phys. Rev., vol. 110, 1965, pp. 1060 - 1061.
17. Ref. 38 of Ch. 1.
18. FARNELL, G.W., "Properties of elastic surface waves", in 'Physical Acoustics", Vol.V1, W.P. Mason and R.M. Thurston, Eds., Academic Press, New York, 1970, pp. 157 - 158.
19. Ref. 17 pp. 170 - 177.
20. Ref. 122 of Ch. 1.
21. SMITH, W.R., GERARD, H.M. and JONES, W.R., "Analysis and design of dispersive interdigital surface wave transducers", IEEE Trans. Microwave Theory and Tech., Vol. MTT-20, No. 7, July, 1972, pp. 438 - 471.
22. BURGESS, A.S., "Coded one-part acoustic surface wave delay lines", Ph. D. Thesis, Elect. Engg. Dept., University of Adelaide, 1974, pp. 73 - 76.
23. NALAMWAR, A.L. and EPSTEIN, M., "Immittance characterization of acoustic surface wave transducers", Proc. IEEE (Left), Vol.60, March, 1972, pp. 336 - 337.

24.  ENGAN, H., "*Excitation of elastic surface waves by spatial harmonics of interdigital transducers*", IEEE Trans. Electron Devices, Vol. ED-16, 1969, pp. 1014 - 1017.

25.  Ref. 108 of Ch. 1.

CHAPTER 3.

1. Television Channels, Standard Intermediate Frequencies and Standards for Limits of Radiation from Receivers - Prepared by Australian Broadcasting control Board, 1971.
2. Technical Standards for Australian Television Service - Determined by the Australian Broadcasting Control Board in pursuance of the Broadcasting and Television Act, 1962 - 1969.
3. Ref. 135 of Chapter 1.
4. Ref. 133 of Chapter 1.
5. FOWLE, E.N., *"The design of FM pulse compression signals"*, IEEE Trans. Information Theory, Jan. 1964, pp. 61 - 67.
6. Ref. 140 of Chapter 1.
7. COURT, I.N., *"Microwave acoustic devices for pulse compression filters"*, IEEE Trans. Microwave Theory Tech. Vol. MTT-17, Nov. 1969, pp. 968 - 986.
8. DARBY, B.J., *"Suppression of spurious acoustic signals in phase coded surface acoustic wave analog matched filters using dual-tap geometry"*, IEEE Trans. Sonics and Ultrasonics, vol. SU-20, No. 4, Oct. 1973, pp. 382 - 384.
9. DeVRIES, A.J., MILLER, R.L. and WOJCIK, T.J., *"Reflection of a surface wave from three types of ID Transducers"*, IEEE Ultrasonics Symposium Proc. 1972, pp. 353 - 358.
10. DeVRIES, A.J. and SUBRAMANIAN, S., *"Overall comparasion between theoretical predictions using the cross-field transmission-line model and experimental measurements of a split-connected transducer"*, IEEE Ultrasonics Symposium Proc. 1973, pp. 407 - 409.

11. CARR, P.H., "*Reduction of reflections in Surface wave delay liners with quarter-wave taps*", Proc. IEEE (Letters), Vol.60, 1972, pp. 1103 - 1104.
12. Ref. 120 of Ch. 1.
13. MARSHALL, F.G., PAIGE, E.G.S and YOUNG, A.S., "*New unidirectional transducer and broadband reflector of acoustic surface waves*", Electronics Letters, Vol. 7, No. 21, Oct. 1971, pp. 638 - 640.
14. Ref. 148 of Ch. 1.
15. COOLEY, J.W. and TUKEY, J.W., "*An algorithm for machine calculation of complex Fourier Series*", Math. of Comput., Vol. 19, 1965, pp. 297 - 301.
16. BURGESS, A.S., "*Numanical computation of Fourier transforms*", IREE Convention Digest, Aug. 1973, pp. 38 - 39.
17. BRIGHAM, O., "*Fast Fourier transform*", Prentice Hall Publication, 1974.
18. Special Issue on Fast Fourier Transform, IEEE Trans. on Audio and Electroacoustics, Vol. AU-17, No.2, June, 1969.
19. HELMS, H.D., "*Fast Fourier transform method of computing difference equations and simulating filters*", IEEE Trans. on Audio and Electroacoustics, vol. AU-15, No.2, June 1967, pp. 83 - 90.

CHAPTER 4

1. Reference 25 of Chapter 1.
2. Reference 26 of Chapter 1.
3. Reference 10 of Chapter 2.
4. Reference 22 of Chapter 2.
5. PHOTOFABRICATION - The new horizon in metalworking, Presented  
by Kodak Company, Rochester, New York, 14650.
6. An Introduction to Photofabrication using KODAK Photosensitive  
Resists, KODAK Publication No. P.79.
7. Proceedings of the second seminar on microminiaturization,  
KODAK Publication No. P.89 April 4th and 5th, 1966.
8. KODAK Plates and Films for Science and Industry, KODAK  
Publication No. P.9, Eastman Kodak Company, Rochester,  
New York, 14650.
9. RESEARCH SOLDER KIT, Indium Corporation of America, New York,  
13503.

CHAPTER 5

1. HELMS, H.D., "*Nonrecursive digital filters: Design methods for achieving specifications on frequency response*", IEEE Trans. Audio and Electroacoustics, Vol. AU-16, No.3, Sept. 1968, pp. 336 - 342.
2. GOULD, B. "*A direct research procedure for designing finite duration impulse response filters*", *ibid*, vol. AU-17, No. 1, March, 1969, pp. 33 - 36.
3. TUFTS, D.W., RORABACHER, D.W. and MOSIER, W.E., "*Designing simple, effective digital filters*", *ibid*, vol. AU-18, No. 2., June, 1970, pp. 142 - 158.
4. SCHROEDER, M.R., "*Synthesis of low peak factor signals and binary sequences with low autocorrelation*", IEEE Trans. on Information Theory, vol. IT-16, No. 1, Jan, 1970, pp. 85 - 89.
5. RABINER, L.R., GOLD, B. and MCGONEGAL, C.A., "*An approach to the approximation problem for nonrecursive digital filters*", IEEE Trans. Audio and Electroacoustics, Vol. AU-18, No. 2, June, 1970, pp. 83 - 106.
6. HERRMAN, O., "*Design of nonrecursive digital filters with linear phase*", Electronics letters, vol. 6, No. 11, May, 1970, pp. 328 - 329.
7. HERRMAN, O. and SCHUESSLER, W., "*Design of nonrecursive digital filters with minimum phase*", *ibid*, vol. 6, No. 11, May, 1970, pp. 329 - 330.
8. HELMS, H.D., "*Digital filters with equiripple or minimax responses*", IEEE Trans. Audio and Electroacoustics, Vol. AU-19, No. 1, March, 1971, pp. 87 - 93.
9. RABINER, L.R., "*Techniques for designing finite duration impulse response digital filters*", IEEE Trans. Communication Technology, vol. COM-19, No. 2, April, 1971, pp. 188 - 195.



10. \_\_\_\_\_ "Linear programme design of finite impulse response (FIR) digital filters", IEEE Trans. Audio and Electroacoustics, Vol. AU-20, No.4, Oct. 1972, pp. 28 - 288.
11. THAJCHAYAPONG, P and RAYNER, P.J.W., "Recursive digital filter design by linear programming", *ibid*, vol. AU-21, No.2, April, 1973, pp. 107 - 112.
12. Special Issue on Digital Filters: The Promise of LSI applied to Signal Processing, *ibid*, vol. AU-16, No.3, Sept. 1968.
13. Special Issue on Digital Filtering, *ibid*, vol. AU-18, No.3, June, 1970.
14. GIBBS, A.J., "Minimum mean-square-error approximation using transversal-type filters", IEEE Trans. Circuits and Systems, May, 1974, pp. 348 - 353.
15. TEMES, G.S. and CALAHAN, D.A., "Computer aided Network Optimization, The State of Art", Proc. IEEE Vol.55, No.11, Nov, 1967, pp. 1832 - 1863.
16. KAISER, J.F., "Digital filters", in System Analysis by Digital Computer, F.F. Kuo and J.F. Kaiser, Eds., New York: Wiley, 1966.
17. Reference 109 of Chapter 1.

CHAPTER 7.

1. Reference 120 of Chapter 1.
2. Reference 121 of Chapter 1.
3. Reference 122 of Chapter 1.
4. Reference 148 of Chapter 1.
5. HARTMAN, C.S., JONES, W.S. and VOLLERS, H., "*Wideband unidirectional interdigital surface wave transducers*", IEEE Trans. Sonics and Ultrasonics, Vol. SU-19, July, 1971, pp. 378 - 381.
6. WORLEY, J.C. and MATTHEWS, H., "*Broadband unidirectional surface wave Transducer*", Paper G-7, IEEE, Ultrasonics Symposium Proc. Oct, 1970.
7. HERRING, F.G., KRENCIK, P.H. and VASILE, C.F., "*High performance surface wave pulse compression*" IEEE Ultrasonics Symposium Proc. 1973, pp. 472 - 477.

CHAPTER 8.

1. Ref. 108 of Ch. 1.
2. Ref. 138 of Ch. 1.
3. Ref. 123 of Ch. 1.
4. Ref. 21 of Ch. 2.
5. Ref. 137 of Ch. 1.
6. MARTIN, T.A., "*A new dispersive delay line*", Presented at the IEEE Ultrasonic Symposium, San. Francisco, Calif. Oct, 21 - 23rd, 1970.
7. Ref. 51 of Ch. 1.
8. HERRING, F.G., KRENCIK, P.H. and VASILE, C.F., "*High performance surface wave pulse compression*", IEEE Ultrasonics Symposium, Proc. 1973, pp. 472 - 477.
9. JUDD, G.W., "*Technique for realizing low time sidelobe levels in small compression ratio chirp waveforms*", *ibid*, 1973, pp. 478 - 481.
10. WEGLEIN, R.D., WAUK, M.T., and NUDD, G.R., "*500 MHz bandwidth surface wave pulse compression filter*", *ibid*, 1973 pp. 482 - 485.
11. MELLON, D.W. and BELL, T.D., "*Development of a UHF surface wave pulse compressor*", *ibid*, 1973, pp. 486 - 489.
12. BUSH, H., "*Application of chirp SWD for spread spectrum communications*", *ibid*, 1973, pp. 494 - 499.
13. JONES, W.S., KEMPF, R.A. and HARTMAN, C.S., "*Practical surface wave chirp filters for modern radar systems*", *Microwave Journal*, May 1972, pp. 43 - 48, 50 & 86.

14. HARRINGTON, J.B. and NELSON, R.B., "*Compressive intercept receiver uses SAW devices*", *ibid*, Sept. 1974, pp. 57 - 62.
15. Ref. 139 of Ch. 1.
16. Ref. 5 of Ch. 3.
17. BRACEWELL, R.M., "*The fourier transform and its applications*", McGraw-Hill Book Company, 1965.
18. Ref. 125 of Ch. 1.

CHAPTER 9.

1. Reference 150 of Chapter 1.
2. Philips Data Handbook - semiconductors and integrated circuits, Part 4a, March, 1973.
3. HEJHALL, R.C., "*Field effect transistor RF amplified design techniques*", Motorola semiconductor Products Inc., a paper presented at Wescon, 1967.
4. Reference 120 of Chapter 1.
5. JONES, W.S., HARTMAN, C.S. and HARRIS, J.S., "*Matching optimization to interdigital surface-wave devices*", Electronics Letters, Vol. 61, No.11, May 1970, pp. 333 - 335.
6. TERMAN, F.E., "*Radio Engineers hand book*", McGraw Hill Book Company Inc., New York, 1943, pp. 148.

CHAPTER 10.

1. Reference 120 of Chapter 1.
2. Reference 121 of Chapter 2.
3. Reference 108 of Chapter 1.
4. Reference 122 of Chapter 1.
5. JAFFE, H. and BERLINCOURT, D.A., "*Piezoelectric transducer materials*",  
Proc. IEEE, Vol. 53, No. 10, Oct, 1975, pp. 1372 - 1386.
6. MITCHELL, R.F., "*Some new materials for ultrasonic transducers*",  
Ultrasonics, April, 1968, pp. 112 - 116.
7. COLLINS, J.H., HAGON, P.J. and PULLIAM, G.R., "*Evaluation of  
new single crystal piezoelectric materials for surface  
acoustic-wave application*", *ibid*, Oct. 1970, pp. 218 - 226.
8. LEWIS, M.F., "*Triple transit suppression in surface acoustic wave  
devices*", Electronics Letters, Vol. 8, 1972, pp. 553 - 554.
9. WAUK, M.T., "*Suppression of spurious triple transit signals in  
acoustic surface-wave delay line*", Appl. Phys. Letters, vol. 20,  
1972, pp. 481 - 483.
10. KLERK de, J., "*Thin film zinc oxide transducers for use in  
microwave devices*", Ultrasonics, July, 1970, pp. 159 - 164.
11. SASAKI, H., CHUBACHI, N. and KIKUCHI, Y., "*Thickness dependence  
of effective coupling factors of ZnO thin-film surface-wave  
transducers*", Electronics Letters, Vol. 9, 1973, pp. 92 - 93.
11. HICKERNELL, F.S., "*D.C. triode sputtered zinc oxide surface elastic  
wave transducers*", J. Appl. Phys. Vol. 44, 1973, pp. 1061 - 1071.
12. EVANS, D.R., LEWIS, M.F. and PATTERSON, P., "*Sputtered ZnO surface-  
wave transducers*", Electronics Letters, vol. 7, 1971, pp. 557-558.

13. SCHNITZLER, P., BERGSTEIN, L. and STRAUSS, L., "*Elastic surface waves: Thin-film transducers and layered system dispersion*", IEEE Trans. Sonics and Ultrasonics, Vol. SU-17, 1970, pp. 185 - 188.
14. HICKERNELL, F.S., SHULDA, G.F., and BRENER, J.W., "*Zinc oxide and cadmium sulphide overloy surface wave transducers*", Paper G-11, IEEE Ultrasonics symposium, San Francisco, Calif. U.S.A., 1970.
15. SANDBANK, C.P., and BUTLER, M.B.N., "*Acoustic surface waves on isopastic glass*", Electronics Letters, vol.7, 1971, pp. 499 - 501.
16. BELLMAN, R., "*Dynamic Programming*", Princeton University Press, 1957.
17. JOSHI, S.G. and WHITE, R.M., "*Dispersion of surface elastic waves produced by a conducting grating on a piezoelectric crystal*", J. App. Phys. Vol.39, 1968, pp. 5819 - 5827.
18. SKEIE, H., "*Electrical and mechanical loading of a piezoelectric surface supporting surface waves*", J. Acoust. Soc. Amer., Vol. 48, 1970, pp. 1098 - 1109.
19. SMITR, W.R., "*Minimizing multiple transit echoes in surface wave devices*", IEEE Ultrasonics Symposium Proc. 1973, pp. 410 - 413.